Insulin resistance and the ability of high-density lipoprotein to provide vascular protection

Jack David Beazer BSc (Hons), MRes

Thesis submitted in fulfilment of the requirements for the degree of Doctor of Philosophy (PhD)

School of Cardiovascular and Metabolic Health,
College of Medical, Veterinary and Life Sciences,
University of Glasgow

November 2023

Abstract

The worldwide prevalence of obesity and its metabolic consequences continues to rapidly increase. Obesity leads to metabolic derangements in insulin signalling and secretion, glucose control, and plasma lipid distribution, resulting in insulin resistance and dyslipidaemia. Over time, this phenotype can lead to pancreatic beta cell failure and type 2 diabetes mellitus (T2DM). The deleterious metabolic changes associated with obesity are causes of vascular dysfunction and are associated with an increased risk of cardiovascular disease (CVD). Notably, obesity-induced dyslipidaemia reduces plasma high-density lipoprotein cholesterol (HDL-C) concentration. HDL-C is well established as an inverse predictor of CVD risk due to its reverse cholesterol transport function, however, pharmacotherapies aimed at raising HDL-C concentration have thus far failed to reduce CVD risk. Attention has therefore turned towards understanding HDL composition and vascular functions, including anti-inflammatory, antioxidant, vasodilatory and anti-thrombotic actions. HDL composition and function is known to be compromised in obesity and T2DM, however, a thorough investigation of HDL composition and vascular function through the full insulin resistance spectrum has not yet been performed. This thesis sought to measure HDL composition and vascular function in a number of previously performed cross-sectional and longitudinal studies including otherwise healthy participants with varying degrees of insulin resistance. HDL composition was assessed using quantitative microplate assays for HDL total protein and cholesterol content and immunosorbent assays for the predominant HDL protein apolipoprotein AI (apoAI). The entire HDL proteome was measured using nano-liquid chromatography mass spectrometry. HDL size was measured using native gel electrophoresis. HDL vascular protective function was assessed by measuring its antioxidant function through paraoxonase-1 (PON-1) activity and its anti-inflammatory activity was measured by assessing the ability of HDL to reduce inflammatory cytokine-mediated adhesion molecule expression in endothelial cells.

This thesis first described the establishment of an assay of HDL anti-inflammatory function in human dermal microvascular endothelial cells (HMEC-1). Healthy control HDL dosed onto HMEC-1 at a concentration of 300 μg/mL apoAI was able to reproducibly reduce vascular cell adhesion molecule 1 (VCAM-1) expression in the face of maximally inflammatory tumour necrosis factor alpha (TNFα) by 60%, with a coefficient of variation of 14.6%. To ensure that remnant salts from the sodium bromide sequential density ultracentrifugation method for the isolation of HDL was not interfering with the cell assay, a comparison of HDL composition, size and function was performed between this technique and biologically inert iodixanol density gradient ultracentrifugation. This thesis described an altered profile of HDL composition between the two isolation techniques, with iodixanol density gradient isolated HDL fractions containing a higher protein content than sodium bromide sequential density ultracentrifugation (10.14 ± 1.49 mg/mL compared to 3.18 ± 1.10 mg/mL respectively, $p < 0.001$, mean ± SD) and a reduction in the proteomic detection of key HDL proteins such as apoAI, apolipoprotein AII and PON-1. HDL size could not be determined in the iodixanol isolated HDL fractions due to contaminating plasma proteins. Though vascular anti-inflammatory function was higher in iodixanol isolated HDL (77.5 ± 4.4 % compared to 58.3 ± 4.8%, mean ± SD, $p = 0.014$) this may have been due to the presence of confounding plasma proteins. Sodium bromide sequential density ultracentrifugation was therefore employed for the remainder of this thesis.

Previous work in this laboratory focussed on HDL composition through healthy gestation and preeclampsia. Pregnancy is characterised by early insulin sensitivity and late insulin resistance, while preeclampsia is associated with increased insulin resistance and inflammation. Despite insulin resistance, in healthy gestation maternal vascular function is improved whereas preeclampsia is characterised by vascular dysfunction. This thesis completed this study of HDL by adding measures of size and anti-inflammatory function. The proportion of large HDL increased at 16 weeks (38.6 ± 5.1 %, mean ± SD), 25 weeks (41.3 ± 5.0 %) and 35 weeks of gestation (40.4 ± 7.8 %) compared to pre-pregnancy (25.4 ± 9.6 %, $p = <0.0001$). This was unchanged in preeclampsia. Surprisingly, once corrected for HDL protein content, HDL anti-inflammatory function was decreased at 16 weeks of gestation (0.5 ± 0.3 %/μg protein, $p <0.001$), 25 weeks

of gestation (0.6 ± 0.3 %/μg, $p < 0.001$), 35 weeks of gestation (0.6 ± 0.3 %/μg, $p < 0.001$) and 13-weeks post-partum (0.8 ± 0.5 %/μg, $p = 0.015$) compared to pre-pregnancy (1.9 ± 1.1 %/μg). HDL anti-inflammatory function was not different in preeclampsia compared to healthy gestation. An assessment of HDL composition and function in pregnancies complicated by gestational diabetes mellitus (GDM) followed. HDL did not differ between healthy third trimester pregnancy and GDM pregnancy by any metric, suggesting that the effect of metabolic changes in gestation override those associated with insulin resistant complications of pregnancy.

A cross sectional comparison of healthy middle-aged men to those with impaired glucose regulation (IGR) and those who performed regular endurance exercise revealed a number of changes in HDL composition. ApoAI was highest in the endurance athletes (1.65 ± 0.62 mg/mL) and lowest in IGR men (0.63 ± 0.18 mg/mL) compared to controls (1.21 ± 0.34 mg/mL), while the acute phase reactant serum amyloid A was highest in IGR men (1.77 [1.15, 2.98] μg/mg HDL protein, median [IQR]) compared to both controls and endurance athletes (0.75 [0.37, 2.40] and 0.75 [0.30, 2.40] μg/mg HDL protein respectively, both $p = 0.042$). Endurance athletes had the highest proportion of HDL 2b, the largest of the HDL subfractions, but HDL size distribution was unchanged between healthy and IGR men. Proteomic analysis uncovered distinct changes in HDL protein composition between the three groups. HDL from IGR men was enriched in inflammation and coagulation related proteins, while endurance athlete HDL was enriched in apolipoprotein AII, apolipoprotein D and the thyroid hormone transporter transthyretin. This suggested that HDL composition reflects underlying systemic physiology. In terms of HDL function, both antioxidant and anti-inflammatory functions were impaired in IGR men but not improved in endurance athletes.

Finally, a comparison of the response to weight gain and subsequent weight loss was performed between healthy young European and South Asian men. South Asians are diagnosed with T2DM on average a decade before their European counterparts and at a lower body mass index, suggesting an ethnic difference in metabolic physiology. Weight gain and weight loss had no major impact on HDL composition or function in Europeans. Compared to Europeans, South Asian HDL

had a higher abundance of inflammatory and coagulation related proteins irrespective of weight gain, while a number of lipid handling proteins such as apolipoprotein CIII and apolipoprotein F were increased in South Asian HDL after weight gain. Both HDL antioxidant and anti-inflammatory functions were not impaired in South Asians despite the changes in HDL composition. This suggested that HDL composition reflects altered lipid handling in South Asians

Taken together, this thesis suggested that HDL composition reflects the systemic environment in which it resides through its scavenger activities, which can sometimes affect its vascular function. It appeared that though HDL function could be reduced, as was the case in IGR men and late pregnancy, improvement in insulin resistance through weight loss or endurance exercise did not improve HDL vascular protective function which suggested a ceiling of HDL function. Given the failure of HDL raising therapies, this thesis suggested that treatment of the underlying pathophysiology in obesity and its complications is likely to improve HDL function.

Table of Contents

List of Tables

List of Figures

Publications and conference participation

Publications

Beazer, J. D. and Freeman, D. J. (2022) Estradiol and HDL function in women – a partnership for life. Journal of Clinical Endocrinology and Metabolism, 107 (5), pages e2192–e2194.

Beazer, J. D. , Patanapirunhakit, P., Gill, J. M.R. , Graham, D. , Karlsson, H., Ljunggren, S., Mulder, M. and Freeman, D. J. (2020) High-density lipoprotein's vascular protective functions in metabolic and cardiovascular disease - could extracellular vesicles be at play? Clinical Science, 134(22), pp. 2977-2986.

Conference poster presentations

High-density lipoprotein protein composition differs between white Europeans and South Asians but is not related to its anti-inflammatory function, Beazer J. D., Ljunggren S., Karlsson H., McLaren J., Gill J. M. R,. Freeman D. J. at Physiology 2023, The Physiological Society Conference, July 2023, (unpublished).

Glycation of high-density lipoprotein proteins differs between age and body mass index matched healthy, risk factor and gestational diabetes mellitus pregnancies, Beazer, J. D., Patanapirunhakit, P., Mulder, M., Graham, D., Ljunggren, S., Karlsson, H. and Freeman, D. J. at the Diabetes UK Professional Conference (Virtual), April 2021. Published in 'Basic and clinical science posters: Pregnancy' (2021) Diabetic Medicine, 38(S1), p. e19_14556.

High density lipoprotein composition is unchanged in gestational diabetes mellitus pregnancies compared to healthy pregnancies, Beazer, J. D., Patanapirunhakit, P., Mulder, M., Graham, D., Ljunggren, S., Karlsson, H. and Freeman, D. J. at the 'Maternal obesity and preeclampsia: common pathways' Biochemical Society/World Obesity Federation Conference, Amsterdam, The Netherlands, November 2019 (unpublished).

Acknowledgement

I'd first like to thank Dr Dilys Freeman for all of your support, advice and encouragement. The honesty, integrity and warmth with which you lead the laboratory group and conduct your interactions with everyone you meet has been an inspiration and had a profound impact on me. I feel extremely fortunate and grateful to have had my PhD training under your supervision and to have been provided with so many fantastic opportunities. Dr Delyth Graham, thank you for your encouragement throughout, particularly during my writing up period. Professor Jason Gill, thank you for providing access to the study samples used in the bulk of this thesis. I thank the British Heart Foundation for funding this research project and am grateful to have received Alexander Fairley and Graham Wilson Travelling Scholarship awards to fund my travel to collaborator laboratories.

This project would not have been possible without a fantastic team of collaborators beyond Glasgow. A special thank you to both Dr Helen Karlsson and Dr Stefan Ljunggren and their colleagues at Linköping University, Sweden. Helen, thank you to both you and your family for making me feel so welcome in your home during my visits. I have so many fond memories of my time with you. Stefan, thank you for all of your help in the lab and with the analysis of the proteomic data. Thanks also to Dr Monique Mulder (Erasmus MC, Rotterdam) for yours and your team's advice on the HDL anti-inflammatory assay, and thanks to Dr Hiten Mistry (Kings College London) for providing the samples needed for the study of preeclampsia. Our monthly HDL collaboration meetings were a highlight of my PhD experience, and I am grateful for all of your encouragement and advice. I have learned so much from each of you.

I'd like to thank Dr Ian Davies for hosting me at Liverpool John Moores University to facilitate the comparison of HDL isolation techniques. This came during the not-so-small challenge of a pandemic, and I'm grateful for all of your assistance in making this visit happen. Thanks to Professor Bruce Griffin at the University of Surrey for kindly sharing your lipoprotein sizing technique and offering your advice on my implementation of it. Here in Glasgow, I would like to thank Professor Will Fuller and his lab group for allowing me to use their gel imaging equipment whilst our laboratory was undergoing refurbishment after the fire.

Dr Ian Salt, thank you for your help with all things endothelial cell and nitric oxide measurement and for originally teaching me many of the basic lab skills that have seen me through this PhD. Thanks to Professor Paul Welsh for your statistical advice and encouragement.

To my examiners, Professor Leanne Hodson and Professor Christian Delles, and convenor Dr Sasha Radjenovic, thank you for a thoroughly enjoyable and constructive *viva voce*. I appreciate the time you took to read and consider my thesis and your suggestions have only enhanced my work. Thanks to all of you for your warm and friendly presence throughout.

Fiona Jordan, thank you not only for your huge help in the lab as our senior research technician, but also for all of the mischief, hilarity and banter. I have lost track of the number of times we have laughed ourselves to tears, and you have been a huge support both scientific and as a friend throughout my time in Glasgow. It would not have been the same experience without you. Patamat Nitiwaranggoon, thank you for teaching me so many of the techniques used in this thesis when I first joined the lab and for making our trip to Sweden together so much fun. Thank you to my Freeman lab mates Xuan Gao, Zoë Lees, Sol Olivera and Max Ralston for making my PhD so enjoyable. I am fortunate to have had such brilliant company beside me to while away the hours in the lab. Thanks to lab aid Marie, your cheerful greeting always brightened up the early starts on HDL isolation days, and thanks also to all of my colleagues past and present in Lab 535. Erin Boland, Chloé Gulliver, Tom Wright and Emma Parsons, thank you for your friendship and for all of the good times both in and outside the lab, especially at the pub or one of our flats! Lastly, Max Hill, thank you for your continued encouragement and friendship over the years.

To my parents, Kelly and Chris, and my brother Oliver, I could not have written this ‘pamphlet’ without your immeasurable love and support. Thank you for always putting things into perspective and keeping my feet on the ground (and for teaching me to use a spoon, Mum!). Nan Christine and Grandad Dave, thank you for all of the encouragement and laughter, especially during our phone calls while I walked home after a long day in the lab.

Lastly, to my fiancée Jamie. Thank you for always being by my side, pushing me forward, and believing in me every step of the way.

Author's Declaration

I declare that this thesis is my own composition and has not been submitted elsewhere for any other degree, diploma or professional qualification at the University of Glasgow or any other institution.

The work presented in this thesis has been carried out by me except where otherwise acknowledged, and all necessary permissions have been obtained for the use of copyrighted materials and the permission explicitly stated where those materials have been reproduced.

Jack David Beazer
November 2023

Abbreviations

ABCA1	Adenosine triphosphate-binding cassette 1
ABCG1	Adenosine triphosphate-binding cassette sub-family G member 1
Akt	Protein kinase B
AMPK	Adenosine monophosphate-activated protein kinase
ANGPTL	Angiopoietin-like protein
ANOVA	Analysis of variance
AO/PI	Acridine orange / propidium iodide
Apo	Apolipoprotein
ATP	Adenosine triphosphate
BHT	Butylated hydroxytoluene
BMI	Body mass index
BSA	Bovine serum albumin
CETP	Cholesteryl ester transfer protein
CVD	Cardiovascular disease
DGU	Density gradient ultracentrifugation
dH_2O	Deionised water
DHA	Docosahexaenoic acid
DMSO	Dimethyl sulphoxide

DPBS	Dulbecco's phosphate buffered saline
DTT	Dithiothreitol
EDTA	Ethylenediaminetetraacetic acid
EL	Endothelial lipase
ELISA	Enzyme linked immunosorbent assay
eNOS	Endothelial nitric oxide synthase
EPS	Early Pregnancy Study
EV	Extracellular vesicle
FACS	Fluorescence-activated cell sorting
FBS	Fetal bovine serum
FET	Frozen embryo transfer
FMD	Flow-mediated dilation
GDM	Gestational diabetes mellitus
GlasVEGAs	Glasgow visceral & ectopic fat with weight gain in South Asians study
GLP1	Glucagon-like peptide 1
GLUT	Glucose transporter
GPIHBP1	Glycosylphosphatidylinositol-anchored high-density lipoprotein binding protein 1
GRI	Glasgow Royal Infirmary

HAEC	Human aortic endothelial cells
HDL	High-density lipoprotein
HDL-C	High-density lipoprotein cholesterol
HDL-CEC	HDL cholesterol efflux capacity
HL	Hepatic lipase
HMEC-1	Human microvascular endothelial cells
$HOMA_{IR}$	Homeostatic model assessment of insulin resistance
HRP	Horse radish peroxidase
HUVEC	Human umbilical vein endothelial cell
ICAM-1	Intercellular adhesion molecule 1
IDL	Intermediate-density lipoprotein
IGR	Impaired glucose regulation
IL-6	Interleukin-6
iNOS	Inducible nitric oxide synthase
IQR	Interquartile range
IRS	Insulin receptor substrate
LCAT	Lecithin:cholesterol acyltransferase
LDL	Low-density lipoprotein
LDL-R	Low-density lipoprotein receptor

LFQ	Label free quantitation
LH	Luteinising hormone
LIPS	Lipotoxicity in Pregnancy Study
LNF	Lane normalisation factor
LPL	Lipoprotein lipase
LRG1	Leucine-rich alpha-2-glycoprotein 1
M-FAT	Role of alternative pathways of triglyceride synthesis in determining insulin sensitivity in muscle study
mRNA	Messenger ribonucleic acid
MWCO	Molecular weight cut off
NFκB	Nuclear factor kappa B
nLC-MS/MS	Nano-liquid chromatography tandem mass spectrometry
NMR	Nuclear magnetic resonance
NO	Nitric oxide
OECD	Organisation for Economic Growth and Development
OGTT	Oral glucose tolerance test
OPLS-DA	Orthogonal projections of latent structures discriminant analysis
PCA	Principal components analysis
PLTP	Phospholipid transfer protein
PON-1	Paraoxonase 1

QQ plot	Quantile-quantile plot
qRT-PCR	Quantitative real-time polymerase chain reaction
RIPA	Radio immunoprecipitation lysis buffer
ROS	Reactive oxygen species
S1P	Sphingosine-1-phosphate
SAA	Serum amyloid A
SAT	Subcutaneous adipose tissue
SD	Standard deviation
SDS-PAGE	Sodium dodecyl sulphate polyacrylamide gel electrophoresis
SDU	Sequential density ultracentrifugation
SEC	Size exclusion chromatography
SRB1	Scavenger receptor B1
T2DM	Type 2 diabetes mellitus
TBS	Tris-buffered saline
TBS-T	Tris buffered saline plus Tween-20
$TGF\beta_2$	Transforming growth factor beta 2
TNFα	Tumour necrosis factor alpha
UC_{Iodix}	Iodixanol density gradient ultracentrifugation
UC_{NaBr}	Sodium bromide sequential density ultracentrifugation

USA	United States of America
VAT	Visceral adipose tissue
VCAM-1	Vascular cell adhesion molecule 1
VIP	Variable influence on prediction
VLDL	Very-low density lipoprotein
WAT	White adipose tissue
ZAG	Zinc-alpha-2-glycoprotein

1 Introduction

1.1 The global obesity problem

The global incidence of overweight and obesity, defined as a body mass index (BMI) of between 25 kg/m^2 and 30 kg/m^2 and over 30 kg/m^2 respectively (Bray, 1987) is an ever-growing global concern. Between 1975 and 2014, the global average incidence of obesity rose in men from 3.2% to 10.8%, and in women from 6.4% to 14.9% (Di Cesare et al., 2016). Domestically, obesity rates are well in excess of the global mean; in 2021, 25.9% of adults living in England and 31% of adults living in Scotland were obese. When including overweight adults, this figure rises to 63.8% and 67% of adults in England and Scotland (Baker, 2023). Western and westernised countries tend to have the highest incidence of obesity. Across the Organisation for Economic Co-operation and Development (OECD), 19.5% of the adult population are obese, likely due to a combination of the abundance and easy access to food and a trend towards decreased physical activity (Blüher, 2019).

1.1.1 Health consequences of obesity

The consequences of being overweight or obese on vascular and metabolic health are long established. Levy et al., (1946) described an increased risk of hypertension when overweight, while Munro, Eaton and Glen, (1949) observed that patients presenting with diabetes mellitus had higher body weight than their control counterparts. It is now widely accepted that obesity is associated with an increased risk of comorbidities affecting almost every facet of physiology, including most cancers, cardiovascular disease (CVD), type 2 diabetes mellitus (T2DM), respiratory diseases such as asthma and musculoskeletal diseases such as osteoarthritis (systematically reviewed by Guh et al., (2009)). Much of this risk is attributable to the pathophysiological adaptation to obesity. The increased risk of cancers has been linked to a pro-inflammatory and growth factor rich environment as a result of tissue damage and repair (Lumeng and Saltiel, 2011), while the increased CVD risk is related to deleterious cardiac remodelling, increased blood pressure and deposition of fatty streaks in the vasculature (Alpert, 2001). The Framingham heart study revealed that 14% of heart failure cases in women and 11% in men could be

attributed to obesity (Kenchaiah et al., 2002). Concomitant with the increasing proportion of obese adults worldwide is an increase in worldwide fasting plasma glucose concentrations. Globally between 1980 and 2008, fasting glucose rose by an average of 0.07 mmol/L in men and 0.09 mmol/L in women each decade. The rise in fasting glucose was higher than the global average in men in western countries (0.12 mmol/L per decade) and in South Asia (0.16 mmol/L per decade in men and 0.20 mmol/L per decade in women) (Danaei et al., 2011). This observed rise in fasting glucose is indicative of prevalent insulin resistance. Obesity and overweight-induced insulin resistance is one characteristic of the metabolic syndrome, and onward development of T2DM, along with the low high-density lipoprotein cholesterol (HDL-C) and increased plasma triglyceride phenotype of dyslipidaemia. Obesity induces a vicious circle of symptoms that feed into one and other; insulin resistance and dyslipidaemia are also risk factors for cardiovascular disease given their deleterious effects on the vasculature. A systematic review including 4.5 million individuals with T2DM revealed that 32% had at least one form of CVD, and 29% had atherosclerosis. The cause of death in half of the individuals in this study was CVD (Einarson et al., 2018).

Obesity places a huge burden on healthcare provision due to its many comorbidities. Cawley and Meyerhoefer (2012) estimated that the treatment of obesity-related illness accounts for 20.6% of healthcare expenditure in the United States of America (USA), while in the United Kingdom obesity could cost 2% of annual health budgets by 2030 (Claire Wang et al., 2011). The non-medical costs of obesity are also high; obesity leads to lower productivity and a higher number of sick days in the workplace (Kleinman et al., 2014) which is estimated to cost the USA $11.7 billion more in lost productivity than for normal-weight employees (Ricci and Chee, 2005). It has also been suggested that a bi-directional relationship exists between mental health conditions and obesity, where those with mood disorders are twice as likely to be obese (Avila et al., 2015).

It is clear that obesity poses huge global challenges. A better understanding of obesity pathology will help in the development of anti-obesity interventions and therapies, crucial to reducing the burden of obesity on individuals, healthcare services and wider society.

1.2 Adipose tissue biology

Obesity is characterised by the accumulation of excess white adipose tissue (WAT). The principal role of WAT is to store energy as triglycerides within adipocytes. As well as storing dietary fat directly, adipocytes also take up and metabolise glucose into triglyceride through *de novo* lipogenesis (DNL). However, this only contributes to a small proportion (~20%) of the adipose tissue triglyceride pool, with the remainder derived from dietary lipid (Strawford et al., 2004). It is thought that the products of adipocyte DNL, including citrate, acetyl-CoA, malonyl-CoA, and palmitate, may have protective effects that maintain physiological adipocyte function (Hsiao and Guertin, 2019). Apart from after a period of fasting or undernutrition, adipocyte DNL remains at a low level (Lee et al., 2013). Lipogenesis begins when pyruvate from glycolysis is used in Krebs cycle in the mitochondria. This produces citrate as a byproduct, which can then be acted upon by a sequence of enzymes including acetyl CoA-carboxylase and fatty acid synthase to produce fatty acids, which are esterified into triglyceride for storage (Song et al., 2018). In fasting conditions, adipocytes hydrolyse triglycerides into glycerol and fatty acids and release them for cellular uptake and metabolism through lipolysis. Lipolysis involves three intracellular lipases: adipose tissue triglyceride lipase, hormone-sensitive lipase and monoglyceride lipase, which sequentially hydrolyse the esters within the triglyceride molecule linking each fatty acid to the glycerol backbone. This facilitates the release of fatty acids from the adipocyte into the bloodstream. Lipolysis is regulated by the actions of insulin, adrenergic signalling and natriuretic peptides, which alter the expression and activity of hormone-sensitive lipase therefore making this enzyme rate-limiting in this process (Arner, 2005). WAT also has endocrine functions, releasing adipokines such as adiponectin which is implicated in glucose and lipid homeostasis (Yamauchi et al., 2001), and leptin which counters the appetite stimulating stomach-derived ghrelin and signals satiety.

As well as adipocytes, WAT contains a diverse array of cell types known collectively as the stromal vascular fraction. This includes endothelial, immune, and mesenchymal stem cells, as well as fibroblast-like preadipocytes (Koenen et al., 2021), which contribute to the ability of WAT to healthily expand by facilitating preadipocyte maturation to increase the number of adipocytes and

angiogenesis to perfuse the expanding tissue with sufficient blood flow. In obesity, WAT dysfunction leads to hypertrophic expansion, where existing adipocytes increase in size without an increase in adipocyte number or new vessels supplying the tissue. Adipocyte integrity is stressed by the increase in volume causing increased lipolysis and free fatty acids and glycerol to leak from the cells. This results in hypoxia and lipid overspill causing macrophages to infiltrate the tissue. This promotes a pro-inflammatory adipose tissue environment (reviewed by Sun et al., (2011)). Chronic over-nutrition with carbohydrates contributes to this phenotype by loading muscle and hepatic glycogen stores to their limit, causing adipocytes to compensate by increasing the rate of lipogenesis and expanding. This phenomenon was observed after four days of a high carbohydrate diet (Aarsland, Chinkes and Wolfe, 1997).

There are two major WAT depots: subcutaneous adipose tissue (SAT) located below the skin, and the deeper-lying visceral adipose tissue (VAT) deposited on and around the internal organs including the liver, stomach and colon. SAT accounts for the majority of WAT and is continuously remodelled based upon physiological energy demand. When the capacity of SAT to store triglyceride is overwhelmed, as in obesity, fat is increasingly stored in VAT. VAT is more responsive to hormonal signalling than SAT and as such releases a greater quantity of fatty acids and secretes a greater quantity of inflammatory cytokines (Lee et al., 2013). It is for this reason, along with the fact that VAT drains through the portal vein and therefore directly loads the liver with glycerol and fatty acids (Björntorp, 1990; Nielsen et al., 2004), that VAT and abdominal obesity are associated more strongly with cardiometabolic disease than BMI and total adiposity (Fox et al., 2007). However, given that SAT accounts for ~85% of body fat storage, and is similarly lipolytic compared to VAT, the impact of SAT dysfunction on cardiometabolic outcomes should not be underestimated (Lee and Fried, 2010). In men, deeper laying SAT correlated with hepatic steatosis and impaired plasma lipid homeostasis (Brand et al., 2021). When WAT is overwhelmed and cannot maintain lipid homeostasis, ectopic fat is deposited outside of adipose tissue and into other tissues, for example the liver (intrahepatic fat), muscle (intramyocellular fat) and heart (pericardial fat). Ectopic fat results from lipid overspill, where both SAT and VAT have reached their capacity to effectively store lipid and is pathophysiological in nature,

adding to cardiometabolic risk by affecting the metabolic function of these tissues. Though a small amount of ectopic lipid droplets can have beneficial effects on cellular metabolism, accumulating excess intracellular lipid can disrupt cell homeostasis and contribute to insulin resistance and obesity-associated disease progression, including cancer and CVD (reviewed in detail by Pressly et al., (2022)).

1.2.1 Differences in adipose tissue distribution by sex and age

There are sex differences in adiposity and adipose tissue distribution; healthy females have a lower muscle mass, higher body fat percentage and tend to store fat in SAT, while healthy males have higher muscle mass, lower body fat percentage but tend to store fat in VAT. This is predominantly mediated by differences in sex hormones, with estradiol having favourable effects on adipose tissue function in women (reviewed by Palmer and Clegg, (2015)). This profile is mirrored in obesity. Schorr et al., (2018) measured the body composition of age and BMI- matched obese men and women using a combination of dual-energy x-ray absorption, computerised tomography and proton magnetic resonance spectroscopy scans. At a similar BMI, women had a higher body fat percentage than men distributed in their lower body in SAT. Men on the other hand had a higher VAT/SAT ratio and higher intrahepatic fat. Measures of lipid and glucose homeostasis making up cardiometabolic risk factors were worse in men compared to women, however, VAT accumulation was more strongly associated with cardiometabolic risk in women than men (Schorr et al., 2018). This apparent contradiction demonstrates that SAT accumulation is metabolically healthier than VAT accumulation, and that it is only at the point where SAT reaches its storage capacity that women deposit VAT, thus contributing more strongly to their cardiometabolic risk. Ageing also has an impact on adipose tissue distribution. A study comparing healthy older (average age of 68 years) and younger (average age of 28 years) males found that the older men had twice the abdominal visceral fat and half the subcutaneous thigh fat than their younger counterparts (Schwartz et al., 1990). In women, menopause was associated with larger SAT and VAT adipocytes, 18% more VAT and a doubling of macrophage infiltration in VAT compared to premenopausal women. Age was positively associated with VAT fibrosis and cytokine production (Abildgaard et al., 2021). These age-related changes may be due to impaired preadipocyte

functions. Preadipocytes from older individuals proliferated at a slower rate than those from younger people *in vitro*, perhaps demonstrating a reduced ability for SAT to expand (Schipper et al., 2008).

1.3 Obesity and insulin resistance

The metabolic syndrome is characterised by a combination of insulin resistance and dyslipidaemia, largely as a result of obesity-associated over-nutrition and adipose tissue dysfunction. In healthy individuals a short-term increase in plasma glucose and triglycerides, for example post-prandially, induces metabolic pathways that maintain their homeostasis. Insulin is the major hormone signal that increases the uptake of glucose and reduces adipocyte fatty acid release. This pathway is impaired in obesity.

1.3.1 Insulin and its role in metabolic homeostasis

Insulin is an anabolic peptide hormone synthesised in granules by the beta cells of the islets of Langerhans within the pancreas. It is released in response to the post-prandial rise in plasma glucose concentration. Beta cells take up glucose through glucose transporter 2 (GLUT2) transporters and rapidly generate adenosine triphosphate (ATP) through glycolysis and Krebs cycle in the mitochondria. Potassium channels sensitive to ATP close, inducing membrane depolarisation and an influx of calcium ions which mediate the exocytosis of insulin containing granules (Ashcroft and Rorsman, 1990; Rorsman and Renström, 2003). Insulin secretion is biphasic, with a rapid first phase in response to rising plasma glucose occurring within 5 minutes of the post-prandial rise in plasma glucose and a second, slower rate of secretion over the course of the following hour (Komatsu et al., 2013). Other hormonal and nutrient factors influence insulin secretion. Gut-derived incretins such as glucagon-like peptide-1 (GLP1) potentiate glucose-stimulated insulin release. Short-term exposure to free fatty acids also increase insulin secretion, however, long-term exposure to fatty acids decreases insulin secretion by beta cells (Komatsu et al., 2013).

Insulin mediates glucose uptake by metabolically active tissues. Insulin-mediated glucose uptake predominantly occurs in skeletal muscle, the liver and WAT, where insulin binding to the insulin receptor induces phosphorylation of its

tyrosine kinases and recruitment of the insulin receptor substrate (IRS). Downstream second messenger signalling results in the phosphorylation of protein kinase B (Akt) which activates a number of substrates involved in metabolic signalling. A detailed review of the molecular pathways of insulin receptor signalling is provided by (Haeusler et al., 2018). The primary cellular response to insulin is the translocation of the glucose transporter GLUT4 to the cell membrane. Though it occurs through the same receptor and signalling pathways, insulin signalling in each of these tissues has different anabolic effects. The majority of glucose uptake in response to insulin occurs in skeletal muscle, where it is stored as glycogen. In the liver, insulin reduces gluconeogenesis by approximately 20% (Gastaldelli et al., 2001) and promotes the storage of glucose as glycogen. In adipose tissue, insulin stimulates lipogenesis and inhibits lipolysis, lowering plasma triglycerides and free fatty acids. Through these actions, insulin reduces both plasma glucose and plasma lipid concentrations. The endothelium is also responsive to insulin, both directly where insulin promotes capillary recruitment throughout skeletal muscle and adipose tissue to facilitate increased glucose clearance, and indirectly whereby endothelial cells transport insulin into the interstitial space (Kolka, 2020). Insulin maintains vascular smooth muscle cell quiescence and reduces their contractility, thereby maintaining perfusion of insulin sensitive tissues (Nakazawa et al., 2005).

1.3.2 Mechanisms and consequences of insulin resistance

Obesity induces insulin resistance due to excess glucose and lipid supply as a result of over-nutrition. There are two pathways responsible for insulin resistance in obesity: lipotoxicity and beta cell dysfunction. Lipotoxicity occurs where lipid overspill from dysfunctional and inflamed WAT leads to elevated plasma lipids and deposition of ectopic fat in the liver and skeletal muscle, causing local inflammation. Intracellular inflammatory signalling interferes with insulin signalling, reducing the action of insulin on these tissues, and impairing glucose uptake. In cultured 3T3-L1 mouse adipocytes, exposure to tumour necrosis factor alpha (TNFα) for 24 hours down-regulated genes encoding proteins involved in insulin signalling, including GLUT4 and IRS1, and those involved in lipogenesis and lipolysis, impairing the metabolic function of these adipocytes (Ruan et al., 2002). In the liver, loss of insulin sensitivity prevents

the inhibition of gluconeogenesis, adding to existing hyperglycaemia (Gastaldelli et al., 2001). In healthy lean subjects, hyperlipidaemia induced by administration of a triglyceride emulsion reduced muscle insulin signalling, as measured by insulin receptor, IRS and Akt phosphorylation, by approximately 60%, despite plasma lipids remaining within the physiological range experienced post-prandially after a high-fat meal (Belfort et al., 2005). In a similar cohort, a physiological increase in free fatty acids by infusion impaired skeletal muscle mitochondrial oxidation and therefore the ability of myocytes to metabolise glucose (Brehm et al., 2006). Insulin resistance in the liver results in over-production of very-low density lipoprotein (section 1.5.1.2), which further exacerbates hyperlipidaemia and induces dyslipidaemia. In response to hyperglycaemia, pancreatic beta cells increase insulin production and secretion and increase in number. However, in the face of rising peripheral resistance to insulin, plasma glucose continues to rise to a point where insulin secretion cannot keep pace with plasma glucose resulting in a state of impaired glucose regulation. Chronic hyperglycaemia and hyperlipidaemia eventually induce beta cell endoplasmic reticulum stress and apoptosis, largely due to an increase in mitochondrial generation of reactive oxygen species (reviewed by Gerber and Rutter (2016)). Over time, this reduces beta cell number and insulin secretion. Continued beta cell failure ultimately results in a dramatic reduction in insulin secretion and the onset of T2DM.

1.4 Dyslipidaemia

Dyslipidaemia results from the mishandling of lipids by adipose tissue, the liver, and plasma lipoproteins. In normal physiology, the exogenous lipoprotein pathway delivers dietary triglycerides to adipose tissue from the gut, while the endogenous pathway delivers triglyceride and cholesterol from the liver to peripheral tissues for use in metabolism (triglyceride) and as a precursor to sterol-based hormones and lipids (cholesterol). In obesity, a combination of excess dietary lipid and the impact of insulin resistance and adipose tissue deposition on lipid homeostasis leads to this system being overwhelmed. Consequently, plasma triglyceride rich lipoprotein concentration is elevated while high-density lipoprotein cholesterol concentration is reduced.

1.4.1 Plasma lipoproteins

Lipoproteins are complexes of lipids and proteins originating from the liver and intestine that carry endogenous and dietary lipids in plasma. Lipoproteins are composed of a hydrophilic phospholipid and unesterified cholesterol outer monolayer and a lipid rich, hydrophobic core containing triglyceride and cholesteryl esters (Figure 1-1). The outer monolayer is studded with proteins, including apolipoproteins, that confer lipid mobilising, cholesterol scavenging and cellular signalling functions. Lipids are liberated from lipoprotein particles through the action of lipase enzymes. Lipoproteins are cleared from circulation by the liver and kidneys. There are five major lipoprotein classes involved in the exogenous (or dietary lipid) pathway and the endogenous (or liver derived lipid) pathway. A third lipid handling pathway is reverse cholesterol transport which is mediated by high-density lipoprotein (HDL).

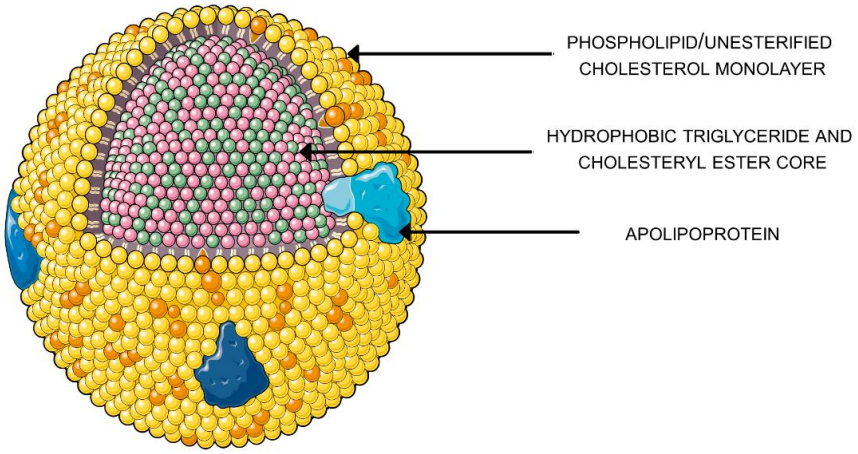

Figure 1-1 Anatomy of a lipoprotein particle Lipoproteins are made up of a core of triglycerides and cholesteryl ester, enveloped by a phospholipid and unesterified cholesterol monolayer studded with apolipoproteins.

1.4.2 Lipases

1.4.2.1 Lipoprotein lipase

Lipoprotein lipase (LPL) is expressed by adipose tissue. It is secreted bound to heparan sulphate proteoglycans, which allow LPL to be picked up by glycosylphosphatidylinositol-anchored high-density lipoprotein binding protein 1 (GPIHBP1) on the vascular endothelium where it hydrolyses triglyceride-rich

lipoprotein-derived triglycerides into fatty acids and glycerol for uptake and metabolism by tissues (Davies et al., 2010). LPL requires lipoprotein-bound apolipoprotein CII (apoCII) as a co-factor in order for its hydrolytic activity to take place, while apolipoprotein AIV (apoAIV) enhances this interaction (Goldberg et al., 1990). Apolipoprotein CIII (apoCIII) on the other hand disrupts apoCII-LPL interactions and inhibits LPL hydrolysis of plasma lipoproteins (Groot et al., 1978), while apolipoprotein E (apoE) has a lesser role in LPL inhibition perhaps by interrupting lipoprotein binding to LPL (Rensen and van Berkel, 1996). Lipoprotein composition therefore has an impact upon LPL activity. Fed or fasting states also affect LPL activity. During fasting, angiopoietin-like protein 4 (ANGPTL4) prevents LPL mediated-lipid uptake by adipose tissue to facilitate triglyceride delivery to peripheral tissues in need of energy (Cushing et al., 2017), while in fed and feeding states ANGPTL8 prevents the action of ANGPTL4 on LPL to increase adipose tissue uptake of triglycerides and decrease plasma triglycerides (Oldoni et al., 2020).

1.4.2.2 Hepatic lipase

Hepatic lipase (HL) hydrolyses lipoprotein triglycerides in the liver and plasma, particularly those in HDL and both intermediate-density lipoprotein (IDL) and low-density lipoprotein (LDL). However, unlike LPL, HL also has phospholipase activity. HL has a role in the hepatic uptake of apolipoprotein B (apoB) containing lipoproteins, their remnants and HDL, independent of its lipolytic activity (Zambon et al., 2000), for example by increasing lipoprotein affinity for scavenger-receptor B1 (SRB1) or the low-density-lipoprotein receptor (LDL-R) (Santamarina-Fojo et al., 2004). As such, HL not only has a role in determining lipoprotein size, but also plasma lipoprotein number. The combination of phospholipid and triglyceride lipolytic activity is particularly important in regulating the size of cholesterol rich lipoproteins such as LDL and HDL.

1.4.2.3 Endothelial lipase

Endothelial lipase (EL) is found on the vascular endothelium and is primarily a phospholipase with minor triglyceride lipase activity. Its function is to breakdown HDL phospholipids into lysophospholipid and fatty acids for intracellular lipid synthesis; mass spectrometric analysis of human aortic

endothelial cells (HAEC) overexpressing EL found significantly higher concentrations of intracellular lipid precursors compared to wild-type cells (Riederer et al., 2012). Like HL, EL also has a role in cellular lipoprotein uptake. EL mediated the uptake of very-low density lipoprotein (VLDL), LDL and HDL *in vitro* in Chinese hamster ovary cells, however, it preferentially internalised the apoB containing lipoproteins (70% of particles bound to EL) compared to HDL (10% of those bound to EL). EL is therefore an important player in the metabolism and size of HDL particles (Fuki et al., 2003).

1.4.3 Chylomicrons and the exogenous lipoprotein pathway

Chylomicrons are the largest and least dense of the lipoproteins, and their primary function is to deliver dietary triglyceride and cholesterol from the gut to adipose tissue and the liver (Figure 1-2). Consumed lipids are emulsified by bile and broken down by lipases in the intestine into fatty acids, which along with cholesteryl esters are taken up by enterocytes. Here, fatty acids are converted into triglycerides. Triglycerides and other dietary lipids including free cholesterol and phospholipids are delivered to the endoplasmic reticulum, where they are packaged with apolipoprotein B48 (apoB48) into chylomicrons by microsomal triglyceride transfer protein. Chylomicrons also host other intestine-derived apolipoproteins, including apoAIV and apoE, though these are not obligate chylomicron apolipoproteins and there are heterogenous populations of chylomicrons. Chylomicrons avoid first pass metabolism by the liver as unlike other dietary nutrients, chylomicrons leave the gut through the lymphatic system and enter the systemic vasculature through the subclavian vein in the thorax (Hussain, 2014). On entry to the circulation, chylomicrons gain other apolipoproteins such as apoCII and apoCIII, which regulate their hydrolysis by LPL. Chylomicron triglycerides are hydrolysed by LPL in skeletal muscle and adipose tissue which causes chylomicrons to shrink in size and become chylomicron remnants. Remnants are taken up by remnant receptors in the liver through recognition of apoE, where they are catabolised, and remaining triglyceride and cholesterol stored for later repackaging into VLDL. Other lipoproteins such as HDL can interact with chylomicron remnants, picking up remnant phospholipids and apolipoproteins (Xiao and Lewis, 2012). Chylomicrons have a density of < 1.006 g/mL (Salter and Brindley, 1988).

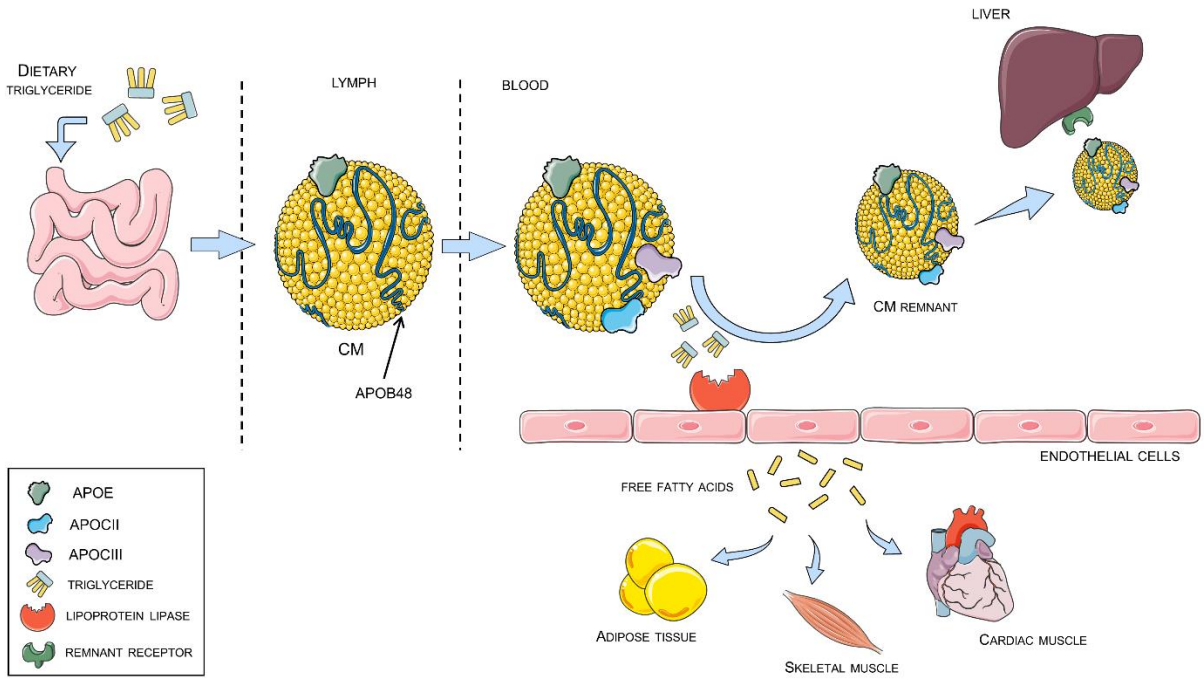

Figure 1-2 The exogenous lipoprotein pathway In response to feeding, the small intestine packages dietary triglyceride and cholesterol with apolipoprotein B48 into chylomicrons (CM), which are secreted into the lymphatic vessels. On joining the circulation, chylomicrons pick up other apolipoproteins such as apolipoproteins CII and CIII which regulate their metabolism by lipoprotein lipase on the vascular endothelium. Lipoprotein lipase hydrolyses chylomicron triglyceride into free fatty acids, which can be stored or metabolised by peripheral tissues. Triglyceride depleted chylomicron remnants are taken up by the liver via recognition of apolipoprotein E.

1.4.4 The endogenous lipoprotein pathway

The endogenous lipoprotein pathway is involved in the distribution of triglycerides to peripheral tissues for use in cell metabolism or storage in adipose tissue (Figure 1-3). The pathway begins with hepatic formation and subsequent secretion of VLDL; hepatic stores of cholesterol and triglyceride, partially derived from the uptake of chylomicron remnants, are packaged with apolipoprotein B100 (apoB100) in the endoplasmic reticulum. VLDL secretion is based upon the availability of triglyceride in the hepatocyte, as well as being inhibited by insulin in order to promote triglyceride storage from circulating chylomicrons (Huang and Lee, 2022). VLDL has a density of less than 1.006 g/mL (Salter and Brindley, 1988). Once released into the circulation, VLDL is hydrolysed by LPL which reduces its size to become IDL, with a density of between 1.006 g/mL and 1.019 g/mL (Salter and Brindley, 1988).

IDL continues to be acted upon by LPL and HL until eventually the lipoprotein becomes cholesterol-enriched LDL, with a density of between 1.019 g/mL and 1.063 g/mL. While VLDL and IDL predominantly deliver triglycerides to peripheral tissues, the primary role of LDL is to provide cells with cholesterol, and to participate indirectly in the return of cholesterol to the liver for recycling or disposal with HDL. LDL is removed from circulation by LDL-R, in both the liver and the vascular endothelium, where the whole particle is endocytosed and catabolised to free cholesterol and membrane lipids. This is particularly important as *de novo* synthesis of cholesterol is energy intensive, thus cells preferentially take up LDL via LDL-R recognition of apoE to maintain cholesterol demands and recycle existing cholesterol (Jeon and Blacklow, 2005). However, the majority of LDL uptake occurs in the liver, where excess cholesterol is packaged into bile for recycling or excretion in faeces, or into VLDL to be re-secreted.

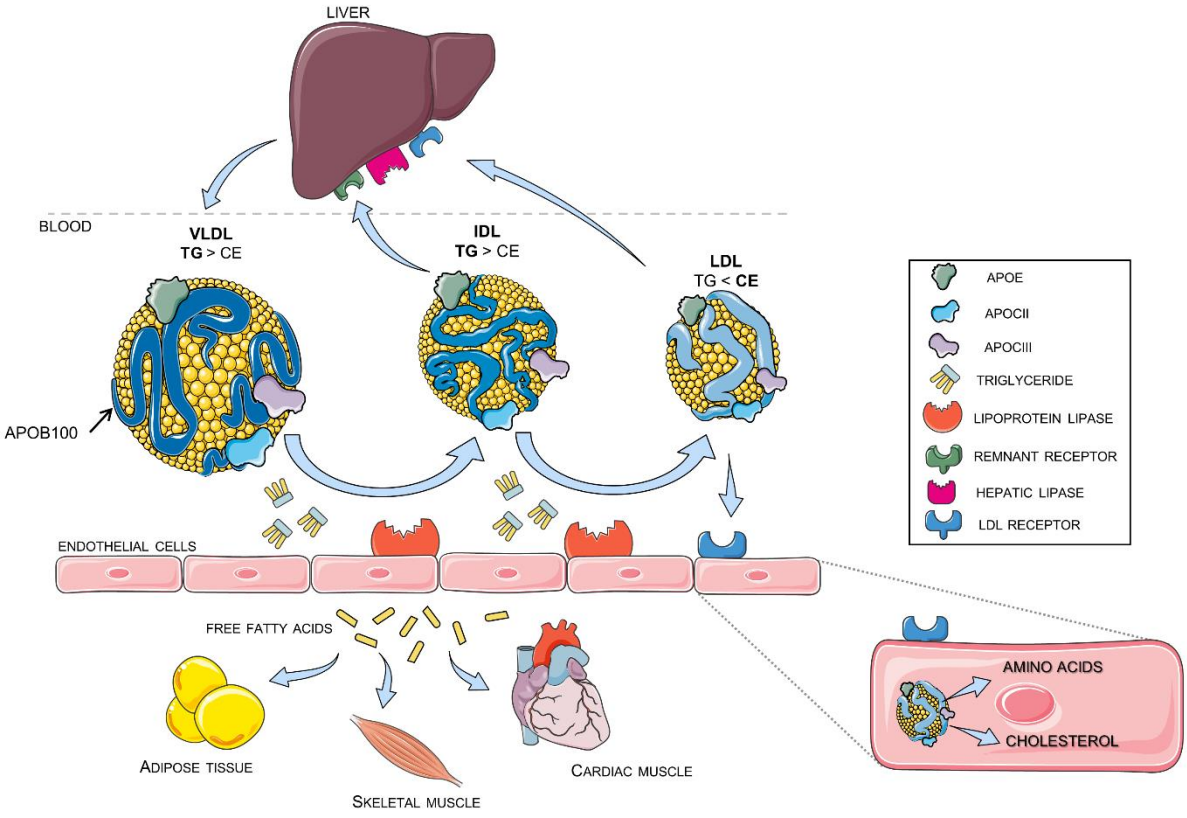

Figure 1-3 The endogenous lipoprotein pathway The liver packages stored triglycerides and cholesteryl esters with apolipoprotein B100 to form VLDL. VLDL is secreted into the circulation and delivers triglyceride to peripheral tissues. The action of lipoprotein lipase shrinks VLDL to IDL. IDL can be directly taken up by the liver through recognition of apolipoprotein E or acted upon by both hepatic lipase and lipoprotein lipase to form cholesteryl ester rich LDL. LDL is either taken up by the liver through the LDL receptor or taken up by endothelial cells where the particle is catabolised to amino acids and cholesterol for use in cellular metabolism.

1.4.5 High-density lipoprotein and reverse cholesterol transport

HDL is the smallest and most dense of the plasma lipoproteins. Unlike VLDL and chylomicrons which are synthesised as a whole particle before secretion, HDL is formed in the circulation through the actions of a number of remodelling enzymes. The liver and intestine synthesise apolipoprotein AI (apoAI), which on secretion receives phospholipids through interaction with ATP-binding cassette A1 (ABCA1) to form nascent pre-ß-HDL (Owen and Mulcahy, 2002). Phospholipid transfer protein (PLTP) also acts upon the nascent particle to provide phospholipids derived from the LPL-mediated hydrolysis of other lipoproteins (Huuskonen et al., 2001). Free cholesterol on the HDL surface is esterified by lecithin:cholesterol acyltransferase (LCAT), after which the resulting cholesteryl esters migrate to the lipophilic core of the lipoprotein. HDL acts as a reservoir for cholesteryl esters and as such interacts with all other lipoproteins to exchange triglyceride and cholesteryl esters through the actions of cholesteryl ester transfer protein (CETP). As HDL accumulates cholesteryl esters it increases in size, first to HDL 3 (with a density of between 1.125 g/mL and 1.21 g/mL) before becoming large buoyant HDL 2 (with a density of between 1.063 g/mL and 1.125 g/mL) (Salter and Brindley, 1988). HL and EL are responsible for the majority of HDL lipolysis and as such regulate HDL size (Annema and Tietge, 2011).

1.4.5.1 Reverse cholesterol transport

While all cells in the body synthesise cholesterol, only the liver has the ability to excrete and catabolise cholesterol, necessitating the retrieval of excess cholesterol from peripheral cells back to the liver. HDL is responsible for this reverse cholesterol transport and the redistribution of cholesteryl esters and triglycerides between the other lipoproteins of the endogenous pathway (Figure 1-4). HDL retrieves cholesterol via ABCA1 in the case of smaller nascent HDL particles and ATP-binding cassette sub-family G member 1 (ABCG1) in larger mature particles (Yu and Tang, 2022), as well as through SRB1, from peripheral cells including endothelial cells and macrophages. Due to its size HDL can access the interstitial spaces and therefore interact with other tissues, including skeletal muscle and adipose tissue. Scavenged free cholesterol is esterified by LCAT, which enables cholesteryl esters to migrate to the core of the lipoprotein.

HDL is constantly remodelled in the circulation, particularly by CETP. CETP exchanges triglyceride and cholesteryl esters between HDL and LDL. Due to the concentration gradient either side of CETP, the direction of travel favours moving a cholesteryl ester from HDL to LDL and triglyceride in the other direction. HDL is cleared from the circulation by the liver and kidneys; hepatic lipase hydrolyses HDL triglyceride and phospholipid leaving de-lipidated apoAI which can be filtered out by the kidneys (Rader, 2006). The liver also takes up whole HDL particles via SRB1 and re-secretes the apoAI component with a small amount of phospholipid, beginning the cycle of reverse cholesterol transport again.

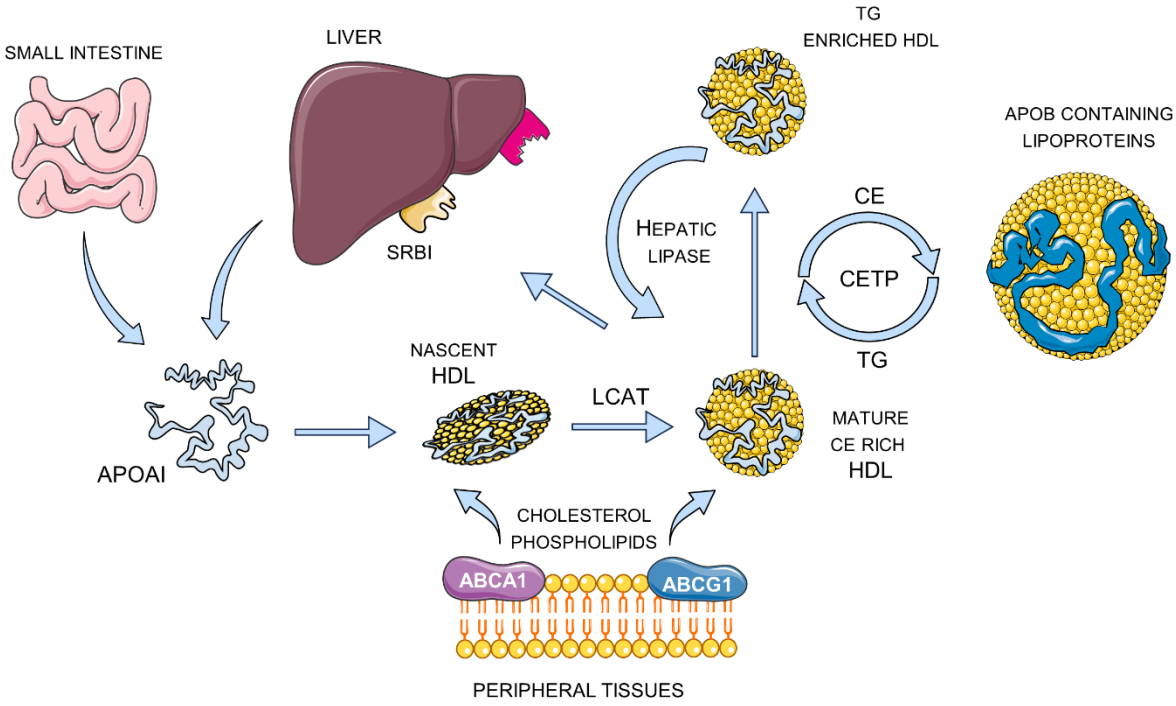

Figure 1-4 HDL metabolism and reverse cholesterol transport Apolipoprotein AI (apoAI) is secreted by the liver and small intestine, where it is loaded with cholesterol and phospholipids through binding to ATP-binding cassette A1 (ABCA1) to form nascent HDL. Lecithin:cholesterol acyltransferase (LCAT) esterifies the free cholesterol on nascent HDL to cholesteryl esters which migrate to the core of the lipoprotein, forming a mature spherical HDL particle. Mature HDL continues to accept cholesterol through ABCG1 and becomes enriched in cholesteryl esters (CE). Cholesteryl ester transfer protein (CETP) remodels mature HDL by swapping apolipoprotein B containing lipoprotein triglyceride (TG) for a HDL CE, enriching HDL in TG. Hepatic lipase hydrolyses HDL TG, making the particle smaller and CE rich. Scavenger receptor B1 (SRB1) specifically takes up HDL CE for recycling or removal in bile.

1.4.6 Mechanisms of dyslipidaemia

A combination of factors affecting all three lipoprotein pathways, the liver and adipose tissue all work in concert towards dyslipidaemia in obesity. Over-nutrition results in increased plasma triglycerides packaged into larger chylomicrons and VLDL, however, there is not sufficient potential for expansion in adipose tissue to store these triglycerides. Insulin resistance in adipose tissue exacerbates the raised plasma triglyceride concentration given disinhibited adipocyte lipolysis, adding to the already raised plasma lipid pool which ultimately is stored in the liver. Obesity and insulin resistance suppress LPL and fatty acid binding protein 4 gene expression in adipocytes, perhaps indicating their reduced secretion (Clemente-Postigo et al., 2011). Fatty acid accumulation also reduces the activity of LPL by displacing it from the vascular endothelium, further reducing lipolytic capacity (Karpe et al., 1992). The rise in hepatic triglycerides and insulin resistance leads to a reciprocal increase in VLDL secretion (Dixon and Ginsberg, 1993). Chylomicrons and VLDL compete for lipolysis by a reduced LPL pool which increases the plasma retention time of these lipoproteins. Incomplete lipolysis by LPL results in a greater number of lipoprotein remnants, which when taken up by the liver through the actions of HL further contribute to the accumulation of hepatic lipid.

Downstream of VLDL, hypertriglyceridemia alters LDL and HDL metabolism, largely due to altered CETP dynamics. In normolipidemic individuals, CETP favours delivering HDL cholesteryl esters to LDL in exchange for triglycerides. However, when plasma VLDL is increased, CETP delivers HDL cholesteryl ester to triglyceride-rich lipoproteins and LDL in exchange for their triglycerides, enriching HDL and LDL with triglyceride (Guérin et al., 2001). Triglyceride-rich LDL has increased affinity for HL and reduced affinity for LDL-R, resulting in small dense LDL with a prolonged plasma retention time (Musliner et al., 1979; Berneis and Krauss, 2002). Enrichment of HDL with triglyceride also enhances its hepatic lipolysis, reducing its size and in turn increasing its clearance from plasma. Obesity and insulin resistance therefore result in reduced HDL-C.

1.5 Vascular consequences of obesity

A major complication of obesity-associated metabolic syndrome is cardiovascular disease. Elevated plasma cholesterol and triglyceride are well established as predictors of heart disease (Kannel et al., 1971), while a meta-analysis of prospective studies undertaken between 1998 and 2004 revealed that the metabolic syndrome is attributable in 17% of CVD cases and 52% of T2DM cases (Ford, 2005), with T2DM itself having additional deleterious effects on the vasculature (Naka et al., 2012). Obesity is known to cause changes in plasma lipids and inflammatory mediators. The vascular endothelium is in contact with these altered plasma factors and therefore is implicated in the vascular consequences of obesity.

1.5.1 Physiological endothelial function

The vascular endothelium lines the interior of every vessel in the body, as well as the endocardial surface within the chambers of the heart. A collagen rich basal lamina separates the endothelium from the contractile smooth muscle cells of the intimal layer of arteries and arterioles (Pugsley and Tabrizchi, 2000). Capillaries lack a smooth muscle layer but are studded with pericytes which control perfusion through these vessels (Attrill et al., 2020). The endothelium responds to a host of physical and biochemical signals which have an impact on vascular tone, for example, the detection of shear stress due to increased blood pressure and consequent vasodilatory signalling (Rubanyi et al., 1986). Endothelial signalling is largely centred around the generation of vasodilatory nitric oxide (NO) by endothelial nitric oxide synthase (eNOS), which has pleiotropic effects on the endothelium and surrounding tissues. As well as inducing vascular smooth muscle relaxation, NO has anti-inflammatory actions such as reducing leukocyte adhesion to the vessel wall through inhibition of intercellular adhesion molecule 1 (ICAM-1) and vascular cell adhesion molecule 1 (VCAM-1) (Carreau et al., 2011). Anti-thrombotic actions of endothelial NO include the reduction of platelet aggregation, a crucial step in clot formation (Riddell and Owen, 1997). Angiogenesis is mediated by the vascular endothelium; vascular endothelial growth factor is a potent activator of eNOS NO production (Kou et al., 2002) and also sensitises other NO signalling pathways, such as by upregulating the expression of eNOS stimulating

sphingosine-1-phosphate (S1P) receptors (Igarashi et al., 2003). Insulin is a potent activator of endothelial NO synthesis, which facilitates adequate blood flow through metabolically active tissues such as skeletal muscle (Steinberg et al., 1994), however, glucose uptake in the endothelium is largely insulin-independent through constitutively expressed GLUT-1 transporters (Ebeling et al., 1998). The endothelium is also crucial to transporting macromolecules from blood through to target tissues, for example fatty acid transport to adipocytes or glucose transport into skeletal muscle (Faulkner, 2021), and as such expresses lipolytic and glucose transport proteins. In normal physiology, endothelial cells are quiescent, and their turnover is slow (Ricard et al., 2021). However, in the face of an inflammatory or unfavourable metabolic environment, endothelial cells become activated and switch their phenotype and behaviour to a dysfunctional state.

1.5.2 Endothelial dysfunction

Endothelial dysfunction induces a number of phenotypical changes, particularly with regard to nitric oxide generation and inflammatory signalling. The uncoupling of eNOS prevents NO generation in favour of reactive oxygen species (ROS). This has inflammatory consequences and leads to protein oxidation and lipid peroxidation. This impairs the ability of the endothelium to produce vasoprotective NO, ultimately leading to vasoconstriction and higher blood pressure. This cycle continues as the shear stress induced by hypertension further activates the vascular endothelium. Loss of NO impairs the anti-inflammatory, anti-thrombotic and angiogenic functions of the vascular endothelium (Cyr et al., 2020). Inflammatory signalling from cytokines including TNFα and interleukin-6 (IL-6) induces nuclear factor kappa B (NFκB) signalling (Mercurio and Manning, 1999), which leads to the production and membrane trafficking of ICAM-1 and VCAM-1 (Sawa et al., 2007) and recruitment of circulating leukocytes. Obesity and its metabolic derangements induce endothelial dysfunction. Increased plasma fatty acid and glucose concentrations impair endothelial NO generation through activation of the inflammatory NFκB pathway (Inoguchi et al., 2000; Kim et al., 2005), while overweight and obese individuals exhibit increased endothelial oxidative stress and upregulate expression of NFκB and the vasoconstrictor endothelin-1 (Silver et al., 2007).

Metabolic syndrome independently predicted endothelial dysfunction measured by flow-mediated dilation of the brachial artery (Melikian et al., 2008).

1.5.3 Atherosclerosis

Endothelial dysfunction in the macrovasculature coupled with dyslipidaemia leads to atheroma formation and vessel narrowing. Atherosclerotic plaques are unstable and can rupture, releasing a thrombus which can block vessels in the heart and brain and cause myocardial infarction and stroke. Atheroma formation begins with vascular inflammation. This results in a more porous endothelium, the production of reactive oxygen species and the recruitment of circulating monocytes. Endothelial porosity allows small, dense LDL and triglyceride-rich remnants to access the interstitial spaces, where they are oxidised by ROS. As well as enhancing endothelial recruitment of monocytes, oxidised lipoproteins are phagocytosed by tissue macrophages and presented by dendritic cells to antibody producing B cells which further adds to the inflammatory environment. Fat-laden macrophages change in phenotype to foam cells, which contribute to fatty lesions in the artery wall. Over time, an atheroma forms, loaded with lipid and a necrotic core of apoptotic foam cells (reviewed by Charla et al (2020)). The inflammatory environment associated with atheroma formation can lead to calcification of the plaque. Passive calcification occurs where calcium arising from apoptotic cells within the plaque is deposited in the remodelled extracellular matrix. Active calcification occurs where pro-inflammatory cytokines induce an osteoblast or osteoclast like phenotype in vascular smooth muscle cells, which leads to secretion of calcium and mineralising proteins such as bone-morphogenetic protein 2 (reviewed by Passos et al (2020) and Doherty et al (2003)). As the atheroma grows, it can protrude through the endothelium, initiating vascular smooth muscle cell recruitment. Smooth muscle cells secrete extracellular matrix factors such as collagen and elastin, resulting in the formation of a fibrous cap. The narrowing of the blood vessel and increased shear stresses on the endothelial surface can lead to rupture of the plaque and consequent thrombus generation. Should the thrombus detach it may lodge in a vessel and prevent blood flow which in the heart can lead to myocardial infarction, and in the brain to an ischaemic stroke (reviewed by Charla et al (2020)). Calcification of the atheroma contributes to plaque stability and could

be used as a marker to predict the risk of atherosclerosis-induced ischaemic events (Wahlgren et al., 2009).

1.6 Factors affecting insulin resistance

1.6.1 Ageing

Ageing is associated with changes in body composition, metabolic physiology and physical activity which together ultimately accrue to elevate insulin resistance in the older population. Ageing induces the loss of skeletal muscle mass; a study comparing otherwise healthy men in their twenties to older men between 60 years old and 75 years old found the older group had 4.3 kg less lean body mass comparted to the younger cohort (Frost et al., 2015). The Baltimore Study of Ageing found that over the seven-year follow-up period, men in the highest quartile of total body lean mass had the lowest risk of developing T2DM (Kalyani et al., 2020). This association was not observed in the female participants in this study, perhaps due to differences in body fat distribution with ageing in men and women (discussed in section 1.2.1). Skeletal muscle is a primary site of glucose uptake and utilisation, and the loss of muscle therefore reduces the volume of tissue available for glucose disposal. Inflammation impairs insulin signalling and ageing is associated with reduced innate and adaptive immune system function (reviewed by Boraschi et al., 2010)). The increase in inflammatory VAT with ageing likely contributes to this inflammatory phenotype. Ageing also induces ectopic fat deposition, further contributing to the insulin resistant phenotype (Guglielmi et al., 2014). Ageing does not reduce beta cell mass but does reduce pancreatic beta cell turnover, which limits the ability of beta cells to regenerate and respond to the post-prandial rises in glucose (Reers et al., 2009), while mitochondrial oxidative and phosphorylation function was 40% lower in older adult skeletal muscle due to ectopic intramyocellular fat deposits (Petersen et al., 2003). Mitochondrial function is key to beta cell insulin secretion and may therefore also play a role in altered beta cell function in aging adults (reviewed in depth by Tudurí et al (2022)). Finally, ageing alters the blood lipid profile to a dyslipidaemia-like state, with an increase in LDL cholesterol and decrease in HDL-C, attributed to reduced clearance of apoB containing lipoproteins from the circulation (Morgan et al., 2016).

1.6.2 Exercise

Exercise is well established as improving insulin sensitivity as a result of the increased metabolic demand of skeletal muscle. A meta-analysis of exercise interventions in otherwise healthy adults across 78 studies found that exercise improves insulin sensitivity (mean effect size 0.38) with a concomitant reduction in fasting plasma insulin concentration (Conn et al., 2014). Exercise has both acute and chronic effects on glycaemic control. Insulin secretion during an oral glucose tolerance test (OGTT) the day after exercise was reduced by 40% compared to baseline in untrained individuals. Exercise trained individuals had lower insulin secretion in response to an oral glucose load at baseline and there was no change in their insulin secretion profile following acute exercise, suggesting a long-term adaptation (Young et al., 1989). Exercise increases GLUT-4 in skeletal muscle through insulin-dependent and independent pathways (such as adenosine monophosphate-activated protein kinase (AMPK) activation), an effect which leads to the reduced insulin secretion post-exercise (reviewed by Bird and Hawley (2017)). Outside of skeletal muscle, exercise training improves adipose tissue insulin sensitivity (Engin et al., 2022) and is also linked to improvements in the lipid profile through increased HDL-C and reduced triglyceride and apoB containing lipoproteins (Kelley and K. S. Kelley, 2006; Stanton et al., 2022a). A meta-analysis of 160 trials investigating the impact of exercise on cardiometabolic risk factors found that those with T2DM or the metabolic syndrome had increased benefit of exercise training, particularly on fasting total cholesterol, LDL cholesterol and fasting insulin concentrations (Lin et al., 2015).

1.6.3 Weight gain and weight loss

Though the effect of obesity on insulin resistance is well characterised, weight gain that remains within the normal healthy body weight range also leads to insulin resistance. In young healthy men with a mean BMI of 21.8 kg/m^2, a 2 kg/m^2 increase in BMI accumulated over 4 months resulted in a 20% increase in insulin secretion, a 50% reduction in insulin clearance and a doubled homeostatic model assessment of insulin resistance ($HOMA_{IR}$) score, with a halving of glucose disposal per picomole/L increase in insulin concentration as measured by euglycaemic clamp (Erdmann et al., 2008). A study understanding the impact of

weight gain from early adulthood (20 years old) to middle age (approximately 50 years old) found that those individuals who increased their weight by 10-19% over the preceding 30 years were three times more likely to have an insulin resistance related syndrome, with this risk increasing to almost five times more likely with weight gain of between 20-29% weight gain (Everson et al., 1998). There are few studies into the underlying molecular pathways responsible for insulin resistance with weight gain. A four-week high-calorie diet in lean individuals, inducing 10% weight gain but remaining within the healthy BMI category resulted in a 40% reduction in insulin receptors on adipocytes isolated from the participants, with a concomitant reduction in IRS-1 tyrosine phosphorylation in response to insulin (Danielsson et al., 2009).

In contrast, weight loss ameliorates insulin resistance. This is the case even where weight loss is moderate, and BMI remains in the overweight category. In a cohort of patients with T2DM, a reduction in BMI from 30.1 kg/m^2 to 27.5 kg/m^2 by consumption of a low-calorie diet returned fasting plasma glucose to control concentrations and enabled complete insulin-mediated suppression of hepatic glucose production during a hyperinsulinemic-euglycemic clamp protocol. Most notably, intrahepatic lipid was decreased by 81% after weight loss, suggesting that improved hepatic insulin sensitivity was responsible for the improvement in glycaemic control (Petersen et al., 2005). In healthy obese individuals, a 6-week low calorie diet resulting in a decrease in BMI from 33.7 kg/m^2 to 29.9 kg/m^2 decreased hepatic triglycerides by 60% and hepatic uptake of free fatty acids by 26% compared to baseline measures, with a 40% reduction in hepatic insulin resistance and improvement in skeletal muscle glucose uptake (Viljanen et al., 2009). In patients with T2DM but not requiring insulin, a medically supervised low calorie diet replacement program for three to five months followed by tailored weight management support resulted in 46% of the intervention cohort participants entering remission from T2DM with a mean weight loss of 10 kg (Lean et al., 2018).

1.6.4 Pregnancy

Healthy pregnancy induces changes in maternal metabolic physiology in order to meet the nutritional needs of the developing and growing fetus. The 40 weeks of gestation are split into the first (0-13 weeks of gestation), second (14-26 weeks of gestation) and third (27-40 weeks of gestation) trimesters. During the first trimester there is implantation of the blastocyte in the uterine wall and formation of the maternal-fetal circulation through the placenta, while in the second and third trimester maternal physiology is altered to support fetal growth, particularly in terms of glucose and lipid handling. Healthy pregnancy is associated with decreased fasting plasma glucose and increased hepatic gluconeogenesis. However, maternal insulin sensitivity steadily decreases through gestation while insulin secretion increases, with a 10% reduction in insulin sensitivity in early pregnancy through to a reduction of up to 78% in late pregnancy, a similar level to that of people with T2DM. This adaptation facilitates sufficient glucose uptake by the fetal-placental unit to provide for the growing fetus. Insulin resistance in pregnancy is driven by placental hormone secretion and inflammation; the fetus elicits an immune response, and as discussed in section 1.3.2 inflammatory signalling interferes with insulin signalling (reviewed by Lain and Catalano, (2007)). Insulin resistance in later pregnancy prevents inhibition of adipocyte lipolysis, increasing the fatty acids available to the fetus (Trivett et al., 2021).

Lipid metabolism through the lipoprotein cascade is also altered in pregnancy. Plasma triglyceride and cholesterol concentration increase markedly through gestation, with triglyceride increasing approximately three-fold and cholesterol two-fold between 10 and 35 weeks of gestation (Sattar et al., 1997). Plasma VLDL concentration increased concomitantly with triglycerides (Sattar et al., 1997), perhaps due to the lack of a compensatory increase in LPL activity in gestation (Kinnunen et al., 1980). An increase in IDL and 70% increase in LDL concentration was linked to an estradiol mediated reduction in hepatic lipase activity in pregnancy, with a trend towards small dense LDL observed in the majority of the study participants (Sattar et al., 1997). There is a transient 42% increase in HDL-C at the establishment of the feto-placental circulation in the first trimester, however this rapidly returns to a gestational baseline 7% higher than pre-pregnant HDL-C (Sulaiman et al., 2016).

Despite an insulin resistant and dyslipidaemia phenotype similar to that observed in the metabolic syndrome, multiple studies have observed improved maternal vascular function through gestation (Dørup et al., 1999; Saarelainen et al., 2006; Stewart et al., 2007). Through measurement of serum nitrite concentrations due to the very short (seconds long) half-life of NO (Csonka et al., 2015), it has been inferred that serum NO increases throughout healthy diet-controlled pregnancy (Choi et al., 2002), perhaps preserving endothelial function. As the placenta is not innervated, NO is an important mediator of placental blood flow, adding to the serum NO pool (reviewed by Lyall and Greer, (1996)). Estradiol concentrations increase through pregnancy, and it is well established that estradiol is vasoprotective, illustrated most clearly by increased cardiovascular risk observed in women coinciding with the precipitous reduction in estradiol post-menopause (El Khoudary et al., 2020). Estradiol has endothelial dependent and independent effects on the vasculature and is a likely contributor to the improved vascular function observed in healthy pregnancy (reviewed by White, (2002)).

1.6.4.1 Pregnancies complicated by obesity

Obesity-associated pathological metabolism has consequences on gestation and the future outcomes for the mother and infant, largely related to pre-existing insulin resistance and inflammation. Though pregnancy is a physiological state of insulin resistance due to the action of pregnancy hormones, obese mothers exhibit exaggerated hypertriglyceridemia and higher plasma VLDL concentration, raised insulin secretion, higher circulating inflammatory mediators and poorer endothelial function than their lean counterparts. HDL-C was also lower in obese mothers, representing a phenotype similar to the dyslipidaemia and insulin resistance observed in the metabolic syndrome in non-pregnant individuals (Ramsay et al., 2002). Lipotoxicity arising from dysfunctional adipose tissue in pregnancy has also been hypothesised to contribute to obesity-related gestational complications (Jarvie et al., 2010). A recent meta-analysis including over 20 million pregnancies across the world found that maternal obesity is associated with an increased risk of a number of maternal and fetal complications, including pre-eclampsia and gestational diabetes mellitus (GDM) (Vats et al., 2021).

1.6.4.2 Preeclampsia

Preeclampsia is severe and sudden onset hypertension in pregnancy, diagnosed by gestational hypertension (blood pressure >140/90 mmHg measured at two separate time points >4 hours apart) occurring after 20 weeks of gestation in a previously normotensive woman and new proteinuria (protein:creatine ratio of >30 or urine protein at a concentration greater than 3 g/L in two random midstream urine samples collected >4 hours apart) without evidence of urinary tract infection (Brown et al., 2001a). It affects approximately 5% of pregnancies worldwide and is a leading cause of maternal death, stroke, and vascular complications (Wójtowicz et al., 2019). It occurs in two forms: early-onset preeclampsia which occurs before 34 weeks of gestation and late-onset preeclampsia which occurs after 34 weeks of gestation, with the early-onset manifestation associated with a more severe disease phenotype and worse maternal and fetal outcomes (Tranquilli et al., 2013; Wójtowicz et al., 2019). Treatment for preeclampsia is placental delivery, hence preeclampsia often leads to emergency premature parturition. A systematic review and meta-analysis of cardiovascular outcomes following preeclampsia, including over 258,000 women who had a preeclampsia pregnancy, calculated a four-fold increased risk of heart failure and two-fold increased risk of other cardiovascular diseases in the 10 years following delivery, independent of age, BMI and traditional risk factors (Wu et al., 2017). Preeclampsia is caused by pathological placentation including improper remodelling of the uterine spiral arteries, primarily as a result of inflammation (Cornelius, 2018). Obesity is therefore a major risk factor for preeclampsia given the inflammatory and metabolic derangements it causes. Insulin resistance in SAT from preeclampsia pregnancies contributes to an increase in the plasma fatty acid pool (Huda et al., 2014), perhaps leading to ectopic and visceral fat accumulation, including in the placenta (Brown et al., 2016). Compared to healthy pregnancy, VAT inflammation and inflammatory mediator secretion is higher which may be a contributor to preeclampsia pathogenesis (Huda et al., 2017). Dyslipidaemia has also been linked to preeclampsia development. The characteristic elevated triglycerides and reduced HDL-C have been associated with the incidence of complicated pregnancy, including preeclampsia and gestational diabetes mellitus (Sattar et al., 1996; Baumfeld et al., 2015).

1.6.4.3 Gestational diabetes mellitus

Obesity is the most significant risk factor for gestational diabetes mellitus (GDM) (McIntyre et al., 2019). GDM occurs in the third trimester of pregnancy and is associated with an impaired adaptation to late pregnancy and increases in insulin resistance. It is phenotypically akin to T2DM, where the pancreas cannot provide sufficient insulin against a background of insulin resistance typically caused by obesity. Impairment of beta cell insulin secretion is maintained 12 weeks after delivery, despite a return to normal glucose homeostasis (Kautzky-Willer et al., 1997). Elevated maternal plasma glucose creates a concentration gradient across the placenta, resulting in higher fetal glucose uptake, lipogenesis and ultimately fetal macrosomia (Desoye and Nolan, 2016). GDM is also a risk factor for preeclampsia (Casey et al., 1997). The most notable long-term consequence of GDM is a seven-fold increase in the likelihood of future T2DM in mothers (Bellamy et al., 2009) and their adult offspring (Clausen et al., 2008). Treatment for GDM mirrors that of T2DM and involves lifestyle modifications, such as improved diet and increased physical activity, or by insulin supplementation where diet and exercise are not sufficient to improved glucose homeostasis. The American Diabetes Association estimate that between 70% and 85% of GDM pregnancies can be managed by lifestyle intervention (American Diabetes Association, 2017). Lifestyle interventions resulted in a four-fold reduction in the incidence of perinatal complications in a case-control study of 1000 GDM pregnancies (Crowther et al., 2005).

1.6.5 South Asians

Recently, there has been a notable acceleration in the incidence of obesity in parts of the world where undernutrition was typically a greater concern, such as in South Asia which includes India, Pakistan, Bangladesh and Sri Lanka (Abarca-Gómez et al., 2017). In India for example, the proportion of obese adults increased by 6.4 percentage points in men and 5.1 percentage points in women between 2015 and 2021, with overweight or obese men and women now accounting for 44% and 41.2% of India's population respectively (Verma et al., 2023). There are ethnic differences in WAT distribution. A meta-analysis of 11 studies comparing South Asians to White Europeans found that at a lower BMI, South Asians have higher SAT and ectopic liver fat but no difference in VAT,

perhaps demonstrating an impaired ability of South Asians to expand their VAT (Iliodromiti et al., 2023). South Asians living in the UK develop T2DM 11 years sooner than their white European counterparts (Mukhopadhyay et al., 2006), while the prevalence of T2DM equivalent to that of white Europeans at a BMI of 30 kg/m^2 was at a BMI of 21.6 kg/m^2 in South Asians (Ntuk et al., 2014). The risk of all-cause mortality is significantly higher in South Asians with T2DM compared to white Europeans (Muilwijk et al., 2019), while hyperglycaemia is more detrimental to left ventricular function in South Asians compared to white Europeans (Park et al., 2014). Understanding the underlying obesity-associated pathophysiology in South Asians compared to white Europeans is important given the increasing South Asian populations in western countries.

1.7 High-density lipoprotein and vascular protection

HDL-C was first established as an inverse predictor of CVD risk during the Framingham heart study in the 1970s (Kannel et al., 1971; Gordon, William P Castelli, et al., 1977). HDL provides vascular protection through reverse cholesterol transport, and therefore it was considered that increasing plasma HDL-C could reduce CVD risk. As a result, a number of pharmacotherapies aimed at increasing HDL-C were trialled, including niacin in combination with statins and CETP inhibitors such as dalcetrapib and torcetrapib (Barter et al., 2007; Boden et al., 2011; Schwartz et al., 2012; Lincoff et al., 2017). Though successful at increasing HDL-C, these interventions did not modify cardiovascular risk. The CETP inhibitor torcetrapib was associated with increased CVD risk and all-cause mortality despite successfully increasing HDL-C by 72% and decreasing LDL-C by 30% (Barter et al., 2007). Due to the lack of improvement in vascular outcomes, pharmacological modulation of HDL-C was abandoned. A recent study of HDL-C and hypertension revealed a U-shaped risk profile in males, with both high and low HDL-C associated with poorer vascular outcomes (Trimarco et al., 2022). Attention has therefore turned towards HDL composition and function and their effects on vascular protection, particularly as the cholesterol efflux capacity of HDL (HDL-CEC) is now recognised as a stronger predictor of cardiovascular outcomes in a disease-free cohort than HDL-C (Rohatgi et al., 2014).

1.7.1 HDL protein composition

1.7.1.1 Apolipoproteins

The predominant apolipoprotein on HDL is apoAI, which accounts for ~70% of HDL protein content. ApoAI confers HDL with cholesterol efflux and vascular protective functions and is a key determinant of HDL structure. ApoAI forms a cage-like structure which exists in a large and small conformation, limiting the volume of the lipid core of the particle (Melchior, Street, et al., 2021). There is a subset of HDL which also contains apolipoprotein AII (apoAII), accounting for a further ~20% of the protein content of those particles (Cheung and Albers, 1984). HDL containing apoAII has a longer plasma retention time (Rader et al., 1991), and can increase the cholesterol efflux capacity of HDL via ABCA1, independent of other HDL proteins and lipids (Melchior et al., 2017). HDL containing apoAII is heterogenous in size compared to the narrowly defined large and small apoAI only HDL particles, as it disrupts the rigid apoAI cage-like structure allowing the helices to slide together and take up a broad range of sizes (Melchior, Street, et al., 2021). Apolipoprotein M (apoM) is also present on HDL. The structure of apoM forms a lipophilic binding pocket which allows HDL to carry the vasoactive lipid S1P (Christoffersen et al., 2011; Ruiz et al., 2017). Through interaction with other lipoproteins and their remnants, other apolipoproteins including apoAIV, apoCII, apoCIII, apolipoprotein D (apoD) and apoE are present on HDL, acting as co-factors and facilitators of HDL metabolism.

1.7.1.2 Paraoxonase-1

Paraoxonase-1 (PON-1) is an enzyme with lactonase and arylesterase activity that confers antioxidant functionality to HDL particles. The enzyme is synthesised in the liver and the majority of PON-1 circulates bound to HDL, perhaps due to the ability of HDL to access interstitial spaces through endothelial transcytosis and prevent oxidative damage (Mackness et al., 1997; Rohrer et al., 2006). PON-1 prevents lipid peroxidation and therefore protects against the formation of oxidised LDL and atherosclerotic plaques in artery walls. This may occur through hydrolysis of lipid peroxides into harmless metabolites, preventing their accumulation on LDL (Mackness et al., 1993). The association of PON-1 with HDL particles is predominantly due to apoAI, however, PON-1 also associates with HDL apoE, though this limits the ability of PON-1 to

prevent LDL oxidation as the enzyme is not stabilised as effectively by apoE compared to apoAI (Gaidukov et al., 2010). Treatment of mildly oxidised LDL with purified PON-1 prevented monocyte recruitment to endothelial cells *in vitro,* further contributing to anti-atherogenic PON-1 functions (Watson et al., 1995). As well as protecting LDL from oxidation, PON-1 prevents HDL lipid peroxidation and recovers cholesterol efflux capacity in oxidised HDL particles *in vitro* (Aviram et al., 1998).

1.7.1.3 HDL proteomics and minor HDL proteins

A landmark study in 2005 revealed a distinct HDL proteome, further advancing our understanding of HDL composition (Karlsson et al., 2005). Given the increasing interest in HDL composition and function, the HDL Proteome Watch was established to maintain a record of proteins identified on HDL. It is accepted as of 2022 that HDL hosts 251 proteins, based on their identification in three separate studies, involved in a wide array of functions including lipid transport, coagulation, immunity/anti-microbial functions and cell-binding (Davidson et al., 2022).

Acute-phase reactants are commonly detected as part of the HDL proteome (Davidson et al., 2022). The acute phase occurs as the initial response to infection or tissue damage and the initial reactants can be positive (or inflammatory) and negative (anti-inflammatory) in nature. A large number of acute-phase reactants are synthesised in the liver in response to inflammatory cytokine signalling and it is therefore unsurprising that many of them are found on HDL (reviewed by Ebersole and Cappelli, (2000)). The chemoattractant serum amyloid A (SAA) is particularly pertinent to HDL composition as it can displace apoAI and phospholipids, thereby remodelling the particle (Miida et al., 1999). It has therefore been proposed that SAA is deleterious to HDL function, by reducing HDL apoAI content and therefore the protective functions it confers to the particle. HDL-CEC is reduced when HDL is enriched in SAA, as is the case in sepsis patients, and remains the case 21 days after recovery (Annema et al., 2010). SAA contains proteoglycan-binding epitopes and can be transferred between lipoproteins through the actions of CETP. An increase in HDL SAA may therefore result in increased apoB-containing lipoprotein SAA, which can more readily bind to the extracellular matrix of atherosclerotic plaques (Wilson et al.,

2018). While control HDL reduces TNFα secretion by peripheral blood mononuclear cells *in vitro*, supplementation of HDL with SAA reverses this effect and enhances the secretion of TNFα, reducing the anti-inflammatory function of HDL (Mao et al., 2017). Given their opposing effects on HDL function, the ratio of PON-1 activity to SAA-1 content of HDL has been proposed as a marker of HDL functionality (Kotani et al., 2013).

Other acute-phase reactants include protease inhibitors such as alpha-1 anti-trypsin. Protease inhibitors are negative acute-phase proteins which act upon leukocyte secreted elastases which break down the extracellular matrix. It is thought that HDL acts as a delivery vehicle to enable protease inhibitor access to the interstitial spaces (Gordon and Remaley, 2017), in a similar fashion to that observed of paraoxonase-1 (Mackness et al., 1997). It is likely the case that complement factors are carried on HDL for the same reason. The complement system forms innate immunity; activation of the complement system by bacterial or viral entry into the bloodstream triggers the complement cascade. This has myriad immune functions, such as triggering the synthesis and secretion of inflammatory mediators such as cytokines and chemokines through NFκB signalling, activation of leukocyte phagocytosis by opsonising pathogens and directly penetrating the bacterial cell wall (Janeway et al., 2001; Reis et al., 2019). Complements C3 and C4 are involved in pathogen opsonisation and return to the liver for phagocytosis by liver macrophages, and their fragments are commonly found on HDL (Davidson et al., 2022).

1.7.2 HDL lipid composition

Lipids account for approximately 50% of the composition of HDL particles. HDL is enriched in phospholipids, predominantly phosphatidylcholine and sphingolipids including sphingomyelin, ceramides, and glycosphingolipids. HDL also hosts free cholesterol, which is eventually esterified by LCAT, and the resulting cholesteryl esters migrate to the core of the lipoprotein. HDL lipids may have a role in the stability and conformation of HDL and its constituent proteins, the efficacy of cholesterol transport and contribute to endothelial signalling. Phospholipids account for the largest proportion (35-50%) of HDL lipids and are delivered to nascent HDL through ABCA1 or in the circulation through the actions of CETP and PLTP. Cholesteryl esters constitute the second most abundant HDL lipid (30-40%

of HDL lipids), unsurprising given the role of HDL scavenging cholesterol from peripheral tissues (Kontush et al., 2013). Though only accounting for 5-10% of HDL lipids, sphingomyelin plays an important role in the structural integrity of HDL; modelling analysis suggests that sphingomyelin alters the conformation of apolipoproteins on the particle surface to facilitate protein-protein and protein-cell interactions (Malajczuk and Mancera, 2023). Sphingomyelin is transferred onto HDL from triglyceride-rich lipoproteins and has effects on lipid-mobilisation enzymes of the lipoprotein cascade. There is evidence that sphingomyelin may inhibit LPL-mediated hydrolysis of chylomicron and VLDL triglycerides (Schlitt et al., 2005), and HDL sphingomyelin inhibits LCAT mediated esterification of free cholesterol (Subbaiah and Liu, 1993). Sphingomyelin may also be implicated in endothelial function, as Muñoz-Vega et al., (2018) only observed HDL-mediated eNOS activation in reconstituted particles containing this lipid. Sphingomyelin-derived ceramides and S1P are also important to cellular signalling and survival (Kontush et al., 2013). The majority of circulating S1P resides on HDL bound to apoM, with the remainder bound to albumin. S1P has multiple functions on the vascular endothelium, including endothelial chemotaxis in angiogenesis and wound healing and the formation of adherens junctions between endothelial cells thus maintaining the endothelial barrier (Christoffersen et al., 2011). Importantly these functions are associated with HDL-bound S1P rather than albumin-bound S1P. Endothelial cells treated with HDL-bound S1P maintained higher barrier function as measured by trans-endothelial electrical resistance for 20 hours post-treatment as compared to only four hours for cells treated with albumin-bound S1P, related to S1P receptor stability. HDL-bound S1P increased the presence of S1P receptor 1 on the endothelial membrane two-fold compared to albumin-bound S1P and increased both total and phosphorylated eNOS protein levels as assessed by confocal immunofluorescence and western blotting respectively (Wilkerson et al., 2012).

1.7.3 HDL vascular protective functions

1.7.3.1 Regulation of vascular tone

HDL regulates vascular tone largely through stimulation of eNOS and the generation of NO. HDL and apoAI both increase the phosphorylation of eNOS in an AMPK dependent manner, and apoAI colocalises with eNOS which might suggest a protein-protein interaction (Drew et al., 2004). Stimulation of eNOS also occurs by HDL binding to SRB1 (Yuhanna et al., 2001) and delivering ceramide (Li et al., 2002). S1P interacting with its receptors (S1PR1 and S1PR3) also results in eNOS stimulation in an Akt dependent pathway (Nofer et al., 2004). HDL and apoAI not only stimulate eNOS activity, but also stabilise eNOS. In human aortic endothelial cells, HDL treatment did not increase eNOS mRNA but lengthened the half-life of eNOS from 81 minutes to 270 minutes through the activation of both extracellular signal-regulated kinase 1/2 and Akt signalling pathways (Rämet et al., 2003). Outside of eNOS stimulation, HDL-bound alpha-1-antitrypsin prevented elastase induced apoptosis of vascular smooth muscle cells, with this protective effect remaining after the removal of HDL from the cells (Ortiz-Muñoz et al., 2009).

1.7.3.2 Antioxidant function

The antioxidant functions of HDL are mainly mediated by PON-1 (section 1.7.1.2), however other HDL proteins and lipids contribute to antioxidant capacity. Inhibition of HDL PON-1 did not impair the ability of HDL to neutralise LDL lipid peroxides when incubated with oxidised LDL (Zerrad-Saadi et al., 2009), suggesting a role for the whole particle in antioxidant function. HDL stimulation of endothelial cells results in the production of NO, which inhibits ROS generation through inhibition of NADPH oxidases (Selemidis et al., 2007). HDL apoAI and apoAII are capable of reducing lipid peroxides by oxidation of their methionine residues (Garner et al., 1998), while CETP preferentially transfers oxidised cholesteryl esters from LDL to HDL (Christison et al., 1995). The composition of the lipid-rich core modulates the anti-oxidative capacity of HDL, with increased triglyceride content destabilising apoAI and perhaps impairing its antioxidative function or abundance (Sparks et al., 1995). ApoD may confer antioxidant properties to HDL particles. Sanchez and Ganfornina (2021) propose that apoD, with the aid of reductase enzymes, can undergo redox

cycling and flit between an oxidised and unoxidised state, though this mechanism requires further investigation.

1.7.3.3 Anti-inflammatory function

Much of HDL anti-inflammatory endothelial function can be attributed to eNOS activation downstream of apoAI and S1P receptor signalling, as NO inhibits the NFκB signalling pathway and prevents the expression of VCAM-1 and ICAM-1 (Kimura et al., 2006; Schmidt et al., 2006) thus inhibiting monocyte recruitment. HDL also prevents monocyte activation directly and inhibits secretion of the inflammatory cytokines TNFα and IL-6 (Gruaz et al., 2010). In both primary human monocytes and coronary artery endothelial cells, HDL prevented cytokine-induced expression of chemokine receptors by inhibiting both NFκB and peroxisome proliferator activated receptor γ (PPAR-γ) signalling pathways (Bursill et al., 2010). ApoAI can prevent neutrophil activation, though it is not clear whether it requires release from HDL to do so, perhaps by SAA-1 during the acute-phase response to inflammation (Liao et al., 2005). Dendritic cells are the antigen presenting cells of the immune system; HDL phospholipids prevent the activation of dendritic cells and the subsequent inflammatory T-helper cell activation of cytotoxic leukocyte functions by decreasing interferon-γ secretion (Perrin-Cocon et al., 2012). HDL apoAI binding to macrophage ABCA1 not only stimulates cholesterol efflux to the lipoprotein but also decreases macrophage secretion of TNFα and interleukin 6, particularly relevant in the context of macrophage infiltration in atherosclerosis (Tang et al., 2009). The induction of transforming growth factor ß$_2$ (TGF-ß$_2$) secretion by endothelial cells treated with HDL 3 (Norata et al., 2005) implicates HDL in the regulation of the active immune system, given the immunosuppressive effects of TGF-ß$_2$ on T-cell proliferation (reviewed by Morikawa et al., (2016)). HDL is the major carrier of apolipoprotein L-1, which has a key role in the innate defence against the *Trypanosoma brucei* parasite transmitted by the tsetse fly. Apolipoprotein L-1 forms anion channels in the trypanosome membrane, causing an influx of chloride ions, altered osmolarity and eventually parasite lysis (Pérez-Morga et al., 2005).

1.7.3.4 Anti-thrombotic functions

While vasodilatory and anti-inflammatory HDL functions contribute to HDL anti-thrombotic function, HDL also exerts effects on platelets and clotting factors. Nitric oxide reduces platelet adhesion (Riddell and Owen, 1997), and exposing platelets to HDL *in vitro* reduces their aggregation in an NO dependent fashion (Chen and Mehta, 1994). HDL binds platelet SRB1 and prevented adhesion molecule expression and the induction of second messenger signalling in response to thrombin (Nofer et al., 1998). Von Willebrand factor is synthesised and secreted by endothelial cells and provides a structure onto which platelets can adhere during clotting. HDL prevents von Willebrand factor from becoming hyper-adhesive though it is not clear by which mechanism, particularly as delipidated apoAI was unable to stabilise this factor (Chung et al., 2016). A study of 136 healthy individuals found that plasma HDL-C was positively correlated with fibrin clot permeability and the speed of clot lysis, implicating HDL in the regulation of clot formation and degradation (Zabczyk et al., 2013).

1.7.4 HDL anti-diabetic functions

HDL also possess insulin sensitising and beta cell protective functions. In a study of thirteen T2DM patients, reconstituted HDL increased plasma insulin and decreased plasma glucose within 4 hours. HDL increased skeletal muscle glucose uptake by 177% compared to placebo, mediated by ABCA1 activation of AMPK (Drew et al., 2009). Both apoAI and apoAII alone or as part of a reconstituted HDL particle increased insulin secretion by pancreatic beta cells though interaction with ABCA1, ABCG1 and SRB1 (Fryirs et al., 2010). Both Han et al., (2007) in C2C12 skeletal muscle cells and Tang et al., (2019) in primary human skeletal muscle cells observed an increase in glucose uptake mediated by apoAI, both by AMPK activation and through enhancement of the insulin receptor / Akt signalling pathway. In a beta-cell tumour cell line, PON-1 increased both insulin secretion and biosynthesis as well as reducing beta-cell oxidative stress, suggesting that HDL may have protective functions on beta-cells (Koren-Gluzer et al., 2011).

1.7.5 Effect of obesity on HDL composition and function

Obesity and T2DM have a number of detrimental effects on HDL composition and function. Enrichment of HDL with triglycerides after three consecutive high fat meals independently associated with endothelial function and HDL anti-oxidative function (Verwer et al., 2020). HDL PON-1 activity is lower in overweight and obese individuals (Doğan et al., 2021) and is a stronger predictor of the incidence of coronary artery disease in T2DM than HDL-C (Mahrooz et al., 2023). Obesity reduces HDL concentration, apoAI content and the proportion of large buoyant HDL 2 particles (Rashid and Genest, 2007), perhaps due to an increase in CETP mass and activity in obese individuals (Arai et al., 1994). HDL from T2DM patients had a greater SAA content and reduced antioxidant and anti-inflammatory function (measured by the ability to prevent LDL stimulated monocyte migration *in vitro*) (Morgantini et al., 2011). HDL isolated from the plasma of abdominally obese individuals was unable to counteract the inhibition of rabbit aortic ring contraction by oxidised LDL, likely due to impaired endothelial protective function (Perségol et al., 2007). Abdominal obesity impairs HDL-CEC and reduces LCAT activity, impairing the ability of HDL to return excess cholesterol to the liver for recycling or removal (Härdfeldt et al., 2022). HDL isolated from obese individuals with the metabolic syndrome had altered apolipoprotein content, with decreased apoAI and apoD and an increase in apoCII and apoCIII, perhaps explaining the reduced anti-inflammatory and antioxidant function and triglyceride enrichment of HDL in obesity (Mocciaro et al., 2022). HDL from patients with metabolic syndrome was had a reduced S1P content and reduced ability to stimulate eNOS activity in endothelial cells compared to controls, but this function of HDL was restored by supplementation of HDL with S1P. Triglyceride enrichment of healthy control HDL did not impair HDL function in this study, suggesting that triglyceride enrichment of HDL does not alter its ability to stimulate eNOS activity and may be more relevant to other HDL functions or its plasma clearance (Denimal et al., 2017).

In the same manner that exercise and weight loss improve insulin resistance (as discussed in sections 1.6.2 and 1.6.3), these interventions also have effects on HDL composition and function in obese individuals. Adherence to a traditional Mediterranean diet increased HDL size and cholesterol efflux capacity (Hernáez et al., 2017), while 4 months of aerobic exercise training in individuals with

T2DM had the same effects (Ribeiro et al., 2008). In overweight and obese men, a high fibre, low fat diet altered HDL form an inflammatory to an anti-inflammatory state, as measured by the ability of HDL to prevent monocyte migration. The same study also observed increase activity of platelet activating factor acetylhydrolase post-intervention, which catabolises platelet activating factor and therefore reflects improved anti-thrombotic activity of HDL (Roberts et al., 2006). Three months of bicycle ergometer training in individuals with metabolic syndrome improved HDL PON-1 activity and a tended towards cholesteryl ester enrichment of the smaller HDL subclasses (Casella-Filho et al., 2011), suggesting improved efflux capacity. Despite no increase in HDL cholesterol concentration, 10 weeks of walk run training in a similar cohort increased HDL PON-1 activity and improved HDL-mediated inhibition of adhesion molecule expression and monocyte recruitment in endothelial cells *in vitro*, while preventing TNFα inhibition of eNOS NO generation (Sang et al., 2015).

1.7.6 Isolation of HDL for downstream analysis

The gold standard technique for the isolation of HDL from plasma is density ultracentrifugation (Beazer et al., 2020). There are two predominant methods of density ultracentrifugation: sequential density ultracentrifugation (SDU) and density gradient ultracentrifugation (DGU). SDU includes multiple centrifugation steps, the first of which removes the lower density lipoproteins before a second step which isolates the HDL fraction. The density buffers used in SDU are typically salt based and use either sodium bromide or potassium bromide. In contrast, DGU is a single step process which separates all of the lipoprotein classes at once, due to the ability of the density solution to form a linear density gradient increasing from the top to the bottom of the ultracentrifuge tube. After centrifugation, the whole ultracentrifuge tube is fractionated, and the lipoprotein content identified by density or apolipoprotein content. The density solutions are typically biologically inert substances such as iodixanol or sucrose. Disadvantages of these techniques are the risk of damage to HDL particles due to shear forces generated by ultracentrifugation, which can strip proteins from the lipoprotein. Plasma protein aggregates of similar density to HDL can be co-isolated with the HDL containing fraction, as can small-dense LDL and extracellular vesicles (EVs) (Beazer et al., 2020). Other techniques for HDL isolation include immunoaffinity and size exclusion chromatography.

Immunoaffinity isolation typically employs antibodies directed against apoAI to capture HDL, however, other lipoproteins such as chylomicrons can also carry apoAI. This technique is a more recent innovation and requires further characterisation of the isolated fractions. Finally, size exclusion chromatography is a fast and economical technique for the isolation of HDL but only results in an enrichment of HDL, not a purified fraction. Similar molecular weight proteins and aggregates may migrate through the column at the same time and therefore contaminate the eluted HDL containing fraction (Beazer et al., 2020). A summary of the advantages and disadvantages of each technique can be found in table 1-1.

Table 1-1 Summary of the advantages and limitations of HDL isolation methods. Used with permission of Portland Press, Ltd, from Jack D. Beazer, Patamat Patanapirunhakit, Jason M.R. Gill, Delyth Graham, Helen Karlsson, Stefan Ljunggren, Monique T. Mulder, Dilys J. Freeman; High-density lipoprotein's vascular protective functions in metabolic and cardiovascular disease – could extracellular vesicles be at play?. Clin Sci (Lond) 27 November 2020; 134 (22): 2977–2986.; permission conveyed through Copyright Clearance Center, Inc.

Isolation Method	Advantages	Limitations
Density Ultracentrifugation	'Gold-standard' method for HDL isolation	Co-isolation of EVs and plasma proteins
	Enables isolation of HDL subspecies separately	Shear forces may damage/remove HDL surface-bound proteins
		Buffers used may interfere with downstream analysis, due to high salt concentration or oxidation
		Lengthy process
		Low throughput process limited by centrifuge capacity
Size Exclusion Chromatography (SEC)	Fast; only requires a single step	SEC eluate is enriched for HDL but still contains contaminants
	Economical	Co-isolation of similar molecular weight plasma proteins
Immunoaffinity	More specific than DUC and SEC	Typically uses antibodies to ApoAI which can be found on non-HDL particles
	Scalable for high-throughput applications	Newer method that requires further characterisation

1.7.6.1 Co-isolation of HDL with extracellular vesicles

EVs are spherical cell-derived particles containing protein, lipid and microRNA that facilitate cell to cell communication. The major subset of EVs are exosomes, which have a density of between 1.13 g/mL and 1.19 g/ml overlapping the density range of HDL. Exosomes are formed intracellularly and through exocytosis are released into the extracellular space, while other types of EVs such as microparticles and apoptotic bodies are formed directly from the cell membrane. All EVs have a lipid bilayer reflective of the cell from which they are derived, and as such typically contain phospholipids, sphingomyelin and ceramides (Pol et al., 2012). Given their bioactive cargo, EVs have functions protective of the vasculature that overlap with those of HDL, including endothelial repair and inhibition of adhesion molecules through delivery of microRNAs 126 and 222 (Jansen et al., 2013; Jansen et al., 2015). Shear stress in human umbilical vein endothelial cells induces the secretion of EVs containing microRNAs 143 and 145 which prevents the de-differentiation of smooth muscle cells (Hergenreider et al., 2012) while TNFα stimulated endothelial cells release EVs containing eNOS that can reduce oxidative stress (Mahmoud et al., 2017). Insulin resistance and high glucose concentrations can alter EV cargo and function. The incubation of endothelial cells with microparticles derived from metabolic syndrome patients inhibited the activity of eNOS irrespective of their cytokine content (Agouni et al., 2008), while endothelial cells cultured in high glucose conditions increased EV secretion three-fold and had higher procoagulant and ROS stimulating activity (Burger et al., 2017). Though EVs likely only make up approximately 1% of the particles in a given HDL fraction isolated by density ultracentrifugation, their larger diameter means they account for approximately 10% of the overall volume (Yuana et al., 2014) and therefore may potentially confound downstream analyses of HDL composition and function. A more detailed review of the overlap between HDL and EVs can be found in Beazer et al (2020).

1.7.7 The use of animal models in HDL research

Though animal models have been frequently used to elucidate the consequences of altered HDL composition, HDL remodelling proteins and subsequent function, there are a number of limitations to consider. In rodents, HDL carries the majority of plasma cholesterol but in humans this role is fulfilled by LDL, suggesting a different function for the lipoprotein. Rodents also lack endogenous CETP, meaning models of HDL remodelling employ genetically modified animals expressing the human protein which does not reflect native physiology. Wild-type rabbits do have endogenous CETP, however they lack apoAII which accounts for a large proportion of human HDL particles. As such, this thesis limits reference to animal studies of HDL composition and function.

1.8 Research questions

The failure of HDL-C raising pharmacotherapies has moved attention towards HDL function. HDL composition is highly heterogenous and likely contributes to HDL functionality, however in-depth analyses of both HDL composition and function together are limited. Though HDL function has been assessed in obesity and T2DM, there has not been a detailed assessment of those HDL metrics throughout the insulin resistance spectrum and in those factors that modulate insulin resistance in otherwise healthy individuals, such as exercise and weight gain or weight loss. How is HDL composition and function altered when insulin resistance is changed physiologically (as in pregnancy) or by weight gain? Does HDL composition and function improve in healthy individuals with exercise? Does the increased risk of T2DM in South Asians have consequences on young and healthy South Asian HDL?

1.9 Hypothesis

I hypothesise that HDL composition influences HDL function with respect to HDL's ability to enhance vascular function and that HDL composition can be altered positively in insulin sensitive conditions and negatively in insulin resistant conditions, thereby improving or impairing its function.

1.10 Objectives

- Establish an *in vitro* endothelial cell assay to measure HDL anti-inflammatory function (Chapter 3).

- Compare HDL isolated from plasma by two different density ultracentrifugation techniques for downstream composition and functional analysis (Chapter 4).

- Measure HDL size and function in healthy pregnancy and preeclampsia, completing a previous study of HDL composition performed in these conditions performed by Patanapirunhakit (2023) (Chapter 5).

- Perform analysis of HDL composition, size and vascular functions in pregnancies complicated by GDM (Chapter 6).

- Compare HDL composition and vascular function in a cross section of men encompassing the full spectrum of insulin resistance, including men with impaired glucose regulation, healthy men and endurance athletes (Chapter 7).

- Test whether HDL composition and function is changed under conditions where insulin resistance is worsened by weight gain in otherwise young and healthy European and South Asian men (Chapter 8).

2 General Methods

2.1 Participant recruitment

Samples used for this study of HDL composition and function were derived from the archival collections of previously performed studies at the University of Glasgow or collaborator institutions. All studies were performed in line with relevant institutional ethical approvals and participants were recruited with informed consent. Full details of each study are given in the appropriate chapters.

2.1.1 Blood sampling

The site of sampling was the antecubital fossa. Venepuncture and cannulation of the median cubital vein was performed by a clinical member of the research team trained in phlebotomy. Blood samples (20-40 mL) were collected in tubes containing ethylenediaminetetraacetic acid (EDTA) or lithium heparin as an anticoagulant. Plasma was separated from whole blood through centrifugation at 1500 x *g* for 15 minutes, 4˚C and stored in aliquots at -80ºC until use.

As the plasma samples used throughout this thesis were from archival collections and therefore had been stored for different durations, the effect of storage time on downstream sample measurements must be considered given there is evidence that storage at -80ºC of greater than five to seven years alters the plasma amino acid and lipid metabolome (Haid et al., 2018; Wagner-Golbs et al., 2019). However, analysis of lipid markers including HDL-C in the same sample for 13 years demonstrated long-term stability (Muzakova et al., 2020). In order to minimise any potential confounding effects duration of storage may have had on experimental inferences, analysis was restricted to being within the bounds of the original studies to ensure that all samples under investigation within each chapter had been stored for the same amount of time.

2.2 Isolation of high-density lipoprotein from plasma

2.2.1 Buffers and solutions

Sodium Bromide (NaBr) density solutions

1.006 g/mL	11.4 g NaCl, 0.1 g EDTA, and 1 mL 1M NaOH made up to 1000 mL with dH_2O
1.182 g/mL	29.98 g NaBr, 100 mL 1.006 g/mL solution
1.063 g/mL	2 parts 1.006 g/mL, 1 part 1.182 g/mL
1.478 g/mL	78.32 g NaBr, 100 mL 1.006 g/mL
1.210 g/mL	2 parts 1.063 g/mL, 1 part 1.478 g/mL

All solutions were checked before use with a density meter (DMA35 V3, Anton Paar, St Albans, Hertfordshire, UK) and adjusted if necessary using further NaBr or the 1.006 g/mL solution.

2.2.2 Sequential density ultracentrifugation

This two-step process sequentially isolates HDL from plasma, resulting in three fractions: VLDL/LDL, lipoprotein depleted plasma, and HDL. Density ultracentrifugation is considered the gold standard technique for isolation of lipoproteins as it results in the cleanest fractions, however there are concerns as to whether isolated HDL particles can be damaged due to the shear forces involved (discussed by Ronsein and Vaisar (2019)). Here the density solutions were made with sodium bromide (NaBr). VLDL and LDL were first removed from plasma by flotation at a density of 1.063 g/mL. Participant plasma (500 µL) was loaded into thick-walled polycarbonate centrifuge tubes (11x34 mm, 1 mL, Beckman Coulter, Brea, California, USA, #343778) and combined with 250 µL of 1.182 g/mL NaBr solution by pipetting multiple times, avoiding bubbles. Where aliquots contained less than 500 µL of participant plasma, Dulbecco's phosphate buffered saline (DPBS, without calcium or magnesium, Thermofisher Scientific #14190-094) was used to make up the difference. Density solution (250 µL 1.063 g/mL NaBr) was layered gently on top of the solution in the tube. The samples were then centrifuged in a Beckman Coulter TLA 120.2 rotor and Optima MAX-TL centrifuge at 100,000 RPM (355,040 x *g* average) for 2.5 hours at 23°C. After this time, the top 500 µL (containing VLDL/LDL) was carefully removed and added to

a clean microcentrifuge tube with a glass pipette. Next HDL was isolated at a density of 1.21 g/mL. The remaining infranatant from the previous ultracentrifugation was combined with 250 µL of 1.478 g/mL NaBr solution, again by pipetting multiple times, before the gentle over layering of 250 µL 1.21 g/mL solution. The density solution combined samples were centrifuged at 100,000 RPM (355,040 x g average) for 5 hours at 23˚C, in the same tube. The resulting top 500 µL supernatant contained HDL and the bottom 500 µL lipoprotein depleted plasma. The VLDL/LDL and lipoprotein depleted fractions were aliquoted and immediately stored at -80˚C.

2.2.2.1 De-salting of sequential density ultracentrifugation isolated HDL

The resultant HDL fractions isolated using NaBr sequential density ultracentrifugation contain high concentrations of salt, which may impact upon HDL functionality and composition in downstream applications. PD MiniTrap G-25 columns (Cytiva, Little Chalfont, Buckinghamshire, UK, #28918007) were therefore used to remove ~90% of remaining salts, according to the manufacturer's protocol. Briefly, columns were emptied of storage solution and the uppermost filter removed before placement into 15 mL centrifuge tubes. To equilibrate the column, 2 mL of DPBS was added and allowed to elute under gravity, after which a further 2 mL DPBS was added and allowed to elute. Both eluates were discarded. DPBS (3 mL) was added, and the column centrifuged at 1000 x *g* for 2 mins at room temperature. Eluted DPBS was discarded, and the column placed in a clean centrifuge tube. Isolated HDL (500 µL) was added to the column and then centrifuged at 1855 x *g* for 5 minutes at room temperature, in an Eppendorf 5910 Ri swing-bucket centrifuge. The desalted eluate containing HDL was aliquoted into clean microcentrifuge tubes and stored at -80ºC.

2.2.3 Iodixanol density gradient ultracentrifugation

The isolation of HDL with NaBr density solutions may have adverse effects on downstream HDL functional assays as a result of osmotic forces and protein degradation. Iodixanol is a high molecular weight, biologically inert polymer that readily forms density gradients. Iodixanol isolation of HDL is faster than sequential density ultracentrifugation as it only requires a single centrifugation step and separates lipoprotein fractions throughout the ultracentrifuge tube.

HDL was isolated from plasma using iodixanol with Dr Ian Davies at Liverpool John Moores University, based on his previously developed method (Harman et al., 2013). Isolation of HDL with iodixanol was not possible in Glasgow due to the need for a near vertical ultracentrifuge rotor.

To generate the density gradients, 15% and 24% (w/v) iodixanol solutions were prepared by diluting Optiprep (Sigma-Aldrich, Gillingham, Dorset UK, #D1556), a 60% w/v solution of iodixanol in water, with DPBS 0.9% NaCl. Participant plasma was mixed with Optiprep to a final concentration of 18.5% (w/v) iodixanol to form the working sample. Initially, 4 mL of the 15% (w/v) iodixanol solution was loaded into polypropylene centrifuge tubes (16x70 mm, 11.2 mL OptiSeal, Beckman Coulter, #362181). A syringe and steel cannula were used to gently under-layer 3 mL of the working sample below the 15% iodixanol layer. Finally, the 24% iodixanol solution (4 mL) was under-layered into the bottom of the centrifuge tube. The syringe was rinsed three times with 70% ethanol and dH_2O between solutions. Loaded centrifuge tubes were sealed with Optiseal plugs and housed in a Beckman Coulter NVT65 rotor. Bronze spacers were placed over the tubes and the caps screwed in before tightening to 180 inch-pounds with a torque-wrench. The samples were centrifuged in a Beckman Coulter XPN ultracentrifuge at 65,000 RPM (352,534 x *g* average) for 3 hours and 10 minutes at 16˚C. After centrifugation samples were fractionated into 500 µL volumes with a Labonco Autodensiflow, Watson Marlow 101U/R pump and Gilson FC203P fraction collector. The density of each fraction was measured using refractometer and converting the refractive index to density using the following equation: $\rho = \eta a - b$ (where a = 3.4193, b = 3.56, η = refractive index, and ρ = density). Fractions containing apoAI were pooled together and concentrated back to the initial volume of plasma used using Vivaspin 6 centrifugal concentrators (Cytiva # 28932296) with a molecular weight cut off of 10,000 Daltons, before storage at -80ºC.

It has been suggested that long term storage of isolated HDL fractions can impact upon particle integrity, composition and function, though the studies in question used different techniques to isolate HDL from plasma compared to those in this thesis which may also impact upon those metrics (Cohn et al., 2004; Holzer et al., 2017). To minimise the impact of storage time confounding

measures of HDL composition and function, for each technique described herein all samples in a given study were analysed at the same time, using the same kits, within the same mass spectrometer runs and the same passage of cells on the same day.

2.3 Cell culture

2.3.1 Cell line

Human microvascular endothelial cells (HMEC-1, ATCC-CRL-3243, LGC Standards, Middlesex, UK) were selected for this work and cultured to supplier protocols.

2.3.2 Culture media

Growth medium

Glutamine free MCDB131 media (Gibco, #10372-019) supplemented with 10 ng/mL epidermal growth factor (R&D Systems, Abingdon, Oxford UK, #236-EG), 1 µg/mL hydrocortisone (Tocris, Abingdon, Oxford UK, #4093), 10 mM L-glutamine (Sigma-Aldrich, G7513) and 10% fetal bovine serum (FBS, Sigma-Aldrich, #F9665).

Low serum medium

Glutamine free MCDB131 basal media supplemented with 0.5% v/v FBS.

Freezing medium

Growth medium (92.5% v/v) and dimethyl sulphoxide (DMSO, 7.5% v/v, Fisher Scientific, Loughborough, Leicestershire UK).

2.3.3 Initial culture

A frozen vial recovered from liquid nitrogen storage was rapidly thawed in a 37°C water bath and the contents transferred into a centrifuge tube containing 9 mL pre-warmed growth medium. Cells were pelleted in a centrifuge at 125 x *g* for 5 mins and the supernatant discarded, removing cryoprotectant DMSO. The pellet was resuspended in growth medium (12 mL) and the cell suspension transferred into a T75 tissue culture flask (Corning, Flintshire, Wales UK). Cell cultures were incubated at 37ºC in a 5% CO_2 atmosphere.

HMEC-1 do not require growth medium to be refreshed between subcultures as they become over-adherent and will not detach from the flask properly at the next subculture, resulting in the risk of over-trypsinisation.

2.3.4 Subculture

The following method is based on T75 culture flasks. Growth medium and sterile PBS were pre-warmed in a water bath. Spent media was aspirated and cells rinsed twice with sterile DPBS to remove serum traces. Trypsin-EDTA (0.25%, 3 mL, LGC Standards #30-2101) was added to the bottom of the flask and incubated for 7 mins to detach cells. Growth medium (9 mL) was added to inactivate the trypsin and to resuspend the detached cells. Further media was added to the flask based upon the desired subcultivation ratio and the cell suspension divided between new culture flask/plates. These were incubated at 37ºC in a 5% CO_2 atmosphere.

2.3.5 Freezing of cell stocks

The following method is based on T75 culture flasks. After following the subculture procedure (section 2.3.4) up to the addition of 9 mL complete media, the cell suspension was transferred into a centrifuge tube and cells pelleted at 125 x *g* for 5 mins. The supernatant was discarded, and the pellet resuspended in 2 mL freezing medium. The DMSO in the freezing media acts as a cryoprotectant by preventing cell damaging crystal formation on freezing. The suspension was transferred into cryovials (1 mL per vial) and placed in a Mr Frosty (Sigma-Aldrich) container overnight in a -80ºC freezer.

The Mr Frosty freezing container gradually cools cells at a rate of -1ºC per minute due to a 100% isopropyl alcohol jacket surrounding the tube-holders. The following day, the cryovials were transferred into a vapour phase liquid nitrogen store.

2.3.6 Cell treatment

Cells were subcultured into 12 well plates prior to treatment. On forming a monolayer, cells were washed twice in PBS and low serum medium (0.5 mL per well) added. Cells were treated with the required dose of drug/biological sample for the requisite time course before lysate preparation.

2.4 Cell lysate preparation

2.4.1 Buffers and solutions

Radio immunoprecipitation lysis buffer (RIPA)

RIPA comprised 150 mM NaCl, 50 mM Tris-HCl pH 7.4, 1% v/v Triton X-100, 0.5% m/v sodium deoxycholate, 0.1% m/v sodium dodecyl sulphate (SDS), 1 mM ethylenediaminetetraacetic acid (EDTA), 10 mM NaF, in dH_2O adjusted to pH 7.4 with concentrated hydrochloric acid.

Complete lysis buffer

Complete lysis buffer comprised RIPA buffer (10mL) with the addition of 1x Roche Complete mini protease inhibitor cocktail tablet (Sigma-Aldrich #11836153001).

2.4.2 Cell lysis

Spent (i.e., conditioned) media was transferred to a pre-chilled centrifuge tube and the cells washed in PBS. Complete lysis buffer (50 µL) was added to each well. The plate was then frozen for 1 hour at -80 ºC. After thawing, each well was scraped immediately, and the lysate added to a pre-chilled microcentrifuge tube. After a brief high-speed vortex, the lysates were incubated on ice for 30 minutes. The lysates were vortexed again at 15 minutes and before centrifugation. After 30 minutes incubation, the lysates were clarified by centrifugation at 17,000 x *g*, 4˚C for 5 mins. The supernatants were transferred into clean prechilled microcentrifuge tubes and the pellets discarded. In the short term, lysates were stored at -20ºC whereas long term storage was at -80ºC.

2.5 Conditioned media preparation

Conditioned media samples were centrifuged at 500 x *g* for 10 min at 4˚C to bring any remaining cell debris or solid contaminants to the bottom of the centrifuge tube. The top three quarters of centrifuged media was retained in fresh pre-chilled microcentrifuge tubes. Samples were stored at -20ºC or -80ºC.

2.6 Bradford protein assay

Bradford's assay for total protein was performed in 96-well plates. The assay works on the principle of Coomassie brilliant blue G-250 dye binding to proteins present in a sample. This results in the formation of protein-dye complexes, shifting the dye from red to blue and a maximum absorption of light at 595 nm. Absorption of light at 595 nm increases with increasing protein concentration (Bradford, 1976).

A standard curve was prepared from a 1 mg/mL bovine serum albumin (BSA) stock solution (Sigma-Aldrich #P0914) by dilution in dH_2O to give 1, 0.75, 0.5, 0.25 and 0.1 mg/mL standards. Deionised water acted as a blank. Samples of unknown protein concentration were diluted appropriately in dH_2O to fit the standard curve. Blank/standards/diluted samples (5 µL) were added in duplicate to the plate. Bradford reagent (250 µL, Thermofisher Scientific #23238) was added to each well. The plate was briefly mixed on a horizontal shaker before a 15 min incubation at room temperature and measurement in a Multiskan FC plate reader (Thermofisher Scientific) at 595 nm. Protein concentration was calculated from the linear equation of the standard curve.

2.7 Total cholesterol quantitation

Total cholesterol in isolated HDL was assessed in 96-well plates using a cholesterol quantitation kit (Sigma-Aldrich, #MAK043) according to the manufacturer's protocol. In this kit, total cholesterol is measured through a coupled enzyme-based system, whereby cholesteryl esters are converted to cholesterol. The final enzymatic product is detected by a cholesterol probe resulting in a measurable colorimetric output. Briefly, a standard curve with 1, 2, 3, 4 and 5 µg cholesterol was prepared in duplicate using the provided

cholesterol standard diluted in assay buffer. Assay buffer alone (50 µL) acted as a blank. HDL samples (5 µL) were added in duplicate to the assay plate. Assay buffer was added to each well to total volume of 50 µL in each well. Reaction mix (50 µL) composed of 44 µL assay buffer, 2µL cholesterol probe, 2 µL enzyme mix and 2 µL cholesteryl esterase was added to each well. The plate was mixed on a horizontal shaker and incubated for 1 hr in the dark at 37°C after which the plate was read at 540nm in a Multiskan FC plate reader. Cholesterol content in µg was calculated based on the linear equation of the standard curve and corrected for the sample volume (5 µL) to give cholesterol concentration in µg/µL. Finally, cholesterol content was expressed in mmol/L by multiplying the cholesterol concentration by 100 and dividing by 38.5.

2.8 SDS-PAGE

Sodium dodecyl sulphate polyacrylamide gel electrophoresis (SDS-PAGE) separates denatured proteins in a sample by molecular weight using electrical current. This separation is achieved by a combination of a protein's mass/charge ratio and the percentage of acrylamide in the gel. Heavier, larger proteins move more slowly than smaller, lighter proteins on the application of electrical current. Gels with higher percentages of acrylamide have smaller pores in the matrix formed on polymerisation, thus excluding larger proteins from being resolved. Gradient gels, such as 4-12% acrylamide, enable the resolution of both large and small molecular weight proteins on the same gel. A molecular weight marker is run in tandem with samples for reference. Polyacrylamide gel electrophoresis was performed using the XCELL Surelock system (Thermofisher Scientific #EI0002), with Invitrogen Bolt 1 mm 4-12% wedge-well pre-cast gels (Thermofisher Scientific #NW04125BOX). Gels were placed into the Surelock tank, and the inner chamber filled with Bolt MOPS running buffer (Thermofisher Scientific #B0001) supplemented with 0.0025% v/v Bolt antioxidant (Thermofisher Scientific #B0005).

Samples of known protein concentration assessed by Bradford assay (section 2.6) were mixed with Bolt 4x lithium dodecyl sulphate sample buffer (Thermofisher Scientific #B0007) supplemented with 200 mM dithiothreitol (DTT) at a ratio of 3:1 and heated at 95°C for 5 minutes. This denatures the proteins in the sample through heat degradation and DTT breaking and preventing the re-formation of

disulphide bonds in folded proteins. An equal amount of protein per sample was loaded onto the gel. The Precision Plus Protein All Blue Standard (4 µL, Bio-Rad Laboratories, Watford, UK, #161-0373) was used as the molecular weight marker. Electrophoresis was conducted at 200V constant for 45 minutes.

2.9 Western blotting

2.9.1 Buffers and solutions

Transfer buffer

Transfer buffer comprised 5% v/v Bolt transfer buffer (Thermofisher Scientific #BT00061), 20% v/v methanol, 0.001% v/v Bolt antioxidant in dH_2O.

Tris-buffered saline (TBS)

TBS comprised 2 mM Tris and 13.7 mM NaCl in dH_2O, adjusted to pH 7.6 with concentrated hydrochloric acid.

Tris-buffered saline + Tween-20 (TBS-T)

TBS-T comprised TBS + 0.1% v/v Tween-20.

Blocking buffer

Blocking buffer comprised 5% w/v low-fat milk in TBS.

Antibody buffer

Antibody buffer comprised 5% w/v bovine serum albumin (Sigma-Aldrich #A3059) in TBS-T.

Total Protein Normalisation

Revert 700 Total Protein Stain Kit (LI-COR Biosciences, Cambridge, Cambridgeshire UK, #926-11016).

2.9.2 Transfer of proteins onto nitrocellulose membranes

Resolved protein gels were placed on nitrocellulose membranes (0.45 µm pore size) and sandwiched between two sheets of 3mm filter paper, all pre-wet with transfer buffer (both Thermofisher Scientific #LC2001).

The sandwich was placed between transfer sponges and stacked into an XCELL Surelock blot module. The module was filled with transfer buffer and the outer tank filled with dH_2O as a heat sink. Electrophoretic transfer was carried out at 25V constant for 1.5 hours. Successful transfer to nitrocellulose was confirmed by the quality of the pre-stained protein ladder on the membrane.

2.9.3 Total protein normalisation

Normalisation of western blots is important to reduce the effect of methodological variability, for example uneven protein loading, on experimental results. Probing for housekeeping proteins and normalising target signal to a housekeeper is one option for normalisation, however this comes with its own flaws, notably the need to select an appropriate housekeeper and optimise a blotting procedure for it. It also requires a degree of certainty that any experimental procedures will not affect housekeeper expression and therefore introduce more variability. Total protein normalisation avoids these flaws as target signal is normalised to the amount of protein loaded into each lane of the gel.

Membranes were rinsed in dH_2O and incubated in methanol activated Revert 700 Total Protein Stain for 5 minutes. After two brief rinses in Revert 700 Wash Solution, the membrane was imaged on a LI-COR Odyssey FC scanner in the 700 nm (red) channel for 2 minutes.

2.9.4 Membrane blocking and primary antibody incubation

Membranes were incubated in blocking buffer for 1 hour at room temperature on a platform shaker to prevent the non-specific binding of antibodies. After blocking, membranes were incubated with mouse anti-human VCAM-1 monoclonal antibody (Santa Cruz Biotechnology Inc, Heidelberg, Germany, #sc-13160) diluted 1:100 in antibody buffer overnight at 4°C on a platform shaker.

2.9.5 Secondary antibodies and membrane visualisation

Membranes were washed in TBS-T three times (5 minutes per wash) before incubation with donkey anti-mouse IgG IRDye 800cw antibody (LI-COR, # 926-32212) diluted 1:10,000 in antibody buffer for 1 hour at room temperature on a

platform shaker. Membranes were visualised using a LI-COR Odyssey FC scanner in both the 700 nm (red, 30 seconds) and 800 nm (green, 2 minutes) channels.

2.9.6 Signal quantification of protein bands

Total protein was first quantified using LI-COR Image Studio Lite software version 5.2, using the total protein normalisation (section 2.9.3) scan. A rectangle was drawn around the perimeter of each lane and the signal value retained. The median background value was calculated from a 3-pixel border at the top and bottom of each rectangle to prevent overlap with neighbouring lanes. A lane normalisation factor (LNF) was calculated using the background adjusted signal values of each lane as follows:

$$Lane\ Normalisation\ Factor = \frac{Total\ Protein\ Stain\ signal\ for\ each\ lane}{Total\ Protein\ Stain\ signal\ from\ the\ lane\ with\ the\ highest\ signal}$$

Secondary antibody signal (section 2.9.5) was then quantified by selecting each band of target signal using the add rectangle tool, which automatically draws a rectangle around the perimeter of the band and corrects for the immediate background signal with a 3-pixel border at the top and bottom of the shape to prevent bleed from neighbouring bands. The signal value was retained and normalised using the LNF values calculated earlier, as follows:

$$Normalised\ Signal = \frac{Target\ Signal}{LNF}$$

Normalised signals were then expressed as percentage of a control sample on each gel.

2.10 Enzyme linked immunosorbent assay (ELISA)

ELISA is a sensitive assay used to detect low abundance targets in biological samples through indirect enzyme activity. The target of interest is sandwiched between a capture antibody bound to the plate and a detection antibody. A streptavidin-horse radish peroxidase (HRP) complex is then bound to the biotinylated detection antibody, which converts 3,3',5,5'-tetramethylbenzidine

substrate solution from colourless to blue in colour. An acidic stop solution stops the reaction and changes the colour to yellow, which can then be measured in a plate reader. The degree of colour change is reliant on the amount of HRP in the well, directly proportional to the amount of target in the sample.

R&D Systems Duoset ELISA kits were used according to the manufacturer's protocol with manufacturer recommended reagent ancillary kits and appropriately diluted samples. All incubations were at room temperature and plates were washed between each stage of the ELISA. Microtiter plates (96-well, Corning) were coated with the supplied capture antibody overnight. Plates were then blocked for 1 hour with reagent diluent before the addition of dilute standards and samples in reagent diluent for 2 hours. The appropriate detection antibody was added to the plate for 1 hour. The plate was then incubated in the dark for 20 minutes with streptavidin-HRP before adding substrate solution for a further 20 minutes in the dark. Finally, without washing, stop solution was added to each well. The plate absorbances were read at 450 nm, and at 540 nm in order to correct for optical imperfections in the microtiter plate. Target concentration was calculated from the 4-parameter logistic equation of the standard curve. Details of each kit used are given in table 2-1.

Table 2-1 R&D Systems DuoSet ELISA kit details.

Catalogue number	Target	Ancillary kit required	Sample type	Sample dilution
#DY206	Interleukin-6	#DY-008B	Conditioned media	1:2
#DY3664	Apolipoprotein AI	#DY-008B	Isolated HDL	1: 25,551
#DY3019	Serum amyloid A1	#DY-009B	Isolated HDL	1:51

2.11 High-density lipoprotein paraoxonase-1 activity assay

2.11.1 Buffers and solutions

Salt Buffer

Salt buffer comprised 20 mM Tris, 1 mM $CaCl_2$ in dH_2O adjusted to pH to 8.0 with concentrated hydrochloric acid.

Phenyl acetate solution

Phenyl acetate solution comprised 3.26 mM Phenyl acetate (Sigma-Aldrich #108723) in salt buffer.

2.11.2 Activity Assay

HDL PON-1 arylesterase activity was quantitated as previously described (Ljunggren et al., 2015). This assay is based upon the hydrolysis of phenyl acetate by PON-1, producing phenol and acetate (Figure 2-1). The rate of phenol production is measured by a plate reader owing to the UV-visible absorption of the aromatic ring present in a phenol molecule at 270 nm.

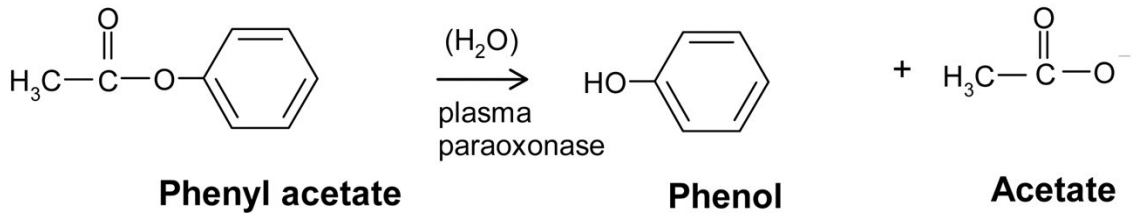

Figure 2-1 - Reaction mechanism of paraoxonase-1 activity assay.
Adapted from (Richter et al., 2008).

Initially each well of a 96 well microtiter plate was loaded with 220 µL dH_2O, to determine its pathlength and allow the SoftMax software to correct absorbance readings to a 1 cm pathlength. Isolated HDL was diluted 1:80 in salt buffer and 20 µL added in duplicate to a UV transparent compatible 96-well microtiter plate (Thermofisher Scientific #8404). Salt buffer alone (20 µL) was used as a blank. Well-mixed phenyl acetate solution (200 µL) was added to each well and the plate shaken for 10 seconds before measurement of the rate of phenol production using the kinetic function of a Spectramax M2e plate reader, at 25°C

every 35 seconds at 270 nm with background correction at 250 nm. The assay was run for 7 minutes for a total of 13 readings. The rate of phenol production (OD/minute, arbitrary units) was calculated from the linear portion of the reaction curve. Concentration per minute was calculated using the Beer-Lambert law using the molar extinction coefficient for phenol of 1310 $\mu mol/L^{-1}\,cm^{-1}$. PON-1 activity was expressed as units (U, $\mu mol/L^{-1}\,min^{-1}$) per mg of HDL protein to compare equally between samples. One sample was used as a control in each run to check inter-assay variability. Across all paraoxonase-1 activity assay plates, inter-assay CV was 5.86%.

2.12 HDL size distribution analysis

HDL size distribution was assessed using native polyacrylamide gel electrophoresis (Native-PAGE). Unlike in SDS-PAGE (section 2.8), samples are not denatured before separation on the gel. As such, proteins remain in their folded structures and, in the case of lipoproteins, particles remain intact. The following method is based on that of Dr Bruce Griffin, University of Surrey, who kindly assisted with the establishment of the technique here at the University of Glasgow. Given that there is debate on the precise size ranges for each HDL subtype and the nature of gel electrophoresis, this method for analysing HDL size is deemed semi-quantitative.

Native-PAGE was performed using the XCELL Surelock II electrophoresis system, using Novex 4-20% tris-glycine wedge-well gels (Thermofisher Scientific #XP04202BOX) submerged in 1x Novex tris-glycine running buffer (Thermofisher Scientific #LC2672). HDL was diluted in 1x Novex tris-glycine native sample buffer (Thermofisher Scientific #LC2673) and 40 µL was loaded into each well of the gel. NativeMark unstained protein standard (5 µL, Thermofisher Scientific #LC0725) was used as the molecular weight marker. Electrophoresis was conducted at 225 V constant for 50 minutes. Gels were then stained for protein in 50 mL QC Colloidal Coomassie stain (Bio-Rad Laboratories #1610803) for 1 hour at room temperature, followed by de-staining in three changes of dH_2O over 1 hour. Gels were imaged using a LI-COR Odyssey FC imager in the 700 nm channel for 2 mins.

To analyse the HDL size distributions, the molecular weight marker was first converted to diameter (in nm) using the calculator based on Erickson (2009) found at 'www.nanocomposix.com/pages/molecular-weight-to-size-calculator'. The standardised retention factor (R_F) for each marker band was calculated relative to the 66 kDa marker band and a linear standard curve drawn. This standard curve was used to calculate the maximum and minimum R_F values for each of the following HDL subtypes based on their diameter: 2b 9.7-12.9 nm, 2a 8.8-9.7 nm, 3a 8.2-8.8 nm, 3b 7.8-8.2 nm and 3c 7.2-7.8 nm (Kontush et al., 2015). The background adjusted signal for each HDL subtype was expressed as percentage of the total background adjusted HDL signal.

2.13 Proteomic analysis of HDL composition

HDL proteomic analysis was performed alongside Dr Helen Karlsson and Dr Stefan Ljunggren at the Department of Health, Medicine and Caring Sciences, Linköping University, Sweden, in July 2019 and June 2022. Between these visits the nano-liquid chromatography mass-spectrometry system was upgraded, necessitating a change in sample preparation and analysis procedure due to the increased sensitivity of the new system. The gestational diabetes mellitus samples were analysed in July 2019, while the M-FAT and GlasVEGAs study samples were analysed in June 2022. The specific details of each methodology are given in the relevant chapters.

2.14 Statistical Analyses

Due to differences in study design and the resulting data, statistical analyses are described separately in each chapter. In all chapters, statistical significance was assumed at $p < 0.05$. All graphs were created with GraphPad Prism software version 9.5 with the exception of the multivariate statistical plots which were created with SIMCA software.

2.14.1 Multivariate statistical analysis of proteomic data

Proteomic datasets are large and require multiple comparisons which increases the risk of type I statistical error, i.e. false positives. Traditionally a corrected probability value is used to counter this risk, for example by Bonferroni

correction, which works well for independent observations but is also highly conservative. In the case of HDL proteomics, it was expected that identified proteins would be correlated with one and other and therefore not independent, rendering Bonferroni correction a poor option to reduce type I error. The multivariate principal components analysis (PCA) and orthogonal projections of latent structures – discriminant analysis (OPLS-DA) were therefore used to identify samples similar to one another based on their protein content and demographics and to identify the proteins and demographic factors important to group separation respectively. These statistical analyses use all of the input data simultaneously to construct new variables that explain the majority of the information, thus enabling the selection of individual input variables that contribute most to a group's phenotype. These models were performed prior to univariate analyses to direct to appropriate univariate analysis of said variables.

SIMCA software was used to generate PCA and OPLS-DA models. All data was centred and scaled using unit-variance scaling (as suggested by van den Berg et al., 2006) before analysis. PCA models use covariance matrices derived from plotting data in 3D space to create latent variables, known as principal components, which explain the variance in the data. The first principal component explains the most variation, while the second principal component explains the second most variation and is perpendicular to the first principal component. Though many principal components are created, the first two contain the majority of the useful information and are used to plot the PCA results. The computation of eigenvalues for the covariance matrices of each sample results in a score value. A score is generated for each sample; samples with similar scores are plotted close together. The accompanying loadings plot identifies the variables that correlate together and their contribution to each principal component. PCA can therefore identify groupings within large datasets in an unsupervised manner, i.e., without prior knowledge of a sample's group membership. PCA scores plots were assessed qualitatively. While PCA gives an overview of sample similarity and the variables that correlate with one and other, it is not a predictive technique. OPLS-DA is a supervised regression and prediction technique where the model identifies variables (X) that predict group membership (Y) and those that do not (which are orthogonal to group membership).

In this way, the horizontal x axis on an OPLS-DA scores plot denotes the degree of difference between the groups, while the vertical y axis indicates the within group variability. Cross validation was used to determine the number of significant model dimensions by removing observations from the model one at a time and comparing the Y predicted by this model with the actual values. To improve interpretability of the OPLS-DA model, variables with a variable influence on prediction (VIP) score greater than one were included in the analysis. The accompanying loadings plot indicates the variables most important to the separation. Variables closer to the group identifiers are more important for separation. OPLS-DA models were assumed statistically significant at $p<0.05$.

3 HDL anti-inflammatory function assay development

3.1 Introduction

This chapter sets out the development of an endothelial cell assay for HDL anti-inflammatory function that will be used in later chapters to assess the relationship between HDL's composition and vascular protective functions. This assay is based upon a commonly published method whereby HDL's ability to inhibit the expression of adhesion molecules in the face of an inflammatory stimulus is measured.

The effect of HDL on adhesion molecule expression was first investigated after evidence emerged that adhesion molecule expression was increased by oxidised LDL in the early stages of atherosclerosis. This led to the assessment of potential inhibitory HDL effects on adhesion molecules in endothelial cells (Cockerill et al., 1995). At physiological concentrations, HDL abolished inflammatory cytokine induced VCAM-1 expression in human umbilical vein endothelial cells (HUVECs). The study demonstrated that this effect was indeed HDL-specific and not due to contaminating factors, with similar results achieved using reconstituted HDL containing solely apoAI, phosphatidylcholine and unesterified cholesterol (Cockerill et al., 1995). The assay has been used to show that smaller HDL has improved anti-inflammatory function (Ashby et al., 1998) and that dietary saturated fat and post-prandial hypertriglyceridemia decrease HDL's anti-inflammatory capacity (Nicholls et al., 2006; Patel et al., 2009). HDL from coronary artery disease (CAD) and myocardial infarction patients has reduced ability to inhibit adhesion molecule expression, as does HDL from those with type 2 diabetes mellitus (T2DM) (Besler et al., 2011; Annema et al., 2016; Ebtehaj et al., 2017). The assay can also be used to assess improvement in HDL anti-inflammatory function, for example via exercise (Sang et al., 2015) or consumption of breakfast in T2DM (Lemmers et al., 2021). There are a number of pathways by which HDL can modulate adhesion molecule expression including via apoAI, the sphingolipid S1P and indirect antioxidant effects (Figure 1-1, Kimura et al., 2006; Schmidt et al., 2006).

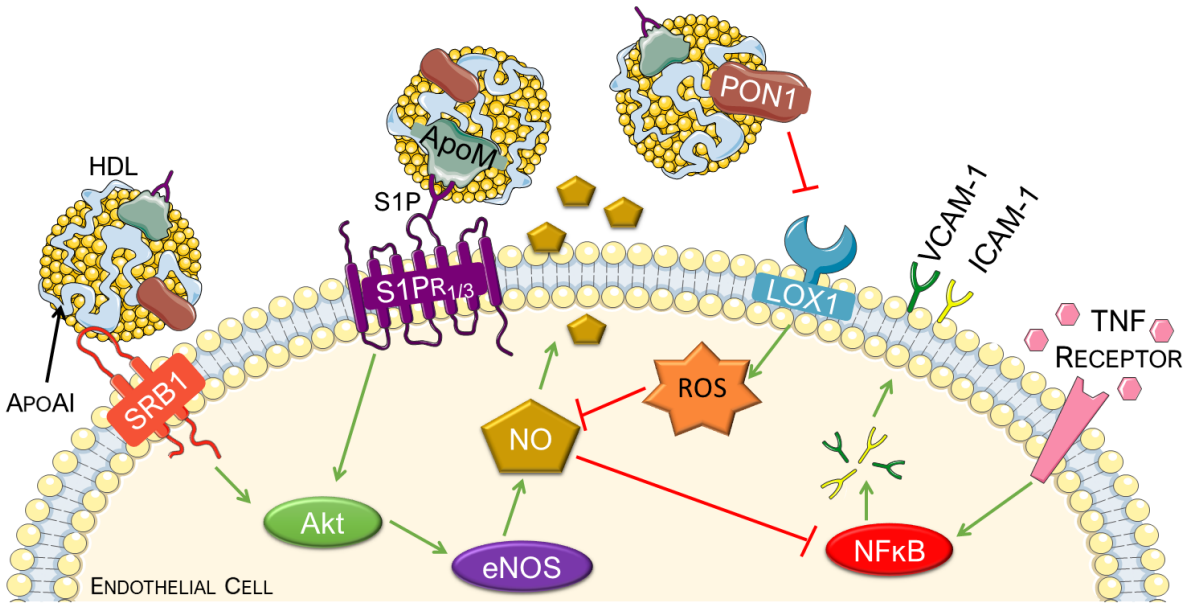

Figure 3-1 HDL protective signalling in endothelial cells: HDL apoAI binds scavenger receptor B1 (SRB1) and HDL S1P binds S1P receptors 1 and 3. Both of these actions instigate Akt signalling which ultimately results in eNOS activation and the generation of nitric oxide (NO). The antioxidant paraoxonase 1 has two linked functions; it prevents the oxidation of LDL which reduces its availability to its receptor LOX-1, and directly reduces the sensitivity of the receptor. Both of these actions prevent reactive oxygen species (ROS) generation which impair eNOS derived NO. These actions of HDL increase NO availability, which has inhibitory effects on nuclear factor κ B (NFκB) and prevents adhesion molecule expression in response to inflammatory stimuli such as tumour necrosis factor α (TNFα). Used with permission of Portland Press, Ltd, from Jack D. Beazer, Patamat Patanapirunhakit, Jason M.R. Gill, Delyth Graham, Helen Karlsson, Stefan Ljunggren, Monique T. Mulder, Dilys J. Freeman; High-density lipoprotein's vascular protective functions in metabolic and cardiovascular disease – could extracellular vesicles be at play?. Clin Sci (Lond) 27 November 2020; 134 (22): 2977–2986.; permission conveyed through Copyright Clearance Center, Inc.

Though the underlying premise of the assay remains consistent throughout these published studies, a key difference exists in the methods used to detect changes in adhesion molecule expression. The original study by Cockerill et al., (1995) measured VCAM-1 expression using fluorescence-activated cell sorting (FACS), which uses live cells that have been incubated with fluorescent antibodies against adhesion molecules and measures the intensity of signal in the samples. Enzyme-linked immunosorbent assays on fixed cells have also been used to detect changes in VCAM-1 expression; like FACS this determines cell surface adhesion molecule expression. Others made use of northern blotting or the modern equivalent quantitative real-time polymerase chain reaction (qRT-PCR) to detect changes in the messenger RNA (mRNA) levels for adhesion molecules, rather than the proteins themselves. Recent studies on mediators of cytokine-

induced endothelial adhesion molecule expression in response to factors outside of HDL have used semi-quantitative western blotting to detect VCAM-1 in a sensitive and repeatable manner (Zhu et al., 2013; Lin et al., 2019; Huang et al., 2023). Due to constraints in access to training and equipment for FACS here at the University of Glasgow, and my previous experience in using western blotting, I chose to measure VCAM-1 expression in this manner. Western blotting measures cytoplasmic and surface VCAM-1 protein in cell lysates. PCR analysis was a potential alternative method for detection of VCAM-1 but was disregarded as increased mRNA transcription does not necessarily equate to increased protein translation. Direct measurement of VCAM-1 protein was preferred as it is ultimately one of the effector molecules in endothelial monocyte recruitment.

Given that HDL anti-inflammatory endothelial signalling centres around eNOS activation (Figure 1-1), I also aimed to measure nitric oxide secretion into the culture media as a secondary measure of HDL function. However, in this assay, the inflammatory stimulus provoking endothelial inflammation post-incubation with HDL also upregulates inducible nitric oxide synthase (iNOS), which produces nitric oxide in concentrations far exceeding that of eNOS and thus obscures eNOS-derived NO. Contrary to constitutive eNOS, inducible NOS has a postulated role in the endothelial dysfunction caused by insulin resistance as a result of oxidative and nitrosative stress and its expression is mediated in part by Akt and NFκB signalling, pathways inhibited by HDL (reviewed in Soski et al., (2011)). I aimed to assess the ability of HDL to reduce inflammation-induced excess NO production as an auxiliary measure of HDL's anti-inflammatory function. This may reveal insulin resistance-altered pathways of modulated adhesion molecule expression.

Simian vacuolating virus 40 large T antigen (SVT-40) transformed HMEC-1 were chosen for this work (Ades et al., 1992) as many of the prevalent consequences of insulin resistance are microvascular in nature, including nephropathy, neuropathy and retinopathy (Petrie et al., 2018a). HMEC-1 share morphological and phenotypical characteristics of their parent primary cells but are far easier to culture, given their ready and consistent growth. These cells have also been validated as appropriate for the study of HDL effects on endothelial function with improved reproducibility compared to primary human umbilical vein

endothelial cells (HUVECs) (Muñoz-Vega et al., 2018). It should be noted that HUVECs are macrovascular in nature which may contribute to the differences in HDL effects between the cell types. In any case, HUVECs would be an inappropriate choice of cell line in the present thesis given that a number of study groups used are women with healthy and insulin resistance complicated pregnancies. HUVECs are fetal in nature and do not reflect maternal endothelial function. Other studies on HDL function have been performed using physiologically relevant macrovascular cells with mixed results lending further support to the use of microvascular cells; Zhang et al., (2002) did not find HDL effects on adhesion molecule expression in human aortic endothelial cells while Besler et al., (2011) did. A study comparing pre- and post-prandial HDL anti-inflammatory function found feeding related differences in HDL in microvascular retinal endothelial cells but not in macrovascular human coronary artery endothelial cells potentially due to diverging endothelial phenotypes (Lemmers et al., 2021).

Cells can be exposed to HDL based on apoAI, cholesterol, or protein concentration. There is no one measure that is superior to the others. As apoAI accounts for the majority of HDL protein and is the dominant functional protein, this measure of the amount of HDL was used. In recognition that HDL cholesterol better reflects particle number, given there are variable numbers of apoAI molecules on a HDL particle, results were presented both as function relative to apoAI and also corrected for HDL cholesterol content. Results were also presented corrected for HDL total protein to reflect the diverse array of proteins associated with HDL and their potential effect on endothelial function. The optimised assay was used to determine how HDL composition affects its anti-inflammatory function.

3.1.1 Aim

- To establish a reproducible endothelial cell assay to measure the anti-inflammatory function of HDL isolated from individuals with varying insulin resistance

3.2 Methods

3.2.1 Study samples selected for assay optimisation

Initially, the recruitment and blood sampling of healthy volunteers was planned to generate a pool of healthy HDL for the optimisation of the assay and subsequent comparison of HDL isolation techniques described in chapter 4. Due to the COVID-19 pandemic and a laboratory fire, this plan could not be enacted. Instead, a random selection of five control and five impaired glucose regulation (IGR) samples from the M-FAT study (chapter 7) were used to develop, optimise and pilot test this HDL anti-inflammatory assay. Demographics for the samples can be found in table 3-1. As these samples were derived from an archival study collection, five samples from each group were chosen to reduce the impact on sample volume and availability for later analysis.

Table 3-1 Demographics of samples used to optimise the assay. Data expressed as mean ± SD.

	Control (n = 5)	IGR (n = 5)	p value
Age (years)	41.2 ± 9.0	56.4 ± 1.6	0.018
BMI (kg/m^2)	23.8 ± 2.3	31.5 ± 4.8	0.019
HbA1c (mmol/mol)	33.8 ± 4.1	55.4 ± 8.6	0.003
HDL (mmol/L)	1.24 ± 0.23	1.15 ± 0.24	0.57
Triglycerides (mmol/L)	1.41 ± 0.43	2.07 ± 1.72	0.49
Total cholesterol (mmol/L)	4.03 ± 0.61	4.09 ± 0.77	0.89
Fasting glucose (mmol/L)	5.14 ± 0.20	8.69 ± 1.06	0.001
Fasting insulin (µU/ml)	6.72 ± 1.37	19.58 ± 21.39	0.25

3.2.2 High-density lipoprotein isolation

HDL was isolated by ultracentrifugation and desalted as per sections 2.2.1 and 2.2.2. For downstream cell culture experiments, only the top 250 µl of the final supernatant was retained to increase HDL concentration. For experiments regarding HDL storage, isolated HDL fractions were frozen with the antioxidant butylated hydroxytoluene (BHT) (0.001%).

3.2.3 Enzyme-linked immunosorbent assay

3.2.3.1 Apolipoprotein AI

Isolated HDL ApoAI content was assayed using an R&D Systems Duoset® ELISA kit according to the manufacturer's protocol (section 2.10).

3.2.3.2 Interleukin-6

Cell culture supernatant IL-6 concentration was assayed using an R&D Systems Duoset® ELISA kit according to the manufacturer's protocol (section 2.10). Concentrations were corrected for baseline IL-6 concentration in untreated cells.

3.2.4 HDL cholesterol content analysis

HDL cholesterol content was measured as per section 2.7.

3.2.5 Endothelial cell culture

HMEC-1 were cultured as described in section 2.3. Cells were grown in 12-well culture plates. Once confluent and forming a monolayer, cells were rinsed twice with DPBS and serum-starved in 0.5 mL basal media supplemented with 0.5% FBS. Cells were immediately exposed to HDL samples for up to 6 hours, after which TNFα prepared in 0.1% BSA in DPBS was added to the cells (5 ng/mL) for up to 24 hours. Media samples were taken for measurement of IL-6 by ELISA (section 2.5) and cells were lysed for SDS PAGE and western blot analysis (section 2.4).

3.2.5.1 Cell viability assessment

For cell viability experiments, cells were trypsinised and resuspended in complete media. Cell suspensions were mixed 1:1 with acridine orange (AO)/propidium iodide (PI) (ViaStain AO/PI staining solution, Nexcelom, Manchester, UK, #CS2-0106) and 20 µL was loaded into a cell counting chamber (Nexcelom SD100 #CHT4-SD100). Cells were counted with a Nexcelom Cellometer Spectrum cytometer and the proportion of live cells calculated. All cells (live or dead) fluoresce green due to the membrane permeability of AO.

PI is only permeable to dead cells and quenches AO fluorescence, resulting in red fluorescence. The Cellometer together with Nexcelom software counts all cells in the chamber (green and red) followed by live cells (green). Cell viability was calculated as the ratio of live cell count to total cell count expressed as a percentage.

3.2.6 SDS PAGE

SDS PAGE was performed as described in section 2.8. Gels were loaded with 20 µg cell lysate per well as determined by Bradford assay and electrophoresed before blotting for VCAM-1 (section 2.6).

3.2.7 Western blotting

Western blotting was performed and analysed as described in section 2.9. Under reducing conditions, VCAM-1 appears as an approximately 100 kDa band on the membrane.

3.2.8 Measurement of *in vitro* endothelial nitric oxide generation

Measurement of NO is challenging given its short half-life and rapid action. As such, assays designed to measure or infer endothelium-derived nitric oxide typically focus on the activity of the enzymes responsible for its synthesis, activation of the sites of NO action, and the products of NO reactions such as nitrite (Csonka et al., 2015). Measurement of nitrite is a common technique for inferring NO generation as it can be readily measured by spectrophotometry (as performed by Choi et al., (2002)) or by converting nitrite back to NO and measuring its reaction, as follows. As nitrite is common in cell culture media, a media only control was included in the analysis and all samples measured corrected for this baseline. Samples of conditioned cell culture medium (50 µL) were taken and mixed with 200 µL of ice-cold methanol. Samples were centrifuged at 17,000 x g at 4°C for 20 minutes and supernatants were stored at -20°C until measurement. Nitric oxide (NO) concentration was determined using a Sievers NO Meter ozone-chemiluminescence technology as described previously (Morrow et al. 2003). Briefly, 20 µL of sample was injected into purging acetic acid supplemented with NaI. Iodide reacts with nitrites in the media sample thus converting back to NO. Inside of the reaction chamber, NO and ozone was

converted into nitrogen dioxide in a chemiluminescent reaction. The intensity of the light emitted was recorded by spectrophotometry at 600 nm and quantified by the instrument. A NO standard curve was obtained by applying linear regression to nitrite samples made in deionised water (20 nM, 50 nM, 100 nM, 200 nM, 500 nM, 1 µM, 2 µM, 5 µM, 10 µM). All samples and standards were measured in triplicate.

3.3 Results

3.3.1 Selection of a TNFα concentration to induce maximal endothelial inflammation

Assay development began with the selection of the optimal TNFα concentration to stimulate endothelial inflammation. HMEC-1 were exposed to 2, 5 and 10 ng/mL TNFα for 17 and 24 hours. Maximal stimulation of IL-6 secretion was at 5 and 10 ng/mL TNFα for 24 hours (Figure 3-2).

As there was no difference between the two concentrations, 5 ng/mL for 24 hours was chosen as the concentration and time course of TNFα stimulation to prevent potential over-stimulation of the cells and consequently an irretrievable inflammatory response.

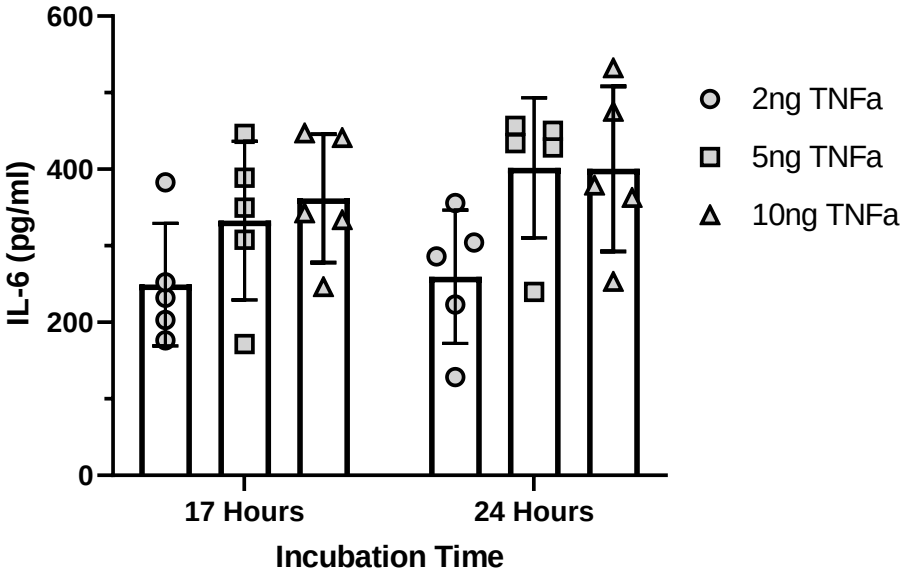

Figure 3-2 Pilot interleukin-6 inflammatory response of HMEC-1 to TNFα: HMEC-1 were exposed to 2, 5 and 10 ng/mL TNFα for 17 and 24 hours and spent media samples assessed for IL-6 concentration by ELISA. Data shown are corrected for baseline IL-6 concentration. Bars indicate mean ± SD, n=5.

3.3.2 Optimisation of western blotting conditions for VCAM-1

Initial western blots performed using an R&D Systems VCAM-1 antibody were of poor quality. To ensure the lysis protocol adequately retrieved protein from plated cells, the pellets left behind after clarifying the lysates were resuspended in sample buffer and run on a separate western blot (Figure 3-3 A). VCAM-1 was not detected in the pellets. The Santa Cruz VCAM-1 antibody was therefore tested and used for this assay. However, a second band at approximately 200 kDa was present even at a range of TNFα concentrations, and the VCAM-1 signal was diffuse (Figure 3-3 Bi). Dithiothreitol (50 mM) was added to the sample buffer to eradicate the dimer band, though the VCAM-1 signal remained diffuse (Figure 3-3 Bii). Bolt antioxidant was therefore added to both the running and transfer buffers, to prevent re-oxidation of the proteins during SDS-PAGE and transfer to nitrocellulose membranes (Figure 3-3 Biii).

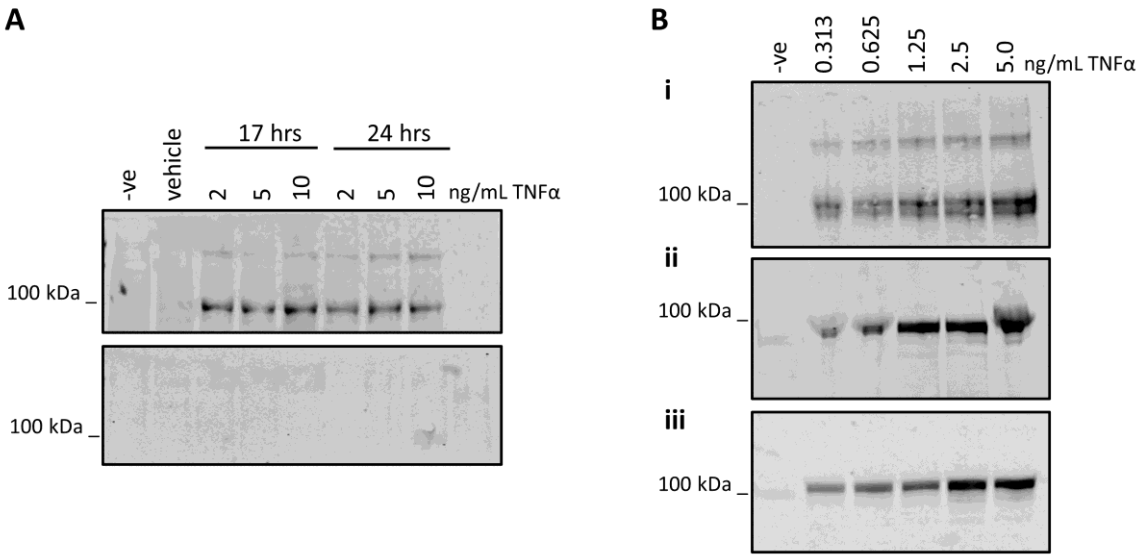

Figure 3-3 Representative Western blots used for optimisation: Initial VCAM-1 immunoblots using R&D systems anti-VCAM-1 antibody were of poor quality (A, top). VCAM-1 was not present in the cell pellets of the same samples (A, bottom). Stepwise improvement of initial western blot quality using Santa Cruz anti-VCAM-1 antibody (Bi) with dithiothreitol (Bii) and with both dithiothreitol and Bolt antioxidant (Biii). -ve, untreated cells; vehicle, 0.1% BSA in PBS.

3.3.3 VCAM-1 response to TNFα

With 5 ng/mL selected as the maximum TNFα concentration based upon the IL-6 ELISA pilot data (section 3.3.1), a concentration/response experiment was performed to assess the linearity of the VCAM-1 response, the sensitivity of the western blot as an experimental output and finally the reproducibility of the assay (Figure 3-4). The VCAM-1 response to TNFα concentrations in the range of 625 pg/mL to 2.5 ng/mL were log linear and detectable on an immunoblot. Overall inter-assay coefficient of variation was 16.4%.

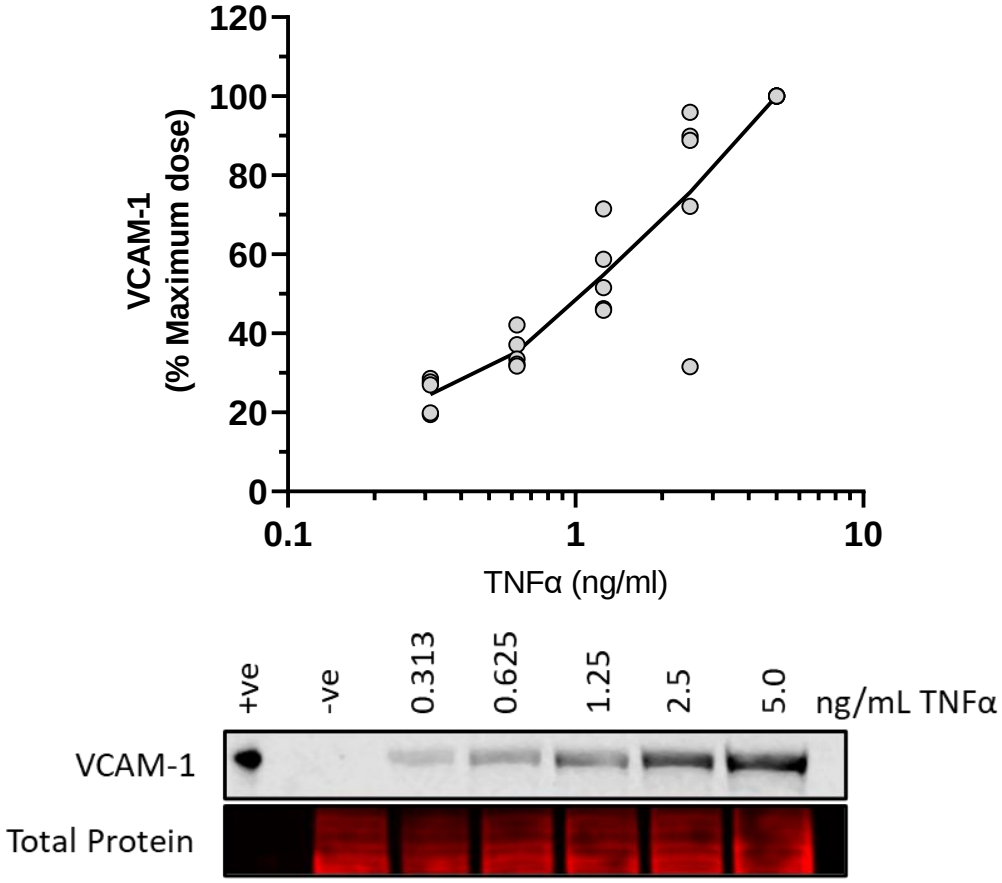

Figure 3-4 Concentration-response of VCAM-1 to TNFα in HMEC-1: HMEC-1 were exposed to a range of doubling TNFα concentrations for 24 hours. Line indicates mean with individual replicates, n = 5. Inter-assay average %CV= 16.4. +ve, recombinant human VCAM-1, -ve, untreated cells.

3.3.4 Pilot assessment of assay function

With the western blotting readout optimised and a suitable concentration of TNFα chosen to stimulate inflammation, a pilot assessment of the assay was performed using five control and five IGR samples from the M-FAT study. HDL

(100 µL) was pre-incubated with HMEC-1 for four hours followed by TNFα stimulation. Both control and IGR HDL inhibited TNFα stimulated VCAM-1 expression (Figure 3-5 A). However, the variability was high in both groups with function ranging from a 4% increase in VCAM-1 to 80% inhibition of VCAM-1 expression. Correcting for HDL apoAI content failed to reduce experimental variability (Figure 3-5 B). Correction by HDL cholesterol content (Figure 3-5 C) and protein (Figure 3-5 D) also failed to improve the variability of the assay. These findings led me to believe that there may be an interfering factor in the assay, potentially from residual salt in the HDL samples leftover from the isolation process.

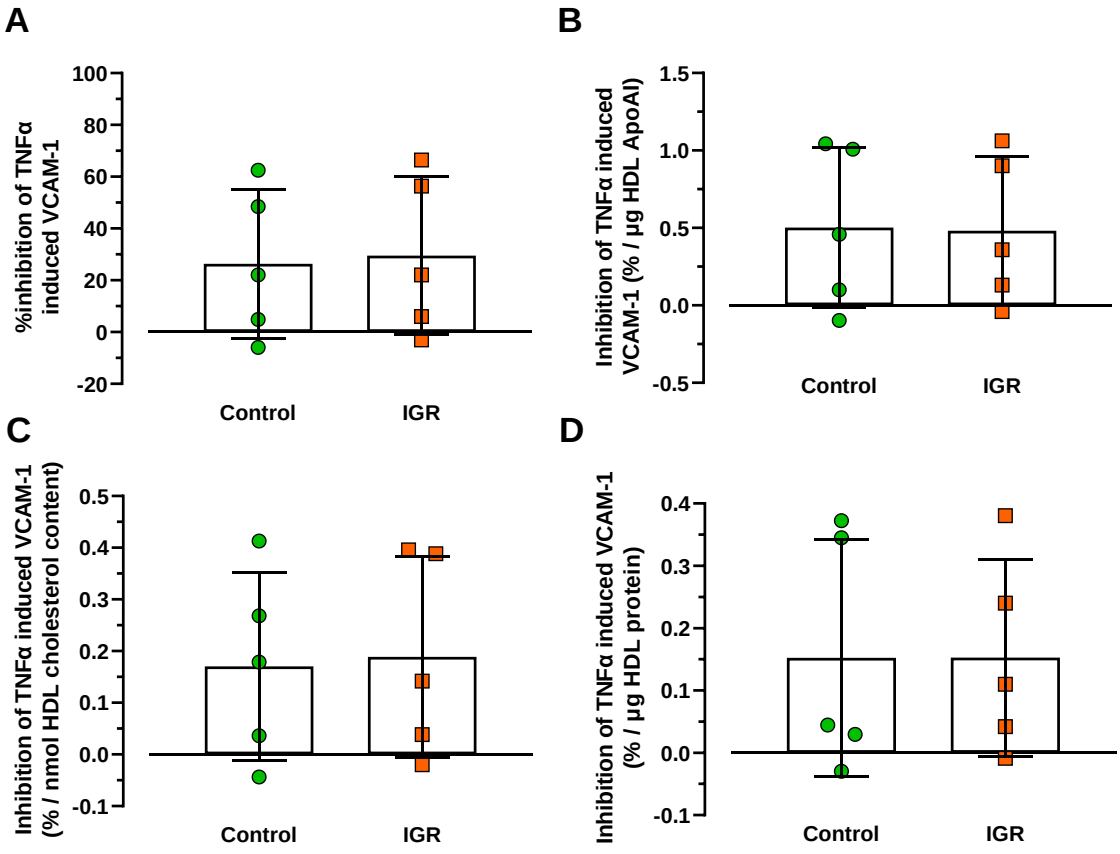

Figure 3-5 Pilot assessment of HDL function in the developing assay: HMEC-1 were pre-incubated with 100 µL HDL for 4 hours before 24 hours incubation in 5 ng/mL TNFα. Data is expressed as uncorrected % inhibition of TNFα induced VCAM-1, corrected per µg ApoAI, corrected per nmol HDL cholesterol content and per µg HDL protein. Bars indicate mean ± SD, n=5.

3.3.5 Establishing the effect of residual isolation buffer sodium bromide on endothelial VCAM-1

After desalting, isolated HDL fractions contain approximately 243 mM NaBr and consequently in the pilot assay cells are exposed to a final concentration of approximately 50 mM NaBr. Historically, isolated lipoproteins were desalted by dialysis in PBS. Based on the hypothetical dialysis of a 500 µL HDL sample in 5 L of PBS, the final NaBr concentration in the culture well would be ~ 5 µM. HMEC-1 were incubated in 5 µM and 50 mM NaBr in the presence and absence of TNFα to assess the impact of NaBr on the endothelial inflammatory response (Figure 3-6). NaBr (50 mM) ablated VCAM-1 expression in HMEC-1 both in the absence and presence of TNFα, while cells exposed to 5 µM NaBr in the presence of TNFα maintained the level of VCAM-1 expression.

Given the cellular response to NaBr, a concentration/response experiment was conducted to ascertain the relationship between NaBr and VCAM-1 expression in response to TNFα stimulation in HMEC-1 (Figure 3-7). NaBr at 100 mM caused cell death, while 50 mM and 25 mM concentrations inhibited VCAM-1 expression. NaBr concentrations between 12.5 mM and 0.39 mM did not affect VCAM-1 expression compared to TNFα alone.

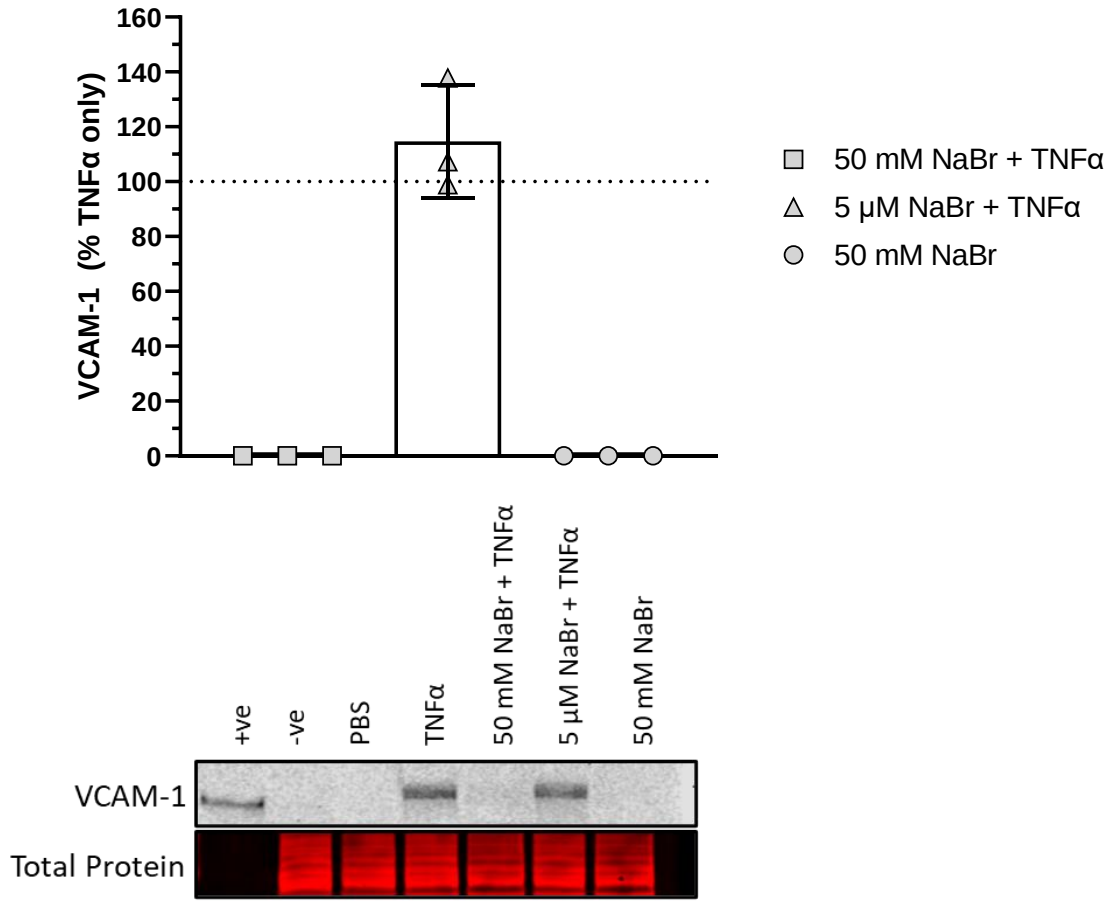

Figure 3-6 Assessment of the impact of residual NaBr on HMEC-1 inflammation: HMEC-1 were pre-treated with NaBr for four hours followed by 24 hours in the presence and absence of 5 ng/mL TNFα. Average %CV = 23.3%.

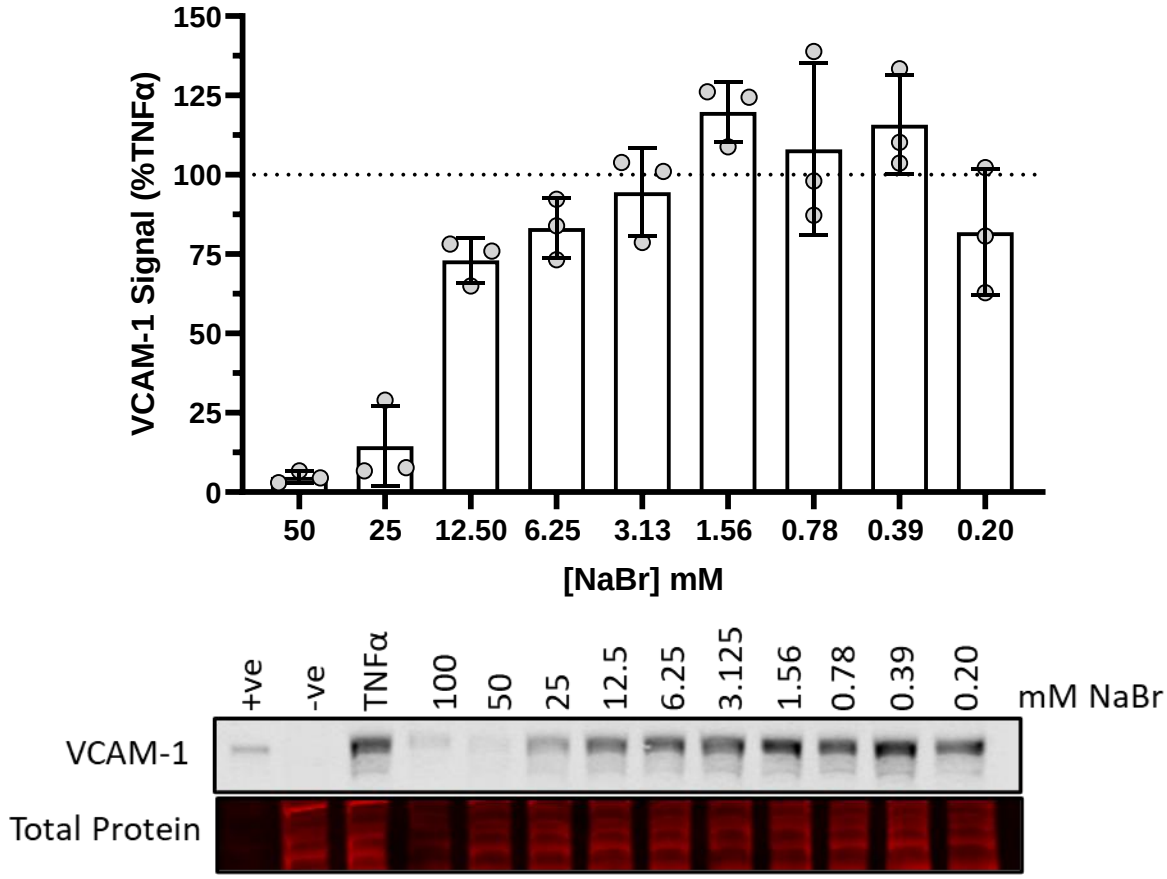

Figure 3-7 Concentration response of NaBr in the presence of 5 ng/mL TNFα
HMEC-1 were treated with doubling concentrations of NaBr for four hours followed by 24 hours in the presence of 5 ng/mL TNFα. Average %CV across concentrations 12.5 mM to 0.20 mM was 12.4%. Bars indicate mean ±SD, n = 3.

Desalting HDL fractions twice using desalting columns results in cells being exposed to approximately 1.56 mM NaBr, within the range of NaBr concentrations that do not affect VCAM-1 expression. Therefore, all subsequent assays were carried out using double desalted HDL preparations.

3.3.6 Selection of an appropriate HDL pre-incubation concentration and time exposure

Having chosen a TNFα concentration and identifying the effect of contaminating NaBr on assay performance, the appropriate concentration and duration of HDL treatment was assessed. HMEC-1 were pre-treated with pooled control group HDL for six, four, two and one hour(s) before the addition of 5 ng/mL TNFα, at concentrations ranging from 7.5 µg/mL - 120 µg/mL apoAI. No concentrations or preincubation durations reduced VCAM-1 expression below TNFα stimulation alone, though the six- and four-hour preincubations increased VCAM-1 the least

(Figure 3-8). Therefore, extended concentration response curves were performed with six- and four-hour HDL preincubations (Figure 3-9). There was no difference between the durations hence a 4-hour preincubation with HDL was chosen. ApoAI concentrations greater than 100 µg/mL reduced TNFα induced VCAM-1 expression.

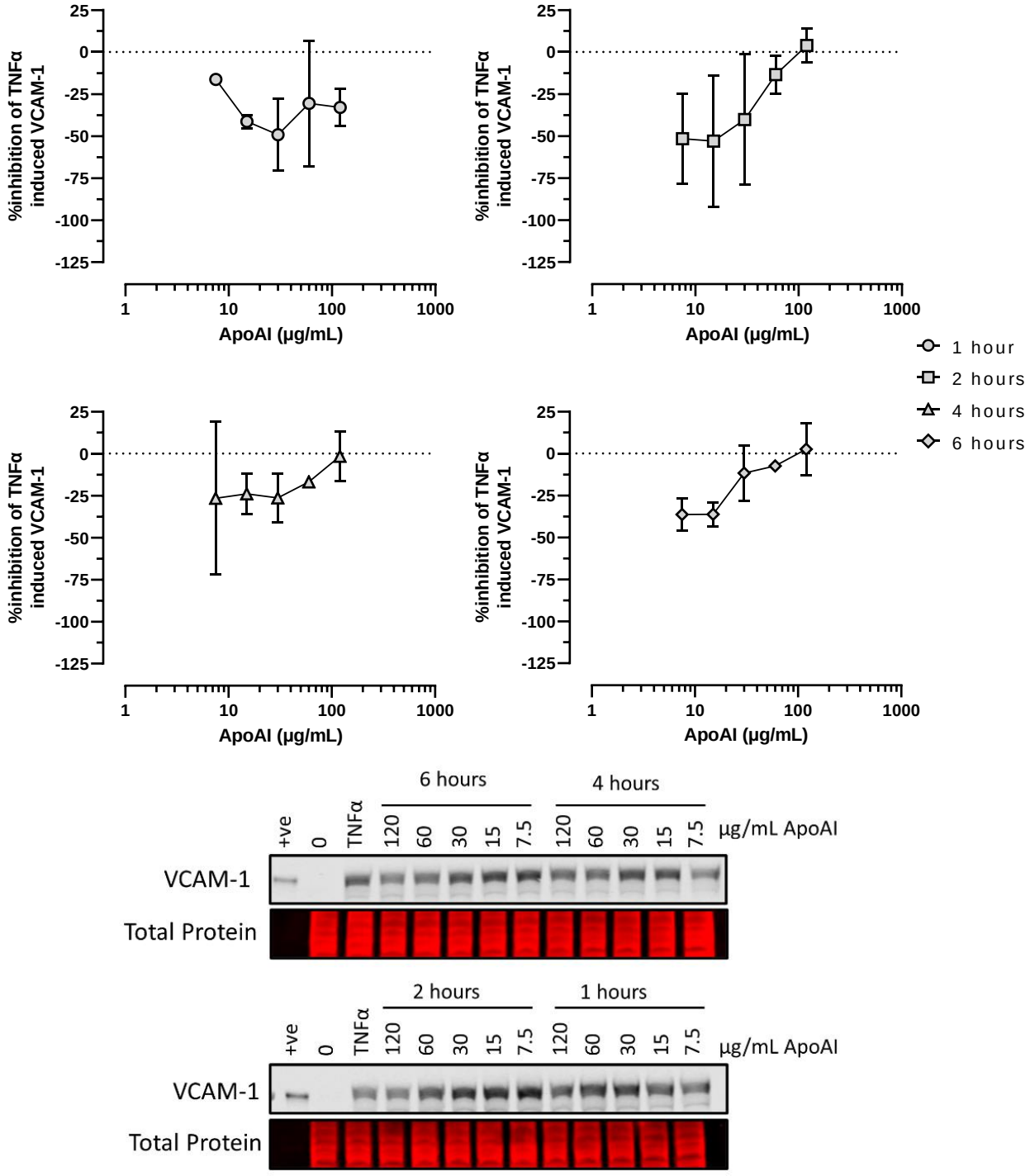

Figure 3-8 Initial HDL concentration-/time- response curves: HMEC-1 were exposed to HDL at doubling concentrations based on apoAI content for 1, 2, 4 and 6 hours. Bars indicate mean ± SD, n = 3. Average %CV = 11.0.

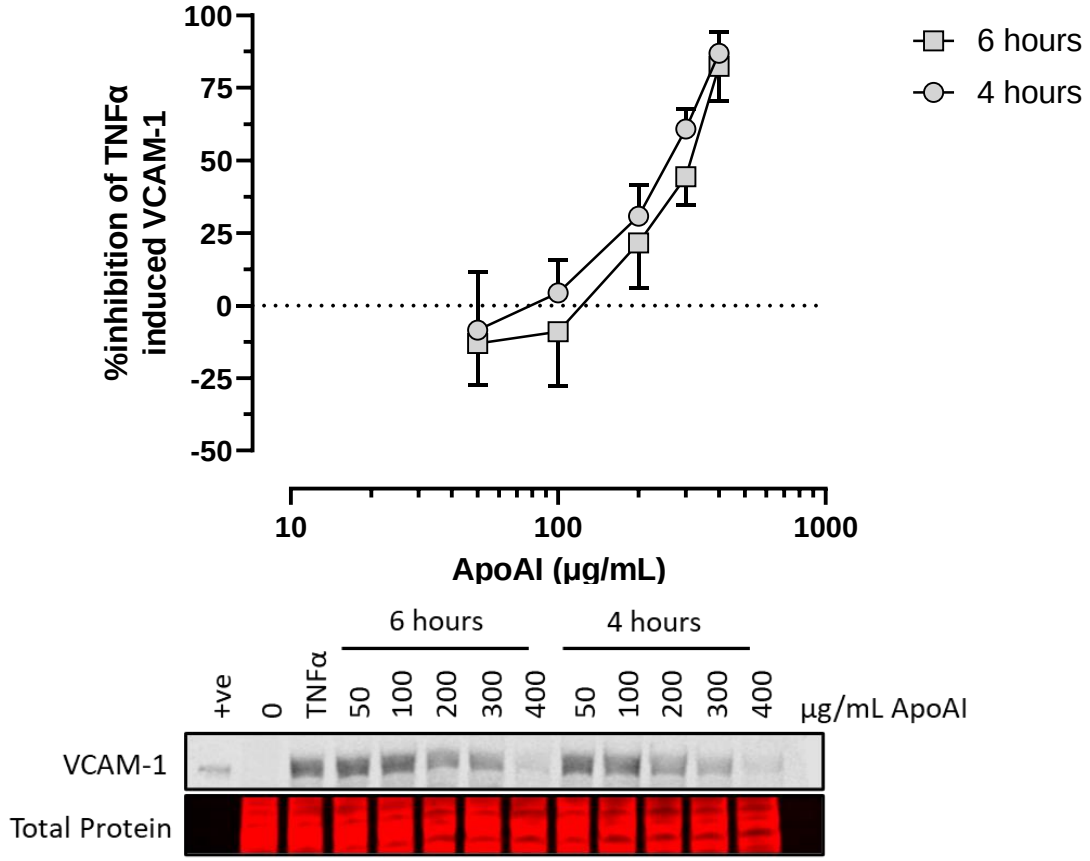

Figure 3-9 Extended HDL concentration-/time- response curves: HMEC-1 were exposed to increasing concentrations of HDL based on ApoAI for 4 and 6 hours. Bars indicate mean ± SD, n = 3. Average %CV at 300 µg/mL apoAI = 14.6. Average %CV at 400 µg/mL apoAI = 51.0.

3.3.7 Assay performance when storing isolated HDL with and without butylated hydroxytoluene

To ensure isolated HDL protein function was preserved against autooxidation during storage, a comparison was made between HDL stored in the presence and absence of 0.001% antioxidant BHT. Storage with BHT for one month did not affect the anti-inflammatory function of HDL (Figure 3-10) and was therefore not used for storage of HDL.

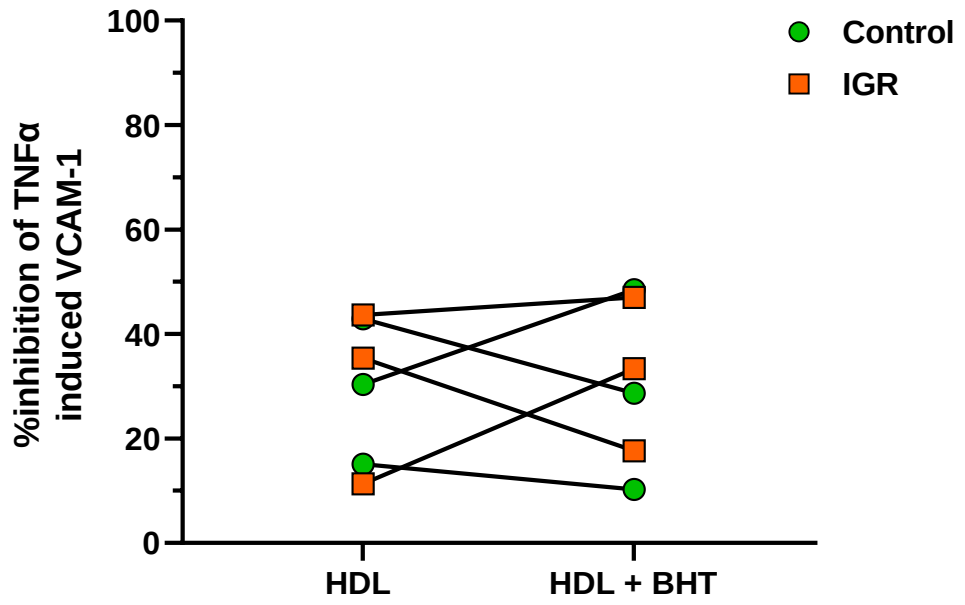

Figure 3-10 Assay performance when HDL stored with and without 0.001% butylated hydroxytoluene: Before- after plot of same pooled HDL samples stored in the presence and absence of 0.001% BHT. Individual values plotted.

3.3.8 Cell viability in diluted media

As HDL apoAI concentration varies between individuals, the volume of HDL added to each well of cells for a concentration of 300 µg/mL apoAI also varies. This has the effect of diluting the culture media. To ensure that dilution of the cell media did not affect cell viability and therefore introduce variability into the assay, cells were grown in cell culture media for the full length of the assay (28 hours) in dilute media. Cell viability across all dilutions averaged 84.57% (Figure 3-11). Thus, volume of HDL added did not affect the performance of the assay.

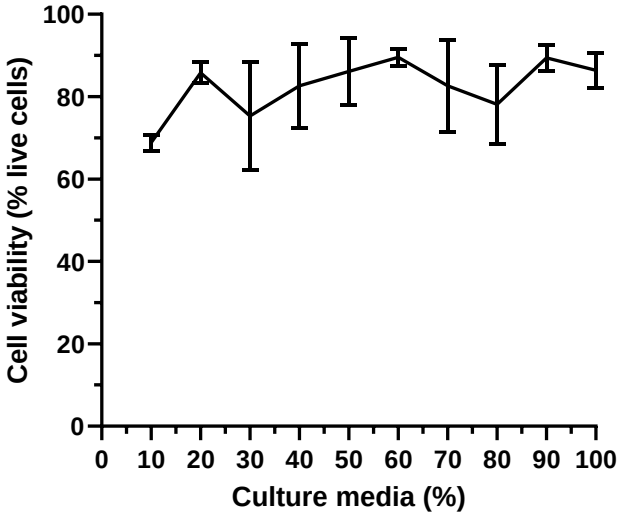

Figure 3-11 Cell viability in diluted culture media: HMEC-1 were incubated for 28 hours in reducing concentrations of complete culture media diluted in DPBS and assessed for viability using a Nexcelcom Cellometer. Bars indicate mean ± SD, n = 3.

3.3.9 Investigating the effect of TNFα on nitric oxide generation

In order to assess the ability of HDL to reduce inflammation-related nitric oxide generation, the effect of TNFα stimulation on NO production was assessed. NO production resulting from TNFα (5 ng/mL) stimulation was highly variable (%CV = 75.1) and ranged from no increase in NO to a five-fold increase in NO compared to untreated cells (%CV = 19.1) (Figure 3-12).

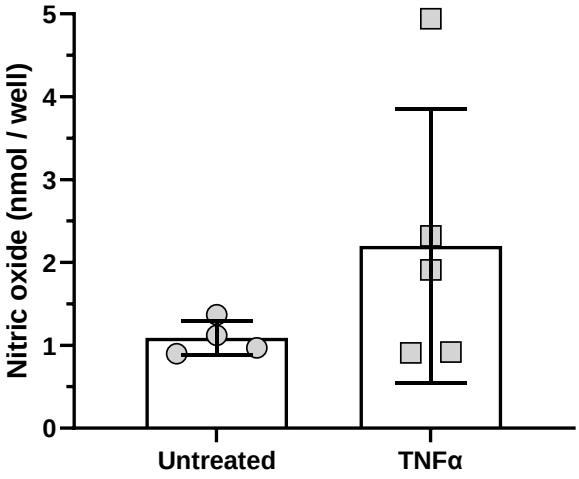

Figure 3-12 The effect of TNFα on HMEC-1 nitric oxide production: HMEC-1 were incubated in the presence or absence of 5 ng/mL TNFα for 24 hours and the amount of nitric oxide produced by the endothelial monolayer measured. Bars indicate mean ± SD, untreated n = 4, TNFα n = 5.

3.4 Discussion

This chapter set out to establish an endothelial cell-based assay to determine HDL's ability to provide vascular protection through its anti-inflammatory function. This involved the selection of the appropriate concentration of TNFα to invoke maximal endothelial inflammation and the optimisation of western blotting for VCAM-1. Pilot experiments revealed the need to adjust the HDL isolation protocol to remove interfering NaBr, and the effect of storage with and without supplementary antioxidant was explored. The viability of cells in diluted media was assessed, as was the suitability of this experimental design for the measurement of endothelial nitric oxide generation. The established assay was used to assess HDL function in individuals with varying degrees of insulin sensitivity and resistance. It was also used to relate HDL composition to its function. Establishing changes in HDL functionality during insulin resistance may go some way to improve understanding of the pathophysiology of metabolic disease and potentially suggest novel therapeutic targets.

Endothelial inflammation in response to TNFα stimulation was first measured by IL-6 secretion into the culture media. IL-6 acts as the initial signal of endothelial injury and inflammation and has pleotropic inflammatory and immune effects. IL-6 can be seen as a general marker of non-specific endothelial inflammation (Müller and Griesmacher, 2000) and therefore IL-6 secretion by HMEC-1 in response to TNFα indicates the overall inflammatory status of the cell. Overstimulation with TNFα may cause an irretrievable inflammatory response in HMEC-1 which may mask the specific VCAM-1 pathway under interrogation. The TNFα concentrations selected for this pilot were based on commonly used concentrations in similar assays (such as by Muñoz-Vega et al., 2018 and Lemmers et al., 2021). IL-6 secretion into the media after TNFα stimulation was highest and most reproducible at 5 ng/mL for 24 hours, therefore this concentration of TNFα was selected to maximally stimulate endothelial inflammation.

Western blotting was chosen as the readout for my adaptation of this anti-inflammatory assay. Western blotting is fast and relatively inexpensive to perform and with appropriate controls can be semi-quantitative. Having optimised the blotting procedure, the appropriate concentration of TNFα to

stimulate VCAM-1 expression was chosen based on a concentration/response curve, with the maximum concentration derived from the pilot IL-6 data. Despite the multiple opportunities for variation to occur in the western blotting protocol, such as gel loading and variable binding of primary and secondary antibody incubations, overall inter-assay coefficient of variation was 16.4% across all concentrations. The VCAM-1 expression in response to TNFα was linear. VCAM-1 signal at all tested TNFα concentrations was detectable. These findings demonstrate the applicability of TNFα induced inflammation and sensitivity of western blotting as an experimental output.

A pilot test of the assay with a 4-hour preincubation, based upon Lemmers et al., (2021), of 100 µL control and IGR HDL yielded highly variable results. The variability persisted even after correction for the key HDL components apoAI, cholesterol and protein, with some samples increasing VCAM-1 expression in HMEC-1. Sodium bromide sequential density centrifugation for HDL isolation results in a significant concentration of NaBr in the isolation buffer, despite desalting, therefore, the possibility of NaBr interfering with the assay was explored. An initial experiment identified that endothelial cells treated with 50 mM NaBr with and without TNFα, failed to induce VCAM-1 expression. Historically, HDL desalting was performed using dialysis, in this case resulting in ~5 µM remaining NaBr. This concentration of NaBr did not impair TNFα induced VCAM-1 expression. However, dialysis is a time-consuming process requiring a large volume of buffer. Based on a 500 µL HDL sample, 5L of PBS would be required. As such, a concentration/response experiment was performed with halving concentrations of NaBr to explore the impact of residual salt on TNFα induced VCAM-1 expression in HMEC-1. High concentrations of NaBr either caused cell death or severely impaired VCAM-1 expression compared to TNFα alone, while concentrations of NaBr between 12.5 mM and 390 µM did not appear to affect VCAM-1 expression. Given that the desalting columns used in the present protocol remove ~90% of remnant salt, it was decided that two passes through the column would result in a final concentration of NaBr of approximately 1.56 mM, removing sufficient salt as to prevent interference in the assay. Though the effect of remnant NaBr has been diminished in the context of this anti-inflammatory assay, it is not clear how remnant NaBr may affect HDL compositional measures such as proteomics. Other HDL isolation

techniques include using iodixanol, an inert polymer that readily forms density gradients under ultra-centrifugal forces, such as in the method developed by Harman, Griffin and Davies, (2013). A comparison of these techniques by Lemmers et al., (2021) showed comparable anti-inflammatory function but further investigation into HDL isolation method effects on downstream HDL composition and function is warranted.

With interfering excess salt now removed from the isolated HDL, experiments were performed to select an appropriate dosing concentration and duration of HDL pre-treatment for optimal anti-inflammatory function. These experiments used pooled control HDL to minimise individual variation. Cells can be exposed to HDL by protein content, cholesterol or by specific functional proteins such as apoAI. ApoAI was chosen as the method by which to expose cells to HDL in this assay as it is the primary and most abundant functional protein on HDL (Soran et al., 2012). There is not a consensus in the literature as to the best method for dosing HDL and no one method is superior to the others. HDL has been exposed to cells based on apoAI (Lemmers et al., 2021), HDL total protein (Vaisar et al., 2018) and by HDL total cholesterol (Annema et al., 2016). As HDL carries multiple apoAI molecules and HDL-C varies between individuals, dosing by apoAI may mean that cells are exposed to different HDL and protein concentrations. For this reason, HDL-C was later included as a covariate when comparing HDL function between individuals. HDL anti-inflammatory function was also expressed in terms of function per nmol cholesterol and µg protein exposed to the cells for context.

Cells were first treated with between 7.5 – 120 µg/mL apoAI for 1, 2, 4, and 6-hour pre-TNFα. This range of concentrations was not sufficient to reduce VCAM-1 expression, though the 4- and 6-hour time courses tended towards reduced expression with the least variability across the concentrations. On extending the range of concentrations to between 50 and 400 µg/mL ApoAI, pre-treating HMEC-1 with pooled control HDL was shown to reduce VCAM-1 expression in response to TNFα. As there was no significant difference between 4- and 6-hour preincubation with HDL, 4 hours was selected for experimental efficiency. ApoAI exposed to cells at 300 µg/mL and 400 µg/mL were most effective at reducing VCAM-1 expression. As the 400 µg/mL concentration was almost completely

inhibiting the VCAM-1 expressed by stimulated HMEC-1, 300 µg/mL apoAI was chosen, with a CV of 14.6%. This resulted in approximately 60% inhibition of TNFα-induced VCAM-1 expression, allowing for the detection of increased and decreased anti-inflammatory function within the limits of detection of the assay.

The isolation buffers used in the ultracentrifugation protocol contain EDTA to prevent oxidation of the HDL-bound proteins, however, this may be lost after desalting. Oxidation is known to affect protein function (Hawkins and Davies, 2019) which may confound the outcomes of this assay. Isolated HDL fractions were therefore stored in the presence or absence of 0.001% BHT and compared for HDL anti-inflammatory function. BHT is commonly used as a food and pharmaceutical industry antioxidant (Lambert et al., 1996). BHT did not improve the function of HDL in this assay and so was not added to the storage protocol.

Variation in individual HDL-C results in differing volumes of HDL for a final concentration of 300 µg/mL apoAI per well of cells. This dilutes the culture media and may affect cell viability. Cell viability remained consistent with diluted media, likely as a result of HMEC-1 being an immortalised cell-line. Early characterisation of HMEC-1 compared to their primary counterparts demonstrated that the cells proliferate in the absence of serum (Ades et al., 1992), suggesting that the cells are capable of survival in low nutrient and growth factor environments. The same authors noted that HMEC-1 grown in varying concentrations of serum were regularly > 99% viable, higher than the findings in this chapter. This is likely due to the 28-hour protocol without the media being refreshed, and the fact that cells were grown to confluent monolayers before experimentation. Dosing with TNFα instigates a strong inflammatory response which increases the metabolic demand on the cells, the result of which is increased cell-toxic waste product concentration in the media and cell death. The death of approximately 15% of cells in a given well in the face of a maximally inflammatory cytokine concentration in this experimental system is therefore not unsurprising and tolerable given experimental conditions.

In this experimental system, the ability to assess HDL inhibition of inflammation-induced NO is hampered by the variability of the endothelial NO response to TNFα. As the large number of study samples to be assayed will need to be split across several culture plates, consistency of the cellular response to TNFα is key to reproducible and interpretable results. While the adhesion molecule response to TNFα was consistent, the NO response was highly variable with a coefficient of variation of 75.1%. This may be due to the duration of this iteration of the assay. In order for iNOS to respond to an inflammatory stimulus it must first be transcribed into mRNA at the gene level and translated into functional protein. It may be that 24 hours is insufficient to enable sufficient iNOS to be translated, leading to variable iNOS induction in TNFα treated cells. As the study plasma samples utilised in this thesis to explore the effect of insulin resistance on HDL function have already been heavily used for their original projects, the volume of plasma remaining precluded the re-design and optimisation of an assay able to assess this facet of HDL protection.

This assay was established using sodium bromide sequential density ultracentrifugation to isolate HDL from participant plasma. Though twice desalting isolated HDL removed the effect of residual NaBr, it was not clear how remnant salt may affect other measures of HDL composition and function. To assess this, the next step was to compare sodium bromide sequential density ultracentrifugation isolated HDL with iodixanol density gradient ultracentrifugation isolated HDL in terms of composition and function. This comparison was performed in the proceeding chapter.

4 A comparison of HDL isolation techniques for subsequent compositional and functional measures

4.1 Introduction

Though the effect of excess sodium bromide left over from sequential density ultracentrifugation was addressed in the context of the HDL anti-inflammatory assay described in the previous chapter, it is unclear how the method used to isolate HDL from plasma might affect measures of HDL composition and function. This is particularly pertinent to salt-based lipoprotein isolation procedures given the high ionic strength of the density buffers and the potential impact this may have on the structure and protein composition of HDL (Timasheff, 1993). For this reason, this chapter aimed to compare sodium bromide sequential density ultracentrifugation (UC_{NaBr}) to iodixanol density gradient ultracentrifugation (UC_{Iodix}) which does not use salt.

Iodixanol is a biologically inert, water soluble 1550 kDa molecule (structure shown in figure 4-1), used clinically as a contrast agent during x-ray imaging. Iodixanol readily forms density gradients and is isotonic with plasma and as such has been used to separate fractions of interest from mixed biological samples including subcellular fractionation of cultured adipocytes (Sadler et al., 2016), the isolation of motile spermatozoa before assisted reproduction (Harrison, 1997) and purifying pancreatic islet cells before clinical transplantation (Noguchi et al., 2009). The use of iodixanol to separate plasma lipoproteins was first established by Graham et al., (1996) as an alternative to salt-based isolation methods. This method was further refined for the isolation and assessment of the major LDL subclasses (Davies et al., 2003) using pre-stained plasma before a similar protocol was developed for HDL (Harman et al., 2013).

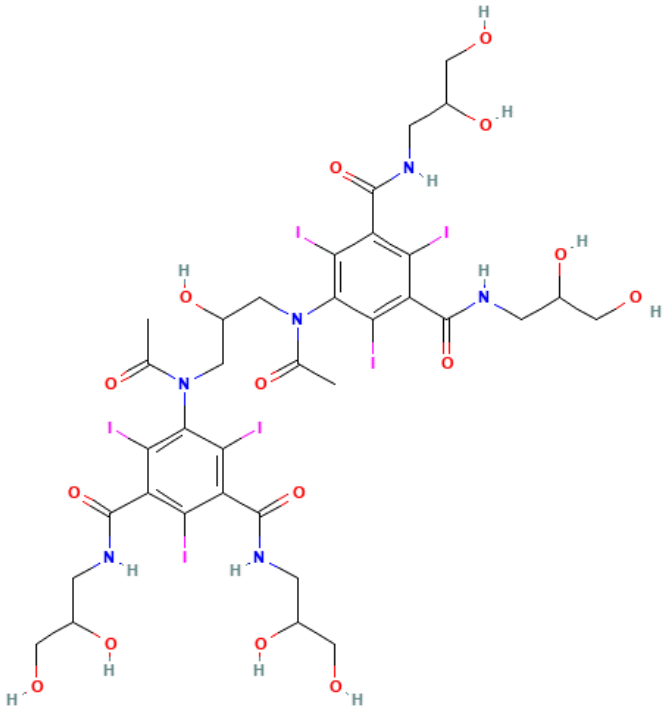

Figure 4-1 Molecular structure of iodixanol Structure sourced from the PubChem library (PubChem CID 3724, https://pubchem.ncbi.nlm.nih.gov/compound/Iodixanol#section=2D-Structure)

Due to the lack of a near vertical ultracentrifuge rotor in Glasgow, HDL was isolated from participant plasma by UC_{Iodix} by the author at Liverpool John Moores University with Dr Ian Davies, who was involved in the optimisation of UC_{Iodix} for LDL and HDL subclass distribution analysis. The same samples were isolated by UC_{NaBr} in Glasgow before a comparison of HDL composition and anti-inflammatory function was performed.

4.1.1 Aims

- To compare the content of the core HDL compositional measures apoAI, total protein and total cholesterol after UC_{NaBr} and UC_{Iodix}.
- To compare the size distribution of HDL after UC_{NaBr} and UC_{Iodix}.
- To determine the proteomic composition of HDL isolated by UC_{NaBr} and UC_{Iodix}.
- To compare the anti-inflammatory function of HDL isolated by UC_{NaBr} and UC_{Iodix} using the endothelial cell assay established in the previous chapter.

4.2 Methods

4.2.1 Samples selected for comparison

Initially, the recruitment and blood sampling of healthy volunteers was planned to generate a pool of healthy HDL for the optimisation of the assay described in chapter 3 and subsequent comparison of HDL isolation techniques described in this chapter. Due to the COVID-19 pandemic and a laboratory fire, this plan could not be enacted. Instead, a random selection of five control and five IGR samples from the M-FAT study (chapter 7) were used to compare the isolation techniques. IGR samples were included to assess whether HDL from this group behaved differently depending on the isolation technique used. Demographics for the samples can be found in table 4-1. As these samples were derived from an archival study collection, five samples from each group were chosen to reduce the impact on sample volume and availability for later analysis.

Table 4-1 Demographic and anthropometric measures of study participants to compare UC_{NaBr} and UC_{Iodix} isolation of HDL from plasma. Data expressed as mean ± SD. Comparisons made using Welch's t test. Statistical significance was assumed at $p < 0.05$.

	Control (n = 5)	IGR (n = 5)	p value
Age (years)	48.0 ± 8.8	52.2 ± 5.9	0.46
BMI (kg/m^2)	24.5 ± 1.2	30.7 ± 1.2	<0.001
Fat %	21.5 ± 3.6	33.5 ± 4.9	0.005
Systolic BP (mmHg)	127 ± 12	141 ± 8	0.10
Diastolic BP (mmHg)	78 ± 6	92 ± 4	0.006
VO_2 max (ml/kg/min)	32.00 ± 5.33	28.80 ± 3.19	0.34
HbA1c (mmol/mol)	32.00 ± 2.76	48.40 ± 6.62	0.005
Total cholesterol (mmol/l)	4.84 ± 1.29	5.28 ± 0.65	0.57
Triglyceride (mmol/l)	1.14 ± 0.45	2.02 ± 1.07	0.19
HDL cholesterol (mmol/L)	1.28 ± 0.34	1.20 ± 0.18	0.70
Matsuda index	6.67 ± 1.63	1.89 ± 0.50	0.003
$HOMA_{IR}$	1.19 ± 0.26	5.26 ± 1.94	0.013

4.2.2 Isolation of HDL

HDL was isolated from participant plasma using both UC_{NaBr} and UC_{Iodix} (detailed in section 2.2). For cell culture experiments, the top 250µL HDL was retained to increase HDL concentration after UC_{NaBr}. HDL was isolated from the plasma of the same individuals using both techniques, however due to plasma volume constraints the plasma used in iodixanol density gradient ultracentrifugation was

a pool of the 15- and 30-minute timepoints of an oral 75g OGTT. These time points were chosen as HDL concentration and composition is minimally altered at this short time after food intake (Lewis and Cabana, 1996).

4.2.3 Measurement of HDL composition

HDL apoAI content was measured using ELISA as per section 2.10. HDL total protein was measured by Bradford assay (section 2.6). HDL cholesterol content was measured by colorimetric assay (section 2.7).

4.2.4 Measurement of HDL size distribution

HDL size distribution was measured with native gel electrophoresis as described in section 2.12.

4.2.5 Proteomic assessment of HDL protein composition

4.2.5.1 Buffers and solutions

Ammonium bicarbonate solution
50 mM ammonium bicarbonate in dH_2O.

Dithiothreitol solution
0.025 M dithiothreitol in ammonium bicarbonate solution.

Iodoacetamide solution
0.075 M iodoacetamide in ammonium bicarbonate solution.

Formic acid solution
0.1% v/v formic acid in dH_2O.

100% acetonitrile

80% acetonitrile solution
80% v/v acetonitrile in 0.1% formic acid.

60% acetonitrile solution
60% v/v acetonitrile in 0.1% formic acid.

4.2.5.2 Peptide isolation procedure

After UC_{NaBr}, HDL samples containing 10 µg protein as determined by Bradford assay were made up to a total volume of 30 µL with ammonium bicarbonate solution. After UC_{Iodix}, remnant iodixanol was removed from isolated HDL using five sequential 4X dilutions with 50 mM ammonium bicarbonate in a 3 kDa molecular weight cut off (MWCO) spin filter (Amicon Ultra 3 K device; Merck-Millipore, Germany) before a volume equating to 10 µg protein was taken for denaturation. Dithiothreitol solution (2 µL) was added, and the samples incubated at 60°C for 1 hour to denature the proteins and break disulphide bonds between cysteine residues of proteins. Samples were left to cool to room temperature before the addition of 2 µL iodoacetamide solution to prevent reformation of disulphide bonds. After 15 minutes at room temperature, 2 µL of trypsin stock solution was added and the samples incubated overnight at 37°C. The peptides were then vacuum dried in a SpeedVac at 35°C for 10 minutes before reconstituting the peptide pellet in 10 µL formic acid solution.

4.2.5.3 Peptide cleaning procedure

Isolated peptides were cleaned using 10 µL ZipTip pipette tips containing 0.6 µL C18 resin (Merck, #ZTC18S). A new ZipTip was activated by pipetting and dispensing three tip volumes of 100% acetonitrile and equilibrated with three tip volumes of formic acid solution. Peptides were loaded into the resin by gently aspirating and dispensing the same sample 10 times. Loaded peptides were washed with six tip volumes of fresh formic acid solution. Cleaned peptides were eluted from the resin by first aspirating and dispensing 10 times into 60% acetonitrile solution, followed by aspirating and dispensing 10 times into 80% acetonitrile solution. As each tip has the capacity to clean 5 µg peptides this cleaning process was repeated twice for each sample to retain 10 µg cleaned peptides. Peptides eluted in the 60% and 80% acetonitrile solutions were combined and dried in a SpeedVac at 35°C for 10 minutes, before reconstitution in formic acid solution. Protein concentration was measured with a NanoDrop ND-1000 UV-visible spectrophotometer by measuring absorbance at 280 nm. Proteins were diluted to 0.05 ng/mL with formic acid solution.

4.2.5.4 Nano liquid chromatography coupled to tandem mass-spectrometry (nLC-MS/MS)

Peptides isolated from HDL samples (200 ng) were separated with a C18 column (100 mm × 0.75 μm, Agilent Technologies, Santa Clara, CA, USA) using the Thermofisher EASY-nLC 1200 system. The mobile phase consisted of a linear gradient of 7 – 40% acetonitrile in 0.1% formic acid over 75 minutes, followed by 40-100% acetonitrile over 13 minutes and finally 2 minutes of 100% acetonitrile. Eluted peptides were transferred via electrospray ionisation to a QExactive HF mass spectrometer (Thermofisher) tandem mass spectrometer where peptide sequences were determined by the collision-induced dissociation method with data-dependent acquisition. Spectra were analysed using MaxQuant software version 2.0.2.0 (Max Planck Institute of Biochemistry, Martinsried, Germany) and peptides identified by comparison with the Uniprot/Swissprot human protein database. Only proteins with two unique peptides appearing in >50% of samples were considered as identified in the analysis. Protein content of HDL was expressed relative to all other proteins across all samples as a label-free quantitation (LFQ) intensity. This method eradicates the need for stable isotope labelling of peptides.

4.2.6 Assessment of HDL anti-inflammatory function

HDL anti-inflammatory function was measured using the assay described in chapter 3. Briefly, HMEC-1 were preincubated with HDL (based on 300 μg/mL apoAI) for four hours before the addition of 5 ng/mL TNFα for 24 hours. Cells were lysed according to section and SDS-PAGE / western blotting was performed for VCAM-1 according to section. Results are expressed as % inhibition of VCAM-1 expressed by cells treated with TNFα alone. Each culture plate contained untreated and TNFα only treated cells; samples were corrected for baseline VCAM-1 expression and normalised to the TNFα only control present on the same plate.

4.2.7 Statistical analysis

All data were analysed using mixed effects models, which can cope with parametric or non-parametric data so long as the resulting residuals are normally distributed. Statistical significance was assumed at $p < 0.05$.

Mixed effects models were performed using Minitab version 20. Proteomic heatmaps were plotted using standardised LFQ intensities. As LFQ intensities were deemed non-parametric, due to their relative nature and the preponderance of zero values, standardisation was performed using the median absolute deviation instead of standard deviation. For each observation, the median was subtracted and the absolute (i.e., positive) value taken and divided by the median. After adjusting for the median absolute deviation, the median of the standardised values was used to plot the heatmap. Bland-Altman analysis was performed to assess agreement between isolation methods where appropriate. The plot was created by plotting the difference in measured value between paired samples against the average measured value. The mean bias was calculated as the average difference between measured values. The limits of agreement were calculated as ± 1.96 standard deviations from the mean difference as per Altman and Bland (1983). All graphs were created using GraphPad Prism version 9.5.

4.3 Results

4.3.1 Description of ultracentrifugation outcomes in both isolation methods

4.3.1.1 Sodium bromide sequential density ultracentrifugation

UC_{NaBr} resulted in a floating layer of lipoproteins based upon the density solutions used. After the first ultracentrifugation with a layer of 1.063 g/mL NaBr solution, a layer of VLDL and LDL was seen at the top of the ultracentrifuge tube and removed. After the second ultracentrifugation using a layer of 1.21 g/mL NaBr solution, the floating lipoprotein layer contained HDL (Figure 4-2).

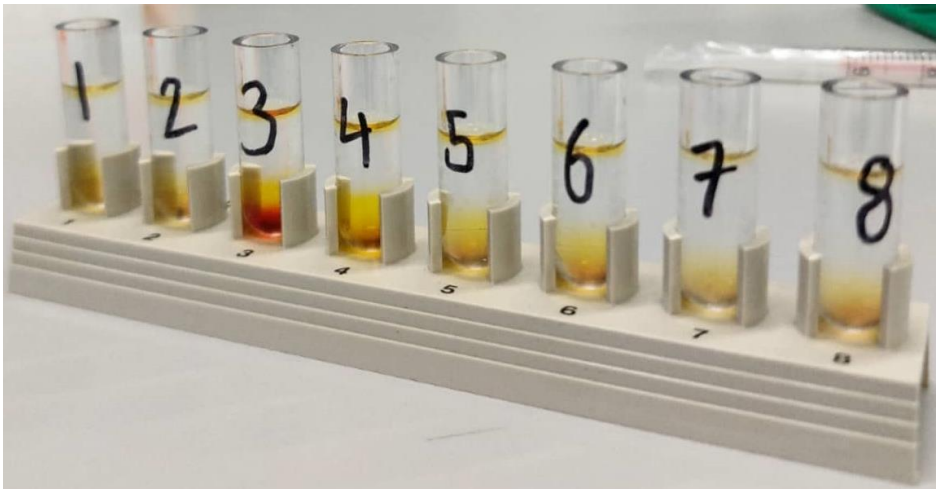

Figure 4-2 Photograph depicting ultracentrifuge tubes after the 1.21 g/mL centrifugation step of sodium bromide sequential density ultracentrifugation. HDL is the yellow band floating at the top of each ultracentrifugation tube.

4.3.1.2 Iodixanol density gradient ultracentrifugation

UC_{Iodix} resulted in three lipoprotein bands in the same ultracentrifuge tube, with VLDL and LDL appearing as a dark band at the top of the tube and HDL separated into the larger and less dense HDL 2 and the smaller and denser HDL 3 (Figure 4-3).

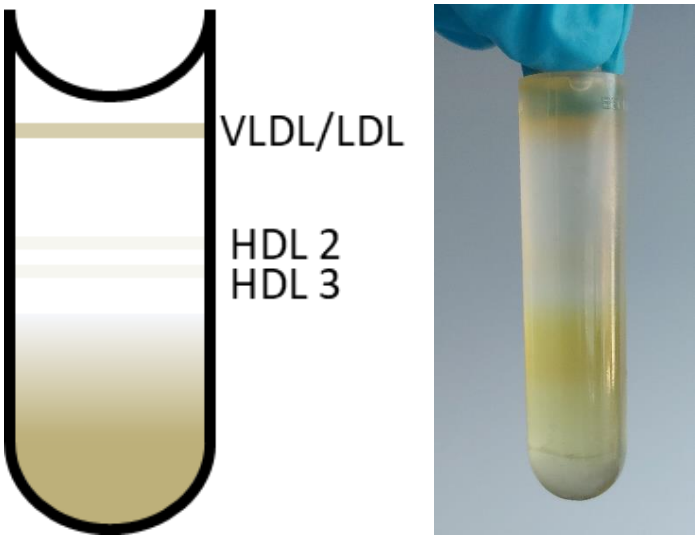

Figure 4-3 Depiction of the outcome of iodixanol density gradient ultracentrifugation. A labelled schematic of the ultracentrifuge tube after the separation of lipoproteins (left) as photographed (right).

Based on the density and apoAI content of each fraction, fractions 6-14 were deemed to contain HDL and were pooled together before concentrating back to the original volume of plasma (Figure 4-4).

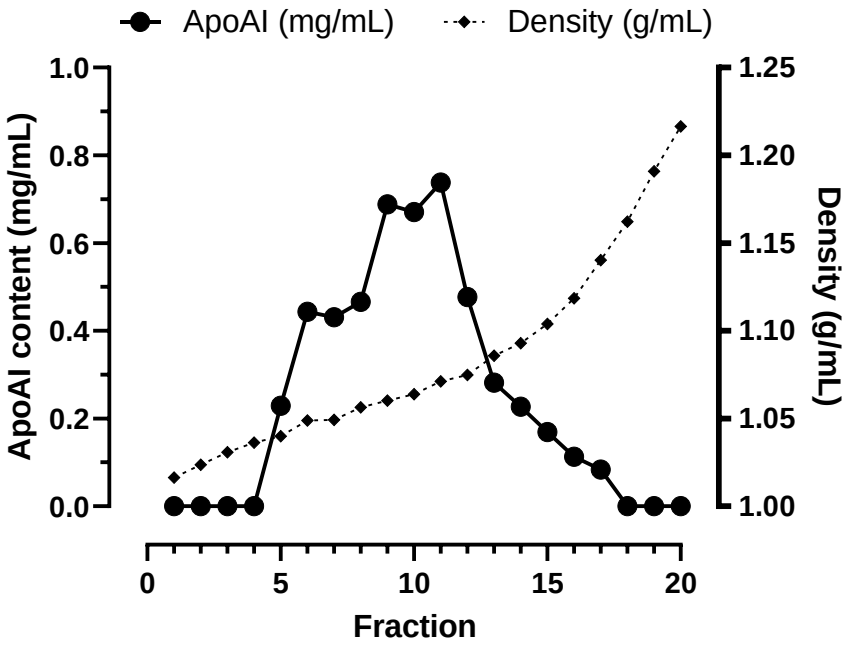

Figure 4-4 The apoAI content and density of each 500 µL fraction resulting from iodixanol density gradient ultracentrifugation. ApoAI content was measured by ELISA and the density of each fraction assessed with a refractometer.

4.3.2 HDL apoAI, total protein and cholesterol content after isolation by ultracentrifugation

HDL apoAI content did not differ by HDL isolation technique (Figure 4-5). However, HDL protein content was significantly higher after UC_{Iodix} compared to UC_{NaBr} (10.14 ± 1.49 mg/mL compared to 3.18 ± 1.10 mg/mL respectively, $p < 0.001$, mean ± SD, Figure 4-6). HDL cholesterol content was significantly lower after UC_{Iodix} compared to UC_{NaBr} (0.82 ± 0.32 mmol/L compared to 2.04 ± 0.59 mmol/L respectively, $p < 0.001$, mean ± SD, Figure 4-7). The interaction effect detected in HDL cholesterol existed between UC_{NaBr} control HDL and UC_{Iodix} IGR HDL which was not a useful comparison in the context of this chapter. A Bland-Altman plot for HDL cholesterol content showed the mean bias ± SD between the isolation methods was 1.22 ± 0.33 mmol/L and the limits of agreement were between 0.57 mmol/L and 1.86 mmol/L (Figure 4-8), with larger differences between the methods at higher HDL total cholesterol concentrations.

There was not a difference detected between control and IGR in any measure by isolation method.

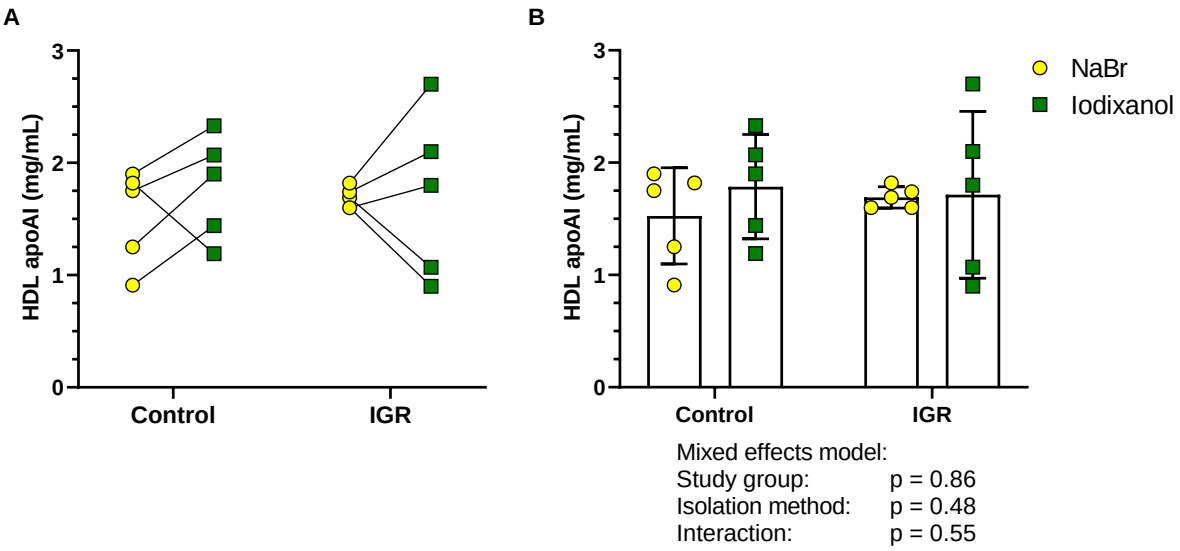

Figure 4-5 HDL apoAI content after sodium bromide sequential density ultracentrifugation and iodixanol density gradient ultracentrifugation. Data expressed as before after plots of individual samples (A) and mean ± SD (B). Comparisons were made using mixed effects model. Statistical significance was assumed at $p < 0.05$.

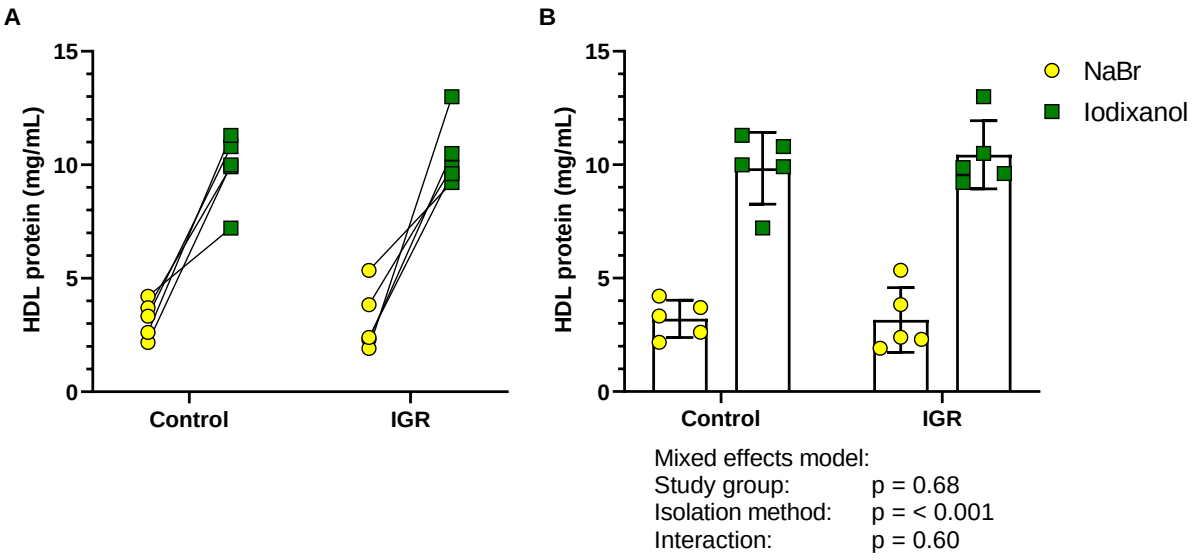

Figure 4-6 HDL protein content after sodium bromide sequential density ultracentrifugation and iodixanol density gradient ultracentrifugation. Data expressed as before after plots of individual samples (A) and mean ± SD (B). Comparisons were made using a mixed effects model. Statistical significance was assumed at $p < 0.05$.

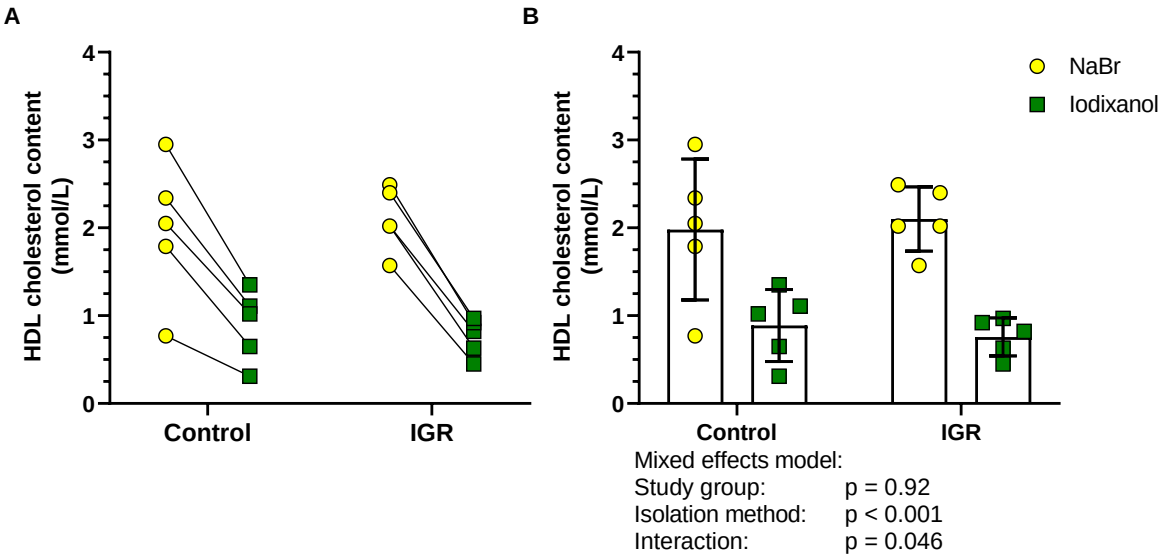

Figure 4-7 HDL cholesterol content after sodium bromide sequential density ultracentrifugation and iodixanol density gradient ultracentrifugation. Data expressed as before after plots of individual samples (A) and mean ± SD (B). Comparisons were made using mixed effects model. Statistical significance was assumed at $p < 0.05$.

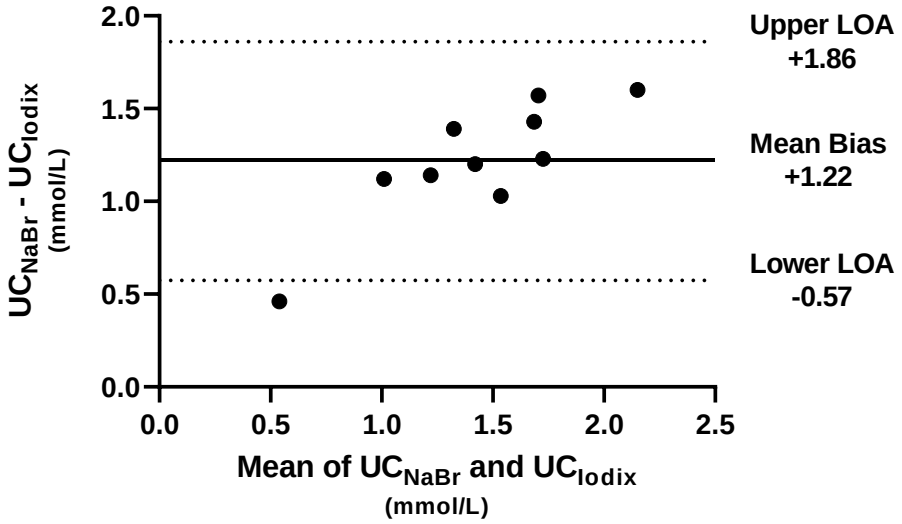

Figure 4-8 Agreement between HDL cholesterol content measures after UC_{NaBr} and UC_{Iodix} represented by Bland-Altman plot. The mean bias between the isolation methods was 1.22 mmol/L and the limits of agreement were between 0.57 mmol/L and 1.86 mmol/L. UC_{NaBr}, sodium bromide sequential density ultracentrifugation; UC_{Iodix}, iodixanol density gradient ultracentrifugation; LOA, limit of agreement.

4.3.3 HDL size distribution after isolation by ultracentrifugation

Native gel electrophoresis of UC_{NaBr} isolated HDL resulted in smooth lane profiles with peaks corresponding to each of the five HDL subclasses (Figure 4-9) and a small peak corresponding to the faint band at the level of the 5.4 nm marker on the gel. Electrophoresis of HDL isolated by UC_{Iodix} resulted in lanes with multiple

bands and a large band at 5.4 nm. The corresponding lane profiles were noisy as a result of the banding and the HDL subclasses could not be delineated (Figure 4-10).

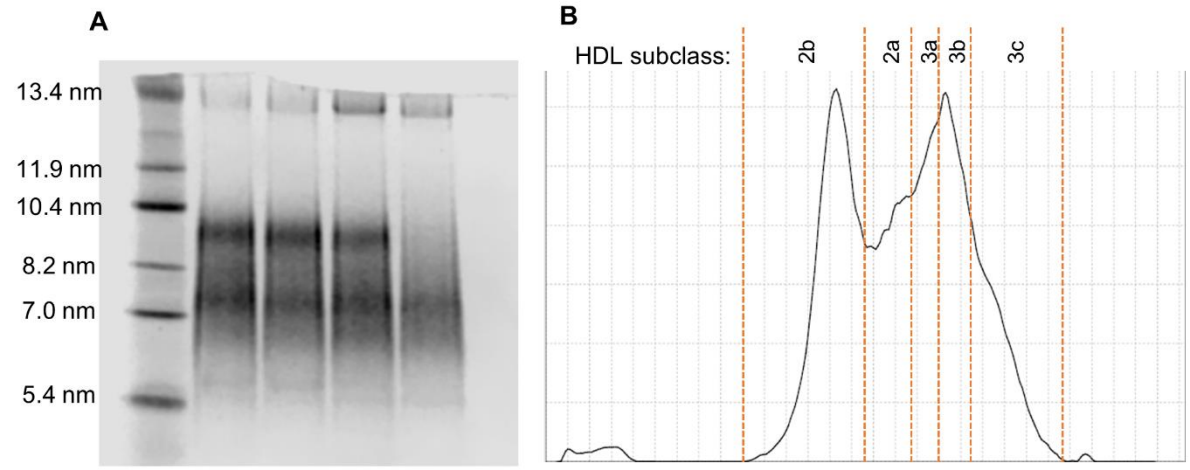

Figure 4-9 HDL size distribution after isolation by sodium bromide sequential density ultracentrifugation. (A) Coomassie blue stained electrophoresed HDL with marker particle diameters indicated. (B) Representative profile of lane 2 with peaks corresponding to each HDL subclass delineated.

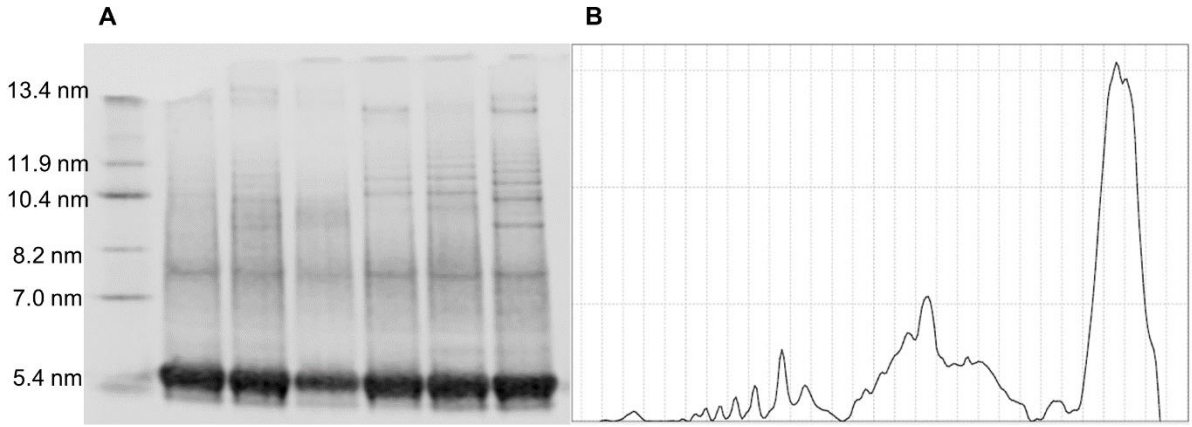

Figure 4-10 HDL size distribution after isolation by iodixanol density gradient ultracentrifugation. (A) Coomassie blue stained electrophoresed HDL with marker particle diameters indicated. (B) Peak profile of the rightmost lane of the gel.

4.3.4 Comparing the proteomic composition of HDL after isolation by ultracentrifugation

There were initially difficulties in preparing the UC_{Iodix} samples for proteomic analysis. After using the same peptide isolation and cleaning protocols as UC_{NaBr}, a broad peak centred around 244 nm was observed in UC_{Iodix} samples, but not in UC_{NaBr} samples, corresponding to iodixanol (Schröder et al., 1997) (Figure 4-11). This was removed by five sequential dilutions using 3 KDa MWCO centrifugal filters.

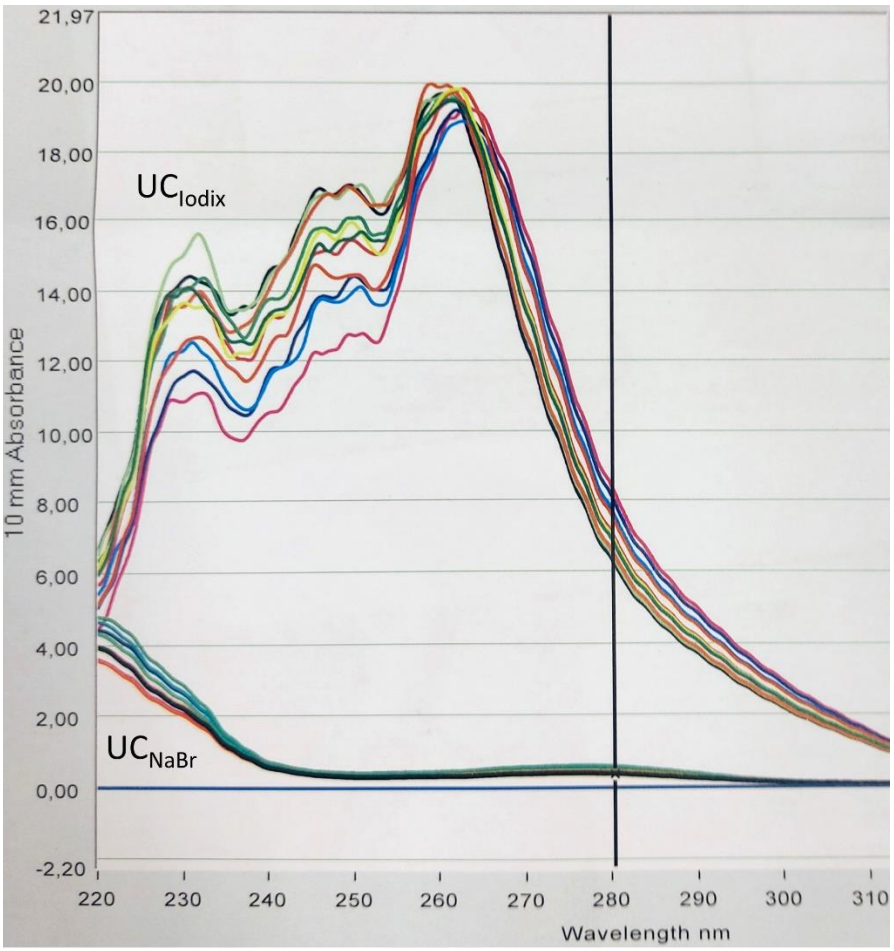

Figure 4-11 Absorbance spectra of UC_{NaBr} and UC_{Iodix} HDL peptides after isolation and cleaning. Peptide concentration was assessed by absorbance at 280 nm. The upper curves represent individual UC_{Iodix} HDL samples, and the lower curves indicate UC_{NaBr} HDL samples. The broad peak centred around 244 nm in the UC_{Iodix} samples corresponds to iodixanol.

With contaminating iodixanol removed, proteomic analysis of HDL isolated by both UC_{NaBr} and UC_{Iodix} revealed 133 proteins present in at least one HDL sample. HDL-associated proteins were identified by their presence in >50% of samples. Of the 133 proteins detected, 103 were deemed HDL-associated. Of those, 52 were

present on HDL isolated by both UC_{NaBr} and UC_{Iodix} (Table 4-2), 7 were present only on HDL isolated by UC_{NaBr} (including CETP and SAA-1, Table 4-3) and 44 were present only on HDL isolated by UC_{Iodix} (Table 4-4).

Table 4-2 List of proteins identified on HDL isolated by both isolation techniques.

Alpha-1-acid glycoprotein 1	Gelsolin
Alpha-1-acid glycoprotein 2	Haptoglobin-related protein
Alpha-1-antichymotrypsin	Hemoglobin subunit beta
Alpha-1-antitrypsin	Hemopexin
Alpha-1B-glycoprotein	Heparin cofactor 2
Alpha-2-antiplasmin	Ig alpha-1 chain C region
Alpha-2-HS-glycoprotein	Ig gamma-1 chain C region
Angiotensinogen	Kininogen-1
Antithrombin-III	Leucine-rich alpha-2-glycoprotein
Apolipoprotein A-I	Lumican
Apolipoprotein A-II	N-acetylmuramoyl-L-alanine amidase
Apolipoprotein A-IV	Phosphatidylcholine-sterol acyltransferase
Apolipoprotein B-100	Phospholipid transfer protein
Apolipoprotein C-I	Pigment epithelium-derived factor
Apolipoprotein C-II	Plasma protease C1 inhibitor
Apolipoprotein C-III	Protein AMBP
Apolipoprotein D	Retinol-binding protein 4
Apolipoprotein E	Serotransferrin
Apolipoprotein F	Serum albumin
Apolipoprotein L1	Serum paraoxonase/arylesterase 1
Apolipoprotein M	Tetranectin
Apolipoprotein(a)	Thyroxine-binding globulin
Beta-2-glycoprotein 1	Transthyretin
Clusterin	Vitamin D-binding protein
Complement C3	Vitronectin
Fibrinogen beta chain	Zinc-alpha-2-glycoprotein

Table 4-3 List of proteins identified only on HDL isolated by sodium bromide sequential density ultracentrifugation

Cholesteryl ester transfer protein
Complement C4-A
Fibrinogen alpha chain
Ig lambda-1 chain C regions
Serum amyloid A-1 protein
Serum amyloid A-4 protein
Serum paraoxonase/lactonase 3

Table 4-4 List of proteins identified only on HDL isolated by iodixanol density ultracentrifugation.

Actin, cytoplasmic 2	Ig kappa chain C region
Afamin	Ig kappa chain V-II region RPMI 6410
Attractin	Ig kappa chain V-III region B6
Beta-Ala-His dipeptidase	Ig lambda-6 chain C region
Carboxypeptidase B2	Ig mu chain C region
Carboxypeptidase N subunit 2	Immunoglobulin lambda-like polypeptide 5
Ceruloplasmin	Insulin-like growth factor-binding protein complex acid labile subunit
Coagulation factor IX	Inter-alpha-trypsin inhibitor heavy chain H1
Coagulation factor V	Inter-alpha-trypsin inhibitor heavy chain H2
Coagulation factor X	Inter-alpha-trypsin inhibitor heavy chain H3
Complement C1r subcomponent	Inter-alpha-trypsin inhibitor heavy chain H4
Complement C1s subcomponent	Kallistatin
Complement C4-B	L-selectin
Complement component C9	Phosphatidylinositol-glycan-specific phospholipase D
Complement factor B	Plasma kallikrein
Complement factor H	Proteoglycan 4
Complement factor H-related protein 1	Prothrombin
Complement factor I	Serum amyloid P-component
Corticosteroid-binding globulin	
Fibrinogen gamma chain	
Haptoglobin	
Hemoglobin subunit alpha	
Ig alpha-2 chain C region	
Ig gamma-2 chain C region	
Ig gamma-3 chain C region	
Ig gamma-4 chain C region	

The median standardised LFQ intensities of the proteins identified on HDL isolated by both ultracentrifugation techniques were plotted against each other in a heatmap (Figure 4-12). The heatmap revealed different abundances of identified proteins in each technique, with a higher relative abundance of apolipoproteins on HDL isolated by UC_{NaBr} and a higher relative abundance of inflammatory and coagulation related proteins on HDL isolated by UC_{Iodix}.

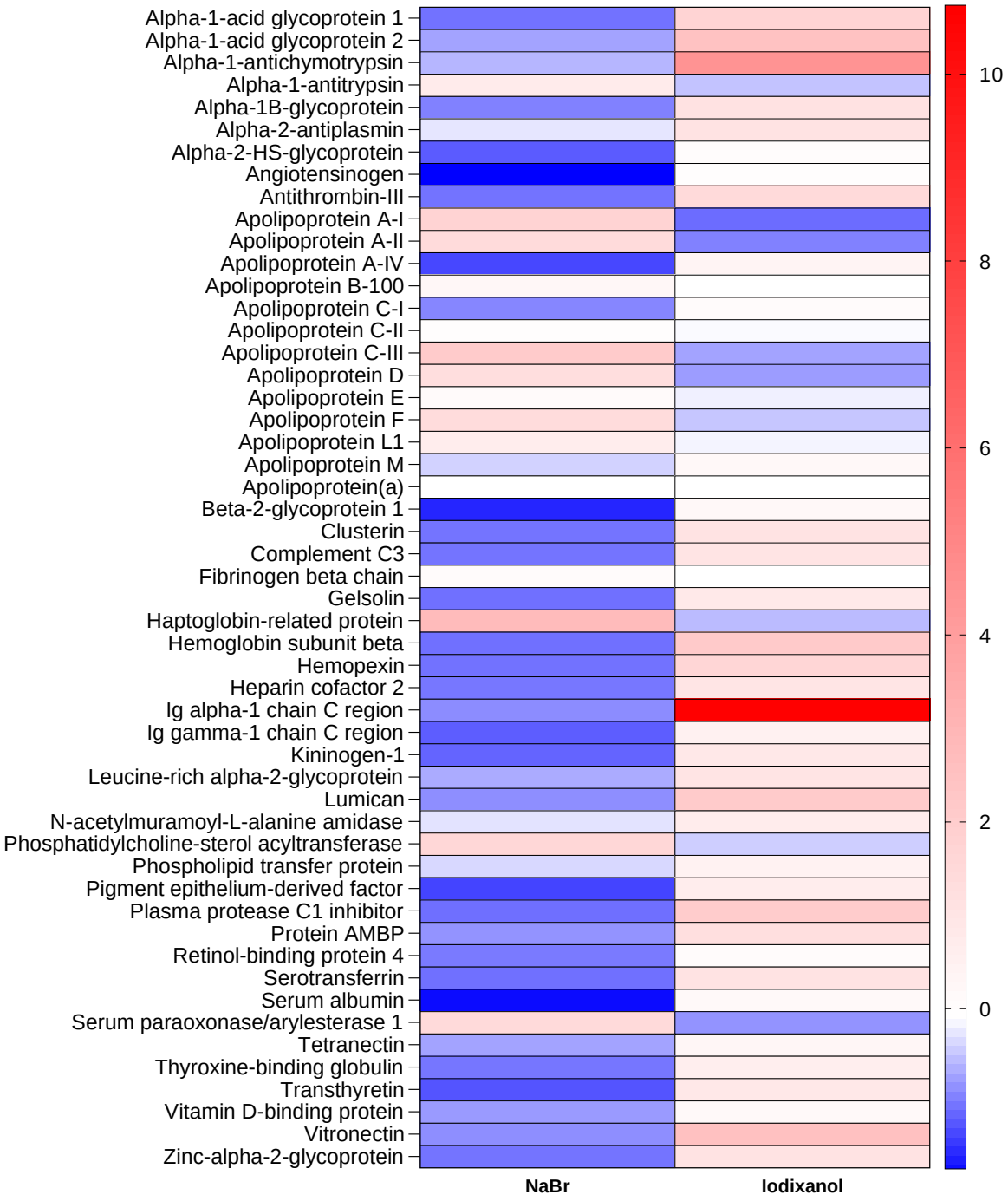

Figure 4-12 Heat map of the relative abundance of proteins identified in HDL isolated using both NaBr and Iodixanol. Heatmap plotted with the median median absolute deviation adjusted LFQ intensity for each protein.

Of the proteins identified on HDL from both isolation techniques, the LFQ intensities of the key HDL proteins apoAI, apoAII and PON-1 were all statistically significantly higher on HDL from UC_{NaBr} (Figure 4-13). There was not a difference between control and IGR in either isolation method.

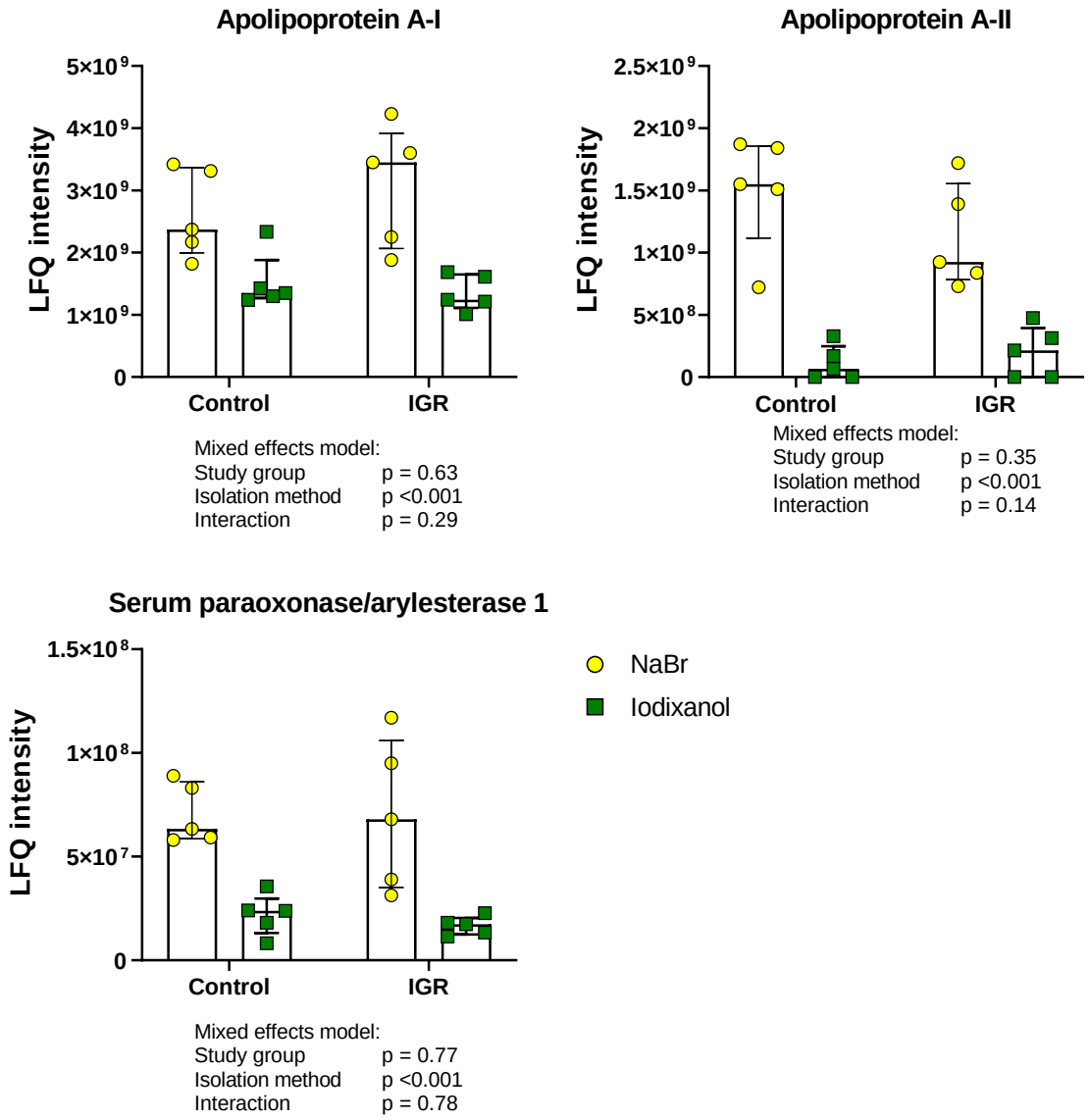

Figure 4-13 Abundance of selected HDL proteins identified on HDL from both NaBr and iodixanol isolation techniques. Data expressed as median ± IQR. Comparisons were made using mixed effects model. Statistical significance was assumed at $p < 0.05$.

4.3.5 The anti-inflammatory function of HDL isolated with each isolation technique

Using the assay established in the previous chapter, the anti-inflammatory function of HDL isolated by ultracentrifugation was compared. HDL isolated by UC_{Iodix} had greater ability to inhibit TNFα-induced inflammation in endothelial cells than HDL isolated by UC_{NaBr} (77.5 ± 4.4 % compared to 58.3 ± 4.8% respectively, mean ± SD, $p = 0.014$, Figure 4-14). There was not a difference between control and IGR in either isolation method.

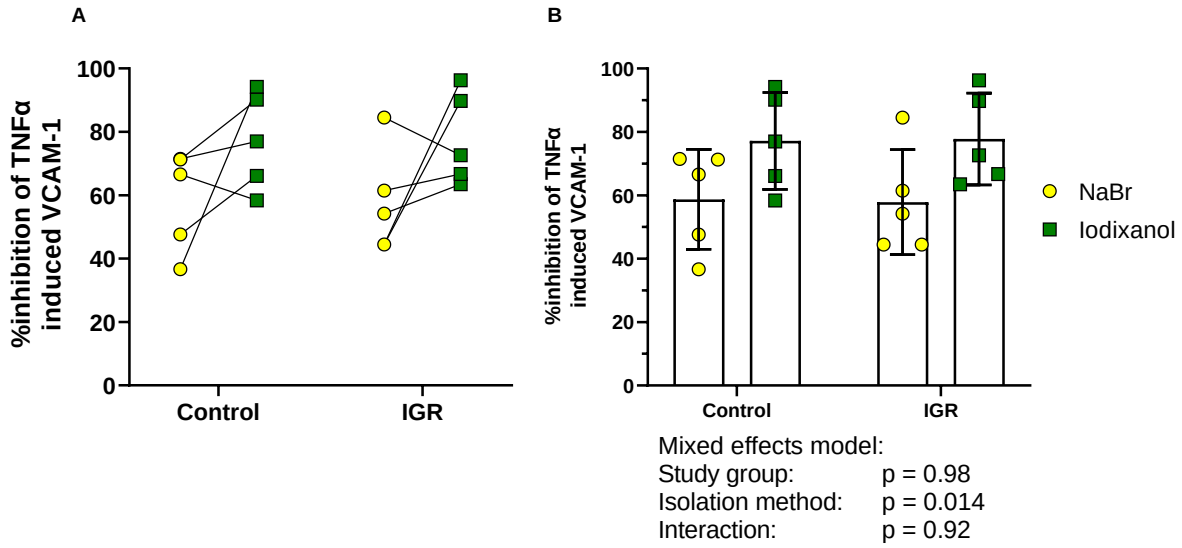

Figure 4-14 The effect of HDL isolation technique on HDL anti-inflammatory function. Data was expressed as before after plots of individual samples (A) and mean ± SD (B). Data expressed as inhibition of TNFα based on 300 µg/mL apoAI (B). Comparisons were made using mixed effects models. Statistical significance was assumed at $p < 0.05$.

4.4 Discussion

This chapter explored how HDL fractions isolated by both UC_{NaBr} and UC_{Iodix} differed compositionally, by size, and when used in endothelial cell assays of anti-inflammatory function, and whether control or IGR HDL responded differently to each isolation method. HDL was isolated at a lower density in UC_{Iodix}, likely as a result of the lower osmotic forces on the lipoprotein particle compared to UC_{NaBr}. HDL apoAI content did not differ between the isolation methods, however, a marked increase in HDL protein content and decrease in HDL cholesterol content were observed in HDL isolated by UC_{Iodix}. It was not possible to compare HDL size by isolation method due to noisy UC_{Iodix} lane profiles. The proteomic content of HDL was different by isolation method, with 7 proteins only identified on UC_{NaBr} HDL (including CETP and SAA-1), 44 proteins only identified on UC_{Iodix} HDL (predominantly complement factors and immunoglobulins) and 52 proteins on HDL isolated by both methods. The key HDL marker proteins apoAI, apoAII and PON-1 were all more abundant in HDL isolated by UC_{NaBr} when measured by nLC-MS/MS. In the previously established endothelial cell assay, UC_{Iodix} HDL had greater anti-inflammatory function than UC_{NaBr} HDL. In all comparisons, control and IGR HDL were not different irrespective of isolation method. UC_{NaBr} was therefore chosen as the optimal

technique for the isolation of HDL for compositional, size and functional measures due to cleaner HDL fractions.

The apoAI content of HDL did not differ between the isolation methods, however, protein content was higher in HDL isolated by UC_{Iodix}. This may be due to the different manner by which HDL is separated from plasma in each technique. In UC_{NaBr} lipoproteins are floated to the top of the ultracentrifuge tube, with a density cushion between the floated lipoproteins and the remaining plasma sample, however, in UC_{Iodix} the whole plasma sample is separated throughout the entire ultracentrifuge tube across a density gradient and as such may lead to protein contamination of the HDL containing fractions. UC_{NaBr} is performed for a longer duration than UC_{Iodix} (7 hrs 30 mins total at 355,040 x g average compared to 3hrs 10 mins at 352,534 x g average respectively) which may cause loosely associated HDL proteins to dissociate from HDL and be found in the lipoprotein depleted plasma fraction. The plasma samples used for UC_{Iodix} were a pool of 15- and 30-minute post-OGTT, which may have an effect on plasma protein levels. Should plasma protein concentration be increased, the association of some of these proteins with HDL may be increased, though there is limited literature from which to understand the acute effects of the consumption of 75g glucose on this metric. HDL cholesterol content was approximately halved after UC_{Iodix} compared to UC_{NaBr}. There is a small degree of small-dense LDL contamination after UC_{NaBr} as seen on the stained sizing gels, however this does not explain the large discrepancy between the isolation methods. A Bland-Altman analysis revealed a tight cluster of observations with a mean bias of 1.22 mmol/L lower HDL cholesterol content after UC_{Iodix}. The wide limits of agreement appear to be driven by the larger differences at higher HDL total cholesterol concentrations, however, the consistency of the mean difference between the cholesterol readings suggested that a methodological factor may be causing the reduced cholesterol measurement. The cholesterol quantitation assay used in this thesis is an enzyme coupled colorimetric assay; there is some evidence that iodixanol alters the performance of particularly colorimetric and enzyme-based biochemical assays (Otnes et al., 2017). As the iodixanol gradients were created at the same time using the same stock solutions, it is likely that the plasma samples contained a similar concentration of iodixanol which may have interfered with the assay to a similar degree in

each sample, perhaps by quenching colour development or by impairing enzyme activity by obscuring substrate binding sites. This may also have had some impact on the protein measurements by Bradford assay. To summarise, HDL apoAI content was not different between the isolation methods. HDL protein content was higher after UC_{Iodix} which might be due to the shorter ultracentrifugation maintaining loosely associated HDL proteins or the separation of plasma throughout a density gradient. Finally, HDL cholesterol content was lower after UC_{Iodix}, but this is likely interference from iodixanol given the consistency in difference between the measurements as described by Bland-Altman analysis.

It was not possible to compare the size distribution of HDL after isolation by the two different techniques as the lane profiles of UC_{Iodix} HDL were noisy due to multiple bands forming on the gel. This was likely a consequence of the higher protein content of HDL after UC_{Iodix} given the gels were stained with the protein stain Coomassie blue G-250. Harman, Griffin and Davies, (2013) acknowledge that plasma proteins may interfere with protein-stained HDL sizing gels after UC_{Iodix} and therefore used sequential density ultracentrifugation with potassium bromide to perform their comparison of methods for assessing HDL subclass distribution. It is therefore likely that the banding seen was caused by plasma proteins, evidenced also by the large band corresponding to serum albumin at the level of the 5.4 nm marker (equivalent to a molecular weight of 66 kDa).

There were challenges in preparing the UC_{Iodix} HDL for proteomic analysis. Mass spectrometers are highly sensitive equipment that require carefully prepared and cleaned samples to prevent damage to the separation columns and detectors. After using the standard peptide isolation and cleaning procedure, iodixanol was detected as a broad peak of absorbance when assessing peptide concentration using the NanoDrop. As a very large 1550 KDa molecule, iodixanol had to be removed from the samples to prevent damage to the mass spectrometer. Initial attempts were made using ice-cold acetone to precipitate HDL proteins, however this proved unsuccessful. As an alternative, filtration and dilution of the UC_{Iodix} HDL using 3 KDa MWCO filters was attempted, with five filtrations required to remove sufficient iodixanol from the HDL fractions.

Proteomic analysis revealed large differences in the protein content of HDL isolated by UC_{NaBr} and UC_{Iodix}. Of the 103 proteins that met the presence in 50% of samples cutoff, 44 proteins were identified only on HDL isolated by UC_{Iodix}. These were predominantly proteins involved in innate immunity, such as immunoglobulins and complement factors typically found in plasma and were therefore likely to be contaminating proteins. Seven proteins were identified only on HDL isolated by UC_{NaBr}. These included CETP and SAA-1, both key HDL proteins involved in its remodelling. This may not necessarily mean that these were not present on HDL from UC_{Iodix} but rather they may be vastly reduced in relative abundance due to the manner in which LFQ intensities are calculated. The remaining 52 proteins were identified on HDL isolated by both techniques, including apolipoproteins and PON-1. Plotting those proteins identified on HDL from both techniques on a qualitative heatmap revealed a distinct pattern of protein abundances for each isolation technique, with apolipoproteins more abundant on HDL from UC_{NaBr} and immune and coagulation related proteins more abundant on HDL from UC_{Iodix}. Univariate analysis of apoAI, apoAII and PON-1, all well established as HDL proteins, revealed significantly higher abundance of these proteins when isolated by UC_{NaBr} compared to UC_{Iodix}. Taken together, the proteomics findings suggest that isolation by UC_{NaBr} results in cleaner HDL fractions with less contamination by plasma proteins. The abundance of plasma proteins in UC_{Iodix} may have obscured the detection of strongly associated HDL proteins such as apolipoproteins. These findings also corroborated the higher HDL total protein content after UC_{Iodix}.

Finally, the anti-inflammatory function of HDL isolated by both UC_{NaBr} and UC_{Iodix} was compared. When exposed to HMEC-1 based on 300 µg/mL apoAI, HDL isolated by UC_{Iodix} was 20 percentage points more effective at reducing TNFα stimulated VCAM-1 expression compared to HDL isolated by UC_{NaBr}. This may be partly due to the biologically inert iodixanol having little impact on cellular functions, whereas the previous chapter demonstrated an effect of NaBr on HMEC-1. However, the confounding impact of the higher protein content and abundance of immune related proteins on HDL isolated by UC_{Iodix} on the measured anti-inflammatory function cannot be discounted. These proteins can also prevent endothelial inflammation; IgG and its fragments were effective in reducing VCAM-1 expression in response to TNFα in primary endothelial cells

(Ronda et al., 2003). However, these findings contrast with the findings of Lemmers et al., (2021) who saw no difference in HDL anti-inflammatory function between the two techniques. This may be due to the differences in the ultracentrifugation techniques used compared to the present study; sequential salt density ultracentrifugation was performed in three steps totalling 108 hours of centrifugation, while the iodixanol technique employed first removed apoB containing proteins before recovering HDL. This may have had the effect of removing abundant plasma proteins in both instances resulting in cleaner HDL fractions, removing confounding protein effects though this was not measured in the study. Due to the large differences in HDL protein content and the potential interference of iodixanol in the cholesterol quantitation assay, HDL anti-inflammatory function was not corrected for HDL protein or cholesterol content.

Taken together, these findings suggest that for the compositional and anti-inflammatory function study of HDL, UC_{NaBr} results in cleaner HDL fractions with less plasma protein contamination than UC_{Iodix}. Iodixanol appeared to interfere with the quantitation of HDL cholesterol content by colorimetric assay which meant that this metric could not be confidently interpreted. Proteomic analysis revealed that key HDL proteins were significantly lower in HDL isolated by UC_{Iodix}, which when coupled with the increase in abundance of proteins known to reduce endothelial activation introduces potential confounding factors into the interpretation of the anti-inflammatory function assay. As such, for the remainder of this thesis UC_{NaBr} was used to isolate HDL from plasma. Having established the optimal parameters for measuring HDL anti-inflammatory function in endothelial cells and the appropriate HDL isolation technique, the next chapter uses the assay to complete a previously performed study of HDL composition in healthy and preeclampsia complicated pregnancy.

5 HDL size and function through healthy gestation and in third trimester pregnancies complicated by preeclampsia

5.1 Introduction

Pregnancy induces significant changes to maternal metabolic physiology in order to provide for the growing fetus. Early pregnancy is characterised by insulin-sensitivity and deposition of adipose tissue in preparation for later fetal growth, while in late pregnancy metabolism shifts to insulin resistance and lipid mobilisation to supply fuel to the rapidly growing fetus. Late pregnancy is also associated with hyperlipidaemia and hypercholesterolaemia (reviewed by Sulaiman et al., (2016)). The expected deleterious consequences of these metabolic changes on the vasculature do not occur during healthy pregnancy; instead, maternal vascular function is enhanced and blood pressure decreases (Lopes van Balen et al., 2017). The establishment of the feto-placental circulation (between 10-15 weeks of gestation) induces a 42% increase in plasma HDL-C, peaking at 20 weeks of gestation, leading to the hypothesis that new HDL of improved composition and vascular functionality is synthesised (Sulaiman et al., 2016). Maternal vascular dysfunction does however occur in pregnancies complicated by preeclampsia. Preeclampsia is characterised by gestational hypertension, proteinuria and insulin resistance after 20 weeks of gestation, while the increase in HDL-C at the establishment of the feto-placental circulation is attenuated compared to healthy pregnancy (Huda et al., 2009). It may be that in preeclampsia newly synthesised HDL is of poorer composition and function which contributes to the impaired vascular phenotype. A more detailed description of the metabolic adaptation to healthy and complicated pregnancy can be found in section 1.6.4.

An analysis of HDL composition and antioxidant function throughout healthy pregnancy and in preeclampsia was performed in the thesis entitled ‘High Density Lipoprotein Composition and Function in Healthy Pregnancy and Preeclampsia’ by Dr Patamat Patanapirunhakit at the University of Glasgow. Briefly, HDL apoAI content increased in late pregnancy, while HDL total cholesterol content was unchanged throughout gestation. Proteomic analysis of HDL revealed changes in proteins related to triglyceride handling, immune

proteins, and coagulation related proteins throughout pregnancy. HDL PON-1 activity was unchanged through gestation. In addition, a comparison of healthy pregnancy to preeclampsia in the third trimester found no difference in HDL apoAI or total cholesterol content. As well as large number of immune and coagulation related proteins, a number of lipid-handling proteins were increased in preeclampsia pregnancy. HDL PON-1 activity was not different between healthy and preeclampsia pregnancy (Patanapirunhakit, 2023). Overall, the changes in HDL composition observed in healthy gestation suggested improved HDL vascular function while those in preeclampsia suggested reduced HDL vascular function, though function was not assessed in the previous work.

The present chapter therefore aimed to add to this previous work by measuring HDL size distribution and anti-inflammatory function throughout gestation and in pregnancies complicated by preeclampsia using samples drawn from the same studies. There is some conflict as to the direction of HDL size changes in healthy pregnancy. Longitudinal studies of HDL size through healthy pregnancy have shown both increased large HDL throughout pregnancy (Fåhraeus et al., 1985; Alvarez et al., 1996) and increased small HDL in late pregnancy (Zeljkovic et al., 2013). A similar split occurred in the limited literature examining HDL size in preeclampsia pregnancies, where Einbinder et al., (2018) found larger HDL compared to healthy pregnancy but Stadler et al., (2023) found smaller HDL in preeclampsia. While neonatal HDL has been shown to have anti-inflammatory effects on the placental vasculature (Del Gaudio et al., 2020), there has not been an examination of maternal HDL anti-inflammatory vascular function throughout healthy pregnancy. This chapter sought to address this gap in the literature. One study demonstrated decreased anti-inflammatory function of HDL from preeclampsia pregnancies (Einbinder et al., 2018); this chapter sought to corroborate this finding.

5.1.1 Hypotheses

- HDL size will increase in late pregnancy due to an increase in HDL-C.
- HDL anti-inflammatory function will increase in late pregnancy as an adaptation to the deleterious metabolic environment seen in late pregnancy.
- PE will have smaller HDL compared to healthy pregnant controls.
- PE will have poorer HDL anti-inflammatory function compared to healthy pregnant controls.

5.1.2 Objectives

- Measure changes in HDL size distribution through healthy pregnancy.
- Measure changes in HDL anti-inflammatory function through healthy pregnancy.
- Compare the size distribution of HDL between preeclampsia pregnancy and matched healthy controls.
- Compare HDL anti-inflammatory function through between preeclampsia pregnancy and matched healthy controls.

5.2 Methods

5.2.1 Recruitment of women with a healthy pregnancy

Following a pregnancy from conception to delivery is a challenge due to the uncertainty around date of conception and the nature of tracking patients through maternity units. As such, healthy pregnancy was modelled as a gestational series by age and BMI matching women from two independent studies performed at the University of Glasgow: The Early Pregnancy Study (EPS) following women through assisted conception, and the Lipotoxicity in Pregnancy Study (LIPS) following women from 16 weeks gestation to 13 weeks after

delivery. Though the timing of the BMI measurement differed between the EPS and LIPS studies, a cross-sectional study including 1,000 Caucasian women found no significant change in BMI through the first trimester (Fattah et al., 2010). As the samples in both of these studies had been heavily used for their originally intended purposes and subsequent studies, a limited volume of plasma in appropriate anti-coagulants were available for use at each time point for a given individual. This chapter used the remaining full sets of samples, totalling 14 women per study. The previous work used 10 women per study and found statistically significant changes in HDL composition, though these HDL samples were lost due to a fire in the laboratory.

5.2.1.1 Early pregnancy study (EPS)

The EPS study was originally collected as part of the PhD thesis entitled 'A study of metabolic and inflammatory pathways throughout gestation' by Dr Christopher Onyiaodike at the University of Glasgow. The study was performed at the Assisted Conception Unit at the Glasgow Royal Infirmary (GRI) between October 2007 and June 2010 under ethical approval from the GRI Ethics Committee (07/S0704/49). The cohort was originally recruited to determine metabolic and immune predictors of successful pregnancy with assisted conception by frozen embryo transfer (FET) (Onyiaodike et al., 2018). Women undergoing FET but with an otherwise regular menstrual cycle were recruited. Women taking exogenous hormones as part of their fertility treatment were excluded. Blood samples were taken daily to detect the luteinising hormone (LH) surge and FET performed three days post-LH surge. Pregnancy was confirmed on day 18 post-LH surge by urinary human chorionic gonadotropin and on day 45 post-LH surge by ultrasound scan. Blood samples were taken at 7 time-points post-LH surge, however the present study made use of four of these: pre-pregnancy (3 days pre-LH surge) and days 18, 29 and 45 post-LH surge. Assuming that the LH-surge occurs on day 14 of the 28-day menstrual cycle, it was classed as 2-weeks of gestation. Days 18, 29 and 45 post-LH surge were therefore deemed equivalent to 4.6, 6.1 and 8.4 weeks of gestation respectively.

5.2.1.2 Lipotoxicity in pregnancy study (LIPS)

This study was performed between March 2010 and November 2011 as part of the PhD thesis entitled 'Anatomical fat distribution and accumulation and lipotoxicity in lean and obese pregnancy' by Dr Eleanor Jarvie at the University of Glasgow. Participants were recruited from NHS Great Glasgow and Clyde maternity units under ethical approval from the West of Scotland Research Ethics Committee (09/S0701/105). The inclusion and exclusion criteria can be found in table 5-1. Healthy pregnant women were recruited at their first antenatal visit to the maternity unit and study visits occurred at 16, 25 and 35 weeks of gestation followed by a post-partum visit after 13 weeks. Fasted blood samples were taken at each visit.

Table 5-1 Inclusion and exclusion criteria for the recruitment of healthy pregnancy in the LIPS study

Inclusion criteria		Exclusion criteria	
i.	Healthy pregnant women aged between 16 and 40 years	i.	Previous fetal loss beyond 12-weeks' gestation
ii.	BMI < 25 kg/m^2	ii.	History of cardiovascular or metabolic disease
		iii.	Pregnancies achieved through assisted conception
		iv.	Multiple pregnancy

5.2.2 Recruitment of women with preeclampsia and healthy matched controls

Preeclampsia and matched healthy control pregnancies were collected as part of the 'Studies into nurturing and development of pregnancies – understanding the genetics of pregnancy and setting up a biobank' ethics application at the University of Nottingham and kindly provided by Dr Hiten Mistry (REC-15/EM/0523). Preeclampsia pregnancies were identified and recruited based upon the International Society for the Study of Hypertension in Pregnancy guidelines (Brown et al., 2001b).This constituted gestational hypertension (blood pressure >140/90 mmHg measured at two separate time points >4 hours apart) occurring after 20 weeks of gestation in a previously normotensive woman and

new proteinuria (protein:creatine ratio of >30 or urine protein at a concentration greater than 3 g/L in two random midstream urine samples collected >4 hours apart) without evidence of urinary tract infection. Preeclampsia patients were categorised as either early- (diagnosis <34 weeks of gestation) or late-(diagnosis >34 weeks of gestation) onset preeclampsia as considered by (Tranquilli et al., 2013). Early- and late-onset preeclampsia pregnancies were matched to pre-term and term normotensive pregnancies. It should be noted that the pre-term normotensive pregnancies may not be strictly healthy owing to premature birth.

5.2.3 Isolation of HDL

HDL was isolated according to section 2.2.2. Only the top 250 µL HDL was retained after ultracentrifugation to increase HDL concentration.

5.2.4 Measurement of HDL size distribution

The size distribution of HDL was measured using native gel electrophoresis as set out in section 2.12.

5.2.5 Assessment of HDL anti-inflammatory function

The anti-inflammatory function of HDL was assessed by measuring the inhibition of TNFα induced VCAM-1 as set out in chapter 3. Briefly, HMEC-1 were preincubated with HDL (based on 300 µg/mL apoAI) for four hours before the addition of 5 ng/mL TNFα for 24 hours. Cells were lysed according to section 2.4 and SDS-PAGE / western blotting was performed for VCAM-1 according to sections 2.8 and 2.9. Results are expressed as % inhibition of VCAM-1 expressed by cells treated with TNFα alone. Each culture plate contained untreated and TNFα only treated cells; samples were corrected for baseline VCAM-1 expression and normalised to the TNFα only control present on the same plate.

5.2.6 Statistical analyses

Demographic data was checked for normality by qualitative assessment of the QQ plot and equality of variances assessed by Brown-Forsythe test. Where data was normally distributed, the data was analysed by Student’s t-test or one-way

ANOVA. Where variances were different between groups, Welch's t-test and ANOVA were used. Where data was not normally distributed, Mann-Whitney U-test or Kruskal-Wallis tests were used to analyse the data.

As a combination of two separately performed studies, careful consideration was given to select the most appropriate method of statistical analysis for the gestational series data. Initially it was considered to analyse each study separately using repeated measures 2-way ANOVA with the non-pregnant time point as the baseline, however, this undermined the study purpose of understanding changes in HDL through pregnancy and reduced statistical power. In consultation with colleagues with statistical expertise (Professor Paul Welsh and Dr Fred Ho, School of Cardiometabolic Health, University of Glasgow), it was decided to analyse this data set using mixed effects models with each study participant identifier included as a random factor to allow for repeated measures. This analysis method factors in any inter-individual variation and as such allows for the analysis of both the EPS and LIPS studies simultaneously. Mixed effects models do not require the input data to be normally distributed or parametric in nature but do assume normality of the resulting residuals. Where residuals were not normally distributed, the input data was log transformed. Mixed effects models were followed by *post hoc* Dunnet multiple comparisons test, compared to the pre-pregnancy time point to simplify the analysis. Anti-inflammatory function data was analysed including HDL-C as a covariate.

The preeclampsia study data was analysed in two ways; one for the effect of preeclampsia compared to healthy control pregnancy, and the other dividing the groups into early- and late-onset preeclampsia and their gestational-age matched controls. As the sizing and function data was non-parametric, Mann-Whitney U-tests were used to compare preeclampsia to controls, while Kruskal-Wallis tests were used when the groups were divided into their preeclampsia phenotypes. A measure of plasma HDL-C was not available for these samples and as such could not be included as a covariate for the analysis of HDL anti-inflammatory function. For all statistical analyses, statistical significance was assumed at $p < 0.05$.

5.3 Results

5.3.1 HDL composition and function through the healthy gestational series

5.3.1.1 Gestational series participant demographics

From the EPS study, 14 women with a mean age of 34.9 years and a pre-pregnant BMI of 26.8 kg/m^2 were matched to 14 women from the LIPS study with a mean age of 33.5 years and a mean booking BMI (at approximately 12-weeks of pregnancy) of 27.7 kg/m^2 (Table 5-2). One sample from the EPS study was not available at 6.1-weeks of gestation leaving 13 samples available for analysis at this time point.

Table 5-2 Characteristics of the EPS and LIPS study participants. Data expressed as mean ± SD and means compared by Welch's unpaired t-test. Statistical significance was assumed at p <0.05.

	EPS (n=14)	LIPS (n=14)	p value
Age (years)	34.9 ± 4.2	33.5 ± 2.1	0.28
BMI (kg/m^2)	26.8 ± 3.9	27.7 ± 4.5	0.58

5.3.1.2 HDL size distribution through pregnancy

There were changes in the proportion of four out of the five HDL subclasses through healthy pregnancy compared to pre-pregnancy. The proportion of each HDL subclass returned to the pre-pregnant baseline at the 13-weeks post-partum time point. The proportion of HDL 2b was significantly higher at 16 weeks (38.6 ± 5.1 %, mean ± SD), 25 weeks (41.3 ± 5.0 %) and 35 weeks of gestation (40.4 ± 7.8 %) compared to pre-pregnancy (25.4 ± 9.6 %, p = <0.0001, Figure 5-1).

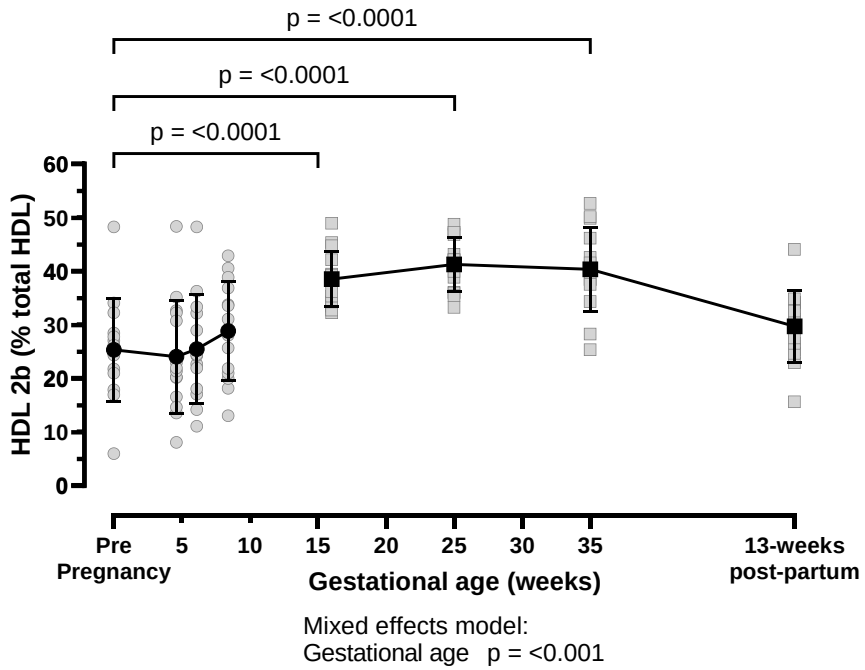

Figure 5-1 The proportion of HDL 2b throughout gestation. Symbols and bars indicate mean ± SD and the grey shapes indicate individual measurements. A line break exists between the EPS (circles) and LIPS (squares) study participants. Data was analysed by mixed effects model followed by *post hoc* Dunnet multiple comparison test. Statistical significance was assumed at $p < 0.05$.

The proportion of HDL 2a was significantly lower at 35 weeks of gestation compared to pre-pregnancy (20.7 ± 3.0 % compared to 25.6 ± 4.1 %, $p = 0.004$, Figure 5-2).

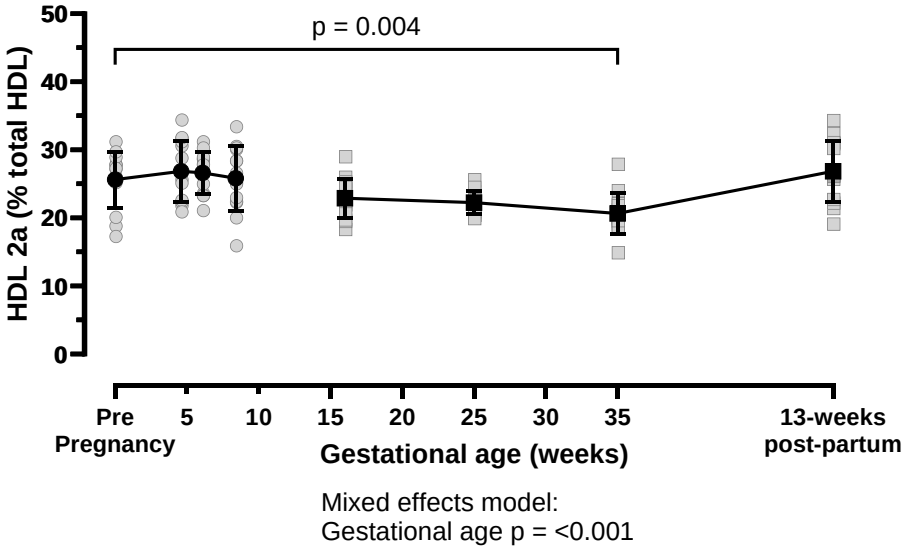

Figure 5-2 The proportion of HDL 2a throughout gestation. Symbols and bars indicate mean ± SD and the grey shapes indicate individual measurements. A line break exists between the EPS (circles) and LIPS (squares) study participants. Data was analysed by mixed effects model followed by *post hoc* Dunnet multiple comparison test. Statistical significance was assumed at $p < 0.05$.

The proportion of HDL 3a was significantly lower at 16, 25 and 35 weeks of gestation (17.6 ± 3.2 %, p = 0.007, 16.9 ± 2.5 %, p = 0.001 and 17.3 ± 3.1 %, p = 0.003 respectively) compared to pre-pregnancy (22.0 ± 3.2 %, Figure 5-3).

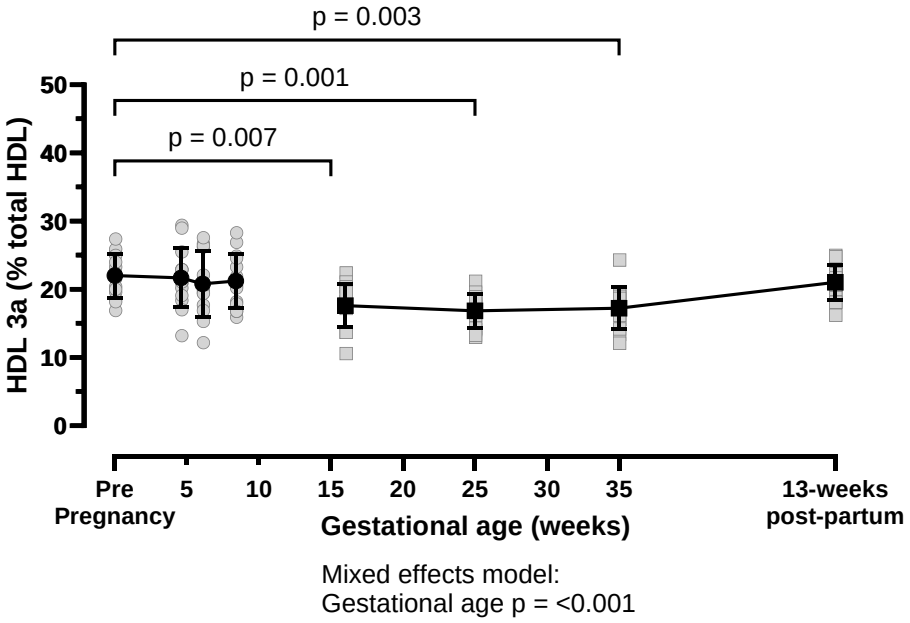

Figure 5-3 The proportion of HDL 3a throughout gestation. Symbols and bars indicate mean ± SD and the grey shapes indicate individual measurements. A line break exists between the EPS (circles) and LIPS (squares) study participants. Data was analysed by mixed effects model followed by *post hoc* Dunnet multiple comparison test. Statistical significance was assumed at $p < 0.05$.

The proportion of HDL 3b was significantly lower at 25 weeks of gestation compared to pre-pregnancy (8.5 ± 1.7 % compared to 11.2 ± 2.8 %, p = 0.031, Figure 5-4).

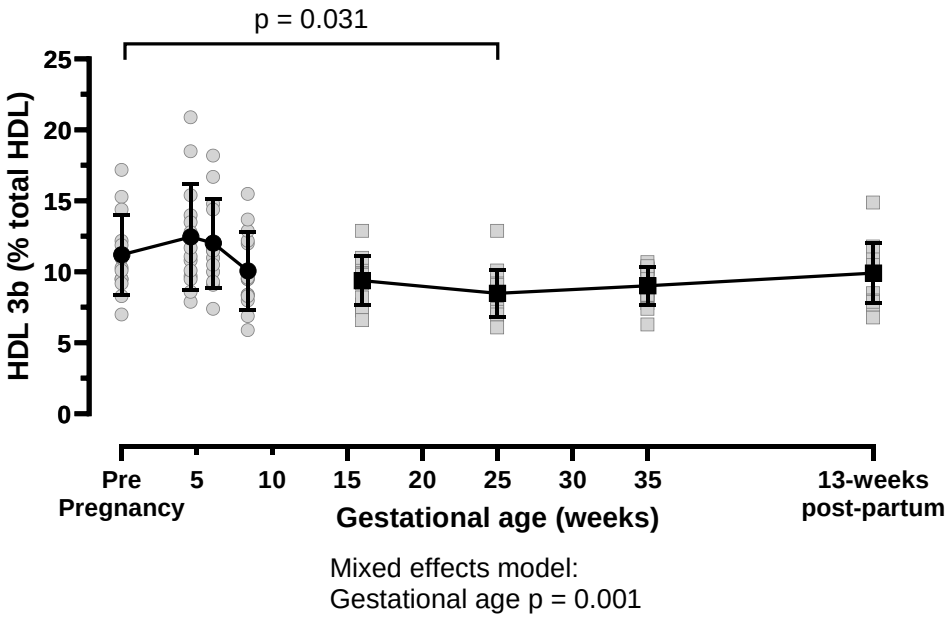

Figure 5-4 The proportion of HDL 3b throughout gestation. Symbols and bars indicate mean ± SD and the grey shapes indicate individual measurements. A line break exists between the EPS (circles) and LIPS (squares) study participants. Data was analysed by mixed effects model followed by *post hoc* Dunnet multiple comparison test. Statistical significance was assumed at $p < 0.05$.

The proportion of HDL 3c was unchanged throughout gestation (Figure 5-5).

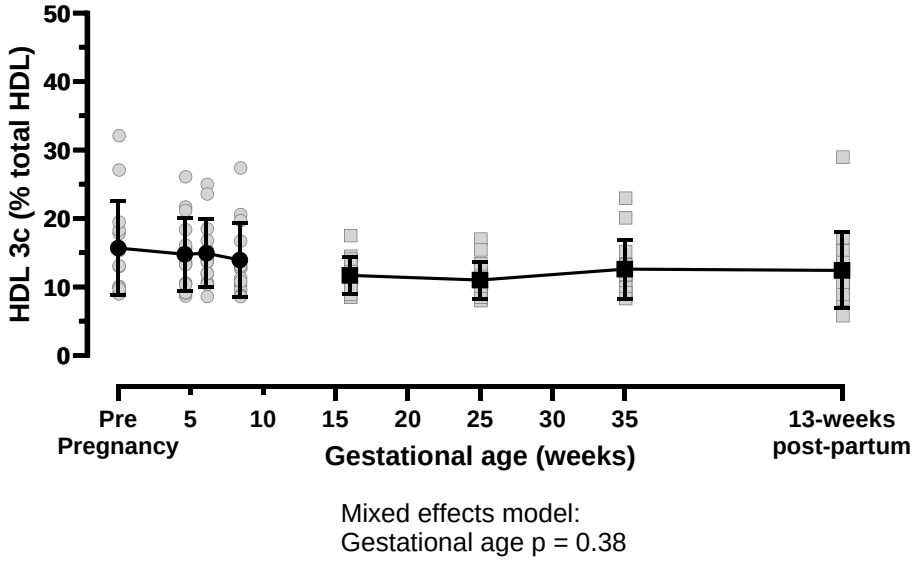

Figure 5-5 The proportion of HDL 3c throughout gestation. Symbols and bars indicate mean ± SD and the grey shapes indicate individual measurements. A line break exists between the EPS (circles) and LIPS (squares) study participants. Data was analysed by mixed effects model followed by *post hoc* Dunnet multiple comparison test. Statistical significance was assumed at $p < 0.05$.

The ratio of HDL 2 to HDL 3 was significantly higher at 16 weeks (1.6 ± 0.4, p = 0.018), 25 weeks (1.8 ± 0.4, p = 0.001) and 35 weeks of gestation (1.6 ± 0.4, p = 0.018) compared to pre-pregnancy (1.1 ± 0.4, Figure 5-6).

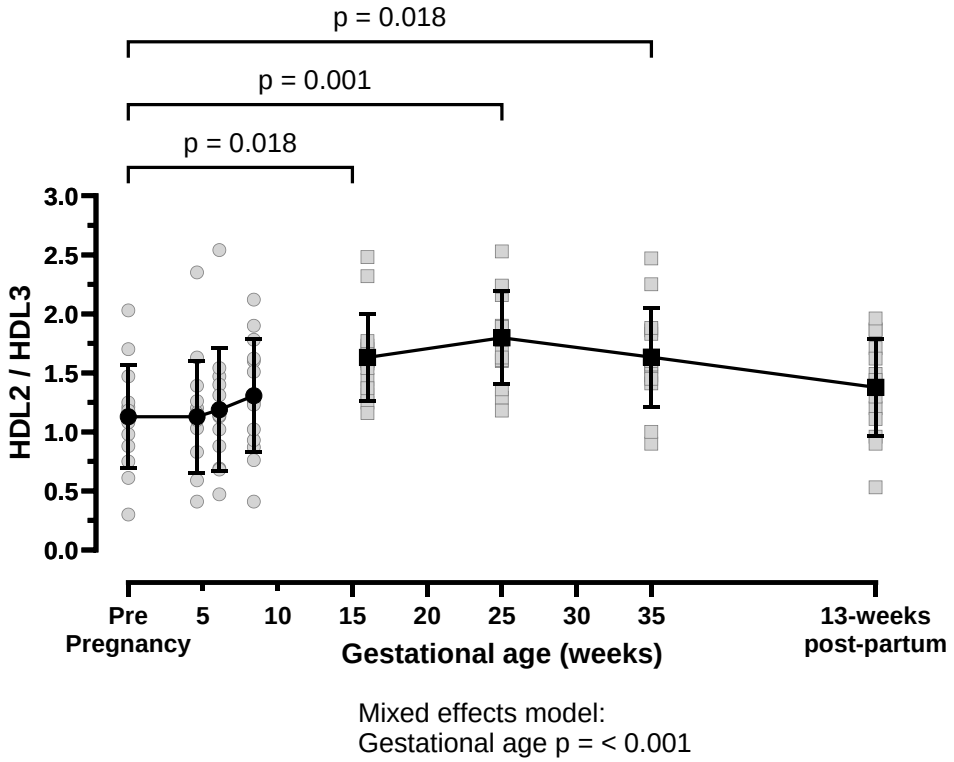

Figure 5-6 The HDL 2/HDL 3 ratio throughout gestation. Symbols and bars indicate mean ± SD and the grey shapes indicate individual measurements. A line break exists between the EPS (circles) and LIPS (squares) study participants. Data was analysed by mixed effects model followed by *post hoc* Dunnet multiple comparison test. Statistical significance was assumed at $p < 0.05$.

5.3.1.3 HDL anti-inflammatory function through pregnancy

When exposed to HMEC-1 based on 300 µg/mL apoAI, HDL anti-inflammatory function as measured by inhibition of TNFα induced VCAM-1 was lower at 16 weeks of gestation compared to pre pregnancy (39.6 ± 19.2 % compared to 64.9 ± 18.8 %, p = 0.008, mean ± SD, Figure 5-7). This was independent of HDL-C (p = 0.62).

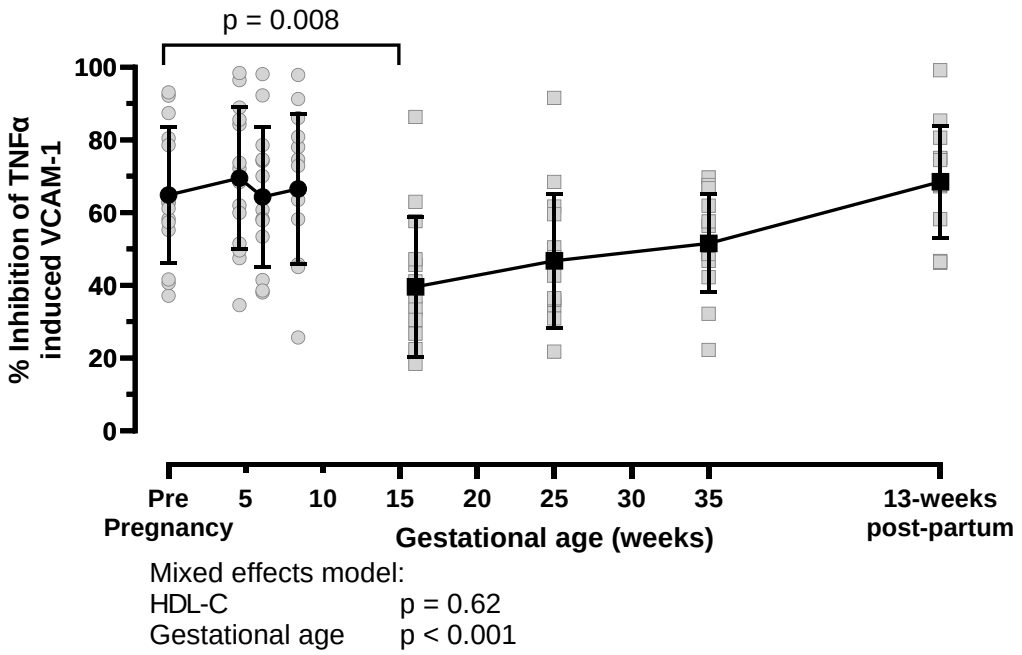

Figure 5-7 The anti-inflammatory function of HDL throughout gestation. Symbols and bars indicate mean ± SD and the grey shapes indicate individual measurements. A line break exists between the EPS (circles) and LIPS (squares) study participants. Data was analysed by mixed effects model followed by *post hoc* Dunnet multiple comparison test. HDL-C was included as a covariate. Statistical significance was assumed at $p < 0.05$.

After correction for HDL total cholesterol exposed to HMEC-1, HDL anti-inflammatory function was lower at 16 weeks of gestation (0.4 ± 0.2 %/nmol), 25 weeks of gestation (0.5 ± 0.3 %/nmol), 35 weeks of gestation (0.6 ± 0.3 %/nmol) and 13-weeks post-partum (0.6 ± 0.2 %/nmol) compared to pre-pregnancy (4.1 ± 3.7 %/nmol, all $p < 0.001$, Figure 5-8). This was independent of HDL-C ($p = 0.42$).

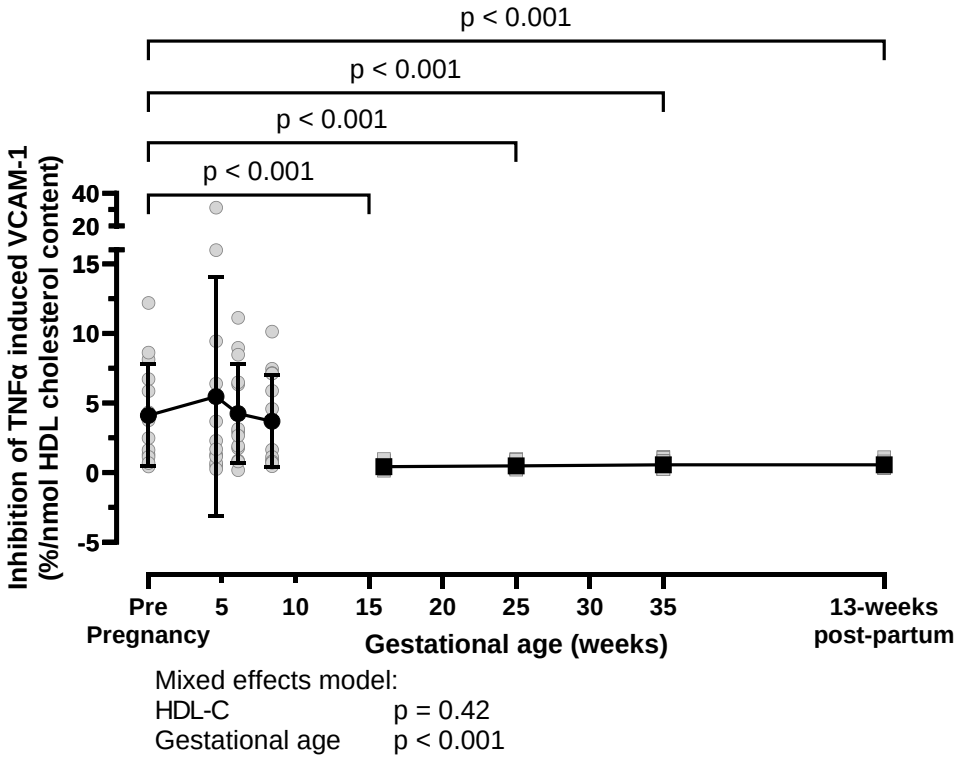

Figure 5-8 The anti-inflammatory function of HDL, corrected for HDL total cholesterol exposed to HMEC-1, throughout gestation. Symbols and bars indicate mean ± SD and the grey shapes indicate individual measurements. A line break exists between the EPS (circles) and LIPS (squares) study participants. Data was analysed by mixed effects model followed by *post hoc* Dunnet multiple comparison test. HDL-C was included as a covariate. Statistical significance was assumed at $p < 0.05$.

After correction for HDL total protein exposed to HMEC-1, HDL anti-inflammatory was lower at 16 weeks of gestation (0.5 ± 0.3 %/µg, $p < 0.001$), 25 weeks of gestation (0.6 ± 0.3 %/µg, $p < 0.001$), 35 weeks of gestation (0.6 ± 0.3 %/µg, $p < 0.001$) and 13-weeks post-partum (0.8 ± 0.5 %/µg, $p = 0.015$) compared to pre-pregnancy (1.9 ± 1.1 %/µg, Figure 5-9). This was independent of HDL-C ($p = 0.86$).

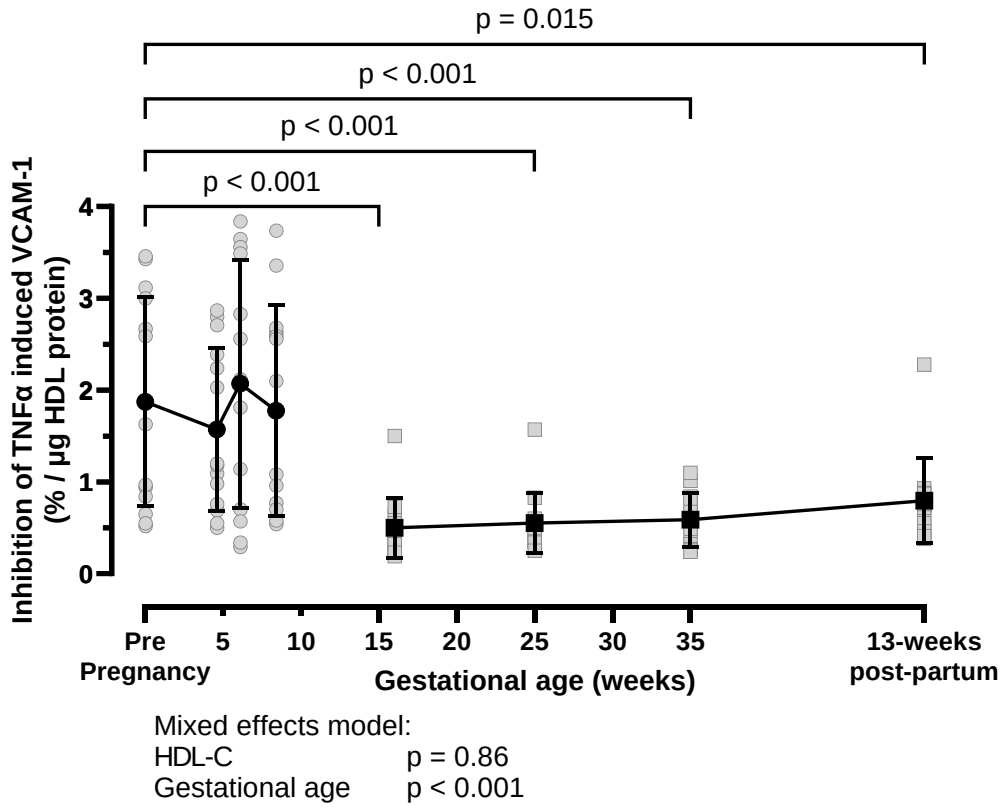

Figure 5-9 The anti-inflammatory function of HDL, corrected for HDL protein exposed to HMEC-1, throughout gestation. Symbols and bars indicate mean ± SD and the grey shapes indicate individual measurements. A line break exists between the EPS (circles) and LIPS (squares) study participants. Data was analysed by mixed effects model followed by *post hoc* Dunnet multiple comparison test. HDL-C was included as a covariate. Statistical significance was assumed at $p < 0.05$.

5.3.2 HDL composition and function in healthy pregnancy compared to pregnancy complicated by preeclampsia

5.3.2.1 Preeclampsia study participant demographics

The characteristics of the preeclampsia study participants can be found in table 5-3. The participants did not differ by age. Early onset pre-eclampsia participants had a significantly higher booking BMI (31.74 kg/m^2) compared to both pre-term and term normotensive controls and late onset preeclampsia. Preeclampsia pregnancies were characterised by higher systolic and diastolic blood pressures than their healthy pregnant counterparts. Gestational ages at delivery were well matched between the groups.

Table 5-3 Characteristics of the preeclampsia study participants. Data expressed as mean ± SD. Data was analysed by Welch's ANOVA and *post hoc* Tukey test or Kruskal-Wallis with *post hoc* Dunn's test. Gestational age at diagnosis was analysed by Welch's t-test. Statistical significance was assumed at $p < 0.05$. Means that do not share a letter are statistically different.

	Pre-term Normotensive (n=18)	Early-onset PE (n=13)	Normotensive (n=16)	Late-onset PE (n=21)	p value
Age (years)	31.3 ± 3.8	31.5 ± 4.6	29.9 ± 4.8	28.2 ± 6.1	0.19
Booking BMI (kg/m^2)	25.2 ± 3.6^A	31.7 ±7.9^B	26.7 ± 5.9^{AB}	27.5 ± 4.9^{AB}	0.021
Booking systolic blood pressure (mmHg)	108 ± 10	115 ± 13	110 ± 11	114 ± 13	0.30
Booking diastolic blood pressure (mmHg)	62 ± 8	66 ± 13	67 ± 8	66 ± 8	0.42
Systolic blood pressure at diagnosis (mmHg)	124 ± 10^A	158 ± 9^B	119 ± 9^A	152 ± 30^B	<0.0001
Diastolic blood pressure at diagnosis (mmHg)	72 ± 10^A	100 ± 6^B	73 ± 10^A	96 ± 4^B	<0.0001
Gestational age at diagnosis (weeks)	N/A	30.5 ± 2.8^A	N/A	36.7 ± 2.4^B	<0.0001
Gestational age at delivery (weeks)	33.3 ± 2.9^A	32.9 ± 3.1^A	39.3 ± 1.0^B	37.9 ± 1.7^B	<0.0001

5.3.2.2 HDL size distribution in preeclampsia

There was no difference in HDL size distribution between healthy pregnancy and preeclampsia pregnancy (Figure 5-10), irrespective of preeclampsia phenotype (Figure 5-11).

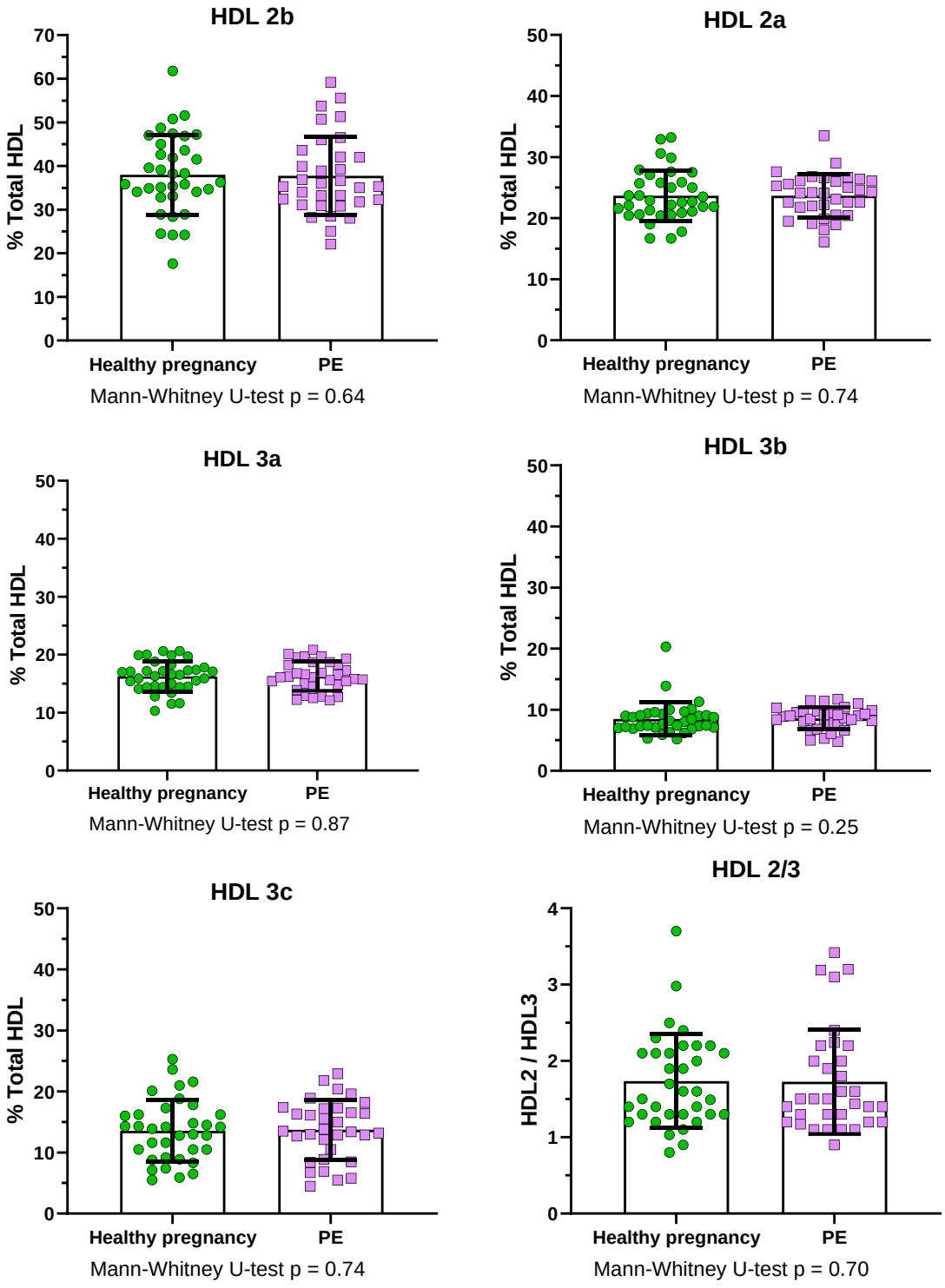

Figure 5-10 HDL subclass distribution in healthy pregnancy and pregnancy complicated by preeclampsia. Data expressed as mean ± SD and comparisons made by Mann-Whitney U-test. Statistical significance was assumed at $p < 0.05$. PE, preeclampsia.

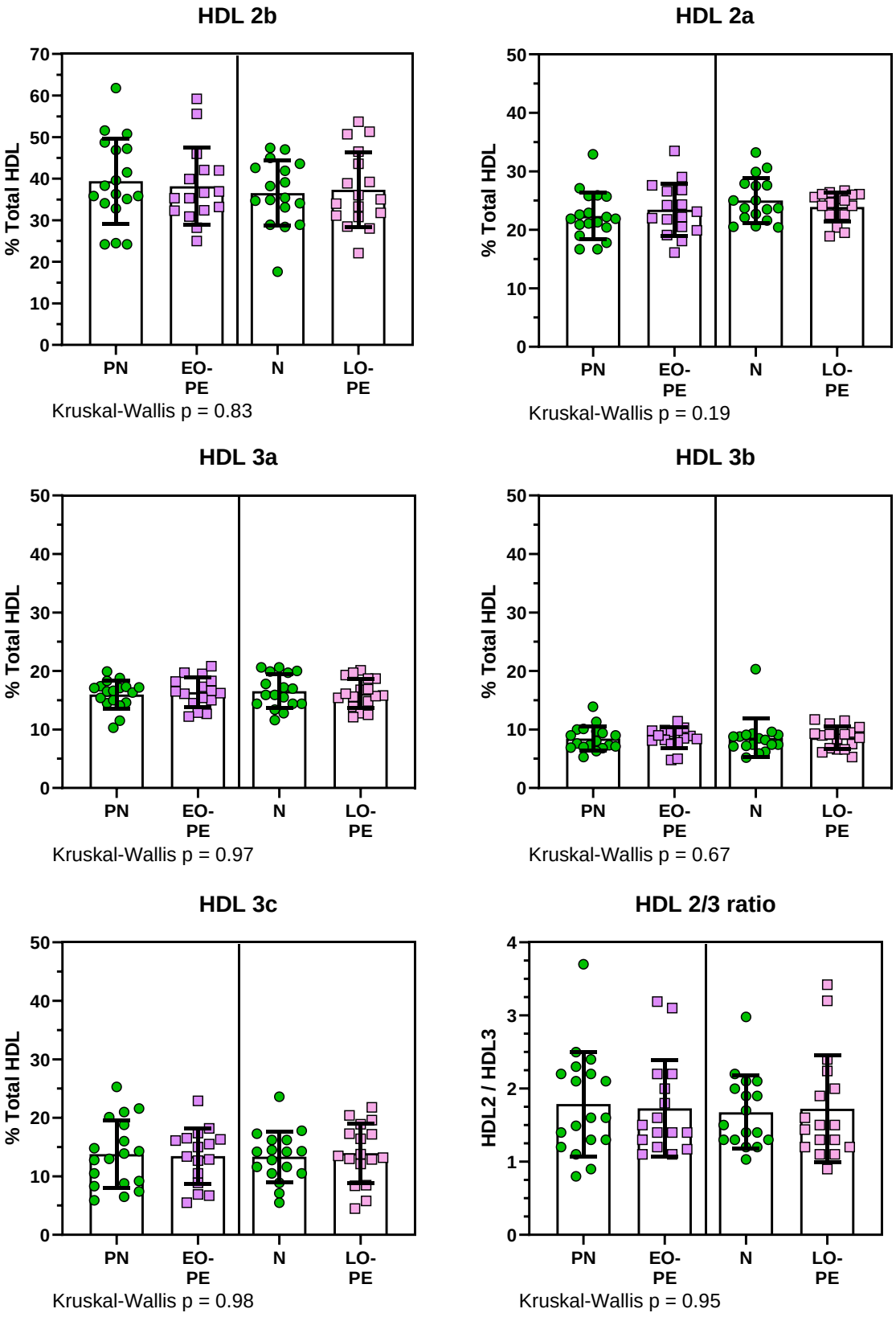

Figure 5-11 HDL subclass distribution between early- and late-onset preeclampsia and gestational-age matched healthy pregnancy. Data expressed as mean ± SD and comparisons made by Kruskal Wallis test. Statistical significance was assumed at $p < 0.05$. PN, pre-term normotensive pregnancy; EOPE, early-onset preeclampsia; N, normotensive pregnancy; LOPE, late-onset preeclampsia.

5.3.2.3 HDL anti-inflammatory function in preeclampsia

There was no difference in HDL anti-inflammatory function between healthy pregnancy and preeclampsia pregnancy (Figure 5-12) irrespective of preeclampsia phenotype (Figure 5-13).

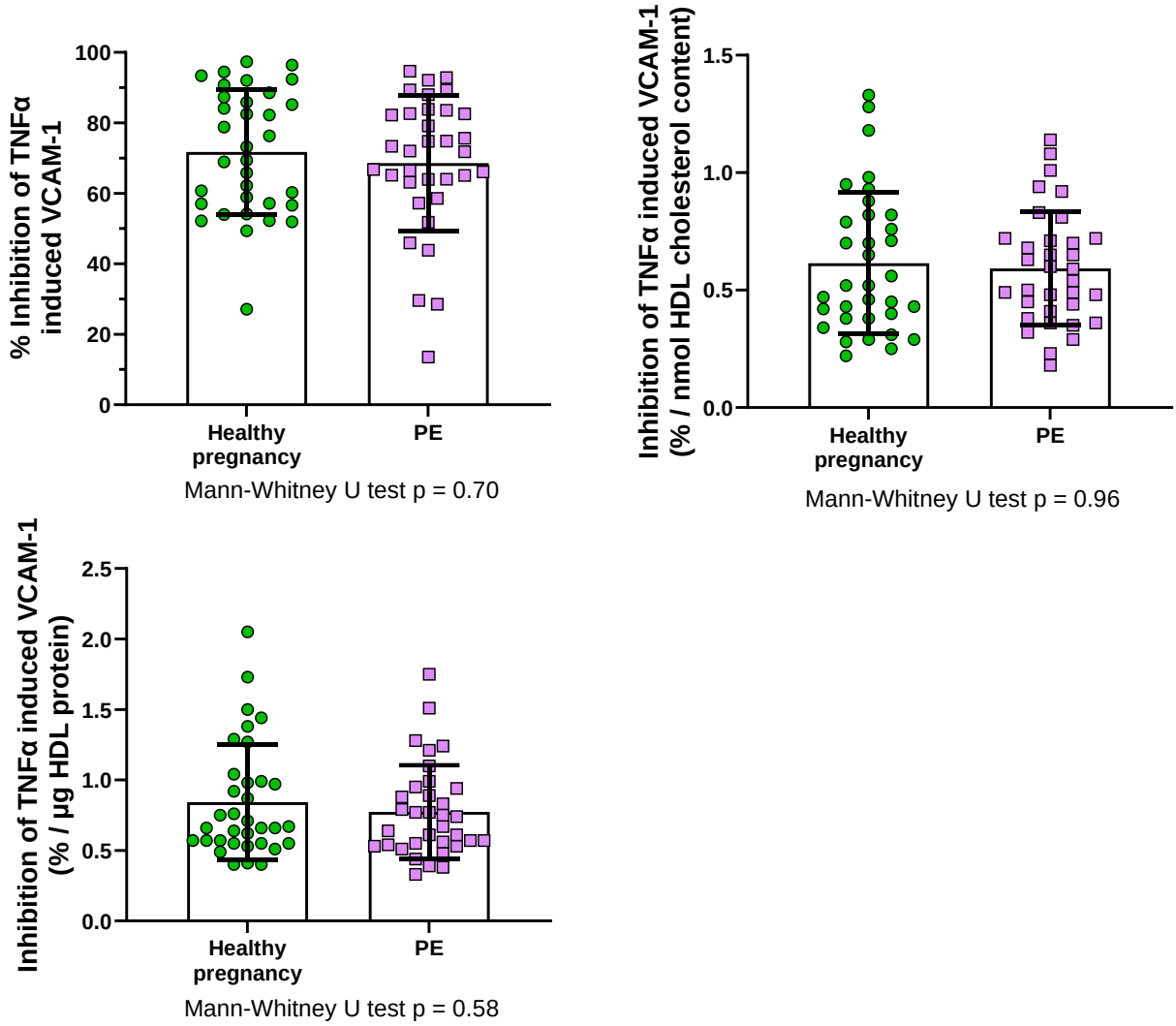

Figure 5-12 HDL anti-inflammatory function in healthy pregnancy and pregnancy complicated by preeclampsia. Data expressed as mean ± SD and comparisons made by Mann-Whitney U-test. Statistical significance was assumed at $p < 0.05$. Data shown as PE, preeclampsia.

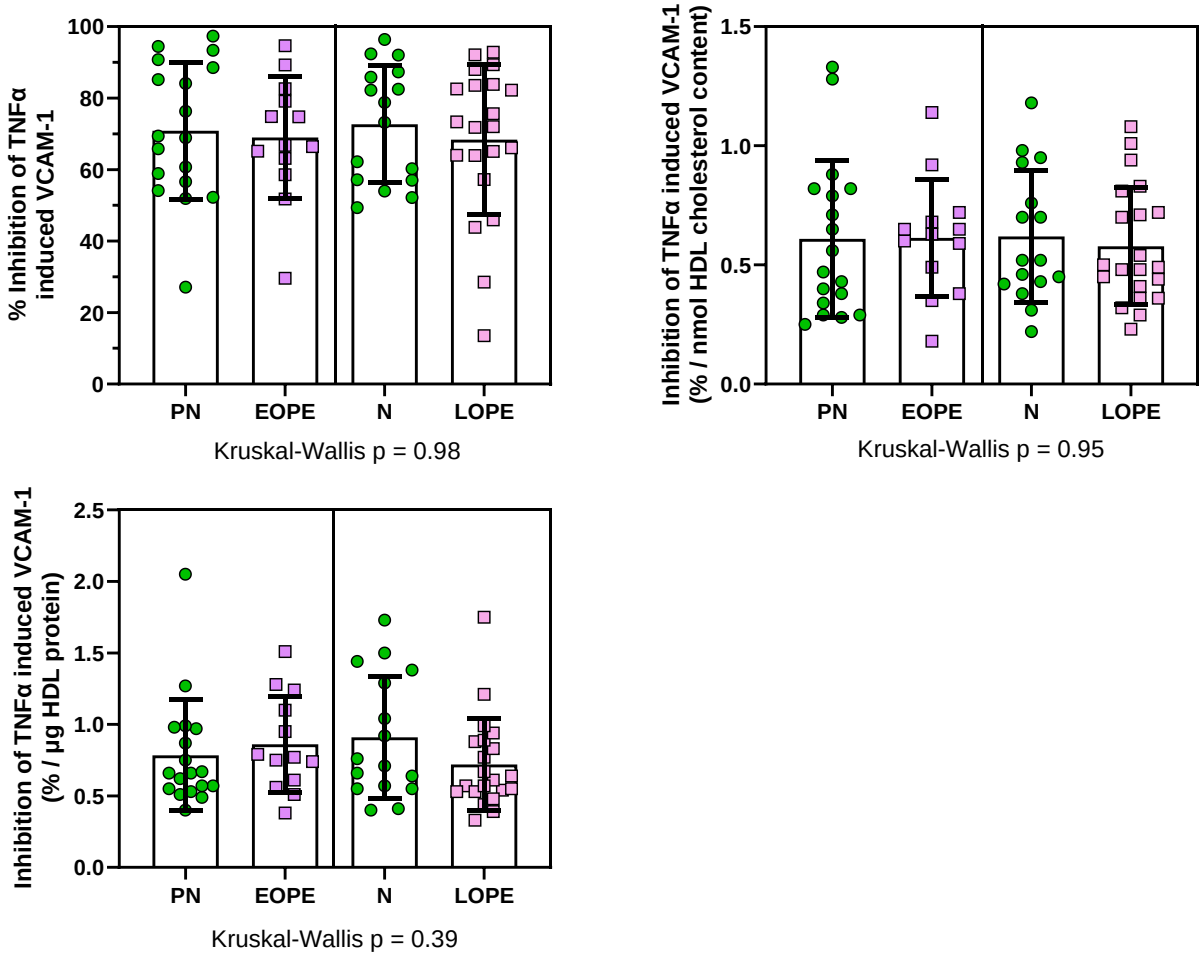

Figure 5-13 HDL anti-inflammatory function in early- and late-onset preeclampsia and gestational-age matched healthy pregnancy. Data expressed as mean ± SD and comparisons made by Kruskal Wallis test. Statistical significance was assumed at $p < 0.05$. PN, pre-term normotensive pregnancy; EOPE, early-onset preeclampsia; N, normotensive pregnancy; LOPE, late-onset preeclampsia.

5.4 Discussion

This chapter set out to measure HDL size and anti-inflammatory function through healthy pregnancy and in pregnancies complicated by preeclampsia, adding to a study of HDL composition previously performed in this laboratory and addressing a gap in the literature. In the study of healthy pregnancy, all of the changes in HDL size and HDL function occurred in the second and third trimester. HDL size increased during the second and third trimesters before returning to the pre-pregnancy size distribution. HDL anti-inflammatory function was reduced at the 16th week of gestation compared to pre-pregnancy when exposed to HMEC-1 based on apoAI. When corrected for both HDL total cholesterol and total protein content, HDL anti-inflammatory function was reduced in late pregnancy and remained so 13 weeks post-partum. There was no difference in either HDL size

or HDL anti-inflammatory function in preeclampsia compared to healthy pregnancy. This remained the case after separating the groups by preeclampsia phenotype and comparison to gestational-age matched controls.

The largest HDL subclass, HDL 2b, was increased in late pregnancy compared to pre-pregnancy, with concomitant late pregnancy decreases in HDL 2a, 3a, and 3b. The smallest HDL subclass, HDL 3c was unchanged throughout pregnancy, suggesting that HDL turnover remains at a steady state through pregnancy. Overall HDL size as inferred from the HDL 2:HDL 3 ratio suggested an overall increase in HDL size in late gestation that returned to the pre-pregnancy size distribution by 13-weeks post-partum. These findings corroborate those of Melchior et al., (2021), who saw a similar change in HDL subclass distribution in healthy second trimester pregnancies compared to non-pregnant controls. Late pregnancy is characterised by hyperlipidaemia which, in the non-pregnant population, leads to smaller triglyceride-rich HDL that is more rapidly cleared from the circulation. These findings suggest that this does not happen during pregnancy, possibly as a means to provide lipid to the growing fetus. The changes in the composition of HDL lipid-handling proteins have already been discussed in the context of changing maternal lipid concentration through pregnancy (Patanapirunhakit, 2023), however these proteins are likely to also be implicated in determining HDL size. HDL apoF and apoAIV were both decreased in late pregnancy (Patanapirunhakit, 2023). ApoF is inactive as a CETP inhibitor when sequestered on HDL (Liu and Morton, 2020) while apoAIV acts as an activator of CETP (Main et al., 1996); these findings suggest inhibition of CETP and consequent HDL enlargement. Both HDL apoCII and apoCIV were also increased in late pregnancy (Patanapirunhakit, 2023). The LPL activator apoCII is increased in hypertriglyceridemia and suggests that triglyceride-rich lipoproteins are efficiently hydrolysed through the lipoprotein cascade (Wolska et al., 2020), reducing triglyceride available for HDL enrichment, reducing HL-mediated HDL lipolysis and reducing plasma HDL clearance thereby allowing increased HDL size in late pregnancy. There is limited literature describing the role of apoCIV in lipoprotein metabolism, though in transgenic mice it was shown to be associated with increased VLDL secretion and delivery of VLDL cholesterol to LDL and HDL (Allan and Taylor, 1996). Taken together, the previously uncovered compositional changes may partially explain the larger HDL and increased

plasma HDL-C observed in late pregnancy. Outside of HDL composition, HDL cholesterol efflux capacity is a determinant of HDL size (Mutharasan et al., 2017). There is a limited literature on HDL cholesterol efflux capacity in pregnancy, though the passive diffusion pathway of cholesterol efflux was increased in second trimester pregnancy compared to non-pregnant controls (Melchior, Swertfeger, et al., 2021), perhaps a contributing mechanism to the larger HDL observed in late pregnancy.

When HMEC-1 were exposed to HDL at 300 µg/mL apoAI, anti-inflammatory function was significantly lower from samples taken at 16 weeks of gestation compared to pre-pregnancy. Anti-inflammatory function tended to be lower through late pregnancy but gradually recovered by 13-weeks post-partum, though these changes were not statistically significant. However, given that HDL apoAI content increased in late pregnancy this may reflect a reduction in anti-inflammatory function per HDL particle; therefore, anti-inflammatory function was corrected for HDL total cholesterol and protein content exposed to the cells. In both cases HDL anti-inflammatory function was significantly lower throughout late pregnancy and did not recover by 13-weeks post-partum, contrary to my earlier hypothesis. This may be due to the compositional changes described by (Patanapirunhakit, 2023), who observed an increase in HDL-associated immune and coagulation related proteins in late pregnancy such as angiotensinogen (~60 kDa), vitronectin (~75 kDa) and prenylcysteine oxidase-1 (~57 kDa). These proteins are all much larger than the vaso-active proteins on HDL, including apoAI (28 kDa), and may therefore interfere with the ability of said proteins to interact with the endothelium. It may be that other HDL functions, such as reverse cholesterol transport or vasodilation, are more important during pregnancy. It has been suggested that cholesterol efflux capacity is important to placental function during pregnancy, and that HDL may be taken up by the placenta in order to deliver cholesterol to the fetus (reviewed by Woollett, Catov and Jones, (2022)). Another possible function for HDL in gestation is in essential fatty acid transport, both for maternal and fetal protection. A study of fatty acid distribution across lipoprotein fractions using samples from the same age- and BMI- matched cohorts as the present chapter found that maternal HDL was enriched in the omega-3 fatty acid docosahexaenoic acid (DHA) in late pregnancy (Zamai et al., 2020).

In non-pregnant individuals, DHA has a number of protective effects on the vascular endothelium (reviewed by Yamagata, (2017)) and increased dietary omega-3 fatty acids have been shown to improve HDL function in those with high cardiometabolic risk (Cartolano et al., 2022). These improvements were characterised by CETP inhibition and larger HDL size which are corroborated by the findings of Patanapirunhakit (2023) and the present thesis. It may be that the enrichment of HDL with DHA in late pregnancy improves maternal vascular function through pathways undetected in the assay developed in Chapter 3. Finally, there is cell-culture model evidence that apoAI derived from non-pregnant HDL donors protects against cytokine inhibition of trophoblast invasion into the placental spiral arteries, key to proper placentation (Charlton et al., 2017). In summary, this first foray into the anti-inflammatory function of HDL throughout healthy gestation showed reduced anti-inflammatory function in late pregnancy. This may be related to compositional changes unfavourable to the vascular endothelium, or due to changes in the dominant functions of HDL outside of anti-inflammatory vascular function such as cholesterol efflux, delivery of fatty acids or protecting placental function.

Having established HDL size and anti-inflammatory function through healthy gestation, these metrics were assessed in preeclampsia pregnancy. Whether separated by preeclampsia phenotype and gestational age-matched healthy pregnant controls, or grouped as healthy compared to preeclampsia pregnancy, there were no differences detected in HDL size distribution, contrary to my hypothesis. There were a number of HDL remodelling and lipid-handling proteins increased in preeclampsia pregnancies in this cohort (Patanapirunhakit, 2023) which may be a compensatory response to maintain HDL size. The LPL inhibitor apoCIII is inactive when sequestered on HDL and was increased on preeclampsia HDL, perhaps maintaining the hydrolysis of triglyceride and preventing their accumulation in and consequent shrinking of HDL. The increased LCAT in preeclampsia HDL may be an adaptation to maintain cholesterol esterification and relocation to the core of the lipoprotein, especially in the face of increased passive diffusion of cholesterol in pregnancy (Melchior, Swertfeger, et al., 2021). Increased PLTP perhaps maintains the phospholipid content of HDL which is an important determinant of HDL size. A full discussion of HDL remodelling can be found in section 1.4.5. Cholesterol efflux capacity could also be at play in

maintaining HDL size in preeclampsia. Mistry et al., (2017) reported increased cholesterol efflux capacity in both maternal and fetal HDL from preeclampsia pregnancies compared to healthy controls, though ABCA1 mediated efflux was decreased. Efflux via ABCA1 favours lipid free apoAI and small HDL, which may indicate preferential efflux into larger HDL subclasses in preeclampsia.

There were no differences detected in HDL anti-inflammatory function between healthy pregnancy and preeclampsia pregnancy irrespective of preeclampsia phenotype. This was unexpected given the reduced anti-inflammatory function of preeclampsia HDL observed by Einbinder et al., (2018), however, this study employed methods distinct from the present thesis. HDL was isolated using a 48-hour ultracentrifugation time, which may have led to the removal of more loosely bound HDL proteins compared to the 7-hour total ultracentrifugation time in the present thesis. HDL was exposed to HUVECs based on 50 µg/mL total protein content; the assay development chapter of the present thesis (Chapter 3) found that exposing cells to 50 µg/mL apoAI was proinflammatory. HUVECs are fetal in nature and do not necessarily reflect maternal endothelial cells. Finally, as explained in section 3.1, macrovascular cells like HUVECs have been demonstrated to lead to highly variable results in assays of HDL anti-inflammatory function. These factors may explain the contradiction between these findings. Given the reduced HDL anti-inflammatory function observed in late healthy pregnancy, and the potentially compensatory compositional changes previously observed on HDL from preeclampsia HDL, it follows that other HDL functions may be more important during preeclampsia pregnancy which have not been measured here. For example, the ability of HDL to protect trophoblast invasion into the spiral artery endothelium described by (Charlton et al., 2017) may be impaired.

A strength of this study was the measurement of HDL size and anti-inflammatory function at eight timepoints throughout pregnancy, including pre-pregnancy and post-partum. This series through gestation was made up of two age- and BMI-matched women, minimising differences between them. HDL composition could be related to its size and function as it had already been assessed in samples from the same cohort. This was the first study to assess HDL anti-inflammatory vascular function throughout healthy pregnancy. Preeclampsia pregnancies were

gestational age-matched to healthy pregnancies to ensure fair comparison of preeclampsia phenotypes given the potential confounding effect of gestational age on HDL size and anti-inflammatory function. However, the gestational series was missing data at the establishment of the feto-placental vasculature (between ~10-15 weeks of gestation), the point at which it has been hypothesised that HDL production is increased (Sulaiman et al., 2016). Given the variability in HDL size and anti-inflammatory function, this study may have been underpowered to detect subtle changes in these metrics in early pregnancy. In terms of the preeclampsia study, the pre-term normotensive control pregnancies could be deemed as unhealthy due to early delivery. Measures of HDL-C were not available in this study which precluded the use of this measure as a co-variate in the HDL anti-inflammatory function data analysis. As a cross sectional study of preeclampsia matched based on gestational age at delivery, it was not possible to follow HDL changes through time in these women. A prospective study designed to follow the same women from pre-conception or very early pregnancy through to delivery, though challenging to perform, may reveal longitudinal changes in HDL composition or function in complicated pregnancies.

In summary, this chapter described an increase in HDL size but decrease in HDL anti-inflammatory function in late pregnancy, but no apparent changes in size or anti-inflammatory function in early pregnancy. This suggests that HDL does not protect the vasculature through anti-inflammatory means in pregnancy, but the increase in size may confer other protective properties such as improved cholesterol efflux or protection of the placenta. Preeclampsia, whether early- or late-onset, did not induce changes to HDL size or anti-inflammatory function beyond that of healthy pregnancy. This suggests that HDL-C may be more important than HDL function in the context of preeclampsia. There are other complications of pregnancy that may impact on HDL composition, size and function, such as gestational diabetes mellitus and risk factors thereof. The next chapter therefore seeks to combine the techniques used by Patanapirunhakit (2023) and those of the present thesis to assess HDL composition, size, and antioxidant and anti-inflammatory function in gestational diabetes mellitus.

6 High-density lipoprotein composition and function in gestational diabetes mellitus

6.1 Introduction

In the previous chapter, measures of HDL size and anti-inflammatory function were added to a previously performed study of HDL composition through healthy pregnancy and preeclampsia. HDL size increased in late pregnancy but was not different in preeclampsia compared to healthy pregnancy, perhaps due to the compositional changes observed by Patanapirunhakit (2023). HDL anti-inflammatory function was decreased in late pregnancy but was not different in preeclampsia pregnancy compared to healthy pregnancy. The present chapter aimed to establish the composition and function of HDL in pregnancies complicated by gestational diabetes mellitus (GDM) compared to healthy pregnancy and pregnancies with risk factors for GDM.

Like preeclampsia, GDM occurs in the third trimester of pregnancy and is characterised by insulin resistance and hyperglycaemia beyond that of healthy late pregnancy. GDM often occurs where pre-pregnancy sub-clinical insulin resistance and beta-cell dysfunction is aggravated by the maternal metabolic adaptation to pregnancy, in particular the switch to insulin resistance in late pregnancy required to facilitate fetal growth (reviewed by McIntyre et al., (2019)). A full discussion of the pathophysiology of GDM can be found in section 1.6.4.3. The underlying causes of GDM are similar to that of type 2 diabetes mellitus (discussed in section 1.3.2), where a number of changes in HDL composition have already been described including reduced HDL size, poorer efflux capacity and reduced vascular protection (Cardner et al., 2020). However, there is a limited and conflicting literature describing maternal HDL composition and function in GDM, though a number of studies focus on fetal and neonatal HDL and their effects on placental function. Pre-conception low HDL-C (Baumfeld et al., 2015) and smaller HDL size in early pregnancy (Mokkala et al., 2020) were predictors of the onset of GDM in late pregnancy, however, Pasternak et al., (2020) describe larger HDL in GDM pregnancy. HDL in the third trimester of GDM pregnancy had reduced PON-1 activity (Camuzcuoglu et al., 2009) compared to healthy pregnant controls, while Stadler et al., (2023) found no differences in antioxidant capacity and PON-1 activity between healthy and

GDM pregnancy. This chapter sought to add to the limited literature by comprehensively assessing HDL composition and function in GDM pregnancy.

6.1.1 Hypotheses

- HDL apoAI, total cholesterol and total protein content will be lower in GDM pregnancy.
- HDL will be smaller in size in GDM pregnancy compared to healthy pregnancy.
- The protein composition of HDL in GDM pregnancy will be different to healthy pregnancy in a fashion deleterious to overall HDL function.
- The antioxidant and anti-inflammatory functions of HDL will be lower in GDM pregnancy.

6.1.2 Objectives

- Isolate HDL from third trimester healthy pregnancies, those with risk factors for GDM and GDM pregnancy.
- Measure HDL apoAI, total cholesterol and total protein content in the three pregnant groups using colorimetric assays.
- Use native-PAGE to measure the HDL subclass distribution in healthy, risk factor, and GDM pregnancy.
- Identify the protein composition of HDL from each pregnant group using mass spectrometry.
- Measure HDL antioxidant function by paraoxonase-1 activity in each pregnant group.
- Measure the anti-inflammatory function of HDL using the assay developed in chapter 3.

6.2 Methods

6.2.1 Recruitment of women with GDM and healthy and risk factor controls

This cohort of pregnant women was recruited as part of the MD thesis 'Vascular function in hyperglycaemic pregnancy: studies into potential mechanisms for adverse obstetric outcomes in diabetes' by Dr Sharon Mackin at the University of Glasgow. This study was sponsored by NHS Greater Glasgow and Clyde and ethics approval granted from the Berkshire B ethics committee. Pregnant women were recruited from the Princess Royal maternity hospital and the Queen Elizabeth University Hospital maternity outpatient unit in Glasgow. Healthy pregnant controls were recruited at the standard 20-week fetal anomaly scan. GDM pregnancies were defined by the International Association of the Diabetes and Pregnancy Study Groups (IADPSG) guideline of fasting glucose ≥5.1 mmol/L and a glucose measurement of ≥ 8.5 mmol/L 2 hours post 75g OGTT. Women with GDM were treated by lifestyle intervention in the first instance and treated with metformin if lifestyle interventions were inadequate in reducing hyperglycaemia. As risk factors for GDM could influence vascular function independent of diabetes mellitus, a further risk factor control group was recruited. This was formed of women with risk factors for GDM including BMI >30 kg/m2, previous GDM, a first degree relative with diabetes mellitus, and previous macrosomic baby or being of high-risk ethnicity (South Asian, Middle Eastern or Black Caribbean). These women were recruited as risk factor pregnancies based on a normal OGTT. A summary of the study inclusion and exclusion criteria are outlined in table 6-1. Four study visits were performed. At visits one and four (at 24-30 weeks and 36-37 weeks of pregnancy respectively), participants had anthropometric measures taken and flow-mediated dilation (FMD) of the brachial artery analysis by ultrasound, followed by a fasted blood sample. At visits two and three, no blood sampling occurred but FMD brachial artery analysis was performed. The present study used 10 age- and BMI-matched samples from each recruited group at the visit 4 time-point, selected based on sample availability and n=10 samples per group required to detect proteomic differences as per Levels et al., (2011) and Patanapirunhakit (2023).

Table 6-1 Inclusion and exclusion criteria for the GDM study

Inclusion criteria		Exclusion criteria	
i.	Aged ≥18 years	i.	Aged ≤18 years
ii.	Singleton pregnancy	ii.	Multiple pregnancy
iii.	Normal 20-week anomaly scan	iii.	Pre-existing cardiovascular or metabolic disease (not including prior GDM)
		iv.	Taking vasoactive medications (excluding Aspirin, levothyroxine, folic acid and vitamins)
		v.	Significant pre-existing illness
		vi.	Congenital anomaly
		vii.	Identified placental anomaly

6.2.2 Isolation of HDL from plasma

HDL was isolated from participant plasma using sodium bromide sequential density ultracentrifugation as described in section 2.2.2. For the analysis of anti-inflammatory function, only the top 250 µL after the 1.21 g/mL step was retained to increase HDL concentration.

6.2.3 Measurement of HDL composition

HDL apoAI and SAA-1 content were measured by ELISA as per section 2.10. HDL cholesterol content was measured by colorimetric assay as per section 2.7 while HDL total protein was measured by Bradford assay as per section 2.6.

6.2.4 HDL size distribution analysis

HDL size was determined by native-gel electrophoresis according to 2.12.

6.2.5 Proteomic analysis of HDL

6.2.5.1 Buffers and solutions

Ammonium bicarbonate solution

25 mM ammonium bicarbonate in dH_2O.

Urea solution

8 M urea in ammonium bicarbonate solution.

Dithiothreitol solution

0.25 M dithiothreitol (DTT) in ammonium bicarbonate solution.

Iodoacetamide solution

0.75 M iodoacetamide ammonium bicarbonate solution.

Formic acid solution

0.1% v/v formic acid in dH_2O.

6.2.5.2 Peptide isolation procedure

HDL samples containing 10 µg protein as assessed by Bradford assay (section 2.6) were vacuum dried with a SpeedVac (Thermofisher Scientific) at 35°C for 10 minutes. Dried proteins were resuspended in the chaotropic urea solution (30 µL) and incubated for 10 minutes at room temperature to denature proteins. Following denaturation, 2 µL dithiothreitol (DTT) solution was added to break disulphide bonds between cysteine residues present in proteins. After 15 minutes with DTT, proteins were alkylated with iodoacetamide (2 µL) for 15 minutes. This prevents the reformation of disulphide bonds by 'capping' the now exposed cysteine residues. Reduced and alkylated proteins were diluted 1:10 with ammonium bicarbonate solution and trypsinised (1:25 w/w trypsin:protein) with trypsin stock solution (200 µg/mL, Promega) overnight at 37°C. The trypsinised peptides were then vacuum dried for 4 hours before the peptide pellets were reconstituted in 160 µL formic acid solution for a final protein concentration of 0.0625 µg/µL.

6.2.5.3 Nano liquid chromatography coupled to tandem mass spectrometry (nLC-MS/MS)

Peptides isolated from HDL samples (250 ng) were separated with a C18 column (100 mm × 0.75 µm, Agilent Technologies, Santa Clara, CA, USA) using the Thermofisher EASY-nLC II system. The mobile phase consisted of 2 – 40% acetonitrile in 0.1% formic acid for 82 minutes, followed by 90% acetonitrile for 8 minutes. Eluted peptides were transferred via electrospray ionisation to a LTQ Velos Orbitrap Pro (Thermofisher) tandem mass spectrometer where peptide sequences were determined by the collision-induced dissociation method with data-dependent acquisition. Spectra were analysed using MaxQuant software version 1.6.3.4 (Max Planck Institute of Biochemistry, Martinsried, Germany) and peptides identified by comparison with the Uniprot/Swissprot human protein database. Only proteins with two unique peptides appearing in >50% of samples were considered as identified in the analysis. Protein content of HDL was expressed relative to all other proteins across all samples as a label-free quantitation (LFQ) intensity. This method eradicates the need for stable isotope labelling of peptides.

6.2.5.4 Post-translational modification analysis of nLC-MS/MS spectra

Methionine oxidation and glycation of identified HDL proteins was subsequently analysed using MaxQuant software with a maximum of six modifications per peptide and similar fragment and parent mass tolerances. Results were expressed as both an LFQ value and the ratio of modified to un-modified protein. The specific glycations searched were as follows: early adduct Fructosyl-lysine (FL, mass 162 Da), advanced glycation end-products (AGEs) Nε-Carboxymethyl-lysine (CML, mass 58 Da), N1-(5-hydro-4-imidazolon-2-yl) ornithine (G-H1, mass 40 Da), Nε-(1-Carboxyethyl)lysine (CEL, mass 72 Da), Nδ-(5-hydro-5-methyl-4-imidazolon2-yl)-ornithine (MG-H1, mass 54 Da), Argpyrimidine (ARGP, mass 80 Da), Pyrroline (Pyr, mass 80 Da), Imidazoline B (IB, mass 142 Da) and 1-Alkyl-2-formyl-3,4-glycosyl-pyrrole (AFGP, mass 270 Da) according to Rabbani et al., (2016). In the post-translational modification analysis, modifications appearing in >50% of samples in any one group were considered as identified in the analysis.

6.2.6 HDL paraoxonase-1 activity assay

HDL paraxonose-1 activity was measured using a kinetic assay as per section 2.11.

6.2.7 HDL anti-inflammatory endothelial function

The anti-inflammatory function of HDL was assessed using the assay developed in chapter 3. Briefly, HMEC-1 were preincubated with HDL (based on 300 µg/mL ApoAI) for four hours before the addition of 5 ng/mL TNFα for 24 hours. Cells were lysed according to section 2.4 and SDS-PAGE / western blotting was performed for VCAM-1 according to sections 2.8 and 2.9. Results are expressed as % inhibition of VCAM-1 expressed by cells treated with TNFα alone. Each culture plate contained untreated and TNFα only treated cells; samples were corrected for baseline VCAM-1 expression and normalised to the TNFα only control present on the same plate.

6.2.8 Statistical analysis

Normal distribution of data was assessed by qualitative assessment of quantile-quantile (QQ) plot. Equality of standard deviation between groups was assessed by Brown-Forsythe test. Where data was normally distributed and standard deviations were equal across groups, comparisons were performed using one-way ANOVA with *post hoc* Tukey test. Where standard deviations were not equal between groups, Welch's corrected one-way ANOVA was used with *post hoc* Dunnett's T3 test. Where data was not normally distributed and could not be normalised by log transformation, Kruskal-Wallis with *post hoc* Dunn's multiple comparison test was used.

For HDL proteomic analysis, data was expressed as an LFQ intensity, a measure that quantifies the relative amount of protein across all samples in a mass spectrometry run without the use of isotope labelling. As the LFQ value is a relative value and there is a preponderance of zero values due to the nature of the methodology, the data is considered non-parametric. Proteomic analyses generate large datasets which require the use of multiple univariate comparisons. These are normally accounted for using corrected p values, for example by the Bonferroni method or by correcting for the false discovery rate

as per the Benjamini-Hochberg procedure. These methods work particularly well where each observation is independent and the n number is very large, however, with smaller n numbers and dependent observations these procedures are highly conservative. HDL hosts a limited number of proteins, and it is expected that these are correlated with one and other. As such, correcting for multiple comparisons is likely to mask true differences between the groups. In consultation with colleagues with statistical expertise, I decided not to correct for multiple comparisons but to qualitatively assess the comparisons based on the variables identified in multivariate analyses, the spread of the data and any unusual observations. The multivariate PCA and OPLS-DA reduce the demographic and proteomic data down to the variables contributing the most information and enable the visualisation of factors that most drive the differences between the groups and were performed according to section 2.14.1.

The gradient gel electrophoresis technique for HDL subclass analysis is semi-quantitative and the output data for each subclass is a percentage of the total HDL signal on the stained gel. As such this data is considered to be non-parametric and therefore Kruskal-Wallis with *post hoc* Dunn's multiple comparison test was used to make comparisons. These analyses were performed using GraphPad Prism software version 9.50.

Functional analyses were analysed by general linear model followed by *post hoc* Tukey test to allow for the inclusion of co-variates. General linear models do not make assumptions about data normality or equality of variances in the same way as ANOVA but do require the resulting residuals to be normally distributed. The normal distribution of residuals were assessed by qualitative assessment of the QQ plot. Non-normal residual distributions were rectified by log transformation of the input data. General linear modelling was performed using Minitab software version 20.3. For all analyses, statistical significance was assumed at $p < 0.05$.

6.3 Results

6.3.1 Characteristics of recruited healthy, risk factor, and GDM pregnancies

The characteristics of the study participants can be found in table 6-2. The three groups were of similar age, BMI and gestational age. While fasting glucose was similar in healthy, risk factor and GDM pregnancy, 2-hour glucose was significantly higher in GDM compared to risk factor pregnancy (8.94 ± 1.88 mmol/L and 5.13 ± 1.01 mmol/L respectively, $p < 0.001$, mean ± SD). Fifty percent of the GDM pregnancy cohort were taking metformin to treat their hyperglycaemia, while the remaining GDM participants were treated by lifestyle intervention.

Table 6-2 Characteristics of selected participants for the study of GDM. Data is expressed as mean ± SD. Data were analysed using one-way ANOVA with *post hoc* Tukey test. The 2-hr glucose was analysed by Student's t-test. Statistical significance was assumed at $p < 0.05$.

	Healthy pregnancy (n=10)	Risk factor pregnancy (n=10)	GDM pregnancy (n=10)	p value
Age (years)	33.5 ± 5.0	31.6 ± 3.9	32.8 ± 6.0	0.72
Gestational age (days)	256 ± 3	255 ± 4	255 ± 2	0.57
Systolic BP (mmHg)	107 ± 16	103 ± 10	98 ± 11	0.35
Diastolic BP (mmHg)	67 ± 11	65 ± 9	62 ± 7	0.52
Booking BMI (kg/m^2)	25.7 ± 3.1	26.2 ± 3.8	25.7 ± 3.4	0.94
Fasting insulin (mmol/L)	10.93 ± 4.80	8.98 ± 4.48	11.39 ± 6.31	0.62
Fasting glucose (mmol/L)	3.96 ± 0.36	4.09 ± 0.37	4.32 ± 0.37	0.14
2 hr glucose (mmol/L)	N/A	5.13 ± 1.01	8.94 ± 1.88	<0.001
HDL-C (mmol/L)	1.82 ± 0.40	1.77 ± 0.33	1.65 ± 0.46	0.68
Triglyceride (mmol/L)	2.81 ± 0.59	2.18 ± 0.66	2.45 ± 0.53	0.083
Cholesterol (mmol/L)	6.92 ± 1.06	6.70 ± 1.29	5.81 ± 1.14	0.12
HOMA-IR	1.54 ± 0.63	1.55 ± 0.97	2.39 ± 1.27	0.14
HbA1c (mmol/mol)	39.3 ± 4.4	36.6 ± 2.7	39.5 ± 3.9	0.19
Metformin	N/A	N/A	5 (50%)	N/A

6.3.2 Core HDL composition in healthy, risk factor and GDM pregnancy

There were no significant differences detected in HDL apoAI, total cholesterol or total protein content between healthy pregnancy, risk factor pregnancy or GDM pregnancy (Figure 6-1).

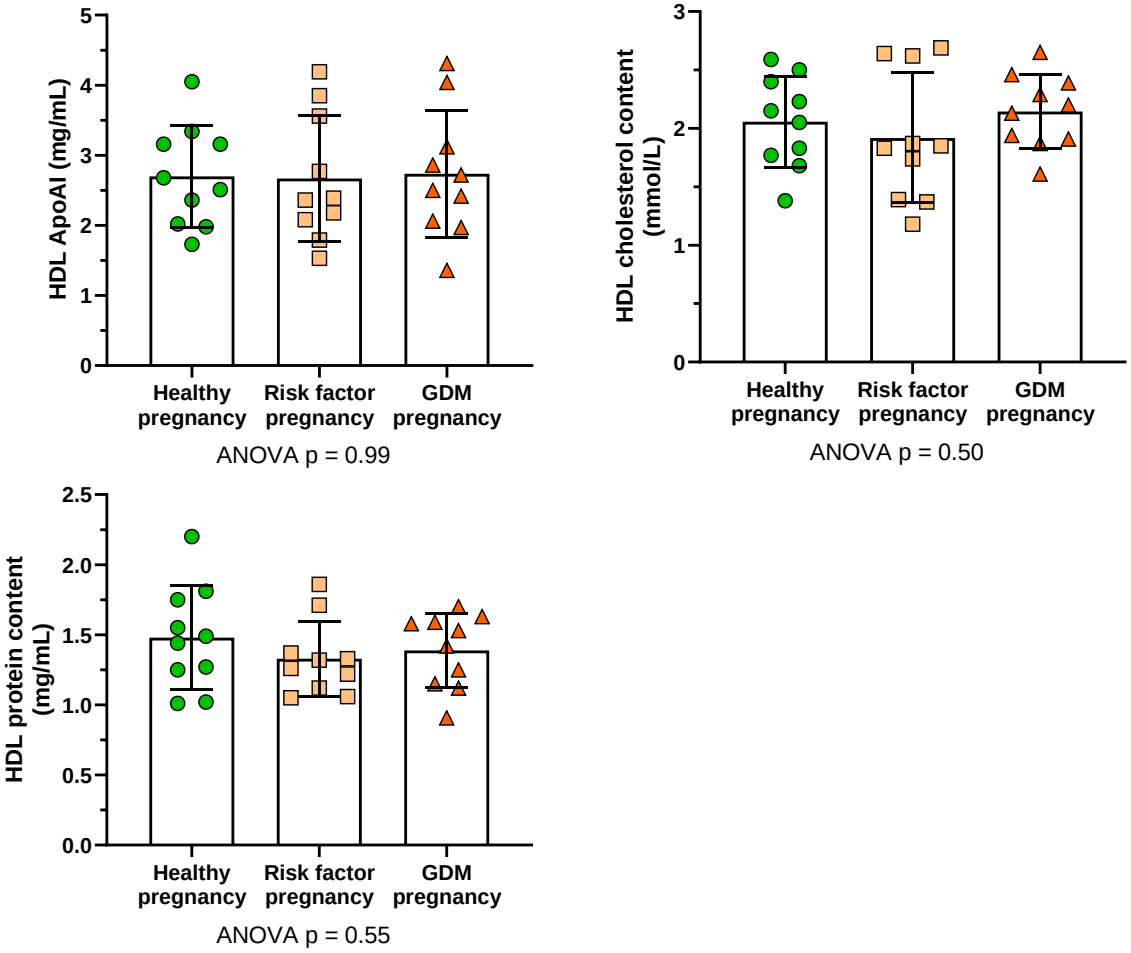

Figure 6-1 HDL apoAI, total cholesterol, and total protein content in healthy, risk factor and GDM pregnancy. Data expressed as mean ± SD and comparisons performed by one-way ANOVA. Statistical significance was assumed at $p < 0.05$.

6.3.3 HDL SAA-1 content in healthy, risk factor and GDM pregnancy

There was not a significant difference in HDL SAA-1 content between healthy, risk factor, and GDM pregnancy (Figure 6-2).

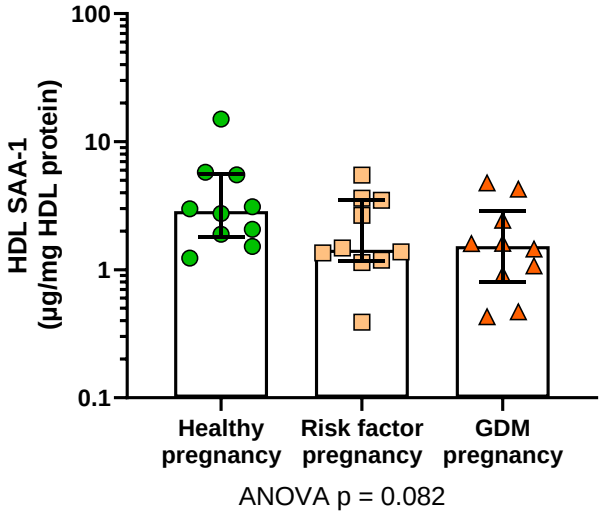

Figure 6-2 HDL SAA-1 content in healthy, risk factor and GDM pregnancy. Data expressed as median ± IQR on a $\log_{10}$ scale for legibility. Comparisons on $\log_{10}$ transformed data were made using one-way ANOVA. Statistical significance was assumed at $p<0.05$.

6.3.4 HDL subclass distribution in healthy, risk factor and GDM pregnancy

There were no significant differences detected in any HDL subclass or in the HDL2/HDL3 ratio between healthy, risk factor and GDM pregnancies (Figure 6-3).

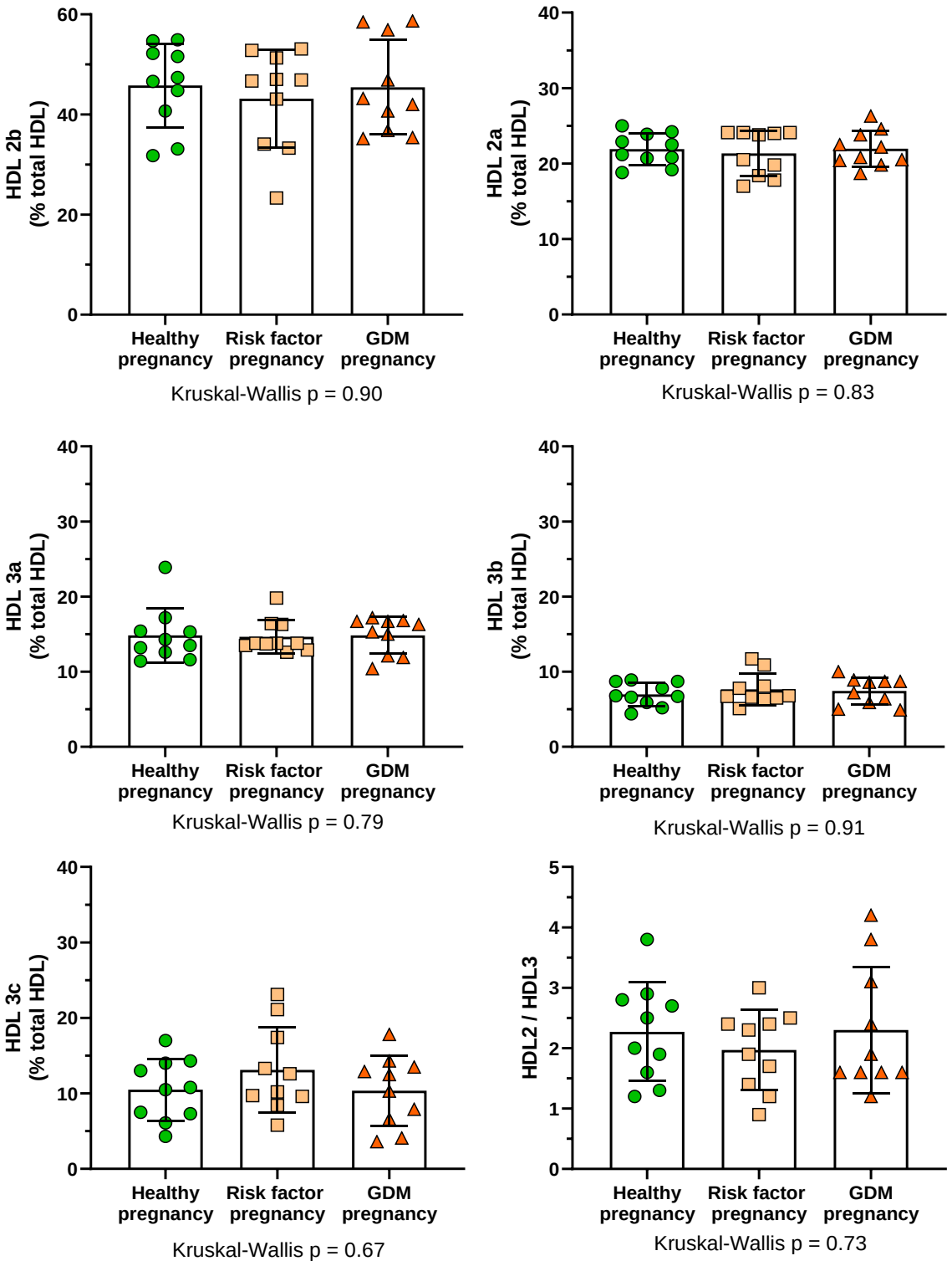

Figure 6-3 HDL subclass distribution in healthy, risk factor and GDM pregnancy. Data expressed as mean ± SD and comparisons made by one-way ANOVA. Statistical significance was assumed at $p<0.05$.

6.3.5 Proteomic analysis of HDL in healthy, risk factor and GDM pregnancy

6.3.5.1 Identification of HDL proteins

Proteomic analysis of HDL from healthy, risk factor and GDM pregnancy revealed 107 proteins identified in at least one HDL sample. After filtering for proteins present on >50% of HDL samples, 63 proteins were deemed HDL-associated (Table 6-3). These included apolipoproteins, HDL remodelling proteins and proteins involved in inflammation, coagulation and immunity.

Table 6-3 List of proteins identified in >50% of HDL samples by nLC-MS/MS in healthy, risk factor and GDM pregnancy

Afamin	Complement C4-B
Alpha-1-acid glycoprotein 1	Fibrinogen alpha chain
Alpha-1-acid glycoprotein 2	Fibrinogen beta chain
Alpha-1-antichymotrypsin	Haptoglobin
Alpha-1-antitrypsin	Haptoglobin-related protein
Alpha-1B-glycoprotein	Hemopexin
Alpha-2-antiplasmin	Heparin cofactor 2
Alpha-2-HS-glycoprotein	Ig gamma-1 chain C region
Angiotensinogen	Ig kappa chain C region
Antithrombin-III	Ig lambda-6 chain C region
Apolipoprotein A-I	Inter-alpha-trypsin inhibitor heavy chain H4
Apolipoprotein A-II	Kininogen-1
Apolipoprotein A-IV	Leucine-rich alpha-2-glycoprotein
Apolipoprotein B-100	Phosphatidylcholine-sterol acyltransferase
Apolipoprotein C-I	Phospholipid transfer protein
Apolipoprotein C-II	Pigment epithelium-derived factor
Apolipoprotein C-III	Platelet basic protein
Apolipoprotein C-IV	Prenylcysteine oxidase 1
Apolipoprotein D	Protein AMBP
Apolipoprotein E	Retinol-binding protein 4
Apolipoprotein F	Serotransferrin
Apolipoprotein L1	Serum albumin
Apolipoprotein M	Serum amyloid A-1 protein
Apolipoprotein(a)	Serum amyloid A-4 protein
Beta-2-glycoprotein 1	Serum paraoxonase/arylesterase 1
Beta-2-microglobulin	Sex hormone-binding globulin
Cathelicidin antimicrobial peptide	Sorting nexin-29
Cholesteryl ester transfer protein	Thyroxine-binding globulin
Chorionic somatomammotropin hormone 2	Transthyretin
Clusterin	Vitamin D-binding protein
Complement C3	Vitronectin
Complement C4-A	

6.3.5.2 Principal components analysis (PCA)

A PCA plot including the demographic and proteomic data as input variables was generated (Figure 6-4). Healthy, risk factor and GDM pregnancy samples did not separate across either the first or second principal component. Two control samples were situated outside the confidence interval of the Hotelling's T2 test.

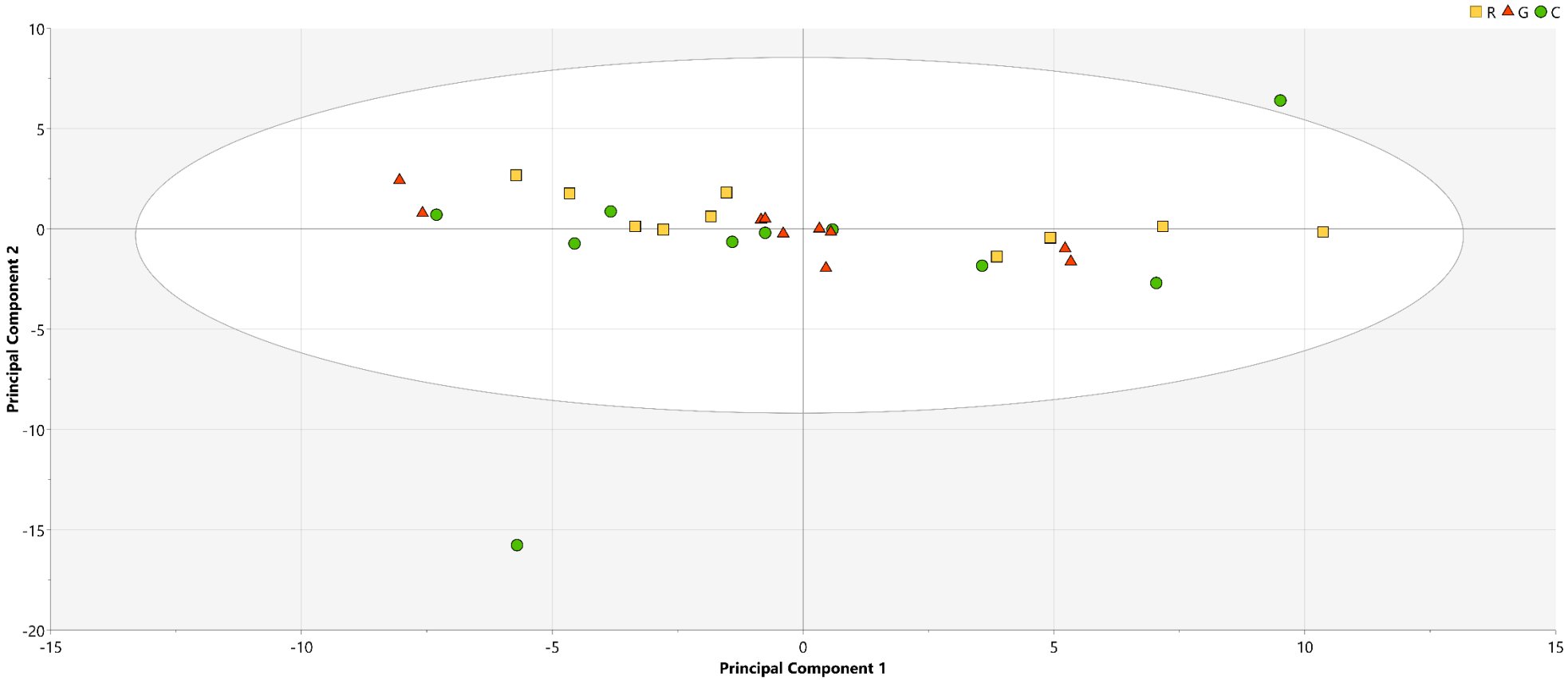

Figure 6-4 Principal components analysis score plot of the healthy, risk factor and GDM pregnancy study samples. Each shape represents an individual study participant. The ellipse represents the confidence region of a Hotelling's T2 test with significance level of p = 0.05. Samples outside the ellipse may be considered as potential outliers. The ellipse represents the confidence region of a Hotelling's T2 test with significance level of p = 0.05. Samples outside the ellipse may be considered as potential outliers. C, healthy control pregnancy, R, risk factor pregnancy, G, GDM pregnancy.

6.3.5.3 Univariate analysis of HDL protein composition

Analysis of the relative abundances of HDL-associated proteins revealed no significant differences in any protein between healthy, risk factor and GDM pregnancy (Figure 6-5).

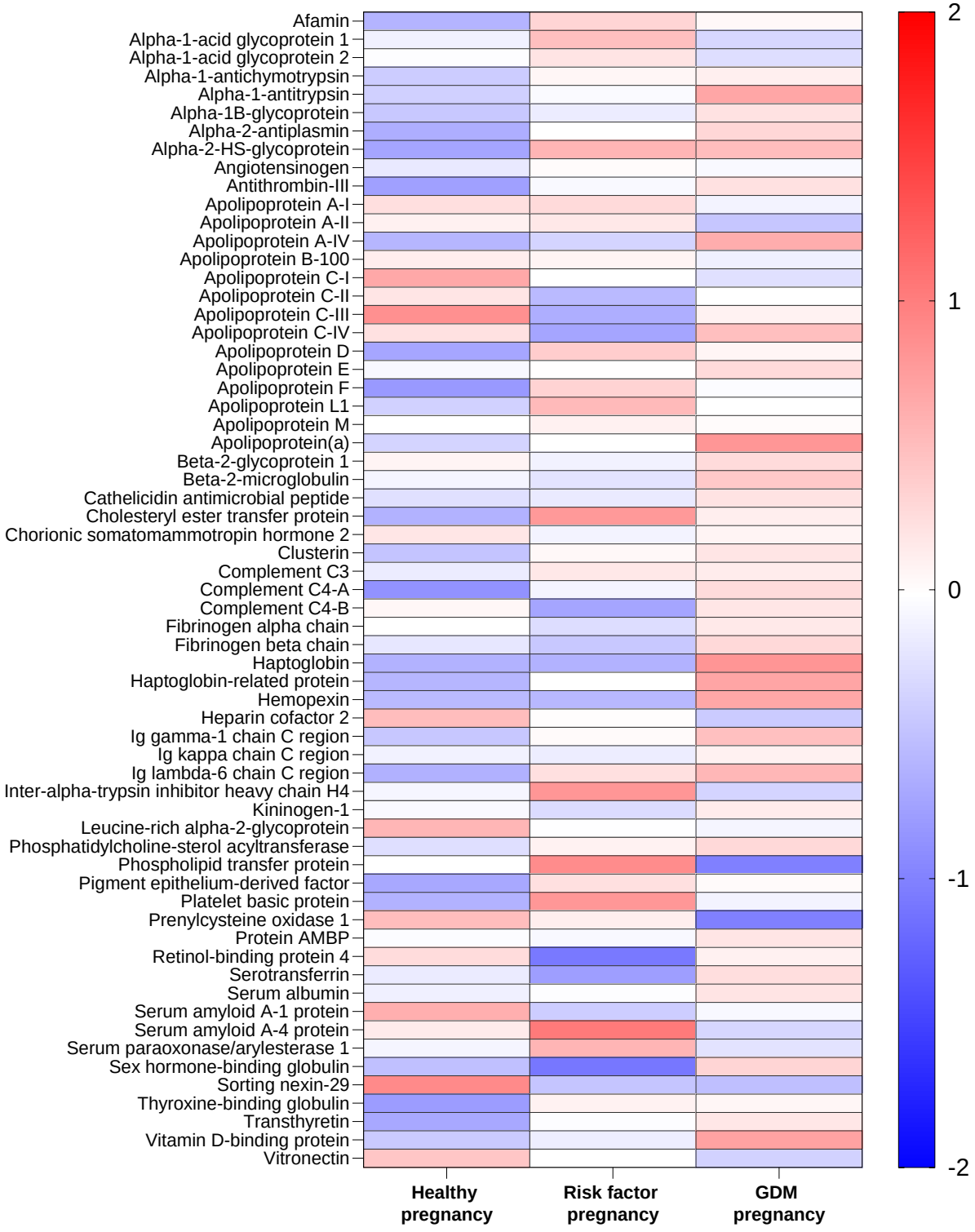

Figure 6-5 Heat map of the relative abundance of HDL-associated proteins in healthy, risk factor and GDM pregnancy. Heatmap plotted with the median median absolute deviation (MAD) adjusted LFQ intensity for each protein. Scale bar indicates median MAD.

6.3.5.4 Methionine oxidation of HDL-associated proteins

Thirteen proteins identified on HDL from healthy, risk factor and GDM pregnancy had oxidised methionine residues (Table 6-4). The degree of methionine oxidation did not differ between the three groups in any of these proteins.

Table 6-4 List of proteins with oxidised methionine residues in healthy, risk factor and GDM pregnancy

Protein name	Amino acid position(s) of modification
Alpha-1-acid glycoprotein 1	129
Alpha-1-antitrypsin	375, 382
Apolipoprotein B-100	31, 801, 812, 2040, 3280
Apolipoprotein C-I	1
Apolipoprotein(a)	3625, 4187
Beta-2-glycoprotein 1	61
Cathelicidin antimicrobial peptide	24
Clusterin	106, 107
Complement C3	1384, 1400, 1407, 1408
Fibrinogen beta chain	397, 403, 456, 468
Hemopexin	229, 255
Serum amyloid A-4 protein	35, 43
Thyroxine-binding globulin	198

6.3.5.5 Glycation of HDL-associated proteins

A full list of proteins with glycated residues can be found in the appendix. Of those proteins, differences in glycation between healthy, risk factor and GDM pregnancy HDL were observed in serotransferrin at arginine residue 162 and lysine residue 163 (Figure 6-6), and in leucine-rich alpha-2-glycoprotein 1 (LRG1) at lysine residues 10 and 41 (Figure 6-7).

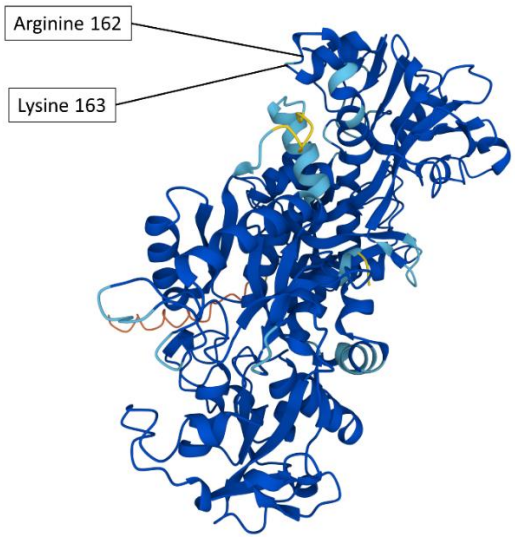

Figure 6-6 Structure of serotransferrin with arginine position 162 and lysine position 163 highlighted Protein structure was predicted using Alphafold DB prediction from EMBL-EBI (Jumper et al., 2021; Varadi et al., 2022). Source sequence was derived from Uniprot entry P02787. Image used under Creative Commons Attribution 4.0 (CC-BY 4.0) licence terms.

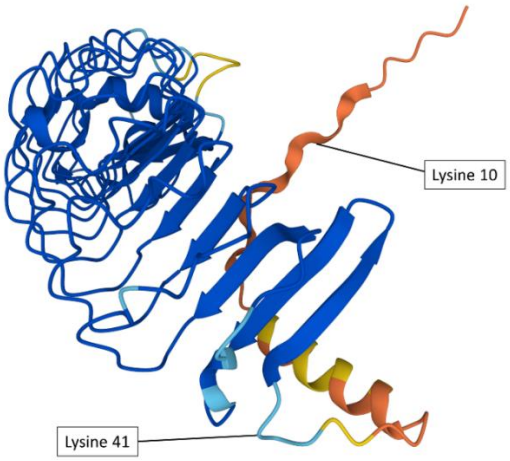

Figure 6-7 Structure of leucine-rich alpha-2-glycoprotein 1 with lysine position 10 and lysine position 41 highlighted Protein structure was predicted using Alphafold DB prediction from EMBL-EBI (Jumper et al., 2021; Varadi et al., 2022). Source sequence was derived from Uniprot entry P02750. Image used under Creative Commons Attribution 4.0 (CC-BY 4.0) licence terms.

Median Imidizilone B glycation of serotransferrin arginine 162 was significantly higher in risk factor pregnancy compared to both healthy pregnancy ($p = 0.0069$) and GDM pregnancy ($p = 0.037$, Figure 6-8). N1-carboxymethy-lysine glycation of serotransferrin lysine 163 was also significantly higher in risk factor pregnancy compared to both healthy ($p = 0.012$) and GDM pregnancy ($p = 0.018$, Figure 6-9). The cluster of individuals with high LFQ intensities in figures 6-8 and 6-9 are the same in both figures.

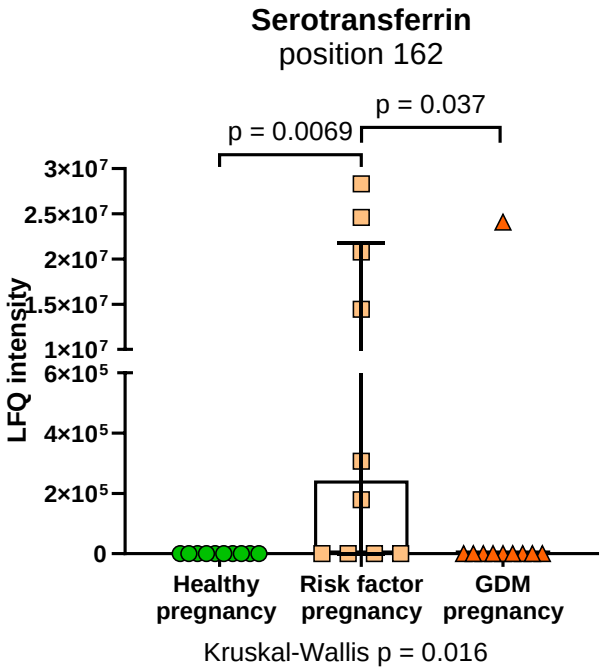

Figure 6-8 Imidizilone B glycation of serotransferrin arginine residue 162 in healthy, risk factor and GDM pregnancy. Data expressed as median ± IQR. Comparisons were made using Kruskal-Wallis test with *post hoc* Dunn's test. Statistical significance was assumed at $p < 0.05$.

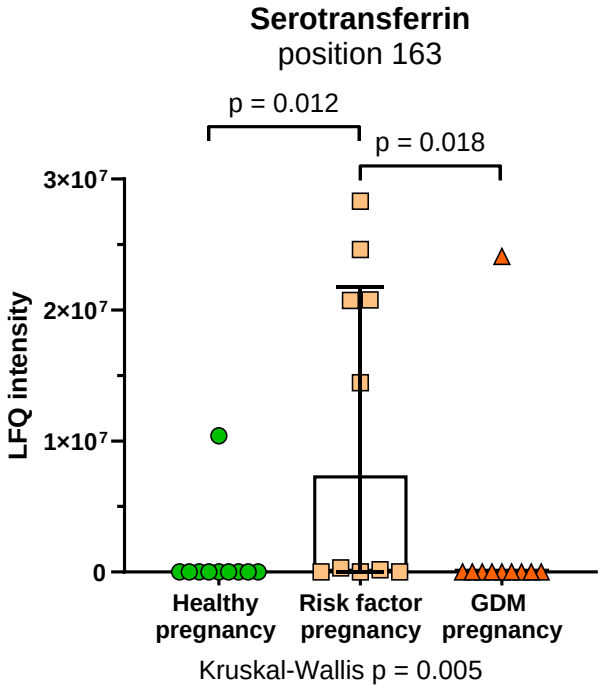

Figure 6-9 N1-Carboxymethyl-lysine glycation of serotransferrin lysine residue 163 in healthy, risk factor and GDM pregnancy. Data expressed as median ± IQR. Comparisons were made using Kruskal-Wallis test with *post hoc* Dunn's test. Statistical significance was assumed at $p < 0.05$.

Median pyrraline glycation of LRG1 at lysine residue 10 (Figure 6-10) and lysine residue 41 (Figure 6-11) was significantly higher in GDM pregnancy compared to both healthy and risk factor pregnancy, both in terms of raw glycation LFQ intensity and the ratio of glycated to unmodified protein. The cluster of individuals with high LFQ intensities in figures 6-10 and 6-11 are the same in both figures.

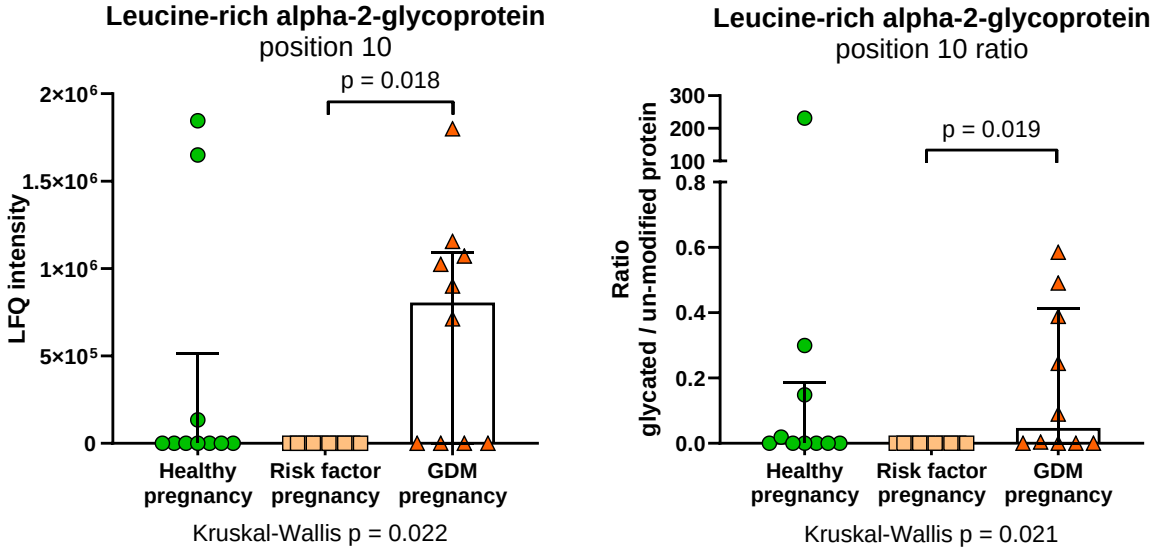

Figure 6-10 Pyrraline glycation of leucine-rich alpha-2-glycoprotein 1 lysine residue 10 in healthy, risk factor and GDM pregnancy. Data expressed as median ± IQR LFQ intensity (left) and ratio glycated/un-modified (right). Comparisons were made using Kruskal-Wallis test with *post hoc* Dunn's test. Statistical significance was assumed at $p < 0.05$.

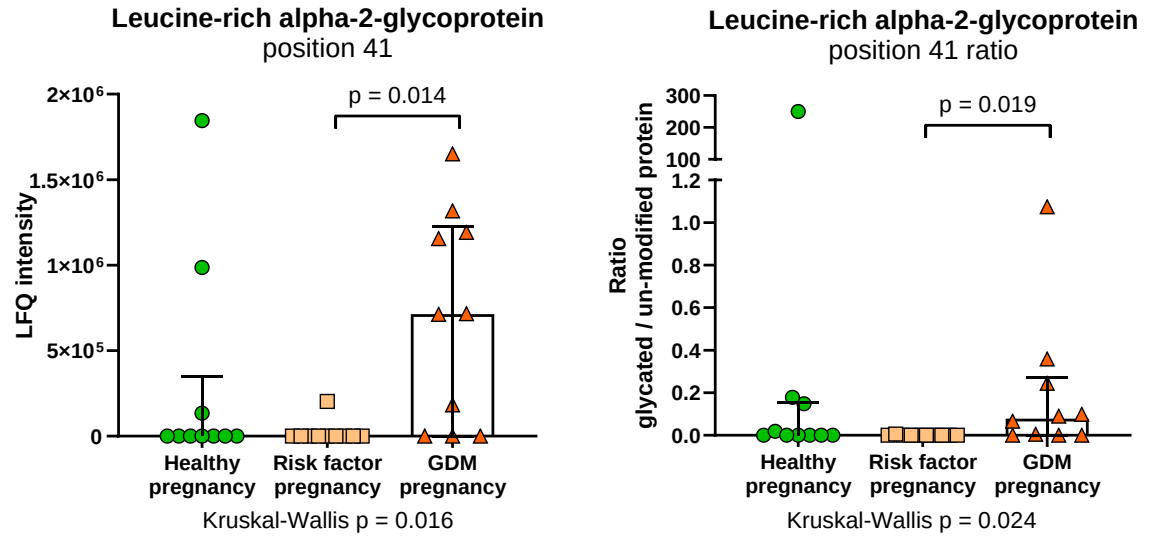

Figure 6-11 Pyrraline glycation of leucine-rich alpha-2-glycoprotein 1 lysine residue 41 in healthy, risk factor and GDM pregnancy. Data expressed as median ± IQR LFQ intensity (left) and ratio glycated/un-modified (right). Comparisons were made using Kruskal-Wallis test with *post hoc* Dunn's test. Statistical significance was assumed at $p < 0.05$.

6.3.6 HDL antioxidant function in healthy, risk factor and GDM pregnancy

Whether corrected for HDL total protein or HDL total cholesterol, there was no significant difference in HDL PON-1 activity between healthy, risk factor and GDM pregnancy (Figure 6-12). The PON-1/SAA-1 ratio was not significantly different between healthy, risk factor and GDM pregnancy (Figure 6-13).

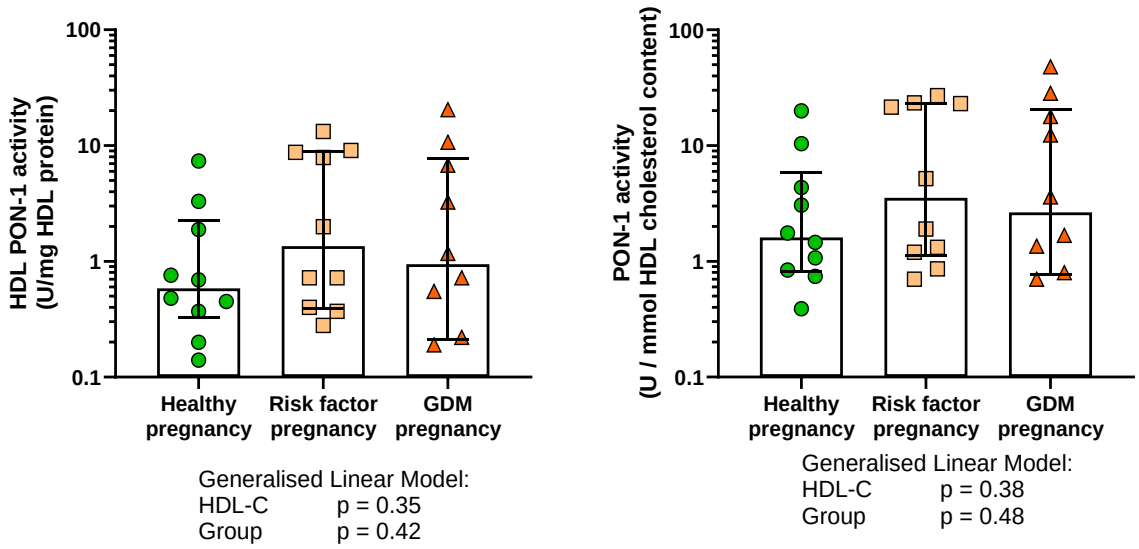

Figure 6-12 HDL paraoxonase-1 activity in healthy, risk factor and GDM pregnancy. Data expressed as median ± IQR on a $\log_{10}$ axis for legibility. Comparisions made using general linear model including HDL-C as a co-variate. Statistical significance was assumed at $p < 0.05$.

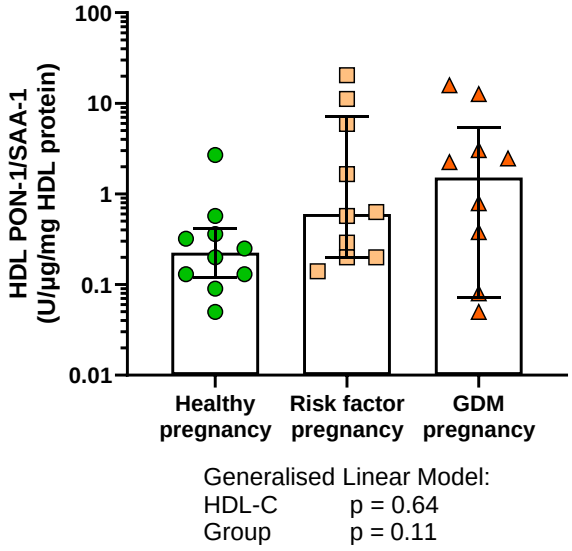

Figure 6-13 The ratio of HDL PON-1 to SAA-1 in healthy, risk factor and GDM pregnancy. Data expressed as median ± IQR on a $\log_{10}$ axis for legibility. Comparisions made using general linear model including HDL-C as a co-variate. Statistical significance was assumed at $p < 0.05$.

6.3.7 HDL anti-inflammatory function in healthy, risk factor and GDM pregnancy

Whether exposed to cells based on 300 µg/mL apoAI, or subsequently corrected for HDL total cholesterol and total protein content, there was not a difference in HDL anti-inflammatory endothelial function between healthy, risk factor and GDM pregnancy (Figure 6-14).

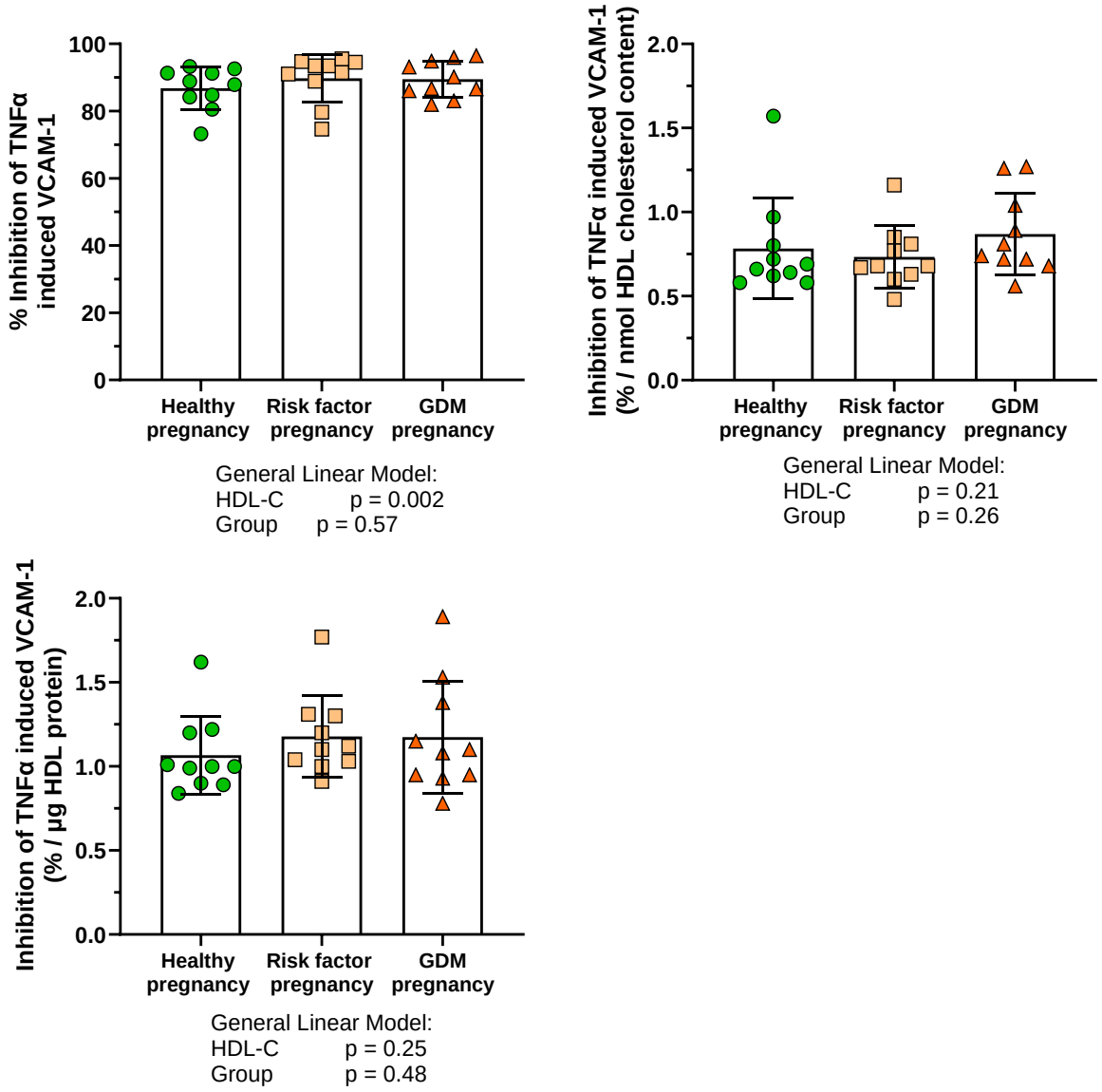

Figure 6-14 HDL endothelial anti-inflammatory function in healthy, risk factor and GDM pregnancy. Data expressed as mean ± SD and comparisons made by general linear model including HDL-C as a co-variate. Statistical significance was assumed at $p < 0.05$.

6.4 Discussion

This chapter set out to establish HDL composition and function in age- and BMI-matched healthy, risk factor and GDM pregnancy. HDL did not differ between these three groups by any compositional or functional measure in this cross-sectional study.

There was not a difference detected in HDL apoAI, total cholesterol or total protein content between the three groups. The primary intervention for GDM pregnancy is dietary. Improvements in diet, in particular reduced carbohydrates, lead to improved serum lipid profiles and potentially improved HDL composition and function (reviewed by Escolà-Gil et al., (2015)). Half of the GDM group were treated with metformin, which modestly increases HDL-C (Wu et al., 1990) and increases apoAI and apoAII on HDL (Schneider et al., 1990). This suggests that the interventions used to treat GDM may recover HDL composition. In late healthy gestation, there is an increase in HDL apoAI that was not attenuated by preeclampsia (Patanapirunhakit, 2023) which may indicate that the pregnancy effect on HDL composition overrides the consequences of any complication, including GDM. HDL SAA-1 content was also not significantly different in GDM pregnancy compared to healthy and risk factor pregnancy, though tended to be lower in GDM pregnancy. This is in contrast to the non-pregnant population, where HDL from women with type 2 diabetes mellitus had increased SAA-1 content compared to healthy controls in a cohort with a similar age, BMI, and rate of metformin use (Griffiths et al., 2017). HDL SAA-1 content did not change through healthy gestation despite the increase in insulin resistance in late pregnancy (Patanapirunhakit, 2023). Taken together, this further suggests that pregnancy itself protects against insulin resistance-driven adverse remodelling of HDL. The distribution of HDL subclasses was not different between healthy, risk factor and GDM pregnancy, reinforced by the lack of difference in HDL2/HDL3 ratio between the groups, likely related to the lack of observed differences in HDL apoAI and total cholesterol which are key determinants of HDL size. In summary, these findings suggest that the deleterious effects on HDL composition observed in insulin resistance in the non-pregnant population may be overcome by the gestational hormone driven effects of pregnancy. It may be that other measures of HDL composition, such as phospholipid and sphingolipid species are more important in the context of pregnancy.

Proteomic analysis revealed 63 proteins associated with HDL in healthy, risk factor and GDM pregnancy. The LFQ intensities of the proteins and the demographic data were used to create a PCA plot to determine similarity between samples. Control, risk factor and GDM pregnancy samples did not separate and were spread throughout the plot, suggesting that the HDL proteome was highly variable in each group and was not different between the three groups. Univariate analysis confirmed this suggestion, with no significant differences observed in any identified protein. This may have been related to statistical power, though the proteomic methodology has power to detect differences between groups with n = 10 per group (Levels et al., 2011), and differences in the HDL proteome between normotensive pregnancy (n=10) and early- and late-onset preeclampsia (n=10) were detected using mass-spectrometry analysis at the same time as the present study of GDM (Patanapirunhakit, 2023). There was a high degree of overlap in the proteins identified on HDL through healthy gestation by Patanapirunhakit (2023) and the present study, with 54 proteins identified in common and nine disparate proteins which included platelet factor 4, zinc-alpha-2-glycoprotein and paraoxonase-3. This might be due to the cross-sectional nature of this study compared to the longitudinal study performed in the previous work; these proteins may have been more abundant in earlier gestation. Patanapirunhakit (2023) detected a further 88 proteins when comparing third trimester healthy pregnancy to preeclampsia, predominantly immune and coagulation related proteins, which is likely a reflection of the response to preeclampsia.

There was however increased glycation detected in two proteins; serotransferrin exhibited higher glycation at two residues in risk factor pregnancy compared to both healthy and GDM pregnancy, while LRG1 exhibited higher glycation at two lysine residues in GDM pregnancy compared to risk factor pregnancy. Serotransferrin is an iron transporter which transfers iron between tissues. There is evidence that increased tissue iron stores are associated with the development of type 2 diabetes mellitus (Golizeh et al., 2017) and GDM (Zhang and Rawal, 2017). Glycation shortens the half-life of serotransferrin (Golizeh et al., 2017) which may suggest that risk factor pregnancies have increased tissue iron which may contribute to their risk for GDM development. Higher glycation of serotransferrin may therefore have a role in the onset of GDM, which is likely

to have been recovered by the subsequent pharmacological and dietary interventions in this group of participants. The consequence of higher LRG1 glycation in GDM pregnancy compared to risk factor pregnancy is less clear. There is conflicting evidence around the role of LRG1, particularly as LRG1 knockout animals appear to exhibit no change in physiology, though there is some consensus that it is a modulator of TGF-ß signalling and therefore has a role in angiogenesis and the stability and deposition of extracellular matrix components (reviewed by Camilli et al., (2022)). In terms of metabolic disease and insulin resistance, Choi et al., (2022) describe LRG1 as a promotor of insulin sensitivity, while He et al., (2021) describe LRG1 as a mediator of insulin resistance. The lack of difference detected between healthy and GDM pregnancy is likely due to a small number of healthy pregnant women with a very high glycated/un-modified LRG1 ratio, i.e that there was very little unmodified LRG1 in these individuals. Despite these differences, there is complexity in interpreting data resulting from the mass-spectrophotometric detection of glycated proteins. Glycation is a non-enzymatic and non-specific reaction, and the glycation of proteins is therefore predicated on the abundance of that protein and the concentration of sugars available to glycate said protein at the time the sample was taken. Both serotransferrin and LRG1 are low abundance on HDL and detected in far fewer studies of HDL composition (Davidson et al., 2022) compared to common proteins such as apoAI, and fasting glucose levels were similar between the three groups. The GDM group were treated with lifestyle modification and metformin, both of which reduce blood sugar levels and therefore the amount of sugar available to glycate proteins. The interpretation of these data should therefore be treated as speculative and requires further study in a larger group of individuals. In summary, the HDL proteome did not differ between healthy, risk factor and GDM pregnancy. There were differences in glycation in two proteins though the consequences of these post-translational modifications are unclear given both experimental limitations and the limited and conflicted literature on serotransferrin and LRG1 in pregnancy and insulin resistance.

Whether corrected for HDL protein or cholesterol content, HDL paraoxonase-1 activity was not different between healthy, risk factor and GDM pregnancy which was in contrast to the decreased serum PON-1 activity in GDM pregnancy

described by Camuzcuoglu et al., (2009). This may be due to differences in PON-1 activity not associated with HDL given whole serum was assessed. The published study populations consisted of 59 control pregnancies and 55 GDM pregnancies, well in excess of the ten participants per group in the present chapter. A power analysis calculated based upon a Cohen's effect size of 0.25 derived from the present chapter revealed a minimum of 45 individuals per group would be required to observe a significant difference at $p = 0.05$ with 80% power, suggesting that this study is underpowered. This may also be the case for the PON-1/SAA-1 ratio, though the high variability in the risk factor and GDM pregnancy suggests that there may be other factors impacting upon this measure of overall HDL function in these groups. It may be the case that this metric is not as useful in the context of pregnancy compared to the non-pregnant population, especially as HDL SAA-1 content and PON-1 activity are not altered through healthy gestation (Patanapirunhakit, 2023). Finally, the anti-inflammatory function of HDL as assessed by inhibition of TNFα stimulated VCAM-1 in HMEC-1 did not differ in healthy, risk factor or GDM pregnancy, whether corrected for HDL cholesterol or protein content. The previous chapter showed a reduction in this measure in late healthy gestation; risk factor and GDM pregnancy did not reduce HDL anti-inflammatory function beyond that of late healthy pregnancy. This may also have been due to lack of power; however, variability was very similar between the three groups and the effect size between them likely to be very small. It may be that any potential significant difference between these groups may not be biologically pertinent.

A strength of this study is that it was a comprehensive study of HDL composition and function in the same women throughout. A second control group, risk factor pregnancy, was included to mitigate any potential confounding effects that GDM risk factors may have on HDL or maternal vascular function. The groups were well matched by age and BMI to avoid potentially confounding effects of these measures. The proteomic analysis was undertaken at Linköping University with Dr Helen Karlsson and Dr Stefan Ljunggren who have significant expertise in lipoprotein proteomics. However, the study was powered for the proteomic analysis which might have precluded the detection of significant differences in the other analyses undertaken. There were a limited number of samples available for analysis which prevented expansion of the group sizes. This study

was cross-sectional in nature; it may be the case that changes in HDL composition and function in GDM may be more apparent in earlier pregnancy. Other measures of HDL composition and function not measured in this thesis, such as sphingolipid content or cholesterol efflux capacity, might differ in pregnancy. Finally, pregnancy and GDM are complex phenotypes. In the groups studied in this chapter, I had three distinct factors at play: an effect of pregnancy, an effect of obesity and other risk factors, and a type 2 diabetes mellitus-like phenotype. Given the complexity in delineating pregnancy effects from the impact of obesity and insulin resistance effects, the inclusion of non-pregnant study participants with these phenotypes as comparator groups in a larger study may help to clarify the individual contributions of those factors. In summary, this chapter described that HDL composition and antioxidant and anti-inflammatory function is maintained in GDM pregnancy. Future studies should attempt to follow women at risk of developing GDM through pregnancy to determine if changes in HDL occur earlier in pregnancy. Studies should also focus on the role of adipose tissue and liver lipid handling in GDM pregnancy, to determine if a pregnancy specific mechanism of insulin resistance occurs. Having thus far explored HDL composition and function in healthy and complicated pregnancies, the next chapter aims to determine the effect of insulin resistance on HDL composition and function in healthy control, endurance athlete and impaired glucose regulation middle-aged men.

7 A cross-sectional study of HDL composition and function with varying insulin resistance in middle-aged men

7.1 Introduction

This thesis has thus far used pregnancy as a model of altered insulin resistance over the relatively short period of gestation. I have shown that HDL size is increased but HDL anti-inflammatory function decreased through healthy pregnancy and that there was no effect of insulin resistance in pregnancy (i.e., GDM pregnancy) over and above these pregnancy-induced changes. HDL assessed in third trimester healthy pregnancy compared to GDM pregnancy showed no difference in any measure of HDL composition or function. Moving on from pregnancy, this chapter sets out to understand HDL composition and function with chronic insulin resistance in a cross-sectional study of middle-aged men, including men with impaired glucose regulation, healthy controls and endurance athletes.

T2DM and exercise alter cardiovascular and metabolic physiology in opposite directions. In T2DM, elevated plasma glucose and insulin levels ultimately provoke oxidative stress, inflammation and the formation of advanced glycation end products all of which have detrimental effects on vascular function. Many of these changes are linked to vascular stiffening and impaired endothelial function (Petrie et al., 2018b). Metabolically, insulin resistance in T2DM is associated with dyslipidaemia and visceral adiposity, both of which also have deleterious effects on vascular function. It is well established that individuals with pre-diabetes are also at increased risk of vascular disease despite being below the clinical threshold for T2DM (Beulens et al., 2019). There have been previous studies into HDL composition and function in T2DM though these largely focus on cholesterol efflux, or recruit participants who are on treatments for their diabetes such as metformin, insulin or sulphonylureas which may have effects on HDL composition and function. Nevertheless, alongside a reduction in cholesterol efflux capacity, Cardner et al., (2020) found HDL from T2DM patients to have adverse changes in composition and reduced vasculoprotective functionality. The effect of exercise on vascular and metabolic health has been well documented. A meta-analysis of 160 randomised control trials found that

exercise increased cardiorespiratory fitness, improved the lipid profile (particularly increased HDL-C) and improved measures of glycaemic control and insulin resistance (Lin et al., 2015). There is mixed evidence of the effects of exercise on HDL composition and function, particularly as many studies focus on short-term training programmes that can take many forms or use exercise as an intervention in individuals with metabolic or vascular disease. Despite the mixed study designs, the overall picture points towards beneficial effects of exercise on HDL function (as reviewed by Ruiz-Ramie, Barber and Sarzynski (2019)).

With HDL known to have effects on glycaemic control and insulin resistance (section 1.7.4), as well as pleiotropic vascular protective functions mediated by its composition (section 1.7), this chapter aimed to compare HDL composition and function between insulin resistant men with impaired glucose regulation, healthy men who exercise minimally, and endurance-trained men covering a full spectrum of insulin resistance through to insulin sensitivity.

7.1.1 Hypotheses

- There is a detrimental profile of HDL composition in IGR men with a related reduction in HDL antioxidant and anti-inflammatory functions compared to control and endurance athlete HDL.

- Conversely, there is a beneficial profile in athlete HDL composition with an associated increase in HDL antioxidant and anti-inflammatory function compared to control and IGR HDL.

7.1.2 Objectives

- Establish the effects of impaired glucose regulation and endurance exercise on measures of HDL apoAI, total cholesterol and total protein content.

- Measure the size distribution of HDL in IGR, control and endurance-athlete men

- Perform proteomic analysis of HDL to understand the effect of insulin resistance and sensitivity on its protein composition and post-translational modification.

- Compare the antioxidant and anti-inflammatory function of HDL from men with varying insulin resistance.

7.2 Methods

7.2.1 Recruitment of healthy, athlete and IGR men

Participants were recruited from the 'Role of alternative pathways of triglyceride synthesis in determining insulin sensitivity in muscle (M-FAT)' study, performed at the Universities of Glasgow and Warwick in 2017 and funded by Diabetes UK. The study was conducted with ethical approval from the West of Scotland Research Ethics Committee 4 (reference number 16/WS/0002). This study set out to determine whether an imbalance of the differing triacylglycerol synthesis pathways in muscle was related to insulin resistance, and if such an imbalance explained the variability of relationship between ectopic triacylglycerol and insulin resistance. The major findings of this study are found in the PhD thesis entitled 'Insulin sensitivity in men with impaired glucose regulation and endurance-trained athletes: the roles of skeletal muscle and adipose tissue' by Dr Anne Sillars at the University of Glasgow. Three groups of men with varying insulin resistance were recruited at GP practices local to the university and at local running, cycling and triathlon clubs. Lean normoglycemic men who did not participate in regular vigorous exercise (normal insulin sensitivity, n = 18), impaired glucose regulation men at high risk of type 2 diabetes mellitus (low insulin sensitivity, n = 17) and endurance athletes undertaking > 5 hours per week of vigorous exercise for at least 2 years (high insulin sensitivity, n = 20) underwent a 2-hour oral glucose tolerance test after an overnight fast, a maximal incremental cycle ergometer test to assess maximal oxygen uptake, and a muscle and adipose tissue biopsy. Inclusion and exclusion criteria for this study are summarised in table 7.1. This study was originally powered to detect a one standard deviation difference with 80% power in intramuscular triglyceride concentration, and this analysis of HDL composition and function used every collected sample.

Table 7-1 Inclusion and exclusion criteria for the recruitment of the M-FAT study

Group	Inclusion criteria	Exclusion criteria
Impaired glucose regulation **Lean normoglycemic controls** (< 1 hour per week vigorous exercise) **and** **Endurance athlete** (>5 hours per week vigorous exercise >2 years)	i. Male ii. Aged 30 – 60 years iii. HbA1c between 6.0 and 6.4% (43.8 – 47.4 mmol/mol) i. Male ii. Aged 30-60 years iii. BMI 18 – 27 kg/m^2 iv. HbA1c <6% (<48.8 mmol/mol) v. No history of cardiovascular, metabolic or systemic disease vi. Not taking drugs affecting carbohydrate or lipid metabolism	i. Female ii. Aged <30 years or >60 years iii. Uncontrolled hypertension >160/90 mmHg on anti-hypertensive medication iv. Previous history of coronary heart disease or stroke v. On any treatment for glucose control vi. Any other serious chronic health conditions.

7.2.2 Isolation of HDL

HDL was isolated from participant plasma samples using sodium bromide sequential density ultracentrifugation according to section 2.2.2. For HDL proteomic analysis, the top 500 µL containing HDL after the 1.21 g/mL centrifugation was collected and passed once through a desalting column. For all other analyses, the top 250 µL HDL 1.21 g/mL centrifugation was collected and passed twice through a desalting column.

7.2.3 Measurement of core HDL composition

ApoAI and SAA-1 content of HDL was measured using ELISA as per section 2.10. HDL protein was measured by Bradford assay (section2.6). HDL cholesterol content was measured by colorimetric assay (section 2.7).

7.2.4 HDL sizing

The size distribution of HDL was measured using native gel electrophoresis as set out in section 2.12.

7.2.5 Proteomic analysis of HDL

HDL proteomics were performed according to section 4.2.5 with post-translational modification analysis of identified HDL proteins performed according to section 6.2.5.4.

7.2.6 HDL paraoxonase-1 activity assay

HDL paraoxonase-1 arylesterase activity was measured using a kinetic UV-visible spectrophotometric method described in section 2.11.

7.2.7 Assessment of HDL anti-inflammatory function

The anti-inflammatory function of HDL was assessed by measuring the inhibition of TNFα induced VCAM-1 as set out in chapter 3. Briefly, HMEC-1 were preincubated with HDL (based on 300 μg/mL ApoAI) for four hours before the addition of 5 ng/mL TNFα for 24 hours. Cells were lysed according to section 2.4 and SDS-PAGE / western blotting was performed for VCAM-1 according to section 2.8 and 2.9. Results are expressed as % inhibition of VCAM-1 expressed by cells treated with TNFα alone. Each culture plate contained untreated and TNFα only treated cells; samples were corrected for baseline VCAM-1 expression and normalised to the TNFα only control present on the same plate.

7.2.8 Statistical Analysis

Normal distribution of data was assessed by qualitative assessment of the QQ plot. Equality of standard deviation between groups was assessed by Brown-Forsythe test. Where data was normally distributed and standard deviations were equal across groups, comparisons were performed using one-way ANOVA with *post hoc* Tukey test. Where standard deviations were not equal between groups, Welch's corrected one-way ANOVA was used with *post hoc* Dunnett's T3 test. Where data was not normally distributed and could not be normalised by log transformation, Kruskal-Wallis with *post hoc* Dunn's multiple comparison test was used.

For HDL proteomic analysis, data was expressed as an LFQ intensity, a measure that quantifies the relative amount of protein across all samples in a mass spectrometry run without the use of isotope labelling. As the LFQ value is a relative value and there is a preponderance of zero values due to the nature of the methodology, the data is considered non-parametric. Proteomic analyses generate large datasets which require the use of multiple univariate comparisons. These are normally accounted for using corrected p values, for example by the Bonferroni method or by correcting for the false discovery rate as per the Benjamini-Hochberg procedure. These methods work particularly well where each observation is independent and the n number is very large, however, with smaller n numbers and dependent observations these procedures are highly conservative. HDL hosts a limited number of proteins, and it is expected that these are correlated with one and other. As such, correcting for multiple comparisons is likely to mask true differences between the groups. In consultation with colleagues with statistical expertise, I decided not to correct for multiple comparisons but to qualitatively assess the comparisons based on the variables identified in the PCA and OPLS-DA analyses, the spread of the data and any unusual observations. The multivariate PCA and OPLS-DA reduce the demographic and proteomic data down to the variables contributing the most information and enable the visualisation of factors that most drive the differences between the groups and were performed according to section 2.14.1.

The gradient gel electrophoresis technique for HDL sizing is semi-quantitative and the output data for each subclass is a percentage of the total HDL signal on the stained gel. As such this data is considered to be non-parametric and therefore Kruskal-Wallis with *post hoc* Dunn's multiple comparison test was used to make comparisons. These analyses were performed using GraphPad Prism software version 9.50.

Functional analyses were analysed by general linear model followed by *post hoc* Tukey test to allow for the inclusion of co-variates. General linear models do not make assumptions about data normality or equality of variances in the same way as ANOVA but do require the resulting residuals to be normally distributed. The normal distribution of residuals were assessed by qualitative assessment of the QQ plot. Non-normal residual distributions were rectified by log transformation of the input data. General linear modelling was performed using Minitab software version 20.3. For all analyses, statistical significance was assumed at $p < 0.05$.

7.3 Results

7.3.1 Characteristics of M-FAT study participants

Demographic and anthropometric data for the M-FAT study participants are described in table 7-2. Mean ages were 53.4, 45.2 and 42.1 years for IGR, control and athlete groups respectively. Mean BMI and HbA1c was highest in the IGR group (30.5 kg/m^2 and 53.4%, $p < 0.0001$). Mean HDL concentration was lowest in the IGR group (1.13 mmol/L, $p = 0.002$). Mean Matsuda index was highest in the endurance athletes (10.8) followed by controls (6.2) and IGR (2.6, $p < 0.0001$). Conversely, $HOMA_{IR}$ was highest in the IGR (5.82) compared to control and athlete (1.36 and 0.99 respectively, $p < 0.0001$).

Table 7-2 M-FAT study participant characteristics: Data expressed as mean ± SD. Comparisons were made by one-way ANOVA and *post hoc* Tukey test. Means that do not share a letter are statistically significantly different.

	IGR (n = 17)	Control (n = 18)	Athlete (n = 20)	p value
Age (years)	53.4 ± 5.0 ^{A}	45.2 ± 9.5 ^{B}	42.1 ± 6.1 ^{B}	0.0001
BMI (kg/m^2)	30.5 ± 3.4 ^{A}	23.8 ± 1.8 ^{B}	23.4 ± 1.5 ^{B}	<0.0001
Body fat %	31.8 ± 7.3 ^{A}	19.4 ± 5.5 ^{B}	13.0 ± 5.8 ^{C}	<0.0001
Waist/Hip Ratio	1.05 ± 0.08 ^{A}	0.93 ± 0.07 ^{B}	0.88 ± 0.06 ^{B}	<0.0001
Systolic blood pressure (mmHg)	142 ± 14 ^{A}	131 ± 12 ^{B}	135 ± 9.7 ^{AB}	0.030
Diastolic blood pressure (mmHg)	90 ± 7.15 ^{A}	80 ± 5.50 ^{B}	79 ± 7 ^{B}	<0.0001
VO_2 Max (mL/kg/min)	31.0 ± 5.6 ^{A}	35.8 ± 5.6 ^{B}	54.7 ± 5.0 ^{C}	<0.0001
HbA1c (mmol/mol)	53.4 ± 9.3 ^{A}	33.1 ± 3.0 ^{B}	34.1 ± 1.9 ^{B}	<0.0001
Total cholesterol (mmol/l)	5.03 ± 1.02	5.02 ± 0.97	5.08 ± 1.04	0.98
Triglycerides (mmol/L)	2.46 ± 1.57 ^{A}	1.71 ± 0.76 ^{A}	1.13 ± 0.51 ^{B}	0.002
LDL cholesterol (mmol/L)	2.63 ± 0.82	2.86 ± 0.88	2.93 ± 0.87	0.60
HDL cholesterol (mmol/L)	1.13 ± 0.24 ^{A}	1.27 ± 0.26 ^{AB}	1.47 ± 0.30 ^{B}	0.002
Fasting insulin (µU/mL)	15.3 ± 13.7 ^{A}	5.9 ± 1.7 ^{B}	4.4 ± 2.0 ^{B}	<0.0001
Fasting glucose (mmol/L)	8.20 ± 1.72 ^{A}	5.17 ± 0.39 ^{B}	4.53 ± 0.39 ^{B}	<0.0001
2-hour glucose (mmol/L)	13.80 ± 3.90 ^{A}	5.04 ± 1.14 ^{B}	4.74 ± 1.23 ^{B}	<0.0001
Matsuda index	2.6 ± 1.3 ^{A}	6.2 ± 1.6 ^{B}	10.8 ± 3.6 ^{C}	<0.0001
$HOMA_{IR}$	5.82 ± 5.83 ^{A}	1.36 ± 0.39 ^{B}	0.99 ± 0.48 ^{B}	<0.0001

7.3.2 HDL apoAI and total cholesterol in IGR, control and athlete men

ApoAI concentration was significantly higher in athlete group HDL (1.65 ± 0.62 mg/mL) compared to both control and IGR men, while controls (1.21 ± 0.34 mg/mL) had significantly higher apoAI compared to IGR (0.63 ± 0.18 mg/mL). The total cholesterol content of HDL was significantly higher in athletes (2.09 ± 0.44 mmol/L) compared to both control (1.54 ± 0.33 mmol/L) and IGR (1.77 ± 0.37 mmol/L (Figure 7-1).

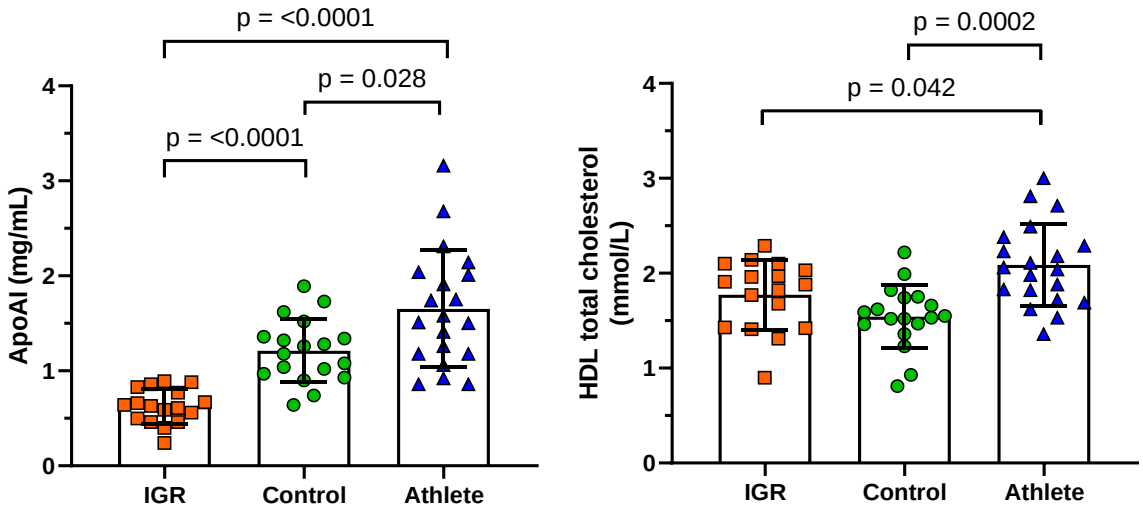

Figure 7-1 HDL apoAI and cholesterol content in the M-FAT study: Data expressed as mean ± SD. Comparisons for apoAI were made with Welch's ANOVA with *post hoc* Dunnet's T3 test, while comparisons for HDL total cholesterol were made with one-way ANOVA and *post hoc* Tukey test. Statistical significance was assumed at $p < 0.05$.

7.3.3 HDL total protein and serum amyloid alpha-1 in IGR, control and athlete men

HDL total protein was significantly lower in control men (0.87 ± 0.25 mg/mL) compared to both IGR (1.16 ± 0.27 mg/mL, p = 0.018) and athlete (1.19 ± 0.37 mg/mL, p = 0.0063) groups. There was no significant difference in HDL total protein between IGR and athletes. SAA-1 was highest in the IGR group HDL (1.77 [1.15, 2.98] µg/mg HDL protein, median [IQR]) compared to both controls and athletes (0.75 [0.37, 2.40] and 0.75 [0.30, 2.40] µg/mg HDL protein respectively, both p = 0.042), with no significant difference apparent between controls and athletes (Figure 7-2).

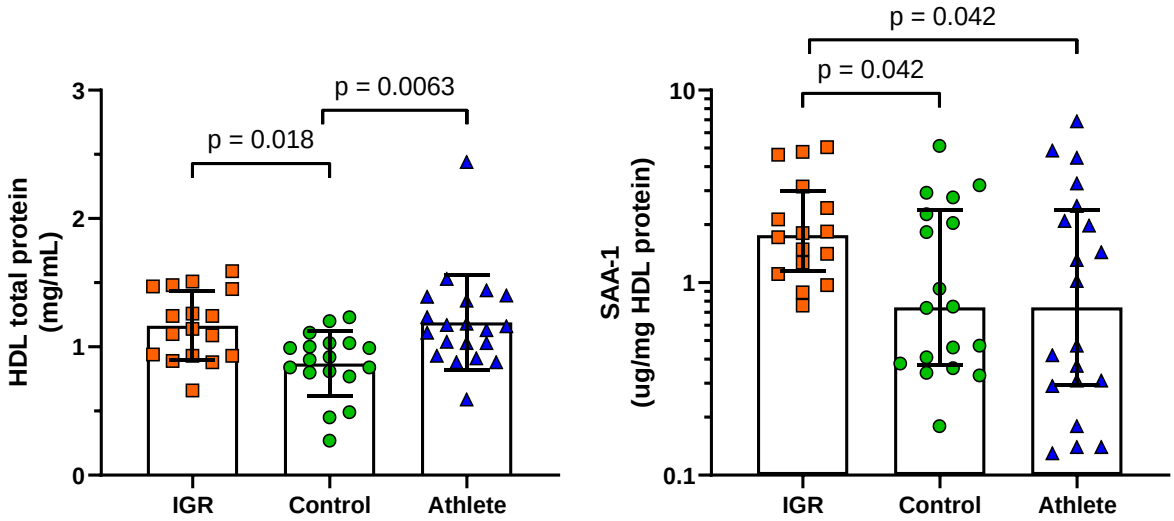

Figure 7-2 HDL total protein and SAA-1 content in HDL from the M-FAT study: HDL total protein data expressed as mean ± SD. HDL SAA-1 data expressed as median ± IQR on a $\log_{10}$ y axis for clear data visualisation. Raw total protein data and log transformed SAA-1 data were compared by one-way ANOVA with *post hoc* Tukey test. Statistical significance was assumed at $p < 0.05$.

The ratio of SAA-1 to apoAI content on HDL was significantly higher in the IGR group (3.48 [1.94, 5.92]) compared to both control and athlete HDL (0.44 [0.29, 1.37] and 0.49 [0.19. 1.55] respectively, Figure 7-3). There was no difference between control and athlete HDL.

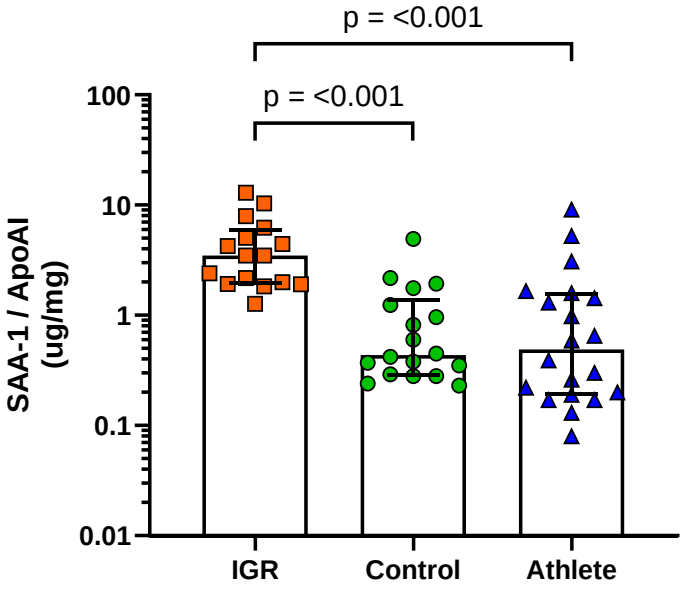

Figure 7-3 HDL SAA-1/ApoAI ratio across the insulin resistant scale: Data expressed as median ± IQR. Comparisons were made with Welch's ANOVA with *post hoc* Dunnet's T3 test on log-transformed data. Untransformed data presented on a $\log_{10}$ axis for clear data visualisation. Statistical significance was assumed at $p < 0.05$.

7.3.4 HDL size distribution in IGR, control and athlete men

HDL 2b made up a significantly larger proportion of athlete HDL compared to IGR (26.1 ± 11.0 % vs 17.3 ± 6.6 %, p = 0.034). There was a trend towards lower percentage small HDL (HDLs 3a, 3b and 3c) in the athlete group, which also had a higher mean HDL 2/3 ratio than the control and IGR groups (1.37 ± 0.61 compared to 0.97 ± 0.33 and 0.98 ± 0.35 respectively), but these were not statistically different (Figure 7-4).

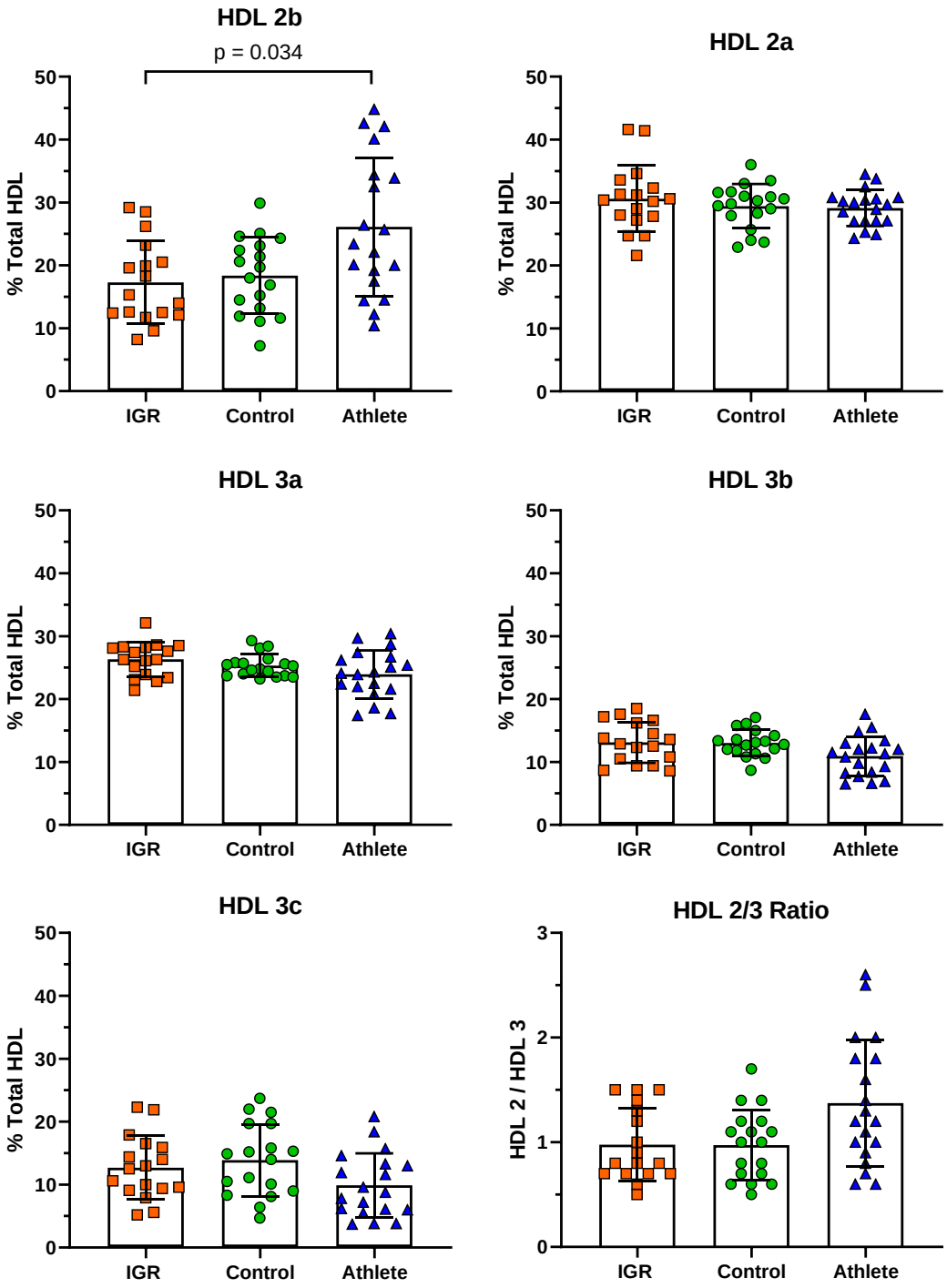

Figure 7-4 HDL subfractions as a proportion of total HDL in the M-FAT study groups: Data expressed as mean ± SD. Comparisons made with Kruskal-Wallis test and *post hoc* Dunn's multiple comparison test. Statistical significance was assumed at $p < 0.05$.

7.3.5 HDL protein composition in IGR, control and athlete men

7.3.5.1 Identification of HDL proteins by nLC-MS/MS

Proteomic analysis of isolated HDL fractions by nLC-MS/MS revealed 109 proteins identified in at least one HDL sample. HDL-associated proteins were determined by including only those proteins present on >50% of HDL samples. Of 109 proteins detected, 59 proteins were deemed HDL-associated (Table 7-3). These included proteins involved in HDL and other lipoprotein metabolism such as CETP and apolipoproteins CI-IV, proteins involved in inflammation and coagulation, and those posited to have roles in insulin resistance.

Table 7-3 List of proteins identified in >50% of HDL samples from the M-FAT study

Alpha-1-acid glycoprotein 1	Ig lambda-1 chain C regions
Alpha-1-acid glycoprotein 2	Kininogen-1
Alpha-1-antichymotrypsin	Leucine-rich alpha-2-glycoprotein
Alpha-1-antitrypsin	Lumican
Alpha-1B-glycoprotein	N-acetylmuramoyl-L-alanine amidase
Alpha-2-antiplasmin	Phosphatidylcholine-sterol acyltransferase
Alpha-2-HS-glycoprotein	Phospholipid transfer protein
Angiotensinogen	Pigment epithelium-derived factor
Antithrombin-III	Plasma protease C1 inhibitor
Apolipoprotein A-I	Protein AMBP
Apolipoprotein A-II	Retinol-binding protein 4
Apolipoprotein A-IV	Serotransferrin
Apolipoprotein B-100	Serum albumin
Apolipoprotein C-I	Serum amyloid A-1 protein
Apolipoprotein C-II	Serum amyloid A-4 protein
Apolipoprotein C-III	Serum paraoxonase/arylesterase 1
Apolipoprotein D	Serum paraoxonase/lactonase 3
Apolipoprotein E	Tetranectin
Apolipoprotein F	Thyroxine-binding globulin
Apolipoprotein L1	Transthyretin
Apolipoprotein M	Vitamin D-binding protein
Apolipoprotein(a)	Vitronectin
Beta-2-glycoprotein 1	Zinc-alpha-2-glycoprotein
Cholesteryl ester transfer protein	
Clusterin	
Complement C3	
Complement C4-A	
Fibrinogen alpha chain	
Fibrinogen beta chain	
Gelsolin	
Haptoglobin-related protein	
Hemoglobin subunit beta	
Hemopexin	
Heparin cofactor 2	
Ig alpha-1 chain C region	
Ig gamma-1 chain C region	

7.3.5.2 Principal Components Analysis

Initially a PCA scores and loadings plot was generated using the demographic and HDL protein data for each sample (Figure 7-5). Athletes, controls and IGRs were separated on a diagonal axis, with the athletes in the top left and the IGR spread across the bottom right. The accompanying loadings plot (Figure 7-6) showed that the first principal component correlated positively with proteins including alpha-1B-glycoprotein and kininogen-1 and negatively with apoAI. The second principal component correlated positively with Matsuda index and VO_2 max and negatively with BMI, fat percentage and plasma triglycerides.

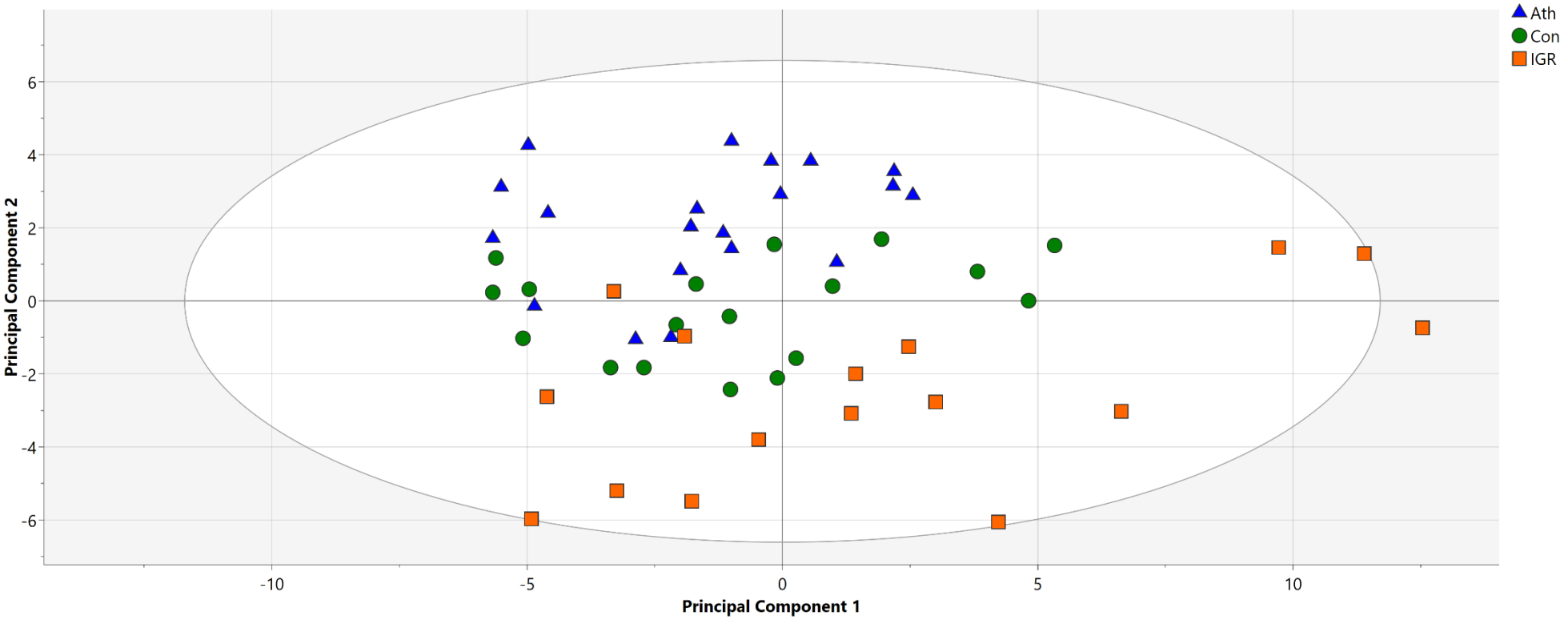

Figure 7-5 Principal components analysis score plot of the M-FAT study samples. Each shape represents an individual study participant. The ellipse represents the confidence region of a Hotelling's T2 test with significance level of p = 0.05. Samples outside the ellipse may be considered as potential outliers.

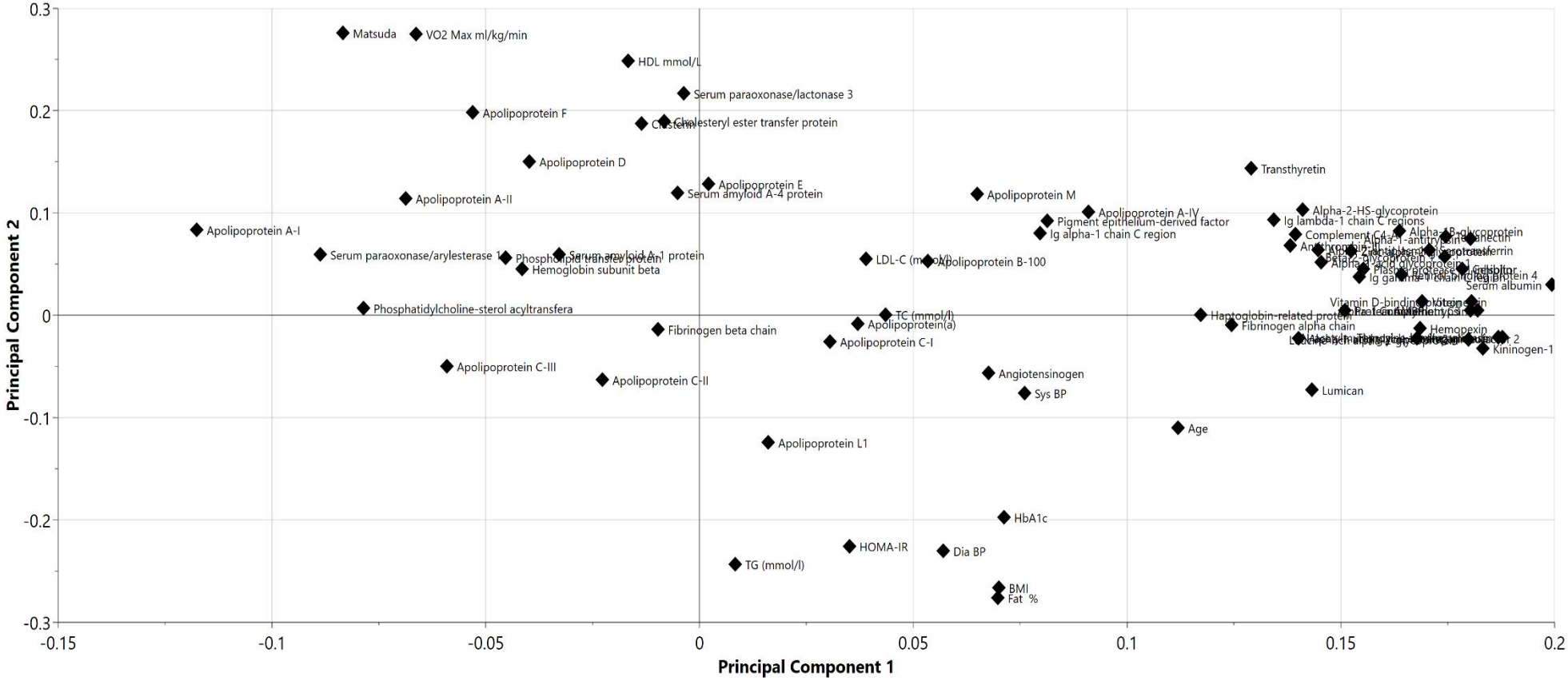

Figure 7-6 Principal components analysis loading plot of the M-FAT study samples. Variables at the extremes of the x axis have a larger positive or negative correlation with the first principal component, while variables at the extremes of the y axis have a larger positive or negative correlation with the second principal component.

7.3.5.3 Orthogonal Projection of Latent Structures – Discriminant Analysis

OPLS-DA was used to understand the degree of separation between the groups and the underlying variables driving any separation. These models were used to identify the contribution of HDL proteins to group separation over and above the separation expected based on their distinct demographic phenotypes. The initial OPLS-DA model (Figure 7-7) confirmed that all three groups were separated. The IGR group was most different to controls and athletes as measured by the distance apart on the x axis, with the most intra-group variation as indicated by the spread across the y axis. The control and athlete group were separated but situated in closer proximity which implied that the differences between those two groups were smaller than those with the IGR group. An OPLS-DA model comparing athletes and controls (Figure 7-8) confirmed that the two groups were clearly separated. The accompanying loadings plot (Figure 7-9) suggested that variables higher in athletes, such as transthyretin and apolipoprotein AII, were more important to separating the groups than factors related to the controls. An OPLS-DA model comparing controls and IGR men and the accompanying loadings plot (Figures 7-10 and 7-11) indicated that higher apolipoprotein F in the control group and a collection of higher inflammatory related proteins in the IGR group contributed most strongly to their separation.

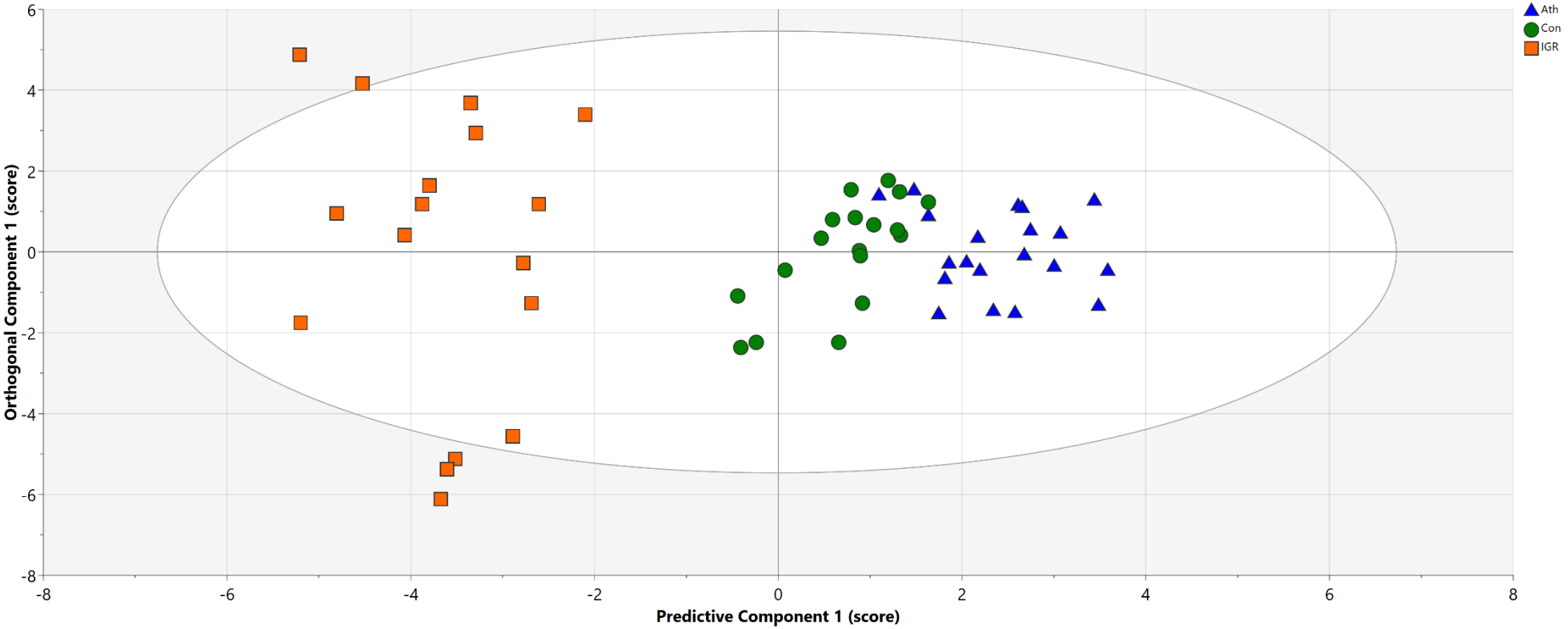

Figure 7-7 Orthogonal projections of latent structures - discriminant analysis score plot of the M-FAT study after VIP selection. The x axis represents between-group variation, and the y axis represents within-group variation. The ellipse represents the confidence region of a Hotelling's T2 test with significance level of p = 0.05. Samples outside the ellipse may be considered as potential outliers.

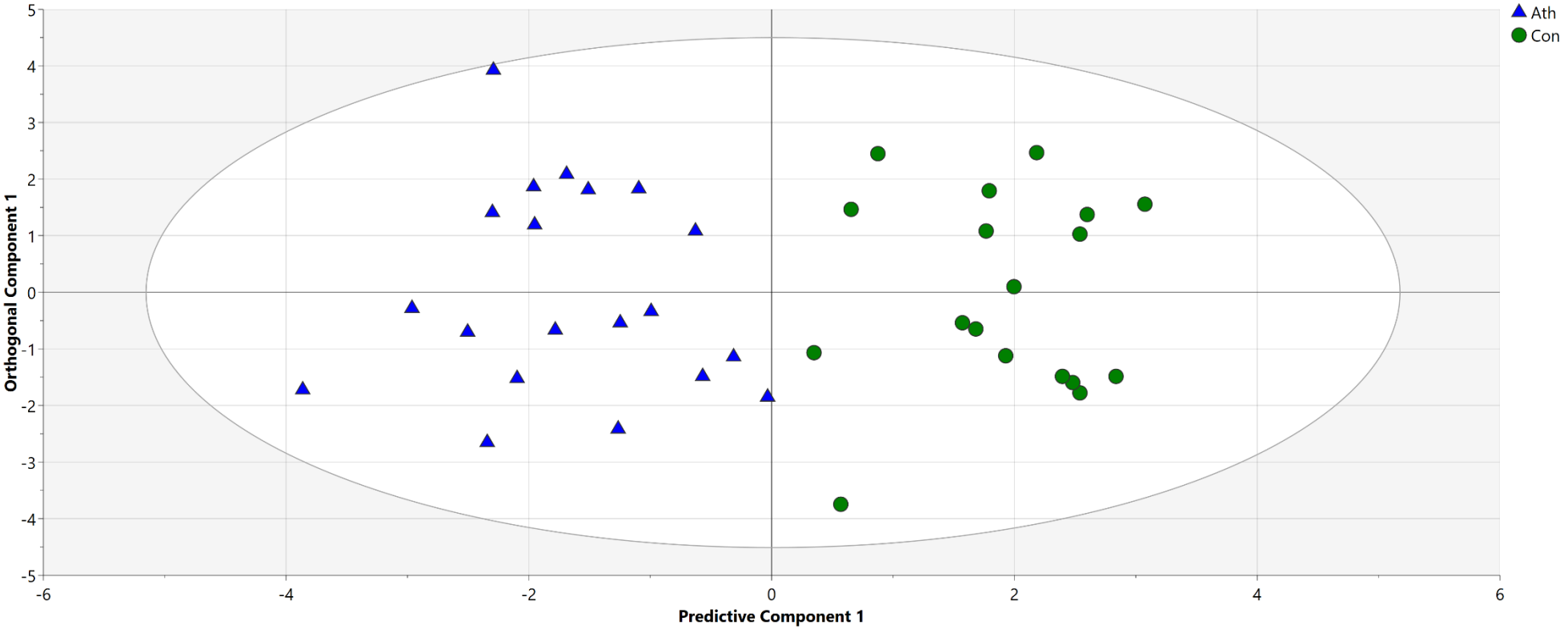

Figure 7-8 Orthogonal projections of latent structures - discriminant analysis score plot of athletes and controls after VIP selection. The x axis represents between-group variation, and the y axis represents within-group variation. The ellipse represents the confidence region of a Hotelling's T2 test with significance level of p = 0.05. Samples outside the ellipse may be considered as potential outliers.

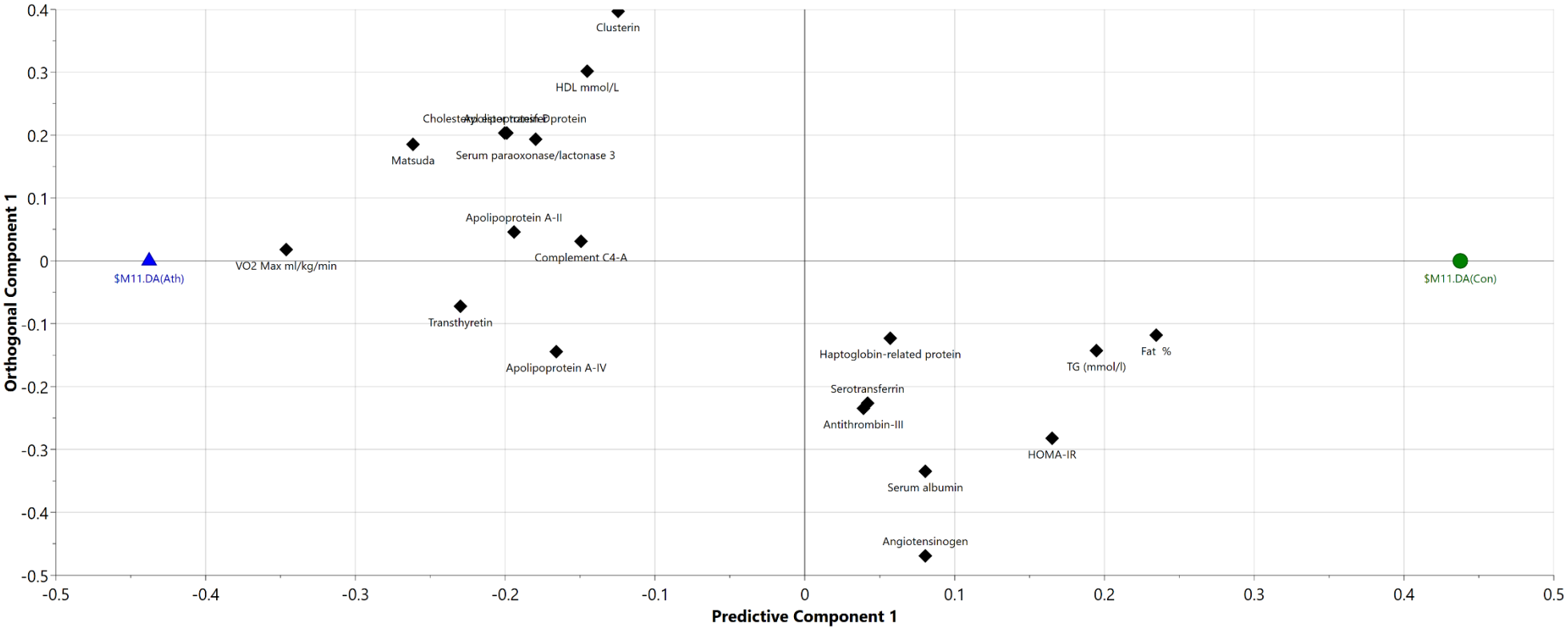

Figure 7-9 Orthogonal projections of latent structures - discriminant analysis loadings plot of athletes and controls after VIP selection. This plot shows the correlations of variables with one and other and their impact on the separation of the groups. Variables located close together are correlated together. Variables closer to the group identifiers are more important to the observed separation.

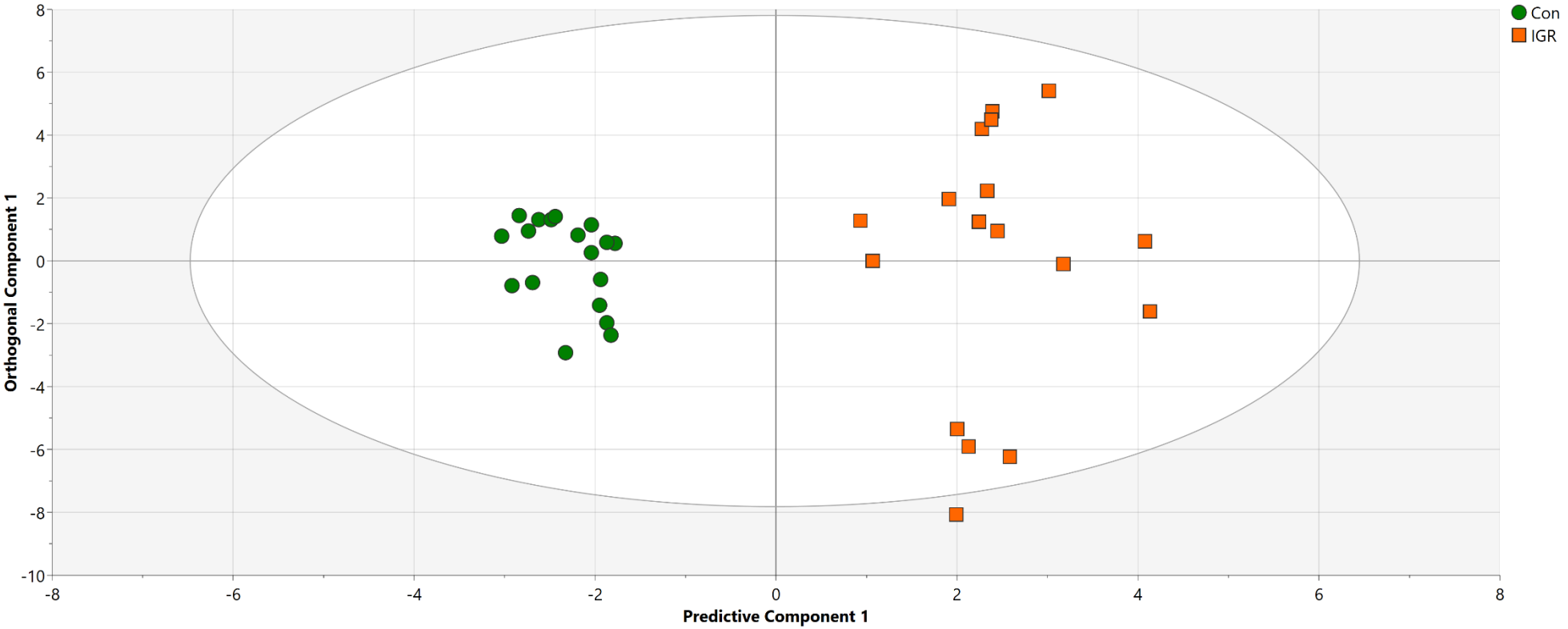

Figure 7-10 Orthogonal projections of latent structures - discriminant analysis score plot of controls and IGR. The x axis represents between-group variation, and the y axis represents within-group variation. The ellipse represents the confidence region of a Hotelling's T2 test with significance level of p = 0.05. Samples outside the ellipse may be considered as potential outliers.

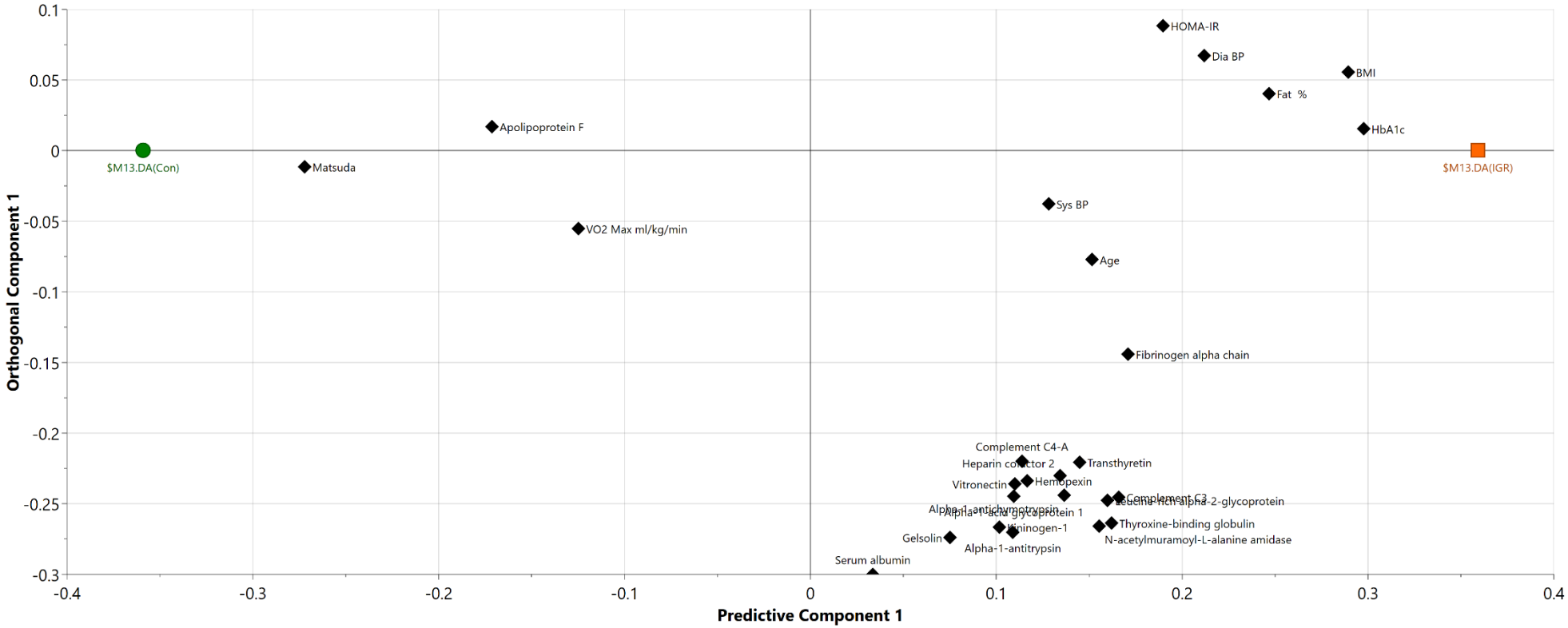

Figure 7-11 Orthogonal projections of latent structures - discriminant analysis loadings plot of controls and IGR after VIP selection. This plot shows the correlations of variables with one and other and their impact on the separation of the groups. Variables located close together are correlated together. Variables closer to the group identifiers are more important to the observed separation.

7.3.6 Differences in HDL protein composition between IGR, control and athlete men

Of those 59 proteins, nine had significant differences in LFQ intensity between the study groups. These included apolipoproteins, proteins involved in coagulation and proteins with implications in bacterial defence, inflammation and vitamin/hormone transport.

Three apolipoproteins were significantly different between the groups of the M-FAT study. ApoAII LFQ intensity was significantly higher in the athlete compared to IGR HDL. ApoD was significantly higher in the athlete compared to control HDL. ApoF was significantly lower in the IGR HDL compared to both control and athlete HDL (Figure 7-12)

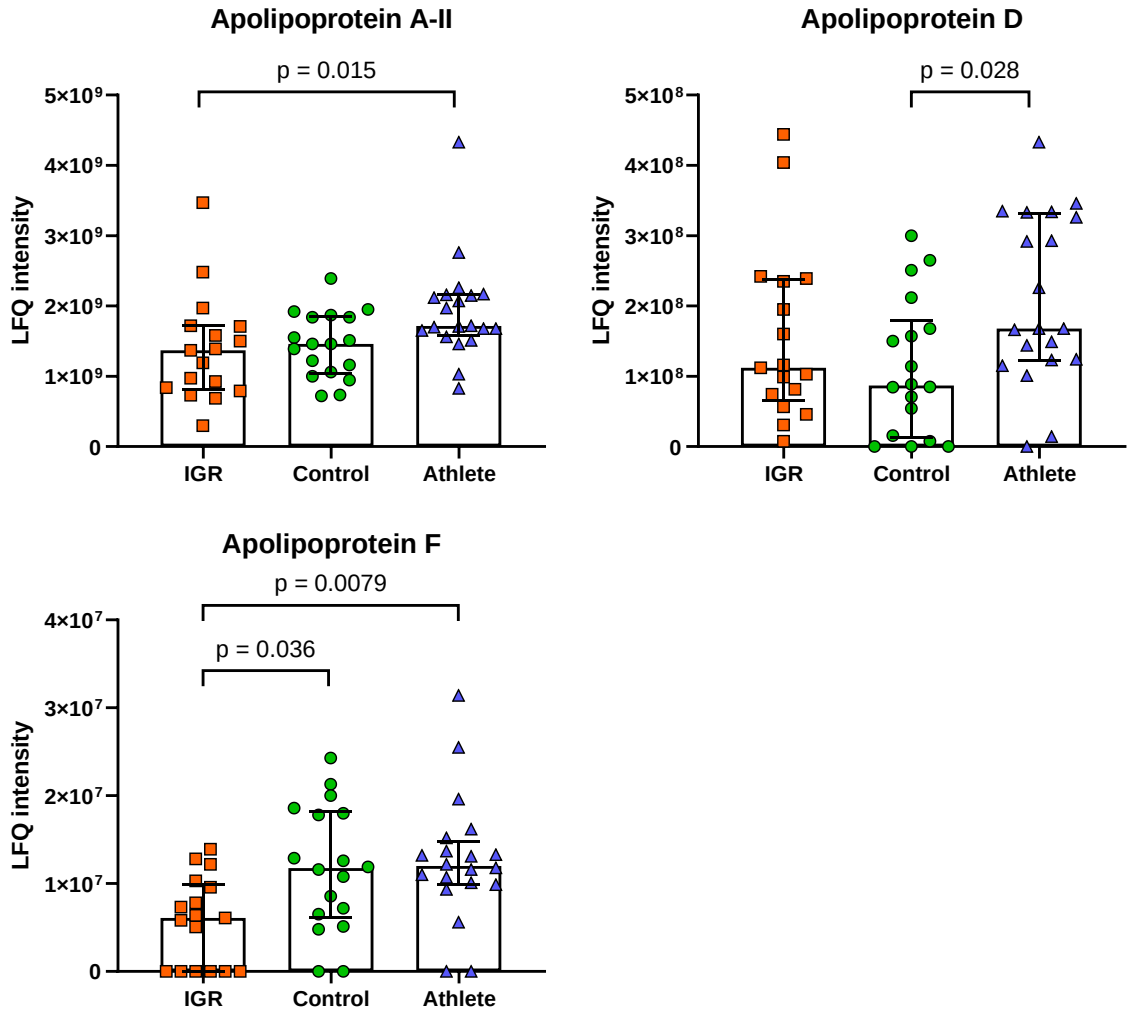

Figure 7-12 LFQ intensities of HDL apolipoproteins with significant differences between groups: Data expressed as median ± IQR. Comparisons made with Kruskal-Wallis and *post hoc* Dunn's test. Statistical significance was assumed at $p < 0.05$.

Two proteins related to coagulation and wound healing were higher in IGR HDL. Fibrinogen alpha chain LFQ intensity was significantly higher in IGR compared to control HDL, while kininogen-1 LFQ intensity was significantly higher in IGR vs athlete HDL (Figure 7-13).

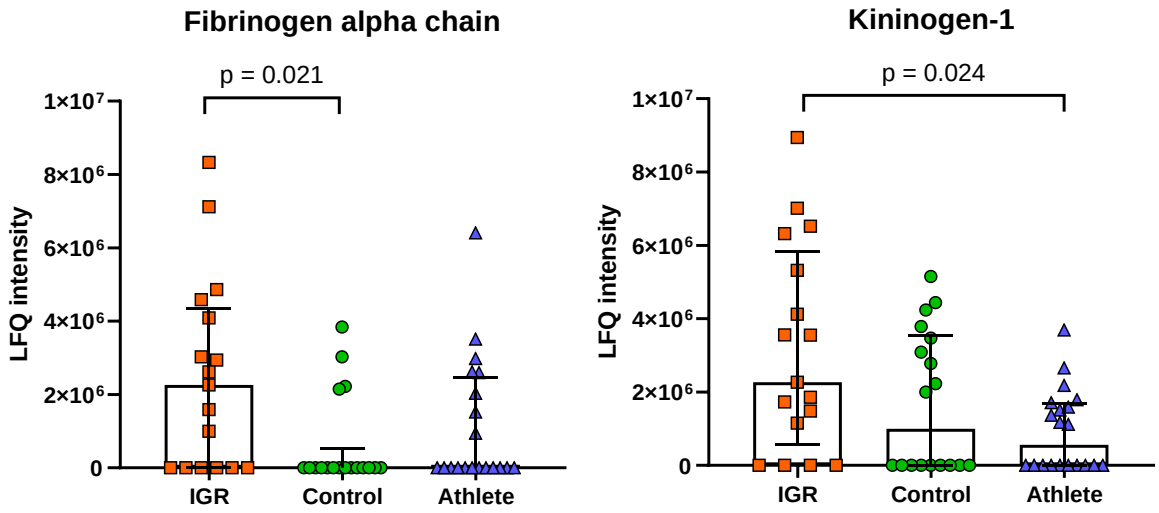

Figure 7-13 LFQ intensities of HDL coagulation-related proteins with significant changes in insulin resistance: Data expressed as median ± IQR. Comparisons made with Kruskal-Wallis and *post hoc* Dunn's test. Statistical significance was assumed at $p < 0.05$.

A further four proteins exhibited significant differences in their LFQ intensity on isolated HDL from the M-FAT study. The acute phase reactant leucine-rich alpha-1 glycoprotein LFQ intensity was significantly higher in IGR HDL compared to both control and athlete HDL. Lumican, a protein involved in fibrosis, LFQ intensity was significantly higher in IGR compared to athlete HDL. The immune enzyme N-acetylmuramoyl-L-alanine amidase LFQ intensity was significantly higher in IGR HDL compared to control and athlete HDL. The thyroxine and vitamin A transporter transthyretin LFQ intensity was significantly higher in athlete HDL compared to control HDL (Figure 7-14).

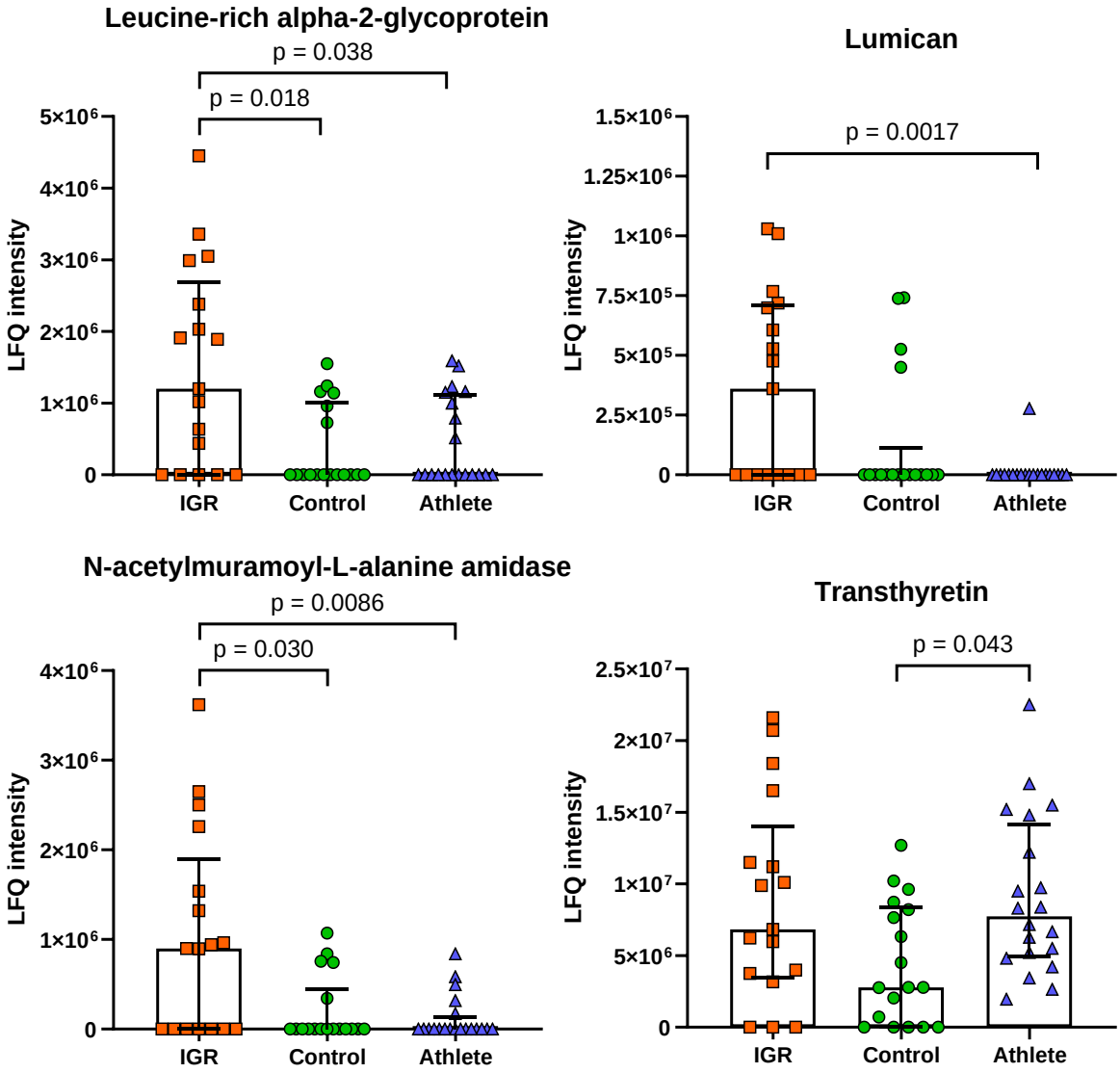

Figure 7-14 LFQ intensities of HDL proteins with miscellaneous functions with significant changes in insulin resistance: Data expressed as median ± IQR. Comparisons made with Kruskal-Wallis and *post hoc* Dunn's test. Statistical significance was assumed at $p < 0.05$.

7.3.7 Post-translational modification of HDL proteins in IGR, control and athlete men

Identified HDL-associated proteins were assessed for post-translational modifications including methionine oxidation and nine distinct glycations. As post-translational modifications could be more prevalent in one group compared to another, modified proteins were included in this analysis if >50% of samples in any one group were modified. Significant differences in methionine oxidation and glycation LFQ intensities and the ratio of modified to unmodified protein were observed in the M-FAT study.

7.3.7.1 Methionine oxidation of HDL proteins in the M-FAT study

Of the 59 identified HDL-associated proteins, four were found to contain oxidised methionine residues (Table 7-4). Significant differences between the groups were found in apoAI at position 136 (Figure 7-15) and apoD at position 177 (Figure 7-16).

Table 7-4 List of HDL-associated proteins with oxidised methionine residues in the M-FAT study

Protein name	Amino acid position(s) of modification
Apolipoprotein A-I	136, 172
Apolipoprotein C-II	82
Apolipoprotein D	177
Serum paraoxonase/arylesterase 1	88

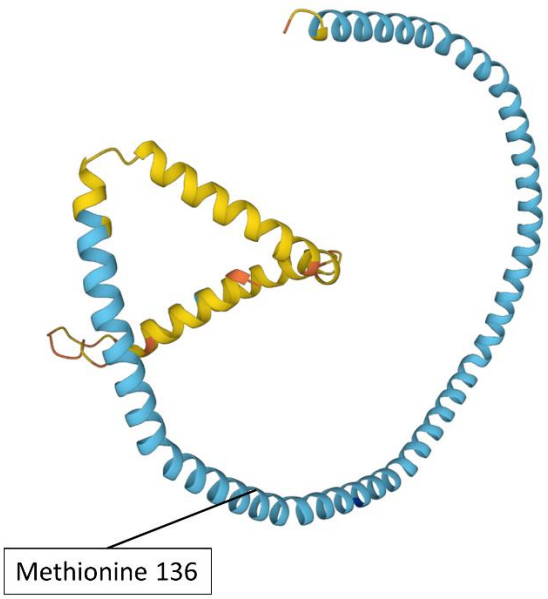

Figure 7-15 Structure of apolipoprotein AI with methionine position 136 highlighted: Protein structure was predicted using Alphafold DB prediction from EMBL-EBI (Jumper et al., 2021; Varadi et al., 2022). Source sequence was derived from Uniprot entry P02647. This sequence includes the 24 amino acid signalling sequence at the N-terminus of the protein. Image used under Creative Commons Attribution 4.0 (CC-BY 4.0) licence terms.

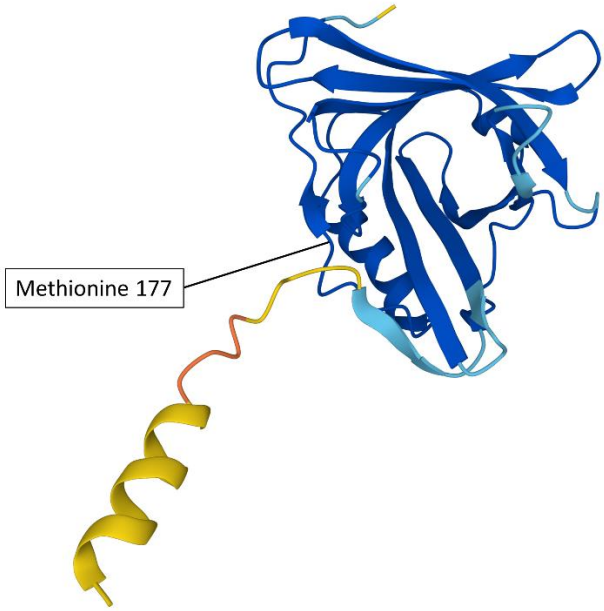

Figure 7-16 Structure of apolipoprotein D with methionine position 177 highlighted: Protein structure was predicted using Alphafold DB prediction from EMBL-EBI (Jumper et al., 2021; Varadi et al., 2022). Source sequence was derived from Uniprot entry P05090. This sequence includes the 20 amino acid signalling sequence at the N-terminus of the protein. Image used under Creative Commons Attribution 4.0 (CC-BY 4.0) licence terms.

The LFQ intensity of apoAI methionine oxidation at position 136 was significantly higher in athlete HDL compared to control. ApoD was oxidised at the methionine residue at position 177 of the protein. Athlete HDL apoD oxidation LFQ intensity was significantly higher than both control and IGR apoD, however the ratio of modified/un-modified apoD at position 177 was significantly higher in IGR HDL compared to athlete HDL (Figure 7-17).

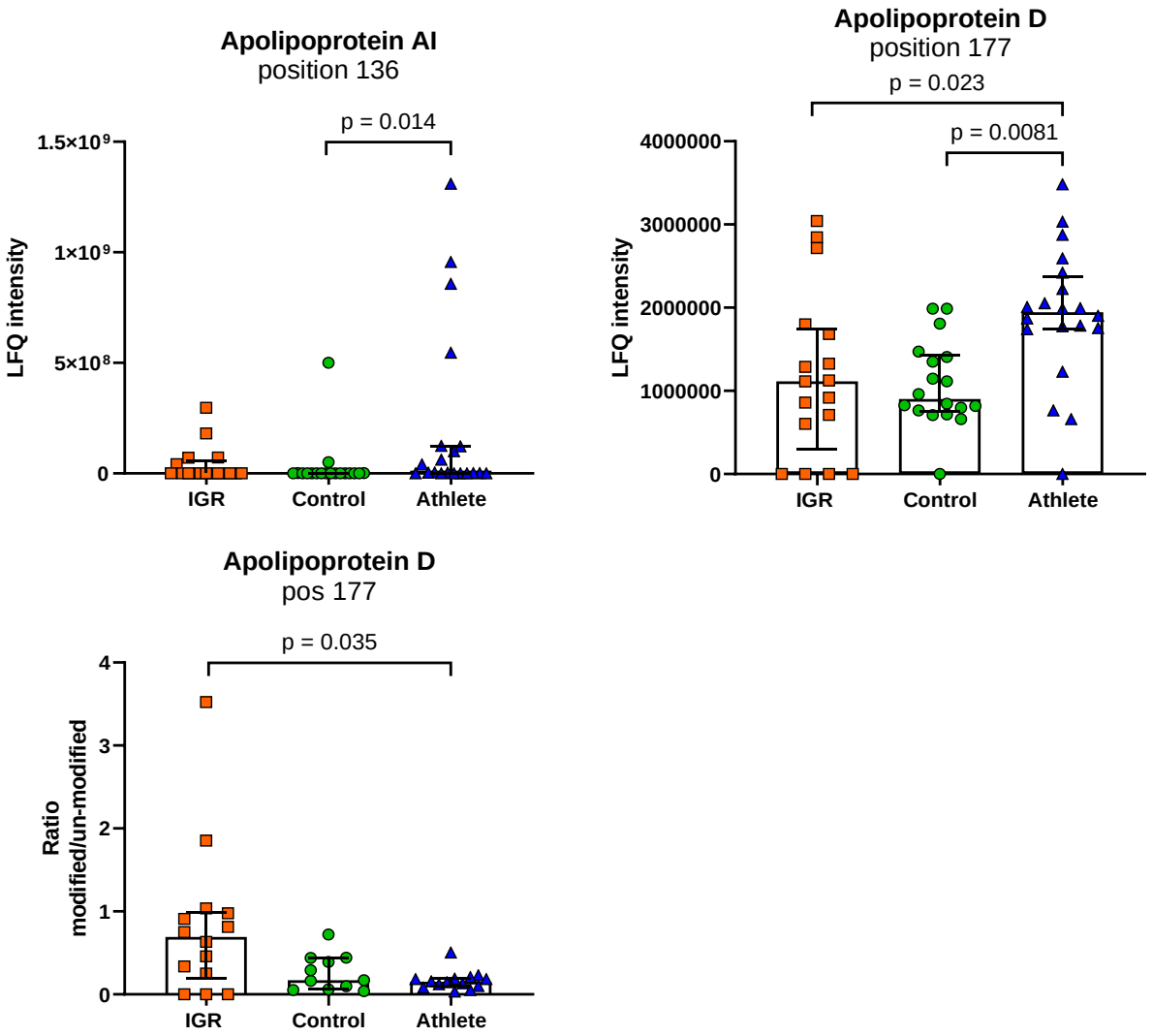

Figure 7-17 LFQ intensity of methionine oxidation of HDL-associated proteins in the M-FAT study: Data expressed as median ± IQR. Comparisons made with Kruskal-Wallis and *post hoc* Dunn's test. Statistical significance was assumed at $p < 0.05$.

7.3.7.2 Glycation of HDL proteins in the M-FAT study

The sole protein identified in the M-FAT study as modified by glycation was apolipoprotein AI. The lysine at position 142 of apoAI was carboxyethyl glycated while the lysine at position 262 was carboxymethyl glycated. The ratio of carboxymethyl lysine glycated to unmodified apoAI at position 262 (Figure 7-18) was significantly higher in the athlete group compared to IGR HDL (Figure 7-19).

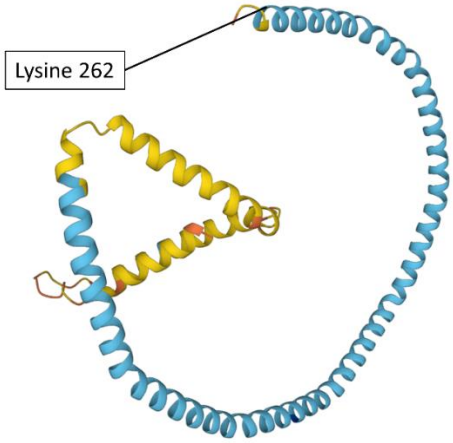

Figure 7-18 Structure of apolipoprotein AI with lysine position 262 highlighted: Protein structure was predicted using Alphafold DB prediction from EMBL-EBI (Jumper et al., 2021; Varadi et al., 2022). Source sequence was derived from Uniprot entry P02647. This sequence includes the 24 amino acid signalling sequence at the N-terminus of the protein. Image used under Creative Commons Attribution 4.0 (CC-BY 4.0) licence terms.

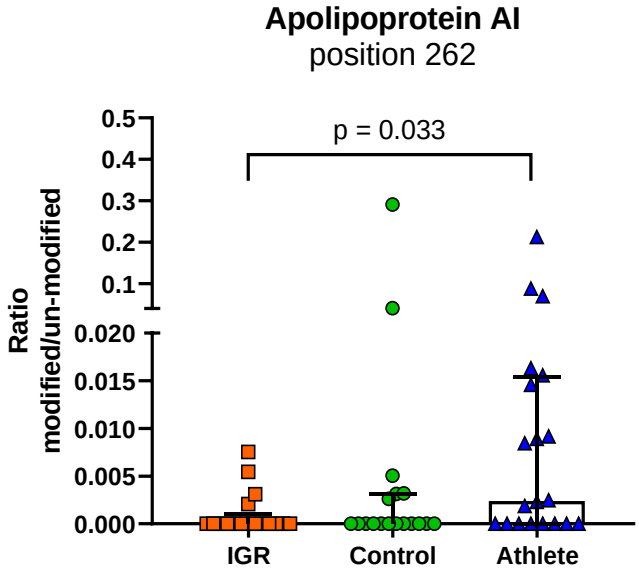

Figure 7-19 The ratio of carboxy-methyl lysine glycation of apolipoprotein AI in the M-FAT study: Data expressed as median ± IQR. Comparisons made with Kruskal-Wallis and *post hoc* Dunn's test. Statistical significance was assumed at $p < 0.05$.

7.3.8 HDL paraoxonase-1 antioxidant function in IGR, control and athlete men

PON-1 activity per mg HDL protein was significantly lower in IGR HDL compared to both control and athletes (10.1 ± 7.3 U/mg HDL protein compared to 22.8 ± 16.2 and 17.7 ± 12.2 U/mg HDL protein respectively). This effect was independent of plasma HDL-C. PON-1 activity per mmol HDL total cholesterol

was negatively associated with plasma HDL-C (p = 0.005). When adjusted for HDL-C, PON-1 activity per mmol HDL total cholesterol was significantly lower in IGR HDL (27.0 ± 20.3 U/mmol HDL total cholesterol) compared to both controls and athletes (51.3 ± 36.2 and 38.7 ± 26.2 U/mmol HDL total cholesterol respectively) (Figure 7-20).

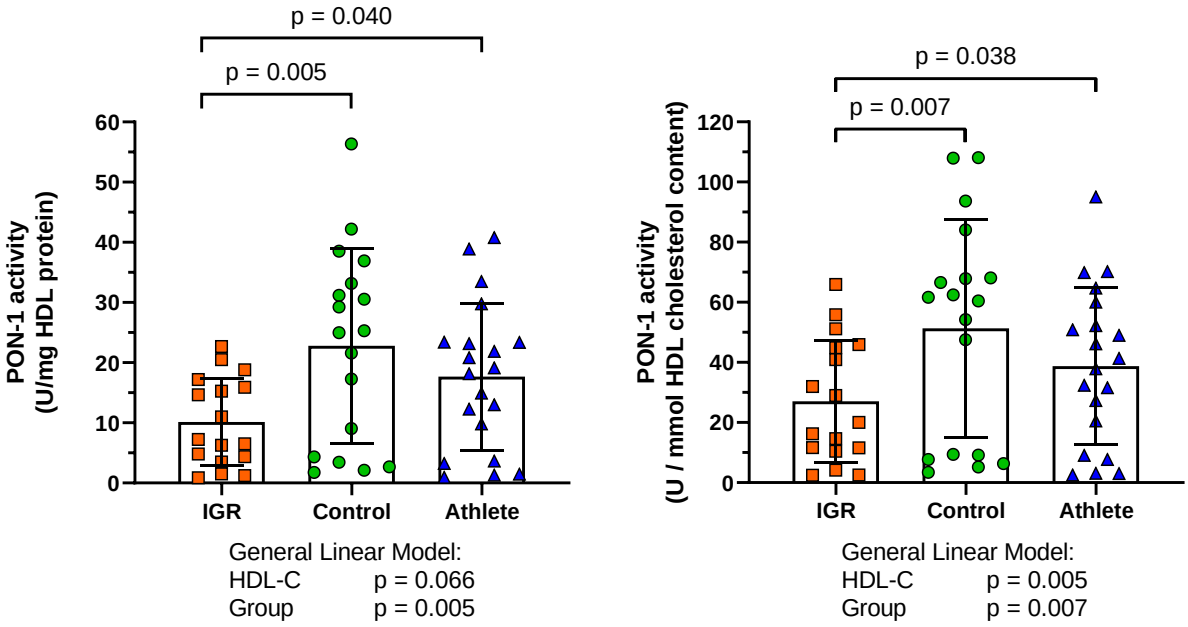

Figure 7-20 HDL paraoxonase-1 activity in the M-FAT study: Data expressed as mean ± SD. Comparisons made with general linear models and *post hoc* Tukey test. HDL-C was included as a co-variate. Statistical significance was assumed at p < 0.05.

7.3.9 HDL anti-inflammatory function in IGR, control and athlete men

Using the assay optimised in chapter 3, the ability of HDL from IGR, control and athlete men to reduce inflammation of endothelial cells was assessed. HDL anti-inflammatory function was independent of plasma HDL-C (p = 0.99) including after correction for HDL total cholesterol and protein (p = 0.34 and p = 0.083 respectively). At an HDL dose of 300 µg/mL apoAI, inhibition of VCAM-1 expression was significantly higher in IGR HDL compared to athlete (83.0 ± 13.2 % compared to 61.4 ± 23.4 %, p = 0.011). Conversely, IGR HDL had significantly lower anti-inflammatory function when corrected for HDL total cholesterol compared to control HDL (0.20 ± 0.06 %/nmol compared to 0.35 ± 0.1 %/nmol, p = 0.003). This pattern continued when correcting HDL anti-inflammatory function for HDL protein; IGR HDL had significantly lower anti-inflammatory

function per mg HDL total protein (0.31 ± 0.11 %/mg) compared to both control and athlete HDL (0.70 ± 0.46 %/mg and 0.57 ± 0.27 %/mg) (Figure 7-21). There was no difference between control and athlete HDL in terms of anti-inflammatory function including after correction for HDL total cholesterol and protein.

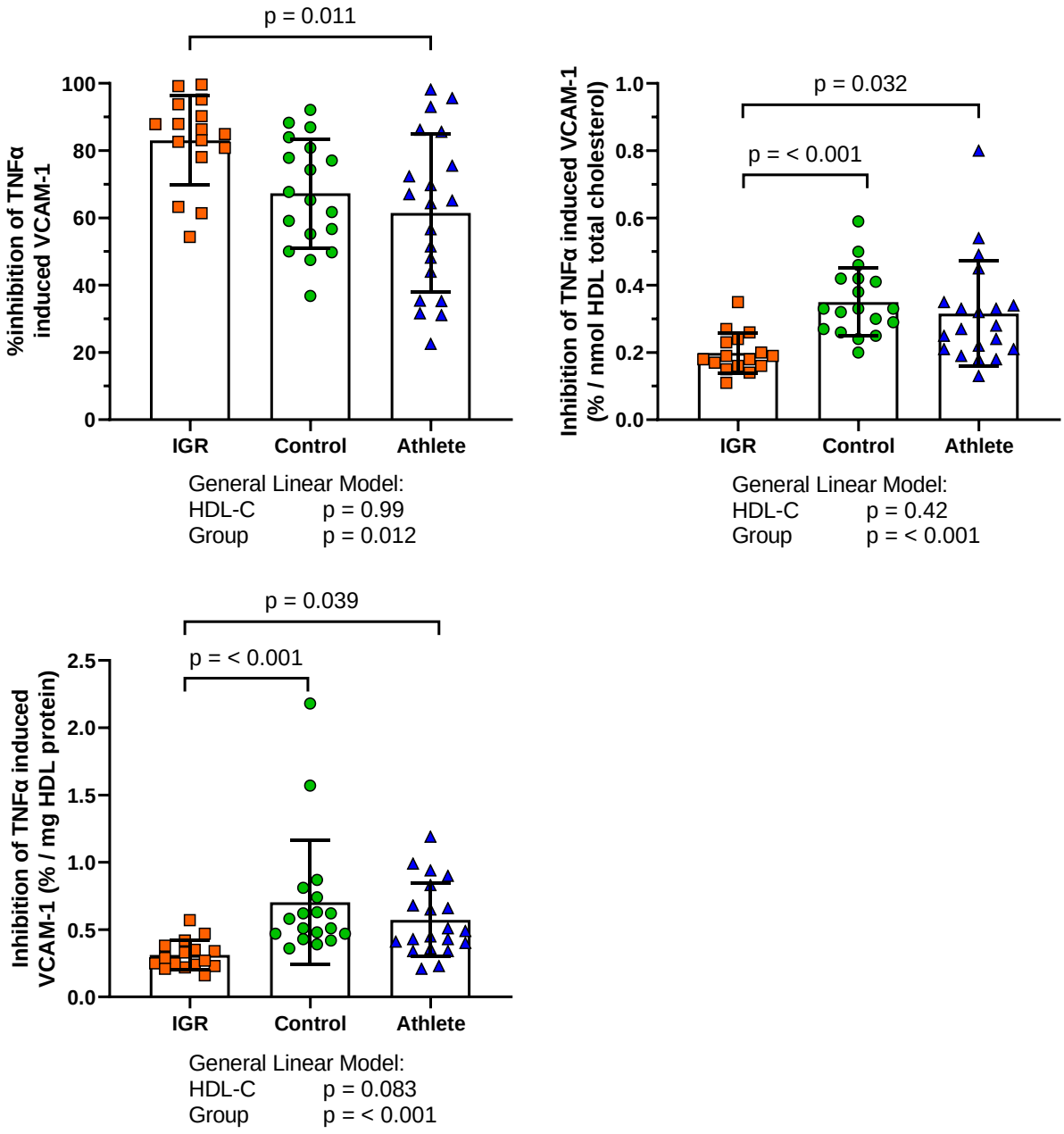

Figure 7-21 Anti-inflammatory function of HDL isolated from M-FAT study participants: Data expressed as mean ± SD. Comparisons made with general linear models and *post hoc* Tukey test. HDL-C was input as a co-variate. Statistical significance was assumed at $p < 0.05$.

7.4 Discussion

This chapter set out to understand HDL composition and function in IGR, control and endurance-athlete men using samples from the previously performed M-FAT study. The three groups were phenotypically very different and core HDL compositional measures differed between IGR, control and athlete HDL. Though athletes had the highest proportion of HDL 2b, overall HDL size distribution was similar between the three groups. OPLS-DA analysis showed that a number of HDL proteins contributed to the separation of IGR, control and athlete men, with univariate analyses revealing nine HDL proteins with statistically different abundances across the three groups of men. Furthermore, apoAI and apoD were shown to be more highly oxidised and apoAI more highly glycated in athlete HDL. Functionally, IGR HDL had the lowest activity of PON-1 while HDL anti-inflammatory activity yielded contrasting results, with IGR HDL having the highest anti-inflammatory function when dosed with apoAI at 300 μg/mL but the lowest once corrected for HDL cholesterol or HDL protein exposed to the cells.

HDL apoAI content is lowest in the IGR group and highest in the athletes, with control HDL apoAI between the two. Given the pleiotropic functions of apoAI, it might be inferred that HDL antioxidant, anti-inflammatory and cholesterol efflux functions are improved with endurance exercise and impaired with IGR. The lower apoAI seen in IGR HDL may be in part due to lower HDL-C. Impaired glucose tolerance has been shown to increase apoAI catabolism by up to 50% compared to controls, thus shortening its plasma lifespan. This may be related to altered HDL composition in IGR (Fré Nais et al., 1997; Pietzsch et al., 1998). HDL-C was not different between athletes and controls, concurring with a meta-analysis of 49 studies which found only a small increase in HDL-C of 2% with exercise (Kelley and Kristi S. Kelley, 2006a). This suggests that the higher apoAI in athletes is not related to an increase in HDL concentration but rather that athlete HDL is enriched in apoAI. Endurance exercise poses increased metabolic demands on skeletal muscle; apoAI has been shown to increase glucose uptake in *ex vivo* human skeletal muscle cells via insulin-dependent and independent mechanisms (Tang et al., 2019). ApoAI enrichment of HDL in athletes could be in response to the increased glucose demand of exercise and may serve to improve their metabolic efficiency. Conversely, reduced apoAI in IGR may be both a driver and consequence of skeletal muscle insulin resistance leading to the onset

of type 2 diabetes mellitus. HDL total cholesterol was highest in the athlete HDL but not different between control and IGR HDL, implying that HDL-CEC is improved with endurance exercise. Direct measurement of HDL-CEC after six-months exercise training in two separate clinical studies showed increased CEC after the intervention (Sarzynski et al., 2018). It should be noted that the athletes in the present study had been performing vigorous exercise for a minimum of 5 hours per week for 2 years or more at the time of recruitment and that no study to date has measured CEC directly in a similar cohort. There was no statistically significant difference between control and IGR in terms of HDL total cholesterol, perhaps due to the fact that the IGR group were identified as such on recruitment and may have only recently developed impaired glucose tolerance. This may also be due to a lack of statistical power to detect a difference between these two groups. In summary, endurance exercise led to higher HDL apoAI and cholesterol content as an adaptation to altered metabolic demands while IGR HDL may only differ from control HDL by these metrics due to decreased plasma HDL-C.

The lower total HDL protein in controls compared to both IGR and athlete was unexpected given that apoAI makes up approximately 70% of HDL protein content and there is a clear difference in apoAI content between the three groups. This may reflect the specificity of the ELISA methodology for apoAI against the broader estimation of total protein by Bradford assay. It could suggest that non-apoAI protein concentration is altered in IGR and athlete HDL, demonstrated by alterations in the abundance of some HDL-associated proteins identified in the proteomic analysis undertaken in this chapter.

Median HDL SAA-1 content was higher in IGR HDL compared to control and athlete HDL, concomitant with the findings of (Cardner et al., 2020) who saw increased SAA-1 in the HDL of T2DM patients. Taken together with the increased SAA-1/apoAI ratio seen in IGR HDL compared to controls and athletes, this finding suggests that deleterious remodelling of HDL by SAA-1 may occur early on in the development of T2DM at the onset of insulin resistance. All individuals in the IGR group had high HDL SAA-1 content, unlike control and endurance athletes where there was a high degree of variability in the SAA-1 content of HDL. Both endurance and acute exercise is known to increase SAA-1 (Bassini et

al., 2022) and this effect remains post-exercise for more than 48 hours (Goussetis et al., 2009). The spread of SAA-1 values seen in the athletes may therefore reflect the time since or the intensity of exercise, where individuals in the group who exercised more recently or more vigorously pre-study enrolment could have increased SAA-1 as a result. It may also be a function of the type of exercise performed; the M-FAT study recruited cyclists, runners and triathletes which could differentially increase SAA-1, much like the findings of Bassini et al., (2022) where altered correlations of SAA-1 with other proteins were seen dependent on the sport performed. The variability of control HDL SAA-1 may be explained in a similar fashion. This group was recruited based on less than 1 hr per week exercise; it may be that some individuals had undertaken their exercise recently prior to enrolment in the study. There is the possibility that some individuals may have been experiencing an underlying asymptomatic infection though this was not assessed at recruitment and any overt illness was a barrier to study enrolment. In summary, the higher SAA-1 content of IGR HDL observed in this chapter corroborated the wider published literature. The variability of SAA-1 content observed on control and athlete HDL is likely related to time since last exercise according to the recruitment criteria.

The assessment of HDL size distribution across the groups found that athletes had the highest proportion of HDL 2b, the largest of the HDL particles, and tended to have the lowest proportion of the smaller HDL 3 particles. This supports the meta-analysis by Kelley & Kelley, (2006b) who found that HDL 2 cholesterol increases post aerobic exercise interventions. This may be explained in part by the increased cholesterol content of athlete HDL. The glycation of lysine 262 of apoAI in athletes may also contribute to their larger HDL phenotype, as disruption of the c terminus has been shown to increase nascent HDL particle size *in vitro* (Vedhachalam et al., 2010). There is higher variability in the proportion of HDL 2b in the athletes, perhaps driven by the higher apoAII content of their HDL. ApoAII containing HDL is more heterogenous in size compared to apoAI-only HDL, which exists as a more narrowly defined small or large diameter particle (Melchior, Street, et al., 2021). Cardner et al., (2020) and Sokooti et al., (2021) both observed smaller HDL in T2DM, while Garvey et al., (2003) reported smaller HDL in individuals with IGR. This is at odds with the present study where there was no difference in HDL size distribution between

control and IGR. This might be due to the method by which HDL was sized; all of the aforementioned studies used nuclear magnetic resonance (NMR) to profile HDL size while the recent study used native-PAGE. There is some disagreement as to whether the two techniques are comparable when sizing lipoproteins: two studies found that they differ substantially, particularly when assaying subjects with diabetes (Witte et al., 2004; Ensign et al., 2006) while one study found that the techniques are comparable with one and other (Arsenault et al., 2010). It is likely that the more detailed NMR can detect subtle differences in particle diameter that are lost with semi-quantitative gel analyses. In summary, while the observation that athlete HDL had the highest proportion of HDL 2b followed the wider published literature, the lack of difference between the HDL size distributions of control and IGR men was at odds with the wider literature perhaps due to the methodology employed.

Proteomic analysis of HDL identified 59 proteins on HDL isolated from participants in the MFAT study. The relative abundances of proteins and the demographic data for each individual was used to create a PCA plot to assess whether samples in the same group were similar to one and other. The PCA separated the groups well along a diagonal axis, with HDL proteins contributing to the principal components. An OPLS-DA model of the three groups of men confirmed that all three groups were different to one and other, with the most within-group variation observed in the IGR group, perhaps unsurprising given that these men may have been IGR for highly variable periods of time. Separate OPLS-DA models comparing athletes and IGR men to the controls identified a number of HDL proteins that contributed to the separation of the groups over and above their demographics; athletes separated from controls based predominantly on apolipoproteins while IGRs separated based upon a constellation of inflammatory and coagulative proteins. These models were performed as a precursor to the univariate analysis of each protein which assisted the interpretation of those findings.

Univariate analyses revealed several proteins were differently abundant in IGR and athlete men, including three apolipoproteins. Apolipoprotein AII was higher in athletes compared to IGR HDL, though this difference was not of great magnitude. More interesting is the uniformity of the athlete group compared to

the more variable control and IGR, suggesting that an exercise-induced increase in apoAII occurs. This adaptation is likely involved in the increased ABCA1-mediated cholesterol efflux in HDL post-exercise observed by Stanton et al., (2022) and may contribute to the reduction in neutrophil activity observed post-exercise (Robson et al., 1999; Furlaneto et al., 2002). ApoD, which forms a heterodimer with apo-AII (Blanco-Vaca et al., 1992), is also increased in athlete HDL compared to control HDL. ApoD is proposed to confer protection from oxidative stress through redox cycling and, at capacity, oligomerisation of oxidised-apoD as described by Sanchez and Ganfornina, (2021). Higher apoD in athlete HDL may be part of the adaptation to exercise described by (Radak et al., 2008) where short bouts of exercise increase oxidative stress, but repeated exercise such as in this group of athletes provokes a systemic antioxidant adaptation and reduces this effect. Arachidonic acid, a precursor for vaso-active compounds such as prostaglandin, has high affinity for apoD and is known to be stored in lipoproteins including HDL. It may be that apoD can regulate the liberation and storage of arachidonic acid depending on specific physiological stimuli (Morais Cabral et al., 1995). Prostaglandins are involved in skeletal muscle vasodilation during exercise (Wilson and Kapoor, 1993), suggesting a role for HDL in delivering arachidonic acid to muscle in athletes to facilitate prostaglandin synthesis. ApoF is inactive as a CETP inhibitor when associated with HDL, and active when associated with LDL (Liu and Morton, 2020). The lower apoF observed in IGR HDL in the present study matched the findings of Cardner et al., (2020) and suggests an early adaptation to insulin resistance related changes in blood lipids to maintain cholesterol homeostasis. The lower HDL apoF may indicate that apoF has shifted onto LDL to inhibit CETP, consequently reducing LDL cholesterol and increasing hepatic LDL uptake to counter the rising plasma triglycerides observed in the IGR group. ApoF mediated inhibition of CETP also prevents the production of atherogenic small dense LDL, a characteristic of insulin resistant dyslipidaemia. ApoF has additional effects outside of lipid homeostasis. HDL-bound apoF protected rat pancreatic beta cells from apoptosis (Cardner et al., 2020) implying that IGRs may lose this protective HDL function. As with apoAII, there was much lower variability in athlete HDL apoF which suggests an exercise adaptation. Exercise upregulates genes associated with the browning of white adipose tissue, which is associated with improved cardiometabolic health (Otero-Díaz et al., 2018;

Becher et al., 2021). HDL apoF promoted mitochondrial respiration in brown adipocytes *in vitro* (Cardner et al., 2020) and may therefore be implicated in exercise-induced adipose tissue browning. In summary, the differences in abundance of apolipoproteins on the HDL of athlete, control and IGR men is likely a reflection of the systemic adaptation to the consequences of either exercise (such as increased oxidative stress) or insulin resistance (such as rising triglycerides).

The other six proteins differentially expressed on HDL among groups have various functions in inflammation, coagulation and endocrine transport. There is a limited literature on these proteins and their associations with HDL; pro-coagulant kininogen-1 associated with HDL isolated from plasma by immunoaffinity columns (Moren et al., 2016) while the 1-2% of plasma transthyretin associated with HDL can alter apoAI mediated cholesterol efflux (Liz et al., 2007). All of these proteins with the exception of transthyretin were higher on the HDL of the IGR group, with insulin resistance known to be linked to increased systemic inflammation and coagulation. It is therefore likely that these proteins identified on HDL are reflecting the chronic inflammation caused by impaired glucose regulation and insulin resistance rather than any metabolic adaptation to HDL *per se*. Transthyretin was higher on athlete HDL compared to control. Exercise increases plasma thyroxine and may therefore also increase plasma levels of its transporter (Refsum and Strömme, 1979). The detection of transthyretin on HDL may reflect this exercise-induced change.

A similar study of the HDL proteome by Vaisar et al., (2018) found differences in the HDL proteome between controls and T2DM patients but these were lost when correcting for multiple comparisons. As it can be expected that individual proteins will change in tandem with one another and are therefore not independent, in this instance it was deemed that correction for multiple comparisons would be excessively conservative and mask the differences between the groups. Many of these proteins appeared in the OPLS-DA loading plots as drivers of separation between the groups after filtering for VIP scores, supporting these univariate findings. It should be noted that Melchior et al., (2017) found that ultracentrifugation markedly decreased the number of proteins identified on HDL by proteomic analysis compared to immunoaffinity

column isolation, particularly those involved in inflammation and haemostasis. It is likely that other plasma proteins that are not typically associated with HDL are found on the HDL of patients with cardiovascular and metabolic diseases by virtue of their increased abundance. These were perhaps not detected in the present study as these loosely associated proteins could have been removed due to the high gravitational and osmotic forces on HDL during sodium bromide density ultracentrifugation. In summary, the limited literature on inflammatory, coagulation and transport proteins and HDL makes interpretation of their different abundances on athlete, control and IGR HDL difficult. It is likely that these proteins are present on HDL due to their increased plasma abundance.

Analysis of the post-translational modification of HDL proteins revealed that apoAI and apoD exhibit methionine oxidation, at positions 136 and 177 respectively, to different degrees between the studied groups. Athlete apoAI methionine oxidation at position 136 was higher than control HDL, though this appears to be driven largely by the small number of individual athletes with much higher apoAI oxidation rather than an athlete group effect. It may also be linked to a structural change in apoAI mediated by the higher apoAII in HDL from endurance athletes, which may expose the methionine residue at position 136 to oxidation (Melchior et al., 2017). ApoD methionine oxidation LFQ intensity was higher in the athletes compared to both control and IGR, however when measuring the ratio of modified to unmodified apoD IGR HDL had a higher proportion of oxidised apoD compared to athlete HDL. The increase in the LFQ intensity of oxidation of athlete apoD is most likely due to the increase in total apoD observed on the HDL in this group and demonstrates the protective oxidation of the apolipoprotein proposed by (Sanchez and Ganfornina, 2021). The increased ratio of modified to unmodified apoD in IGR HDL perhaps indicates increased oxidative stress in IGRs with less efficient redox cycling of apoD compared to the conditioned endurance athletes. Methionine 177 forms part of the loop structure of apoD; loops not only guide the structure of a protein but also hold sites of activity crucial to protein function (Dhar and Chakrabarti, 2014) which suggests that this may be a key site of apoD protective action.

Glycation of apoAI at position 262 was increased in athlete HDL compared to IGR HDL, confirming the findings of Van Den Eynde et al., (2020) who saw increased overall glycation in the plasma of active older adults compared to their sedentary counterparts. This may be a consequence of the role apoAI has in increasing glucose uptake in skeletal muscle (Tang et al., 2019), where the local concentration of glucose increases due to the heightened metabolic demand of muscle and therefore leads to increased glycation of proteins. Carboxymethyl glycation is an advanced glycation end-product which irreversibly binds to proteins and alters their function. Lysine 262 resides in the c-terminus of apoAI. Post-translational modification of the c-terminus of apoAI reduces lipid binding and cholesterol efflux capacity (reviewed in detail by Shao, (2012)). However, in endurance athletes this may be a protective effect as discussed by (Riechman et al., 2009). Cholesterol has anabolic effects on skeletal muscle and has pleiotropic roles in muscle signalling, anti-inflammation and membrane localisation of transporters and signalling molecules. The reduced cholesterol efflux capacity of HDL with glycated apoAI may be a passive protective mechanism preventing the removal of excess cholesterol from conditioned/conditioning muscle at times of increased glucose demand. Not every athlete exhibited increased apoAI glycation; the level of glycation on apoAI may be related to the intensity of exercise performed before, or the time since exercise pre-recruitment to the study. In summary, the higher post-translational modification of apolipoproteins on athlete HDL may be a consequence of the metabolic demands of exercise. Whereas glycation and oxidation are typically detrimental to proteins and tissue, in athletes the higher glycation and oxidation of specific HDL apolipoprotein residues may be protective of muscle.

Whether corrected for HDL protein content or cholesterol content, HDL PON-1 activity was lower in the IGR compared to both control and athletes independent of HDL-C. This is in contrast to Kopprasch et al., (2003) who found that there was no difference between control and impaired glucose tolerance individuals. This is likely attributed to the larger disparity in $HOMA_{IR}$ between control and IGR observed in the present study compared to the more similar $HOMA_{IR}$ between the two in the contrary study. The findings of the present study do however corroborate the reduced PON-1 activity in individuals with T2DM compared to

controls observed by Ebtehaj et al., (2017). A longitudinal case-control study of US air force pilots over 20 years found that lower PON-1 activity was associated with increased risk of developing T2DM (Crow et al., 2018), further corroborating the present findings. Given the overall antioxidant adaptation to exercise-induced oxidative stress, it was unexpected that PON-1 activity was not higher in the athlete HDL compared to control. A recent meta-analysis of studies investigating the effect of exercise on PON-1 found that both acute and chronic exercise had negligible impact on the serum activity of PON-1 (Taylor et al., 2022). The authors suggest that the lack of increased activity is due to the fact that PON-1 predominantly has effects in the interstitial spaces which would not be detected by a serum measure. As the present study measures HDL PON-1 activity isolated from plasma, the same caveat may apply here.

Assessment of the anti-inflammatory function of HDL yielded contrasting results. When dosed onto HMEC-1 at 300 μg/mL apoAI, IGR HDL had higher anti-inflammatory function compared to athlete HDL. This is inconsistent with the apoAI and SAA-1 data where IGR HDL displayed unfavourable compositional measures supposed to impact on its endothelial function. It may be that there is a compensatory increase in apoAI functionality resulting from its decreased HDL concentration. When dosing cells with 300 μg/mL apoAI, a larger volume of HDL is required to compensate for the lower apoAI concentration. It is more likely that other drivers of HDL anti-inflammatory function, for example S1P, are therefore also dosed at a higher concentration thus giving the impression that apoAI mediated anti-inflammatory effects are increased. This was corrected for by adjusting the inhibition of VCAM-1 for the amount of cholesterol and protein dosed onto the cells for each study participant. After correction, IGR HDL had lower anti-inflammatory function per both nmol HDL cholesterol content and mg of HDL protein compared to both controls and athletes. Correcting for HDL cholesterol content reflects the entire particle contents including the various lipid species and proteins, implying that whole particle anti-inflammatory function is reduced in IGR HDL. The reduction in HDL anti-inflammatory function per mg of HDL protein implies that the protein makeup of IGR HDL specifically is detrimental to its ability to protect the endothelium from inflammatory stimuli. A similar study using the same cell line assessing HDL anti-inflammatory function by measuring NFκB activation found that T2DM HDL increased NFκB activity

compared to controls, mirroring the results of the present study (Vaisar et al., 2018). The authors dosed HDL onto cells at a concentration of 50 µg/mL HDL protein, whereas the average concentration of HDL protein dosed onto cells across all samples in the present study was 345.5 µg/mL, approximately seven times higher, though this does not appear to have attenuated any differences between the groups through overstimulation of the cells. Other studies have reported findings consistent with this report of decreased HDL anti-inflammatory function in T2DM (Ebtehaj et al., 2017; Lemmers et al., 2021). A systematic review by Lemmers et al., (2017) found that though HDL anti-inflammatory function is indeed decreased in T2DM there is significant heterogeneity of methodologies and variations of dosing HDL. There has been a report that HDL anti-inflammatory function was not impaired in T2DM (Denimal et al., 2017), however the authors used macrovascular HUVECs and as discussed in section 3.1 HDL exerts its anti-inflammatory function predominantly in the microvasculature. There was no difference between control and athlete HDL in terms of anti-inflammatory function, perhaps not unexpected given that Stanton et al., (2022) found limited differences between the two after moderate intensity exercise based on inhibition of ICAM-1. The same study found a reduction in ICAM-1 expression with high-intensity exercise but no effect on VCAM-1 expression. Again, it is difficult to compare this study with the present chapter's findings: macrovascular cells were used and treated with HDL at 1 mg/mL apoAI for 16 hours, much longer than the 4-hour preincubation with 300 µg/mL apoAI in the present study, and the inflammatory stimulus was 0.1 ng/mL TNFα for 5 hours compared to 5 ng/mL TNFα for 24 hours in the present study. It is likely that the high level of apoAI in the media overnight paired with a mildly inflammatory dose of TNFα masks deficiencies or improvements in HDL anti-inflammatory function post-exercise. In summary, when exposed to endothelial cells based on apoAI IGR HDL performed as well as control HDL but better than athlete to prevent TNFα induced inflammation. However, when accounting for the whole HDL particle whether based on HDL cholesterol content or HDL protein content, IGR HDL was the least anti-inflammatory in this experimental design, suggesting that whole particle anti-inflammatory function aside from apoAI is impaired.

A strength of this study was the broad range of insulin sensitivity across the three groups, providing a cross-sectional overview of HDL composition and function. The IGR men were recruited before formal diagnosis and treatment of T2DM thereby removing any potential confounding treatment effects from this analysis. The three groups were demographically and anthropometrically very different by design with a clear phenotype in each group. A limitation of this study is that the IGR men are likely to have been IGR for a relatively short period of time without symptoms which may have meant that some changes, such as in HDL size or proteins identified, may have been below the threshold for detection. The breakdown of athletes by exercise type was not collected on recruitment thereby preventing detailed conclusions on the effect of different sports on HDL composition and function. The proteomics methodology resulted in a semi-quantitative relative LFQ value which meant that proteins of high abundance could diminish the detection of less abundant proteins, and as described in section 6.4 the interpretation of glycated protein abundance is challenging given the non-specific nature of the modification and its dependence on glucose concentration and protein abundance. The PON-1 assay employed only assessed the arylesterase activity of the enzyme; it may be that the other enzymatic activities are altered differently in the groups. The cell line used here is representative of the dermal microvasculature. HDL from these groups may have altered anti-inflammatory function in cell-types more relevant to diabetes complications specifically such as in retinal or renal microvascular cells. It was difficult to compare the findings of the present study with the wider literature in detail given the heterogeneity of methods for HDL sizing, anti-inflammatory function and compositional assessment. Finally, the study was powered to detect a one standard deviation difference in intramuscular triglyceride content. This is a large difference, and this study may therefore have been underpowered to detect more subtle changes in HDL composition and function.

In summary, this chapter demonstrated that there are alterations in HDL composition and function with both impaired glucose regulation and exercise. Compositionally, the changes to HDL in IGR men reflected pathophysiological changes in inflammation and coagulation, while HDL changes in athletes support the adaptation to the altered metabolic and oxidative environment associated with exercise. Functionally, IGR HDL had reduced antioxidant function and, after

taking into account whole particle composition, reduced anti-inflammatory function. Athlete HDL did not differ from control HDL functionally. The proportion of large HDL was increased in athletes but not affected by insulin resistance. Overall, it can be concluded that HDL has a ceiling of function that cannot be increased, as evidenced by the overall lack of change in athletes, but can be decreased, such as seen in IGR men. Future studies following this work could study younger men participating in more vigorous exercise compared to the current cohort, to understand whether HDL is more plastic in younger men and whether more intense exercise could impact measures of HDL composition and function. A similar study in females in three phenotypically similar groups may also reveal a sex difference in the HDL response to insulin sensitivity, particularly given the impact of female sex hormones on HDL function (Beazer and Freeman, 2022). As a cross-sectional study, it could not be assessed how HDL changed compositionally and functionally from un-trained to trained athlete or from healthy to IGR. A longitudinal study design with an intervention to manipulate insulin resistance/sensitivity may further unravel the relationship between HDL's vascular protective functions and its composition.

8 HDL composition and function in Europeans and South Asians before and after weight gain

8.1 Introduction

In the previous chapter, I showed that there were compositional and functional differences in HDL from middle-aged IGR men compared to controls and athletes in a cross-sectional study design. I also showed that HDL appeared to have a functional ceiling, as evidenced by the lack of HDL differences between controls and athletes despite their different anthropometric and metabolic profiles. However, the cross-sectional study design was unable to reveal how HDL may change in the same individual with altered insulin resistance over time, nor did the population studies provide information on insulin resistance in younger males. All of the men in the M-FAT study were of white European descent, yet it is well established that there are ethnicity differences in the prevalence and aetiology of insulin resistance which may impact on HDL composition and function, particularly in South Asians (discussed in section 1.6.5). In this chapter, I aimed to establish the effect of altered insulin resistance on HDL composition and function in healthy young men of both white European and South Asian descent. Insulin resistance was modulated by weight gain (increasing insulin resistance) and weight loss (decreasing insulin resistance). Much of the research into HDL composition and function with insulin resistance focuses on cross-sectional studies comparing controls and overweight/obese individuals, while studies into the effect of weight loss often have overweight or obese groups as the baseline (discussed in section 1.6.3). This chapter addressed this gap in the literature by first focusing on weight gain and weight loss induced changes in HDL composition and function in healthy young white Europeans, before comparing the European and South Asian HDL response to weight gain.

8.1.1 Hypotheses

- HDL composition, function and size are adversely affected by weight gain in Europeans and South Asians.

- South Asian HDL composition, function and size will be more strongly negatively impacted by weight gain than European HDL.

- Subsequent weight loss will return HDL composition, function and size back to baseline or further improve these measures in Europeans.

8.1.2 Objectives

- Measure HDL composition at baseline and in response to weight gain and subsequent weight loss.

- Measure the size distribution of HDL subclasses with weight gain and subsequent weight loss.

- Perform proteomic analysis of HDL and understand the effect of weight gain/weight loss on HDL protein content.

- Assess the antioxidant and anti-inflammatory function of HDL with weight gain and weight loss.

- Compare the composition, function and size response of white European HDL and South Asian HDL to weight gain.

8.2 Methods

8.2.1 Recruitment of healthy men for a longitudinal study of weight-change induced alterations in insulin resistance

This cohort was originally collected as part of the 'Glasgow visceral & ectopic fat with weight gain in South Asians (GlasVEGAs)' study, performed at the University of Glasgow in 2018 and funded by the European Medical Information Framework (project number 60315/1, clinicalTrials.gov identifier: NCT02399423). The major findings of this study can be found in the PhD thesis entitled 'Adiposity and

diabetes risk mechanisms in South Asians' by Dr James McLaren at the University of Glasgow. This study set out to compare the physiological and metabolic changes associated with weight gain and subsequent weight loss in young, lean South Asian and European men. Participants were asked to gain ~7% of their baseline body weight over 4-6 weeks by eating until fuller than usual and increasing intake of high sugar snacks, and subsequently lose 7-15% body weight over the following 12 weeks. Weight loss was achieved either through the well know Weight Watchers diet plan or through alternate day fasting. Before each study visit participants were provided with all of their food based on measured energy expenditure in order to maintain their weight for three days prior to metabolic and anthropometric measurements. At each study visit, participants gave a fasted blood sample before consuming a standard mixed test meal (containing ~800 kcal, 37% fat, 47% carbohydrate, 17% protein) and undergoing a mixed-meal tolerance test. Whole-body MRI scans were taken to measure changes in subcutaneous, visceral and liver fat distribution with weight gain and weight loss. Participant fitness at each study visit was also measured with a continuous incremental uphill walking treadmill test. This study was powered to detect a one standard deviation difference with 90% power in insulin sensitivity and adipocyte size after the study intervention and this chapter used all available study samples (n = 21 Europeans and n = 14 South Asians). Inclusion and exclusion criteria are summarised in table 8-1.

Table 8-1 Inclusion and exclusion criteria for the recruitment of the GlasVEGAs study

	Inclusion criteria		Exclusion criteria
i.	Male	i.	Diabetes mellitus (as diagnosed by physician or HbA1c ≥ 6.5% on screening)
ii.	Of white European or South Asian descent (self-report of both parents white European, Indian, Pakistani, Bangladeshi or Sri Lankan origin)	ii.	History of cardiovascular disease
		iii.	Regular vigorous exercise
iii.	Aged 18-45 years	iv.	Smoking
iv.	BMI <25 kg/m^2	v.	Drugs or supplements known to impact carbohydrate and lipid metabolism
v.	Weight stable for 6 months (± 2 kg)	vi.	Any serious illnesses

8.2.2 Isolation of HDL

HDL was isolated from participant plasma as described in section 2.2.2. For HDL proteomic and composition analysis, the top 500 µL containing HDL after the 1.21 g/mL centrifugation was collected and passed once through a desalting column. For all other analyses, the top 250 µL after the 1.21 g/mL centrifugation was collected and passed twice through a desalting column to increase HDL concentration.

8.2.3 Measurement of core HDL composition

HDL apoAI and SAA-1 were measured using ELISA as described in section 2.10. HDL total protein was measured by Bradford assay according to section 2.6. HDL cholesterol content was measured by colorimetric assay as described in section 2.7.

8.2.4 Measurement of HDL size distribution

The size distribution of HDL was measured using native gel electrophoresis as set out in section 2.12.

8.2.5 Proteomic analysis of HDL

Isolated HDL was prepared and analysed by mass spectrometry at the same time as the M-FAT samples, according to the method described in section 4.2.5 with post-translational modification analysis of identified HDL proteins performed according to section 6.2.5.4.

8.2.6 HDL paraoxonase-1 activity assay

HDL paraoxonase-1 arylesterase activity was measured using a kinetic UV-visible spectrophotometric method described in section 2.11.

8.2.7 Assessment of HDL anti-inflammatory function

The anti-inflammatory function of HDL was assessed by measuring the inhibition of TNFα induced VCAM-1 as set out in chapter 3. Briefly, HMEC-1 were preincubated with HDL (based on 300 µg/mL ApoAI) for four hours before the

addition of 5 ng/mL TNFα for 24 hours. Cells were lysed according to section 2.4 and SDS-PAGE / western blotting was performed for VCAM-1 according to sections 2.8 and 2.9. Results are expressed as % inhibition of VCAM-1 expressed by cells treated with TNFα alone. Each culture plate contained untreated and TNFα only treated cells; samples were corrected for baseline VCAM-1 expression and normalised to the TNFα only control present on the same plate.

8.2.8 Statistical analyses

As an interventional repeated measures study, the same individuals were followed with weight gain and weight loss. However, repeated measures ANOVA and the non-parametric equivalent Friedman test require a balanced study design, i.e., the same number of individuals in each group. As some men were lost to follow up at both weight gain and weight loss, the assumptions of repeated measures ANOVA and Friedman tests were violated and not appropriate in this instance. For this reason, general linear models were used with the participant identifier included as a random factor. General linear models do not require the input data to be normally distributed but do assume normality of the resulting residuals. Where residuals were not normally distributed, the input data was log transformed. Where residuals were not normally distributed, but the input data contained a large proportion of zeros, such as with proteomic LFQ intensities, the data was imputed by adding the minimum non-zero value to all data points before log-transforming (West, 2022) as logarithmic functions cannot be applied to zero values. The minimum non-zero value was selected to maintain the scale of the data; LFQ intensities are typically greater than $1x10^5$ and zero values do not necessarily mean absence of protein but very low levels of expression. The minimum non-zero value was therefore taken as the limit of detection for a given protein. All analyses pertaining to the white European men only were performed with general linear models with *post hoc* Tukey test. For comparisons between white Europeans and South Asians, mixed effects models were used in place of repeated measures two-way ANOVA, which does not have a non-parametric equivalent and cannot handle unbalanced groups (Muhammad, 2023). Mixed effects models have the same assumptions as general linear models and therefore the input data was treated in the same manner. Participant ID was included in the mixed effect models and the interaction term of ethnicity and study visit was added to the model. Comparisons were made

with *post hoc* Tukey test. Statistical significance was assumed at $p < 0.05$ for all comparisons. All statistics were performed using Minitab version 20.

8.3 Results

8.3.1 Characteristics of GlasVEGAs study participants

Demographic and anthropometric data for the GlasVEGAs study participants are described in table 8-2. It should be noted that the majority of South Asian participants were lost to follow up at the weight loss visit rendering statistical analysis including this study visit futile, however the demographic data has been shown in full for completeness. Analyses pertaining to European men included all three study visits, while analyses comparing the two ethnicities were limited to baseline and weight gain measures only to maintain statistical power.

Europeans and South Asians did not differ in age and increased their BMI similarly with weight gain. Cardiorespiratory fitness as measured by VO_2 max was higher in Europeans irrespective of study visit and was reduced irrespective of ethnicity with weight gain. Fasting and 2 hr glucose was unchanged in either ethnicity with weight gain, however, mean fasting insulin was markedly increased with weight gain in South Asians (6.0 μU/mL at baseline compared to 16.5 μU/mL with weight gain, $p < 0.001$). Mean $HOMA_{IR}$ was also increased in South Asians with weight gain (1.30 at baseline, 3.60 with weight gain, $p < 0.001$). HDL-C did not differ between Europeans and South Asians after the weight loss visit was excluded from the analysis.

Table 8-2 GlasVEGAs study participant characteristics: Data expressed as mean ± SD. P values are assumed significant at $p < 0.05$ as assessed by mixed effect models.

	Baseline		Weight gain		Weight loss		p value		
	EU (n=21)	SA (n=14)	EU (n=21)	SA (n=14)	EU (n=16)	SA (n=3)	Ethnicity	Study visit	Interaction
Age (years)	22.1 ± 3.1	23.1 ± 3.2	22.1 ± 3.1	23.1 ± 3.2	22.1 ± 3.4	24.0 ± 3.6	0.14	0.93	0.93
BMI (kg/m^2)	22.3 ± 1.5	21.7 ± 2.7	23.7 ± 1.7	23.2 ± 2.9	22.2 ± 1.4	20.6 ± 2.0	0.40	<0.001	0.39
Systolic blood pressure (mmHg)	128 ± 11	120 ± 9	126 ± 8	124 ± 11	124 ± 9	108 ± 7	0.054	0.085	0.144
Diastolic blood pressure (mmHg)	76 ± 7	71 ± 8	70 ± 5	76 ± 8	69 ± 7	68 ± 7	0.36	0.39	0.085
VO_2 max (mL/kg/min)	51.7 ± 5.6	44.0 ± 2.9	48.0 ± 5.0	41.6 ± 4.5	49.4 ± 7.3	45.0 ± 1.3	<0.001	<0.001	0.65
Fasting glucose (mmol/L)	5.0 ± 0.8	4.8 ± 0.4	5.0 ± 0.9	4.7 ± 0.5	4.9 ± 0.6	4.9 ± 0.3	0.33	0.98	0.87
2 hr glucose (mmol/L)	4.8 ± 1.0	5.2 ± 0.8	5.0 ± 1.0	5.4 ± 1.0	4.7 ± 0.8	5.6 ± 0.8	0.52	0.25	0.44
Fasting insulin (μU/mL)	6.1 ± 4.8	6.0 ± 3.4	6.1 ± 2.9	16.5 ± 19.4	4.8 ± 2.2	6.0 ± 2.5	0.11	<0.001	0.006
$HOMA_{IR}$	1.32 ± 0.96	1.30 ± 0.74	1.37 ± 0.69	3.60 ± 3.63	1.03 ± 0.49	1.31 ± 0.59	0.076	0.001	0.01
Total cholesterol (mmol/L)	4.24 ± 0.64	4.16 ± 0.85	4.63 ± 0.92	4.69 ± 1.02	4.31 ± 0.85	3.31 ± 0.08	0.58	<0.001	0.23
Triglycerides (mmol/L)	0.81 ± 0.30	1.09 ± 0.51	0.95 ± 0.54	1.37 ± 0.72	0.83 ± 0.33	0.86 ± 0.11	0.11	0.009	0.33
HDL cholesterol (mmol/L)	1.48 ± 0.63	1.31 ± 0.30	1.50 ± 0.29	1.27 ± 0.37	1.50 ± 0.34	1.09 ± 0.09	0.004	0.004	0.004
Liver fat fraction (%)	2.1 ± 1.2	4.1 ± 3.6	3.1 ± 3.9	7.7 ± 13.0	0.8 ± 0.5	1.0 ± 0.3	0.011	0.36	0.99

8.3.2 The effect of weight gain and weight loss on white European HDL composition and function

8.3.2.1 HDL apoAI and total cholesterol content in white Europeans with weight gain and weight loss

Weight gain and weight loss did not alter either apoAI or the total cholesterol content of HDL in white Europeans (Figure 8-1).

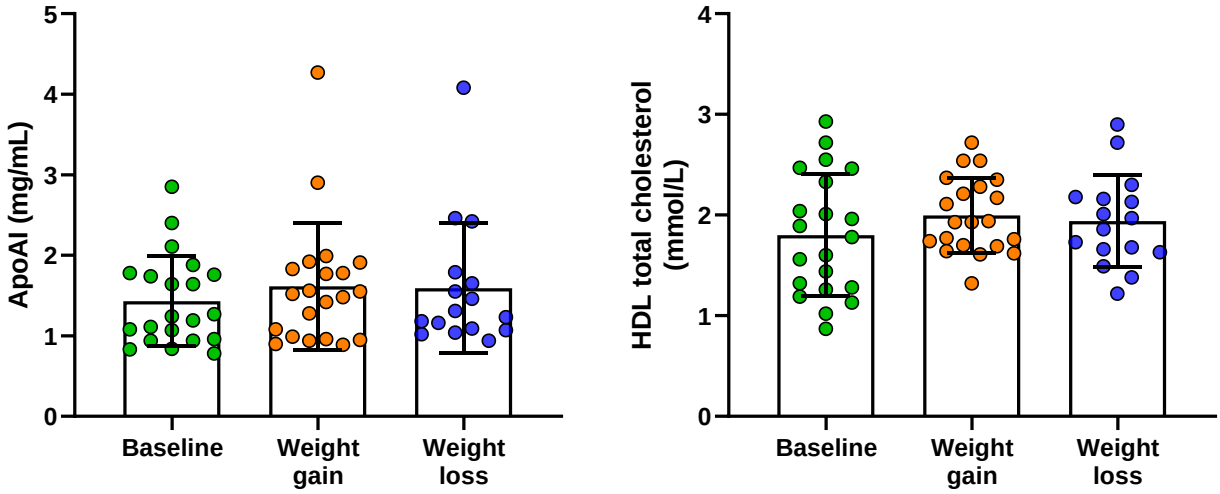

Figure 8-1 HDL apoAI and total cholesterol in the white European cohort of the GlasVEGAs study: Data expressed as mean ± SD. Comparisons made by general linear model. Statistical significance was assumed at $p < 0.05$.

8.3.2.2 HDL total protein and SAA-1 content in white Europeans with weight gain and weight loss

There was no statistically significant difference in HDL total protein content with weight gain or weight loss (Figure 8-2). HDL SAA-1 content tended towards a decrease with weight loss (baseline 0.90 [0.61, 1.30] µg/mg HDL protein, weight gain 1.09 [0.71, 2.04] µg/mg HDL protein, weight loss 0.64 [0.40, 1.21] µg/mg HDL protein, median [IQR]) but did not reach statistical significance. There was one individual with particularly high SAA-1 content of HDL at weight loss (Figure 8-2).

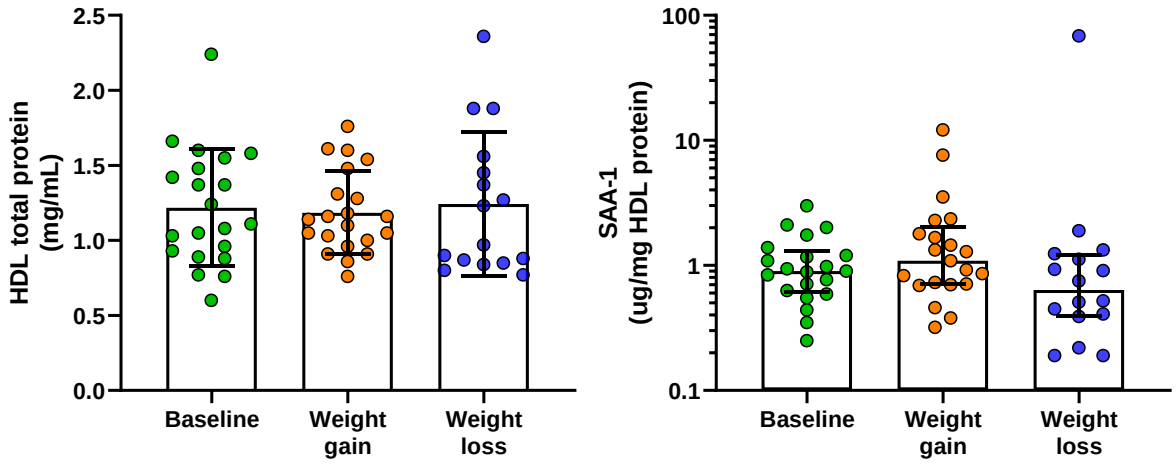

Figure 8-2 HDL total protein and SAA-1 content in the white European cohort of the GlasVEGAs study: Total protein data expressed as mean ± SD. SAA-1 data expressed as media ± IQR and shown on a $\log_{10}$ axis for better data visualisation. Comparisons made by general linear model. Statistical significance was assumed at $p < 0.05$.

8.3.2.3 Size distribution of HDL in white Europeans after weight gain and weight loss

The percentage of HDL 2b appeared to decrease with weight gain in Europeans but this difference was not statistically significant (28.0 ± 8.37 % at baseline compared to 25.0 ± 6.61 % with weight gain, p = 0.065, mean ± SD). Subsequent weight loss returned the percentage of HDL 2b back to the baseline proportion (30.9 ± 9.84 % with weight loss, p = 0.004). There was a modest increase in HDL 3c with weight gain (13.9 ± 4.03 % at baseline compared to 16.2 ± 4.07 % with weight gain, p = 0.026) and weight loss appeared to return the proportion of HDL 3c back to baseline though this was not statistically significant (13.2 ± 5.84 %, p = 0.059). Finally, the HDL 2/3 ratio was increased after weight loss compared to weight gain (1.59 ± 0.82 compared to 1.15 ± 0.33 respectively, p = 0.015, all figure 8-3).

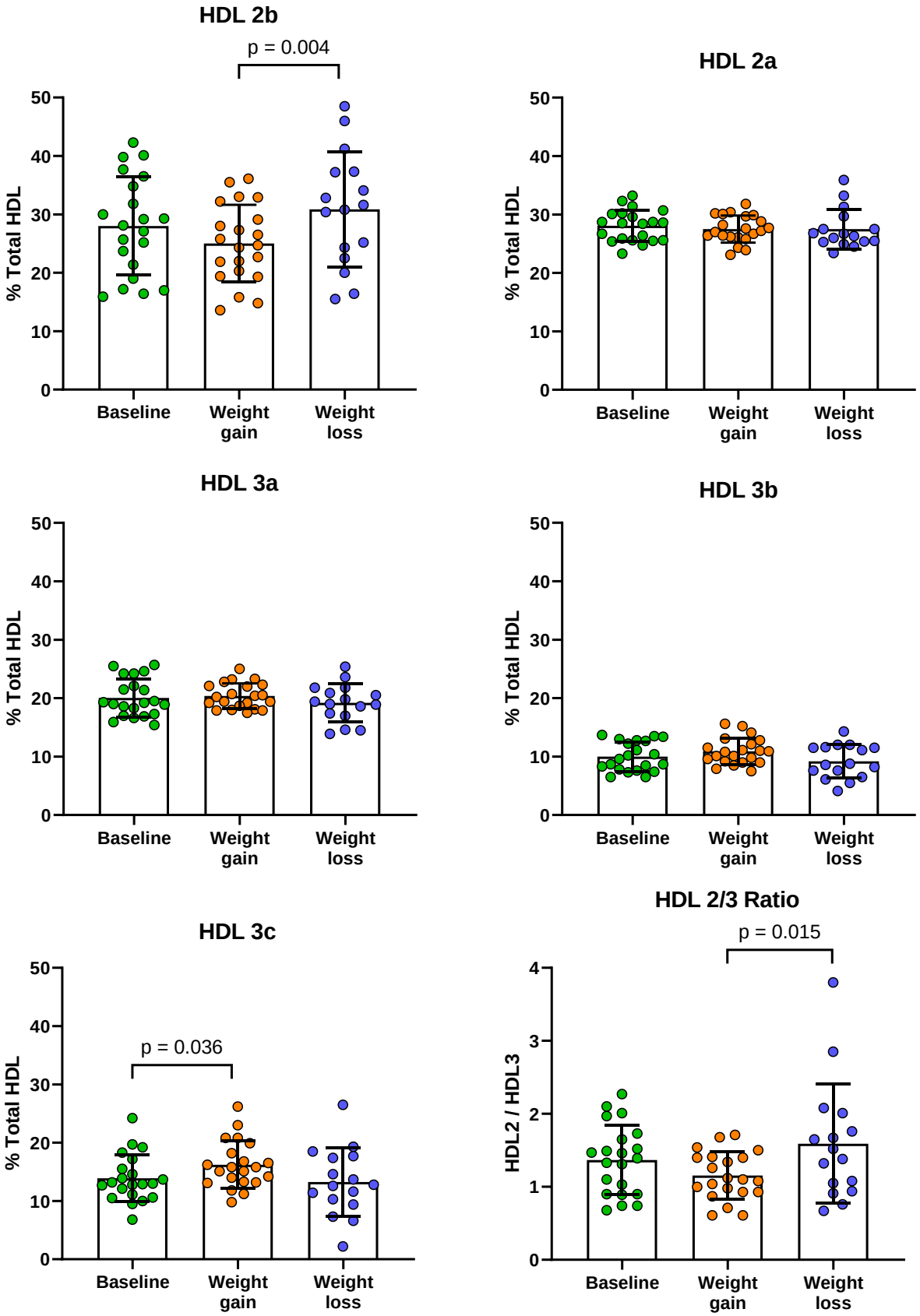

Figure 8-3 HDL size distribution in white Europeans: Data expressed as mean ± SD. Comparisons made by general linear model followed by *post hoc* Tukey test. Statistical significance was assumed at $p < 0.05$.

8.3.2.4 Identification of HDL proteins in the GlasVEGAs study

Proteomic analysis of HDL revealed 149 proteins in at least one HDL sample. Of these, 50 proteins were present in >50% of HDL samples cut off and were deemed HDL-associated. These proteins are listed in table 8-3.

Table 8-3 List of proteins identified in >50% of HDL samples in the GlasVEGAs study

Alpha-1-acid glycoprotein 1	Hemoglobin subunit beta
Alpha-1-acid glycoprotein 2	Hemopexin
Alpha-1-antichymotrypsin	Heparin cofactor 2
Alpha-1-antitrypsin	Ig alpha-1 chain C region
Alpha-1B-glycoprotein	Ig gamma-1 chain C region
Alpha-2-antiplasmin	Ig kappa chain C region
Alpha-2-HS-glycoprotein	Ig lambda-1 chain C regions
Angiotensinogen	Kininogen-1
Apolipoprotein A-I	Phosphatidylcholine-sterol acyltransferase
Apolipoprotein A-II	Phospholipid transfer protein
Apolipoprotein A-IV	Pigment epithelium-derived factor
Apolipoprotein C-I	Protein AMBP
Apolipoprotein C-II	Retinol-binding protein 4
Apolipoprotein C-III	Serotransferrin
Apolipoprotein D	Serum amyloid A-1 protein
Apolipoprotein E	Serum paraoxonase/arylesterase 1
Apolipoprotein F	Serum paraoxonase/lactonase 3
Apolipoprotein L1	Tetranectin
Apolipoprotein M	Transthyretin
Beta-2-glycoprotein 1	Vitamin D-binding protein
Carbonic anhydrase 1	Vitronectin
Cholesteryl ester transfer protein	Zinc-alpha-2-glycoprotein
Clusterin	
Complement C3	
Complement C4-B	
Fibrinogen beta chain	
Gelsolin	
Haptoglobin-related protein	

8.3.2.5 OPLS-DA of white Europeans with weight gain and weight loss

The OPLS-DA model generated using the HDL proteins and demographics as variables did not show any separation between Europeans at baseline, or with weight gain and with weight loss (Figure 8-4).

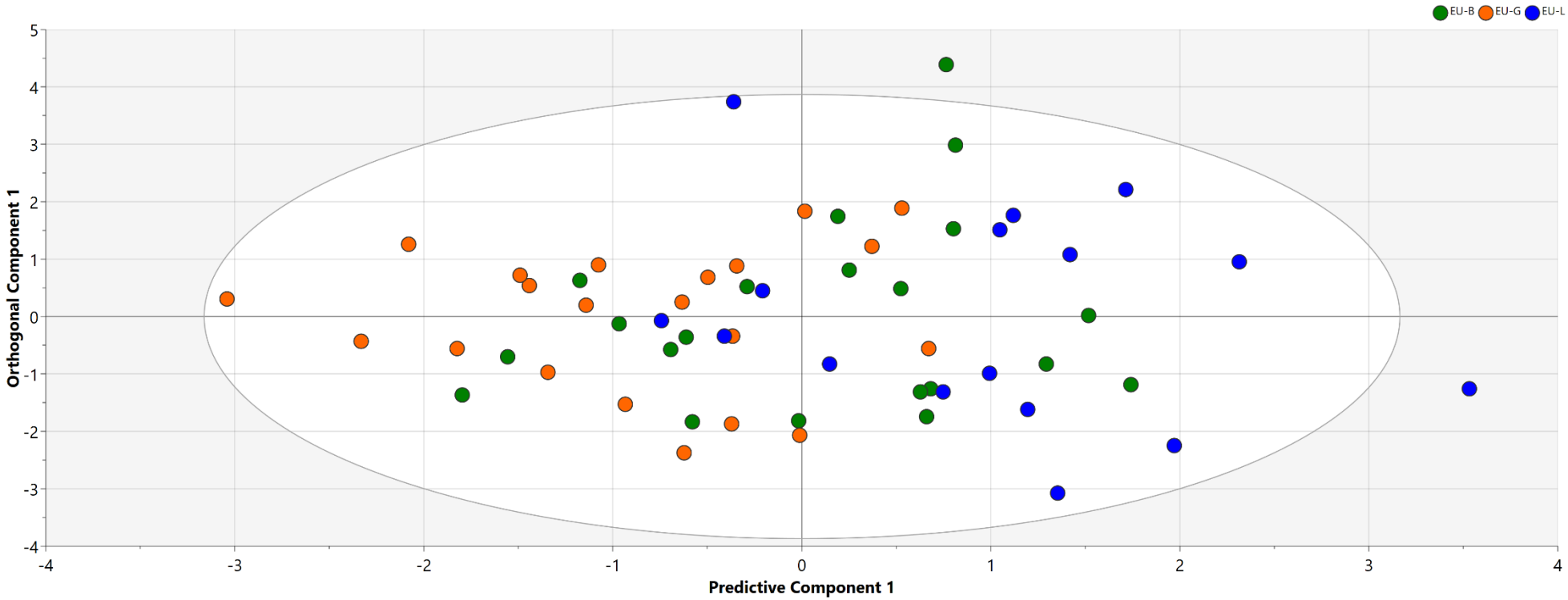

Figure 8-4 Orthogonal projections of latent structures - discriminant analysis score plot of the GlasVEGAs European men after VIP selection. The x axis represents between-group variation, and the y axis represents within-group variation. The ellipse represents the confidence region of a Hotelling's T2 test with significance level of p = 0.05. Samples outside the ellipse may be considered as potential outliers.

8.3.2.6 Differences in HDL protein composition in white Europeans with weight gain and weight loss

Of the 50 identified HDL proteins, two had significant changes in abundance on HDL after weight loss in Europeans (Figure 8-5). The LFQ intensity of serum paraoxonase/arylesterase-1 was decreased after weight loss, while the adipokine zinc-alpha-2-glycoprotein (ZAG) was increased after weight loss in European men.

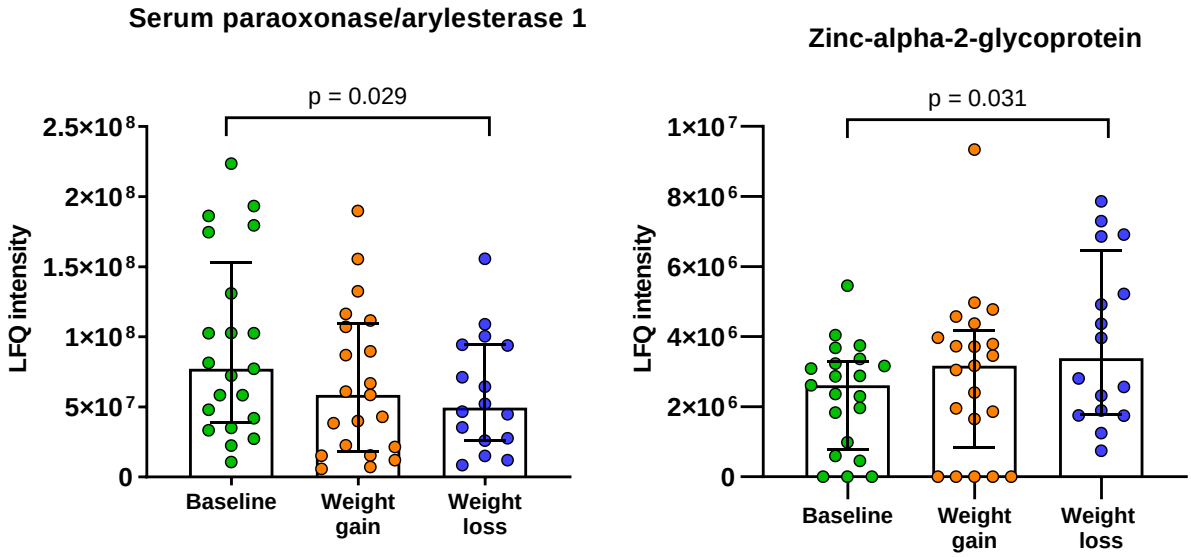

Figure 8-5 HDL serum paraoxonase-1 and zinc-alpha-2-glycoprotein content change with weight loss in white Europeans: Data expressed as median ± IQR. Comparisons made by general linear model followed by *post hoc* Tukey test. Statistical significance was assumed at $p < 0.05$.

8.3.2.7 Methionine oxidation of identified HDL proteins in white Europeans after weight gain and weight loss

Of the 50 identified HDL-associated proteins, three contained oxidised methionine residues (Table 8-4).

Table 8-4 List of HDL-associated proteins with oxidised methionine residues in the GlasVEGAs study

Protein name	Amino acid position(s) of modification
Apolipoprotein A-I	136, 172
Apolipoprotein D	177
Apolipoprotein E	26

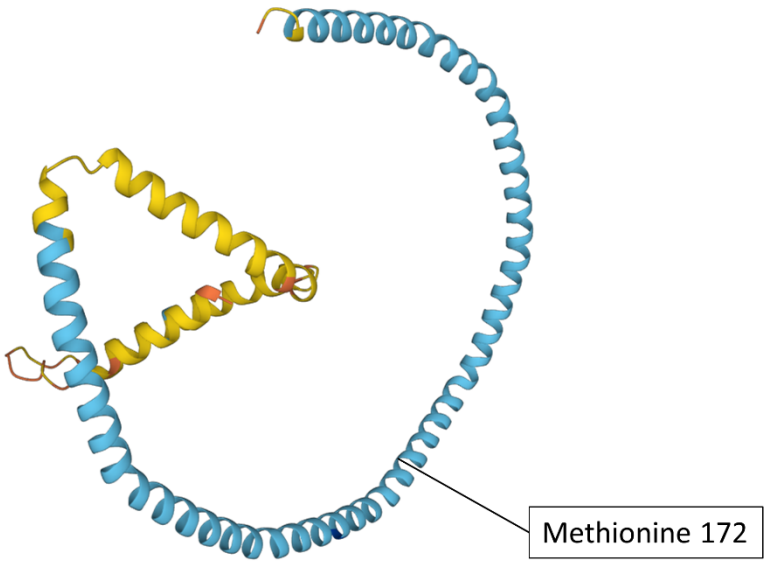

Figure 8-6 Structure of apolipoprotein AI with methionine position 172 highlighted: Protein structure was predicted using Alphafold DB prediction from EMBL-EBI (Jumper et al., 2021; Varadi et al., 2022). Source sequence was derived from Uniprot entry P02647. This sequence includes the 24 amino acid signalling sequence at the N-terminus of the protein. Image used under Creative Commons Attribution 4.0 (CC-BY 4.0) licence terms.

The LFQ intensity of apoAI methionine oxidation was significantly reduced after weight gain compared to baseline in white Europeans (Figure 8-7).

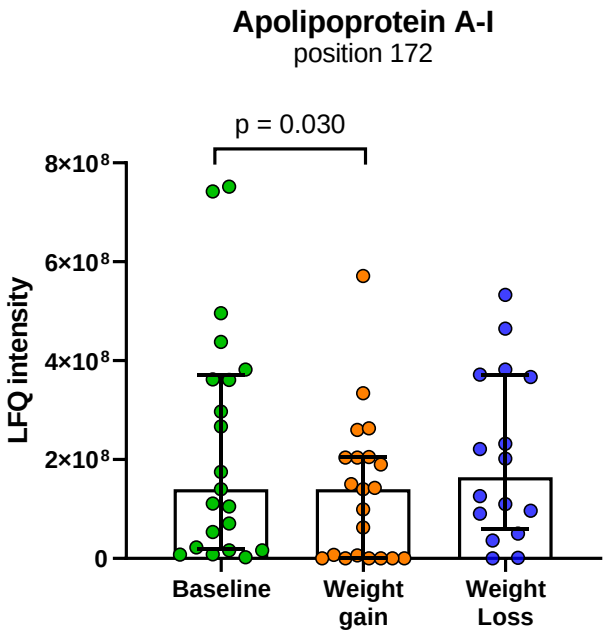

Figure 8-7 Methionine oxidation of HDL apoAI at position 172 in white Europeans: Data expressed as median ± IQR. Comparisons were made by general linear model followed by *post hoc* Tukey test. Statistical significance was assumed at $p < 0.05$.

8.3.2.8 Glycation of identified HDL proteins in white Europeans after weight gain and weight loss

There was both carboxymethyl and 1-alkyl-2-formyl-3,4-glycosyl-pyrrole (AFGP) glycation of alpha-1-antitrypsin detected at lysine residues 355 and 359, however, there were no significant differences detected in the abundance of these modifications after weight gain and weight loss.

8.3.2.9 HDL paraoxonase-1 activity in white Europeans after weight gain and weight loss

Whether corrected for HDL protein or cholesterol content, HDL PON-1 activity did not differ from baseline after weight gain or weight loss (Figure 8-8). There was not a difference in HDL PON-1/SAA-1 ratio after weight gain or weight loss (Figure 8-9).

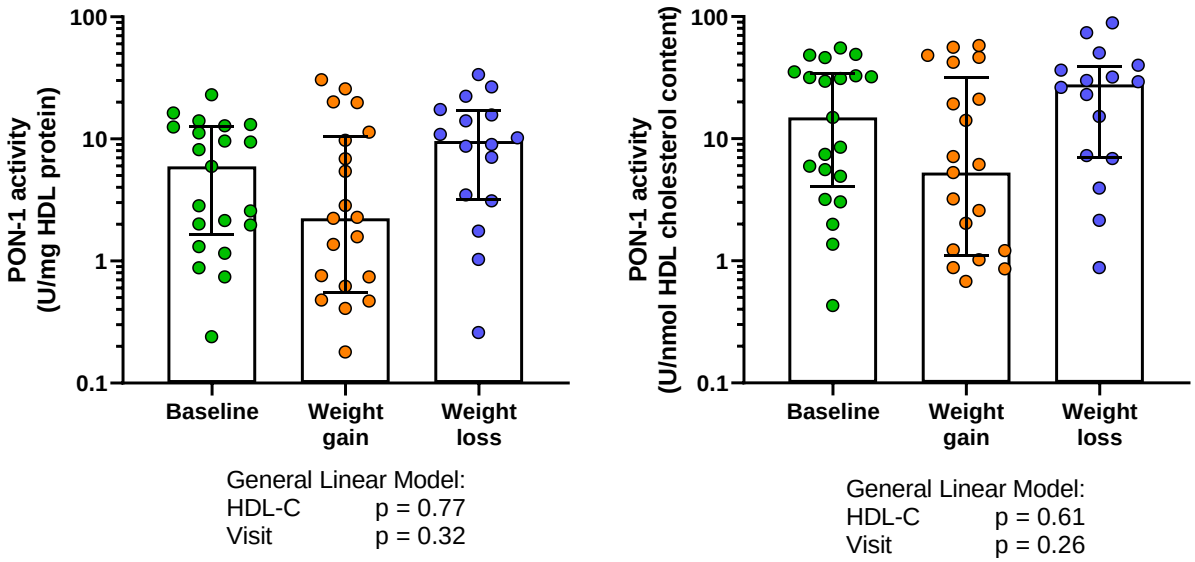

Figure 8-8 HDL paraoxonase-1 arylesterase activity in the white European cohort of the GlasVEGAs study: Data expressed as median ± IQR and shown on a $\log_{10}$ axis for clear visualisation. Comparisons were made by general linear model with HDL-C as a co-variate. Statistical significance was assumed at $p < 0.05$.

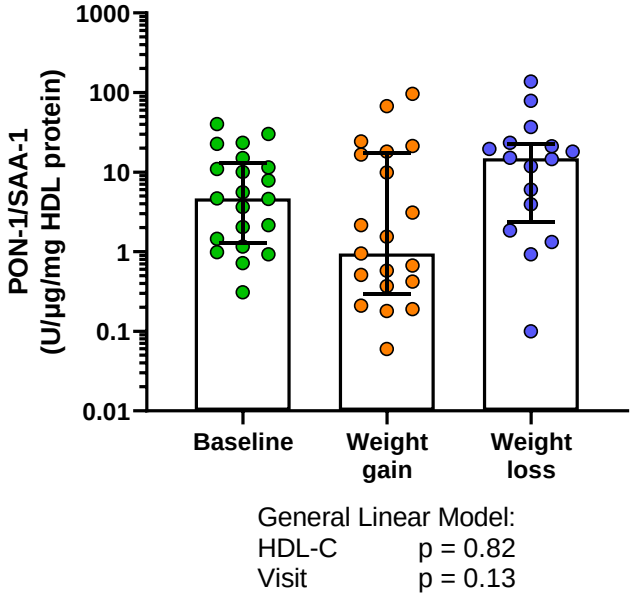

Figure 8-9 The ratio of HDL PON-1 activity to SAA-1 content in the white European cohort of the GlasVEGAs study: Data expressed as median ± IQR and shown on a $\log_{10}$ axis for clear visualisation. Comparisons were made by general linear model with HDL-C as a co-variate. Statistical significance was assumed at $p < 0.05$.

8.3.2.10 Anti-inflammatory function in white Europeans after weight gain and weight loss

The anti-inflammatory function of HDL remained constant after weight gain and weight loss, whether corrected for the HDL total cholesterol or total protein content exposed to the endothelial cells (Figure 8-10).

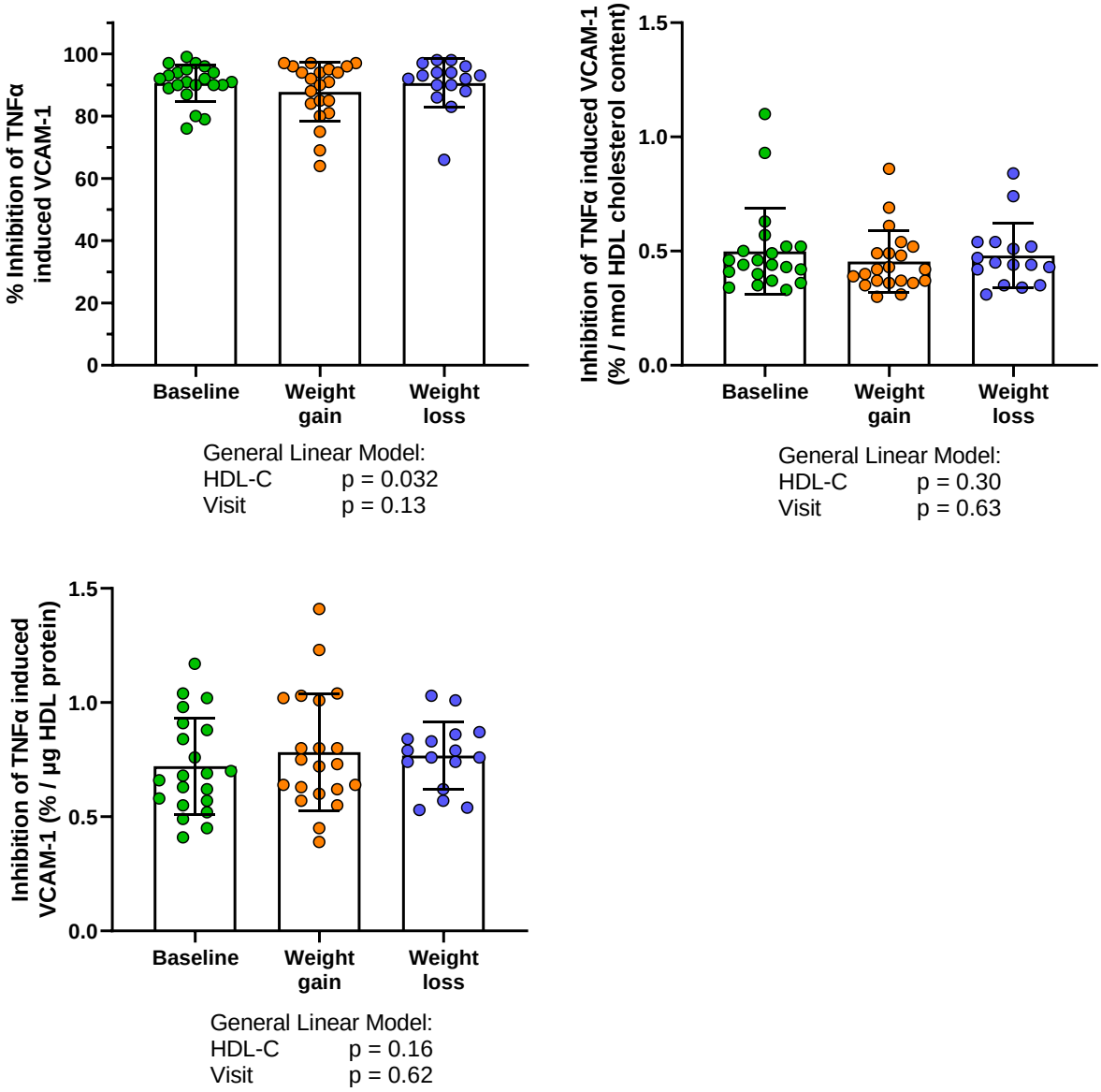

Figure 8-10 HDL anti-inflammatory function in white Europeans of the GlasVEGAs study: Data expressed as median ± IQR and shown on a $\log_{10}$ axis for clear visualisation. Comparisons were made by general linear model with HDL-C as a co-variate. Statistical significance was assumed at $p < 0.05$.

8.3.3 Differences in HDL composition and function between white Europeans and South Asians at baseline and in response to weight gain

8.3.3.1 HDL apoAI and total cholesterol in white Europeans and South Asians with weight gain

Europeans and South Asians responded similarly to weight gain, with unchanged HDL apoAI and total cholesterol content (Figure 8-11).

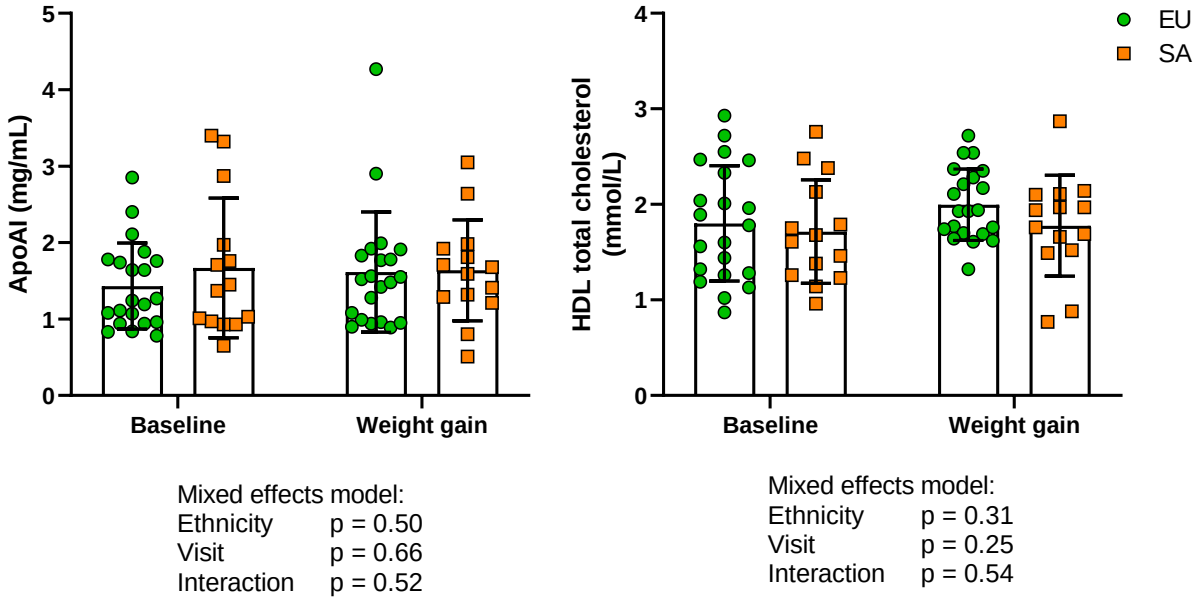

Figure 8-11 HDL apoAI and total cholesterol content in white Europeans and South Asians after weight gain: Data is expressed as mean ± SD. Comparisons were made by mixed effects model. Statistical significance was assumed at $p < 0.05$.

8.3.3.2 HDL total protein and SAA-1 content in white Europeans and South Asians with weight gain

HDL total protein and SAA-1 content was not different between Europeans and South Asians with neither changed with weight gain (Figure 8-12).

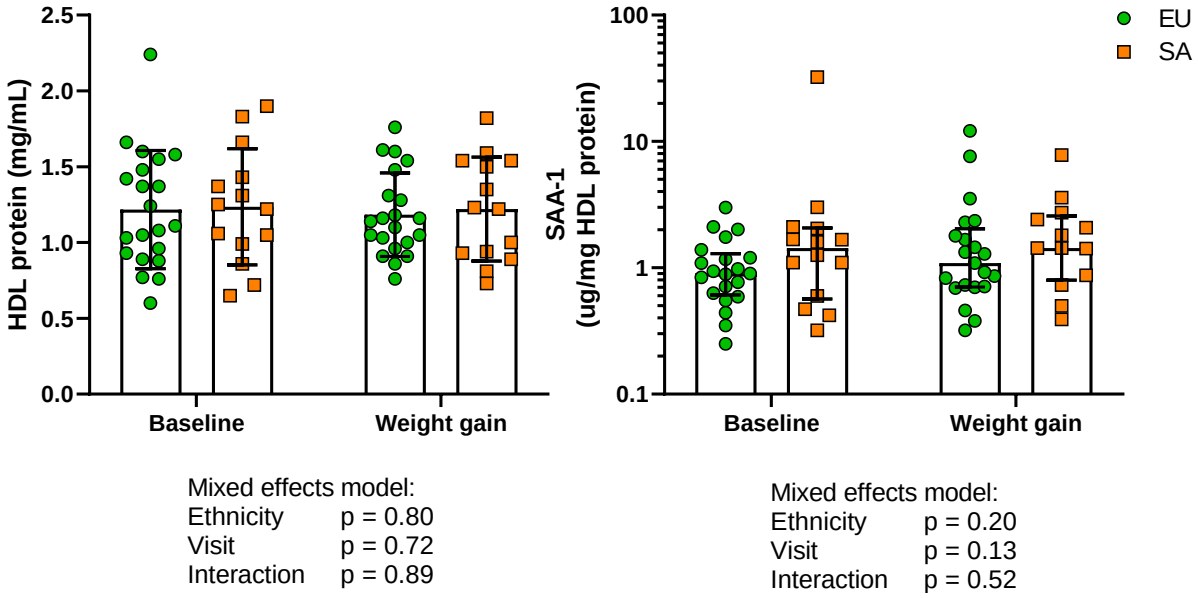

Mixed effects model:
Ethnicity p = 0.80
Visit p = 0.72
Interaction p = 0.89

Mixed effects model:
Ethnicity p = 0.20
Visit p = 0.13
Interaction p = 0.52

Figure 8-12 HDL total protein and SAA-1 content in white Europeans and South Asians after weight gain: HDL protein data is expressed as mean ± SD. HDL SAA-1 data is expressed as median ± IQR and shown on a log10 axis for clear visualisation. Comparisons were made by mixed effects model followed by *post hoc* Tukey test. Statistical significance was assumed at $p < 0.05$.

8.3.3.3 HDL size distribution in Europeans and South Asians after weight gain

The proportion of HDL 2b was not different between Europeans and South Asians but was reduced by weight gain (p = 0.001). There was an interaction effect in the proportion of HDL 2a post-weight gain, with Europeans reducing and South Asians increasing the proportion of HDL 2a. The HDL 2/3 ratio, reflective of overall HDL size, was decreased by weight gain (p = 0.015) but not different between the two ethnicities (Figure 8-13).

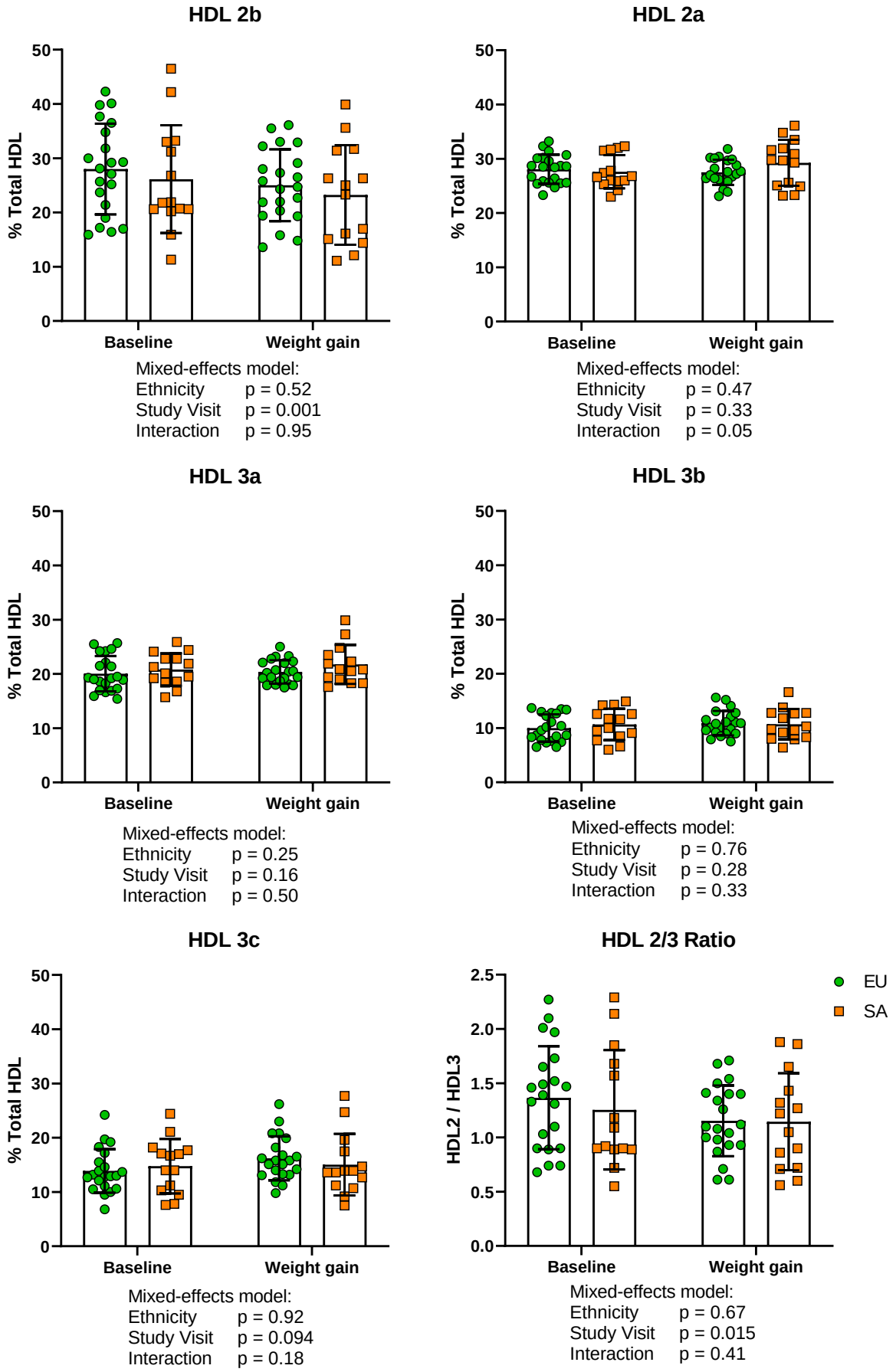

Figure 8-13 HDL size distribution in white Europeans and South Asians: Data expressed as mean ± SD. Comparisons were made by mixed effects model followed by *post hoc* Tukey test. Statistical significance was assumed at $p < 0.05$ for pairwise comparisons.

8.3.3.4 HDL proteins identified on white European and South Asian HDL

Due to sample volume constraints, four South Asian samples were missing from proteomic analysis, resulting in n = 11 at baseline and n= 13 with weight gain in this ethnicity. A full list of the 50 proteins identified on HDL from this study can be found in table 8-3.

8.3.3.5 OPLS-DA of white European and South Asians at baseline and weight gain

An OPLS-DA model showed clear separation between Europeans (to the left of the scores plot) and South Asians at baseline (to the right of the scores plot) (Figure 8-14). The loadings plot indicated that three demographic factors, including plasma triglycerides, and a constellation of HDL proteins contributed most to the separation after filtering for variables with a VIP score of greater than 1 (Figure 8-15). ApoAI and apoF were important to the separation for the Europeans at baseline, while apoAIV, ZAG and apoL1 were important to the separation for South Asians at baseline. A further OPLS-DA model comparing Europeans and South Asians after weight gain showed clear separation between the two groups (Figure 8-16). The corresponding loadings plot indicated that while demographic measures such as $HOMA_{IR}$ contribute to the separation, HDL proteins including apolipoprotein CIII and complement C4-B are important to group separation (Figure 8-17).

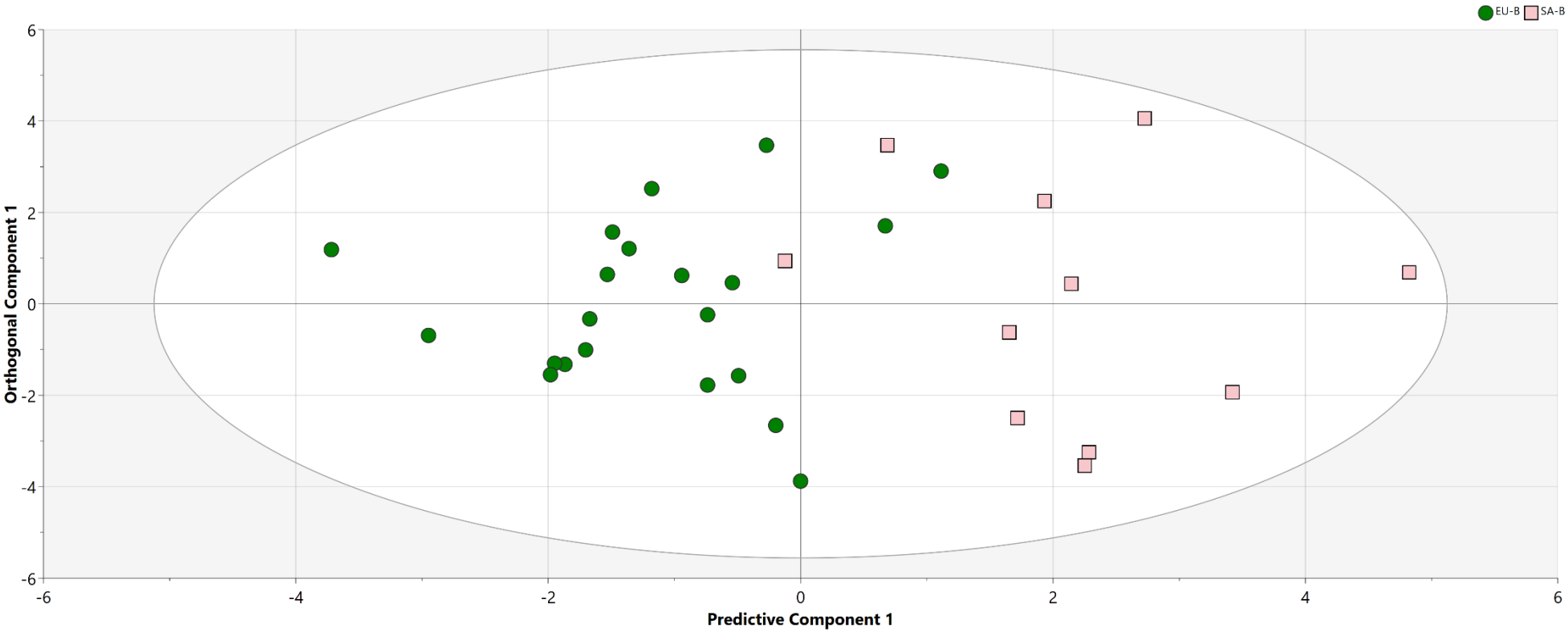

Figure 8-14 Orthogonal projections of latent structures - discriminant analysis score plot of the European and South Asian men at baseline after VIP selection. The x axis represents between-group variation, and the y axis represents within-group variation. The ellipse represents the confidence region of a Hotelling's T2 test with significance level of p = 0.05. Samples outside the ellipse may be considered as potential outliers.

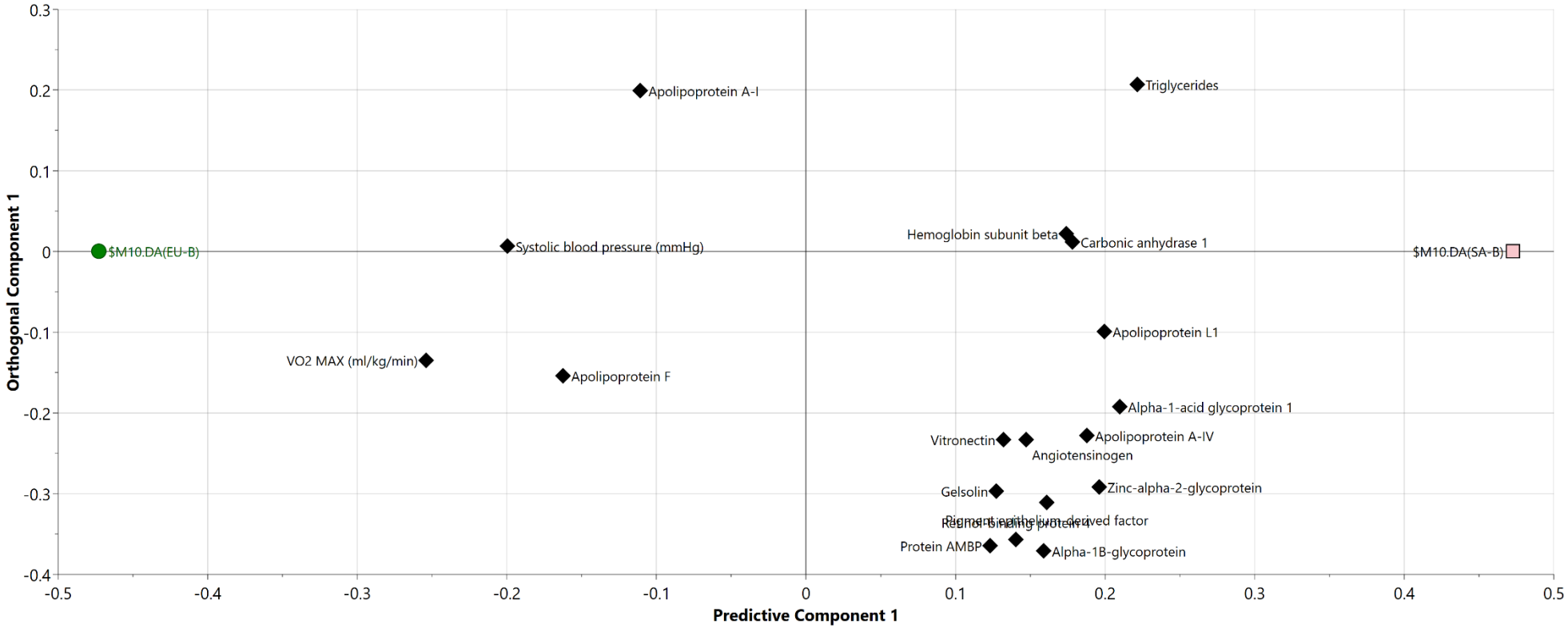

Figure 8-15 Orthogonal projections of latent structures - discriminant analysis loadings plot of the European and South Asian men at baseline after VIP selection. This plot shows the correlations of variables with one and other and their impact on the separation of the groups. Variables located close together are correlated together. Variables closer to the group identifiers are more important to the observed separation.

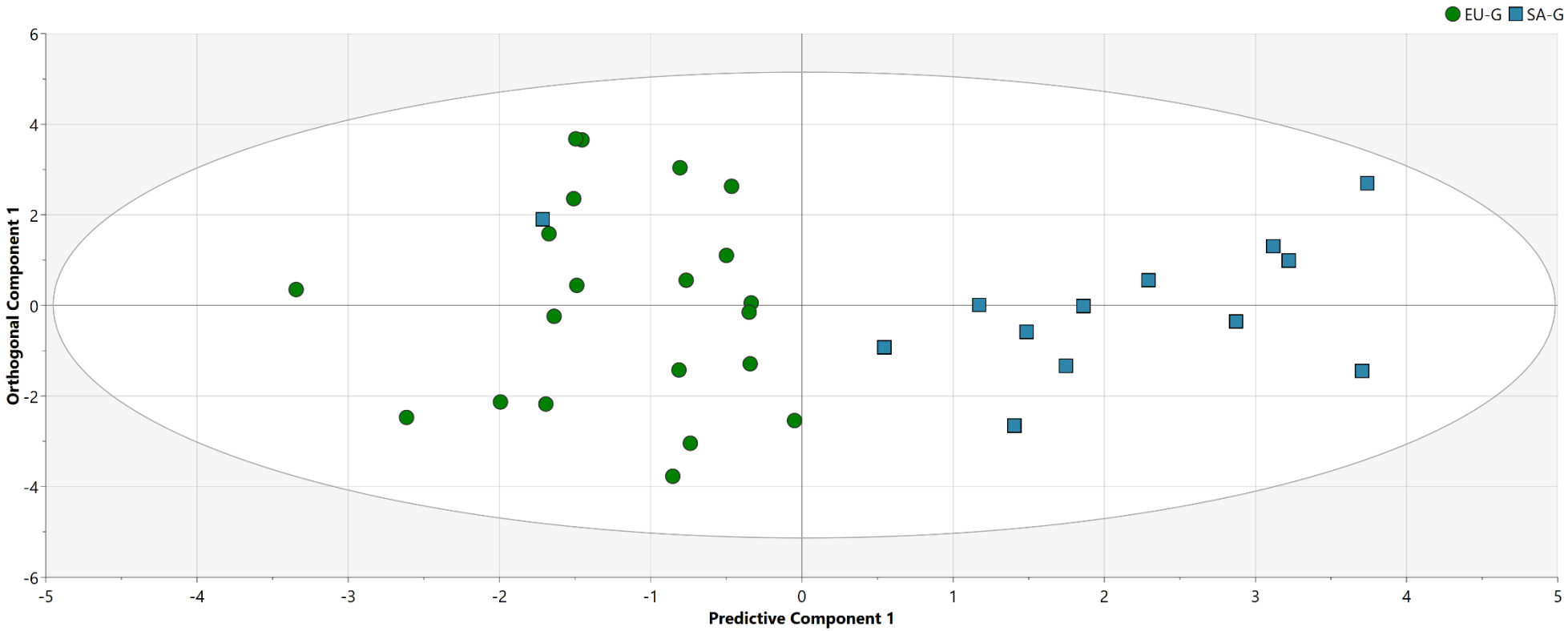

Figure 8-16 Orthogonal projections of latent structures - discriminant analysis score plot of the European and South Asian men with weight gain after VIP selection. The x axis represents between-group variation, and the y axis represents within-group variation. The ellipse represents the confidence region of a Hotelling's T2 test with significance level of p = 0.05. Samples outside the ellipse may be considered as potential outliers.

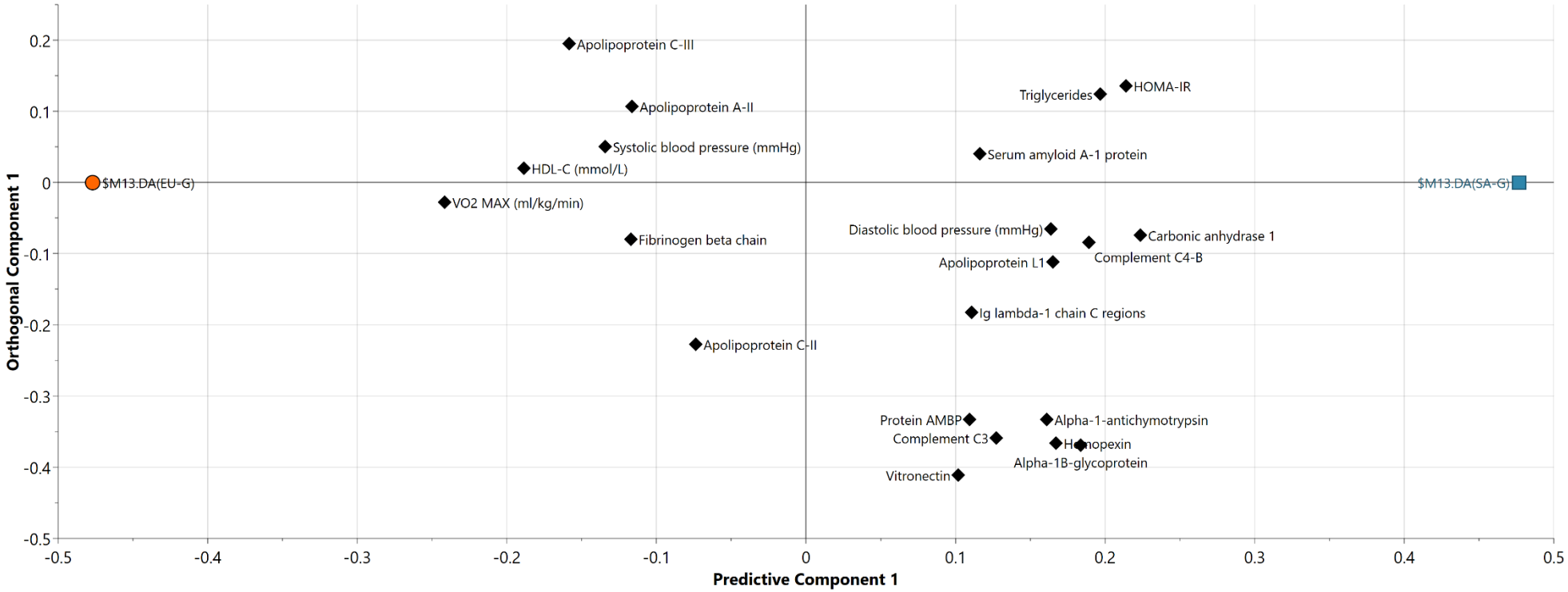

Figure 8-17 Orthogonal projections of latent structures - discriminant analysis loadings plot of the European and South Asian men with weight gain after VIP selection. This plot shows the correlations of variables with one and other and their impact on the separation of the groups. Variables located close together are correlated together. Variables closer to the group identifiers are more important to the observed separation.

8.3.3.6 Changes in the HDL proteome with weight gain in Europeans and South Asians

Of the 50 identified HDL proteins, 17 had significant differences when comparing the European and South Asian response to weight gain, including apolipoproteins, immune-related proteins and adipokines. There were four apolipoproteins with significant differences in their LFQ intensities on HDL when comparing Europeans and South Asians. ApoAIV LFQ intensity was higher in South Asians ($p = 0.011$) but did not change with study visit in either ethnicity. There was an interaction effect in apoCIII and apoF. The LFQ intensity of HDL apoCIII increased in Europeans but decreased in South Asians after weight gain. The LFQ intensity of HDL apoF decreased in Europeans but increased in South Asians post weight gain (Figure 8-18).

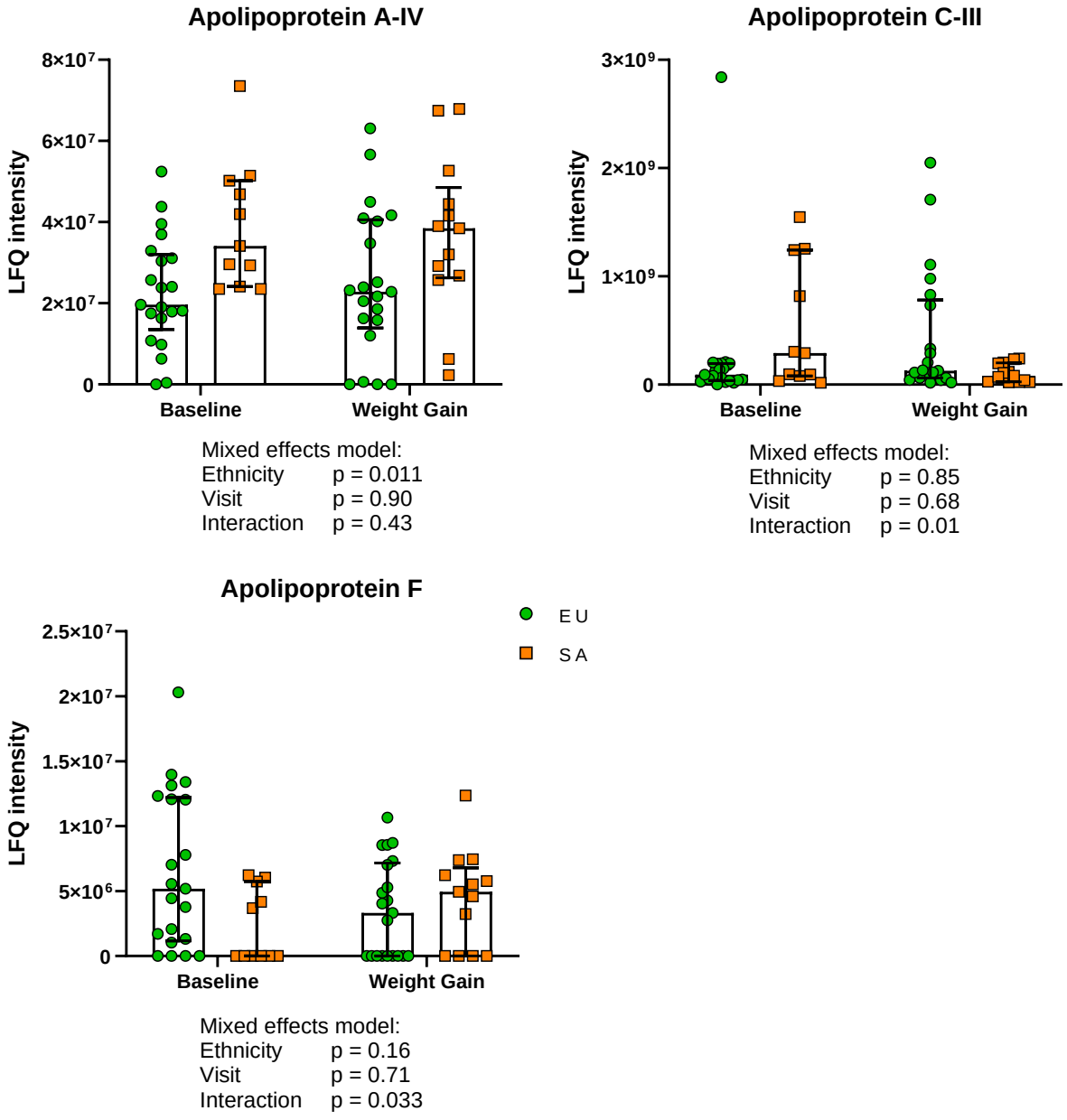

Figure 8-18 Apolipoprotein content of HDL in the GlasVEGAs study: Data expressed as median ± IQR. Comparisons were made by mixed effects model followed by *post hoc* Tukey test. Statistical significance was assumed at $p < 0.05$ for pairwise comparisons.

As these apolipoproteins are involved in triglyceride handling, the relationship between the change in these proteins after weight gain with the change in liver fat fraction was explored. Only the change in apoCIII with weight gain correlated with the change in liver fat with weight gain (Figure 8-19).

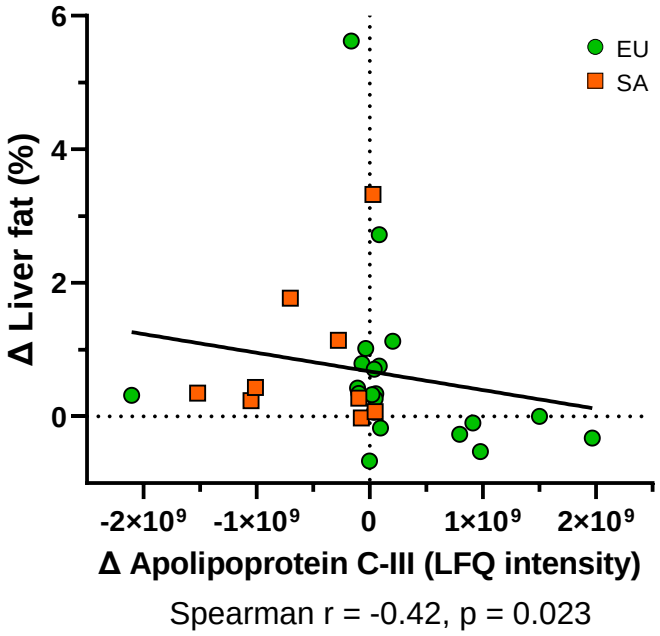

Figure 8-19 The correlation of weight gain induced change in HDL apoCIII and liver fat percentage: Correlation was assessed by Spearman's Rank test. Statistical significance was assumed at $p < 0.05$.

Five proteins identified on HDL with differences when comparing Europeans and South Asians were immune-related. The LFQ intensities of complement C3 ($p = 0.038$), gelsolin ($p = 0.043$), hemopexin ($p = 0.004$) and Ig kappa chain c region ($p = 0.049$) were all higher in South Asian HDL compared to European HDL irrespective of weight gain. The LFQ intensity of complement C4-B was also higher in South Asian HDL compared to European HDL ($p = 0.040$). After weight gain, complement C4-B was significantly higher in South Asian HDL compared to European HDL ($p = 0.026$) (Figure 8-20).

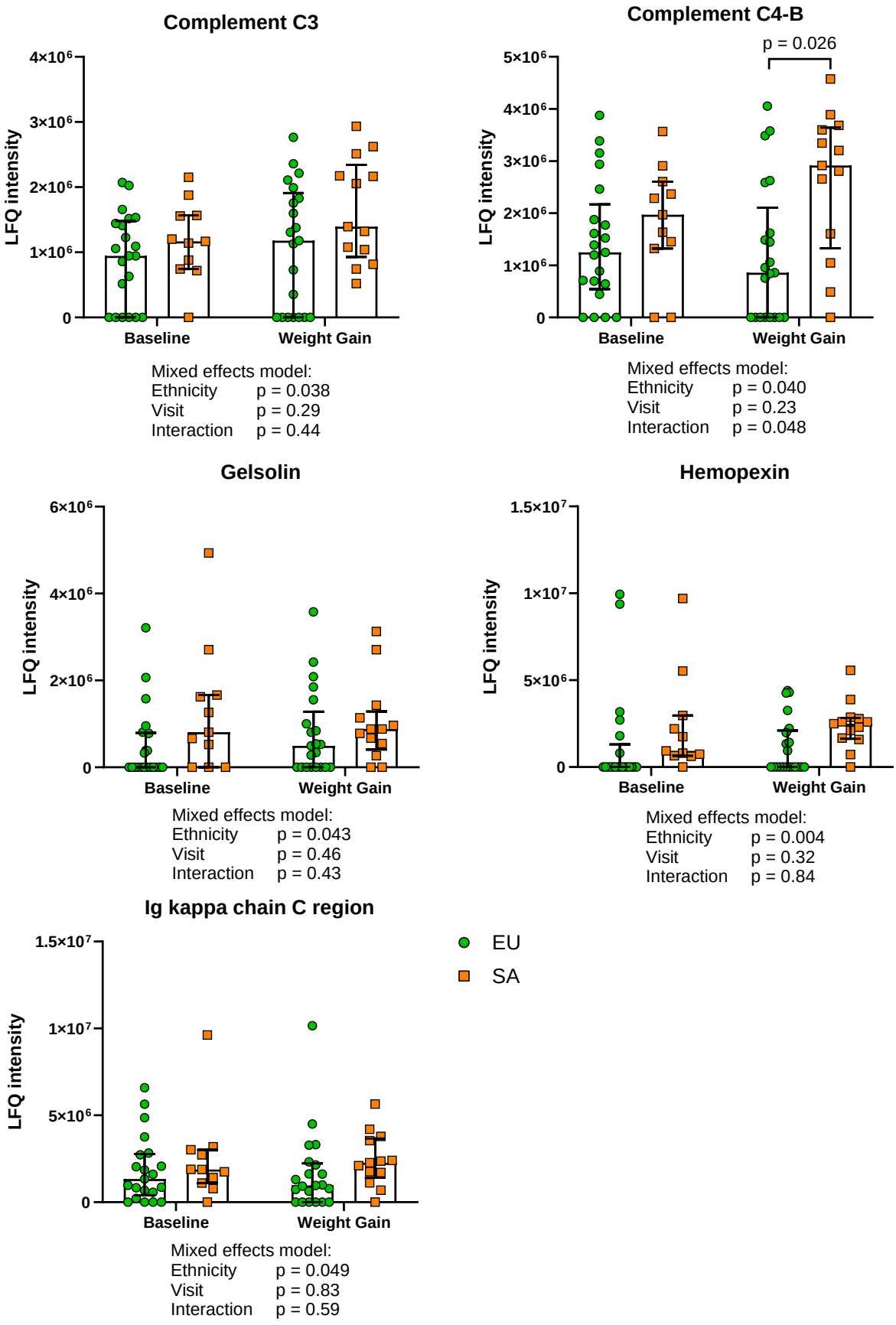

Figure 8-20 Immune-related proteins on HDL from the GlasVEGAs study: Data expressed as median ± IQR. Comparisons were made by mixed effects model followed by *post hoc* Tukey test. Statistical significance was assumed at $p < 0.05$ for pairwise comparisons .

Two adipokines identified on HDL when comparing Europeans and South Asians had significant differences. The LFQ intensity of both retinol-binding protein 4 (RBP4) and ZAG were higher in South Asian HDL compared to European HDL irrespective of weight gain (p = 0.048 and p= 0.041 respectively) (Figure 8-21).

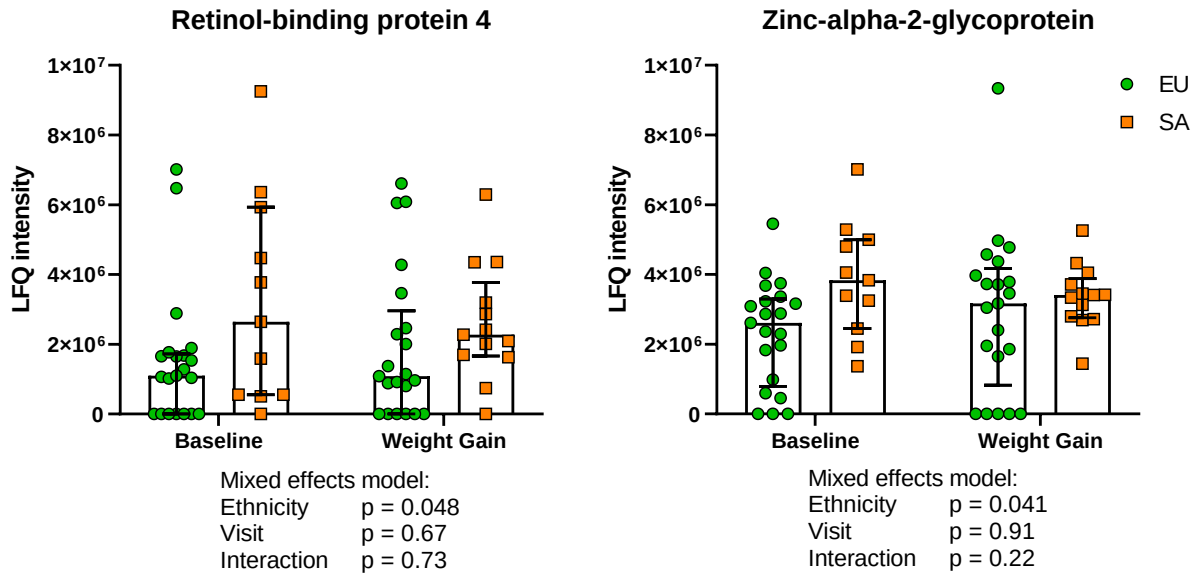

Figure 8-21 Adipokine content of HDL with weight gain in Europeans and South Asians: Data expressed as median ± IQR. Comparisons were made by mixed effects model. Statistical significance was assumed at $p < 0.05$ for pairwise comparisons .

The antioxidant paraoxonase/arylesterase-1 LFQ intensity did not differ between ethnicities, but overall was reduced with weight gain (p = 0.033) (Figure 8-22).

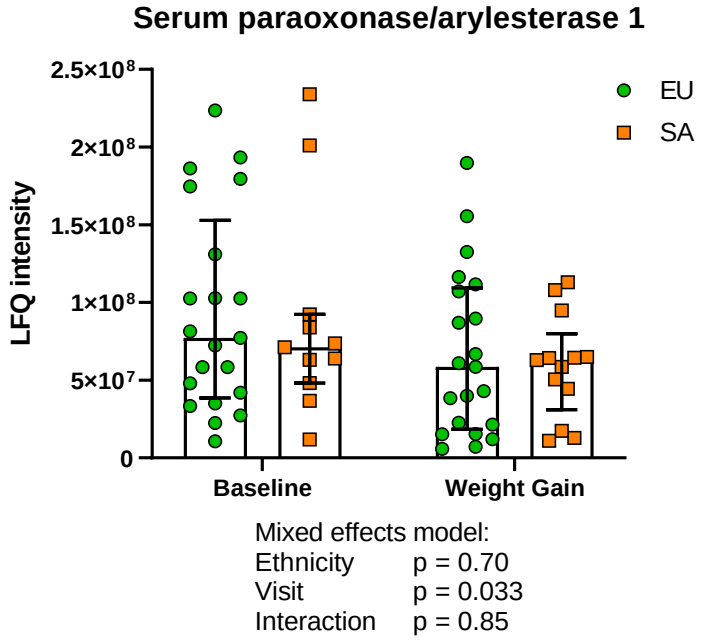

Figure 8-22 Paraoxonase/arylesterase-1 content of HDL in white Europeans and South Asians with weight gain: Data expressed as median ± IQR. Comparisons were made by mixed effects model followed by *post hoc* Tukey test. Statistical significance was assumed at $p < 0.05$ for pairwise comparisons.

Finally, five further miscellaneous proteins were different between the HDL of South Asians and Europeans. The LFQ intensities of alpha-1B-glycoprotein, carbonic anhydrase 1, protein AMBP and vitronectin were all higher in South Asian HDL compared to European HDL irrespective of weight gain (Figure 8-23).

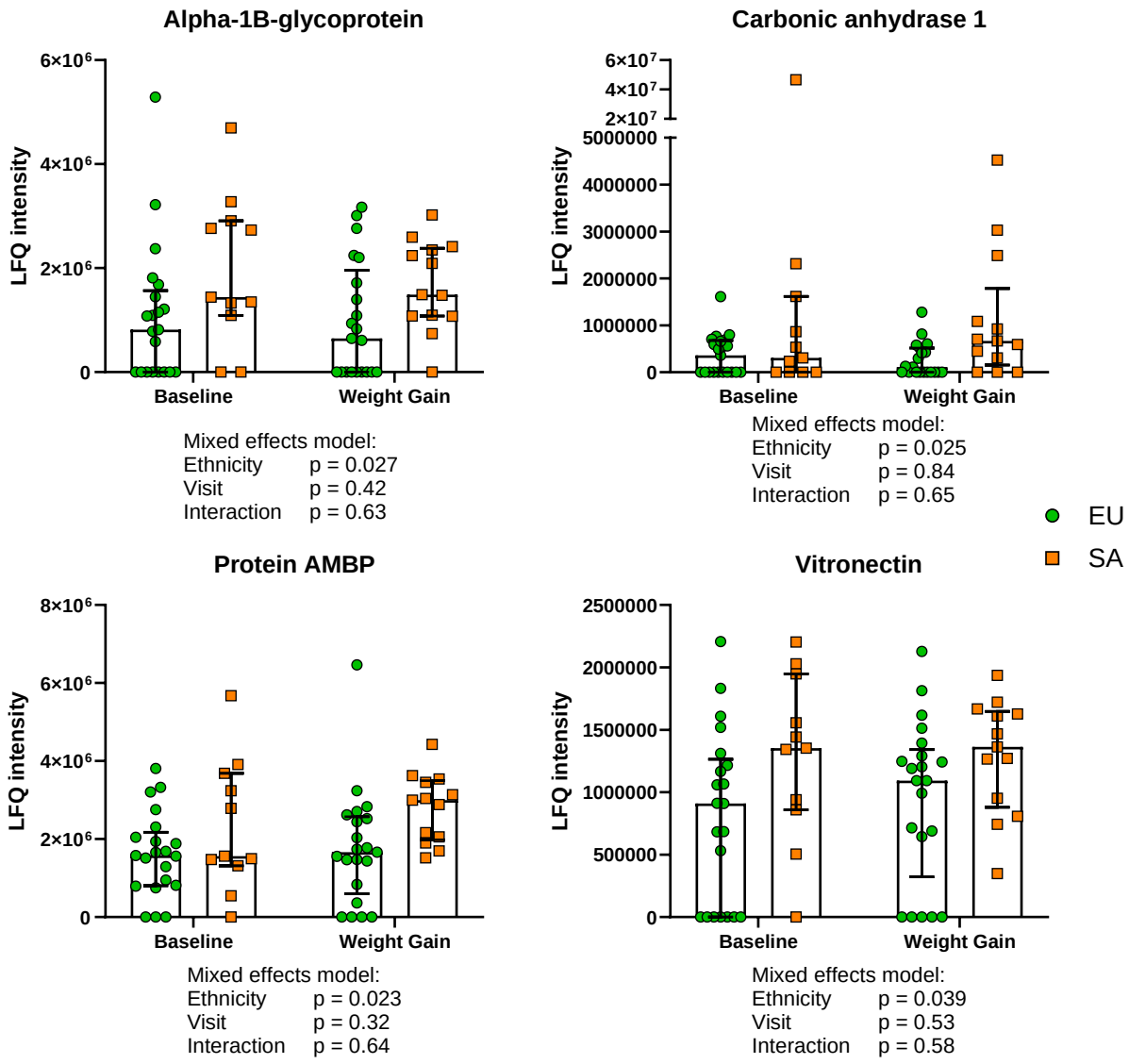

Figure 8-23 Miscellaneous proteins identified on HDL with weight gain in white Europeans and South Asians: Data expressed as median ± IQR. Comparisons were made by mixed effects model followed by *post hoc* Tukey test. Statistical significance was assumed at $p < 0.05$ for pairwise comparisons .

8.3.3.7 Post-translational modification of identified HDL proteins in white Europeans and South Asians in response to weight gain

A list of HDL-associated proteins exhibiting oxidised methionine residues in the GlasVEGAs study can be found in table 8-4 and a description of glycated HDL-associated proteins can be found in section 8.3.2.8. There were no differences detected in the post-translation modification of HDL proteins between white Europeans and South Asians or with weight gain.

8.3.3.8 HDL paraoxonase-1 activity in white Europeans and South Asians in response to weight gain.

Whether corrected for HDL protein or total cholesterol content, HDL PON-1 activity was not affected by either ethnicity or weight gain (Figure 8-24).

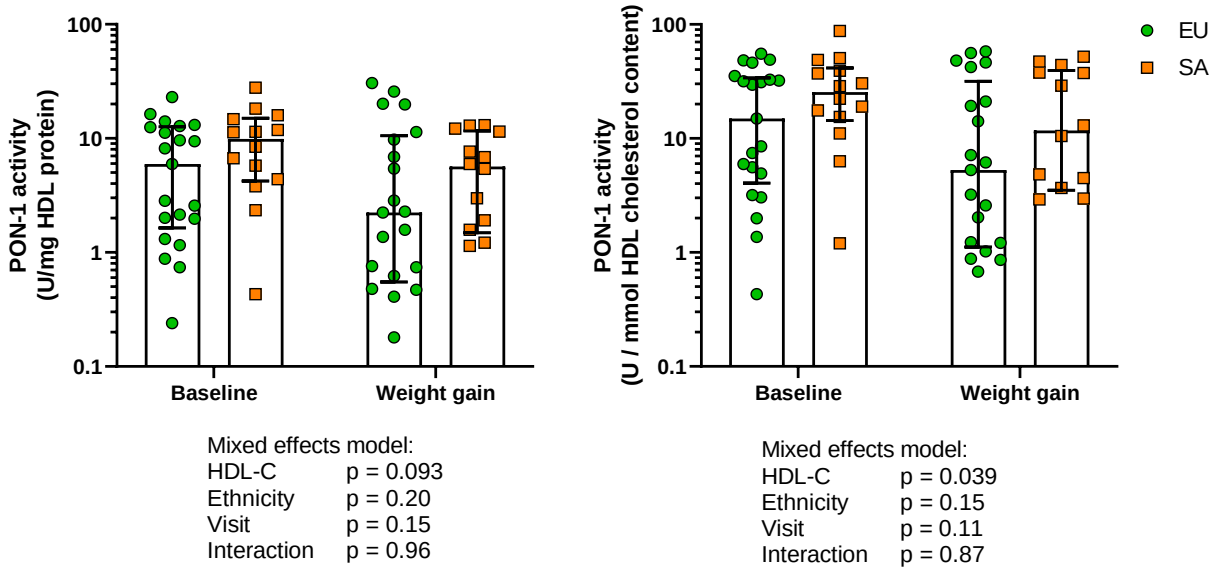

Figure 8-24 Paraoxonase-1 arylesterase activity in the HDL of white Europeans and South Asians with weight gain: Data expressed as median ± IQR and shown on a log10 axis for clear visualisation. Comparisons were made by mixed effects model. Statistical significance was assumed at $p < 0.05$.

The ratio of PON-1 activity to SAA-1 content in HDL from Europeans and South Asians did not differ by ethnicity or weight gain (Figure 8-25).

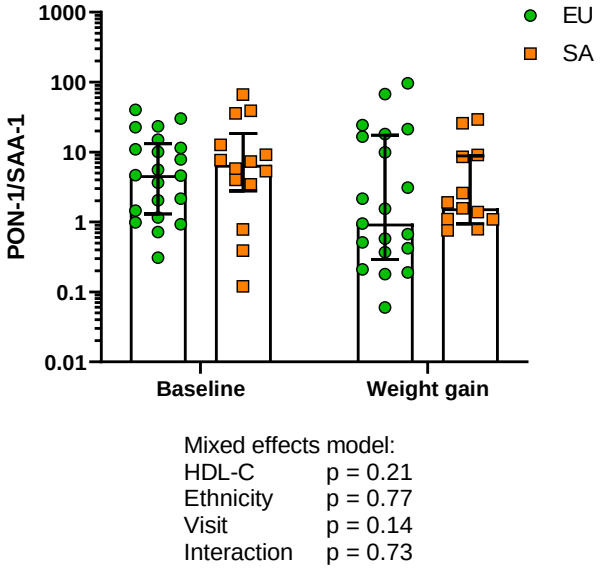

Mixed effects model:

HDL-C	p = 0.21
Ethnicity	p = 0.77
Visit	p = 0.14
Interaction	p = 0.73

Figure 8-25 The ratio of paraoxonase-1 activity and SAA-1 content of HDL in Europeans and South Asians in response to weight gain: Data expressed as median ± IQR and shown on a log10 axis for clear visualisation. Comparisons were made by mixed effects model. Statistical significance was assumed at $p < 0.05$.

8.3.3.9 The anti-inflammatory function of HDL in Europeans and South Asians in response to weight gain.

The anti-inflammatory function of HDL was not affected by ethnicity or weight gain. This was still the case after correction for HDL total protein and HDL cholesterol exposed to the cells (Figure 8-26).

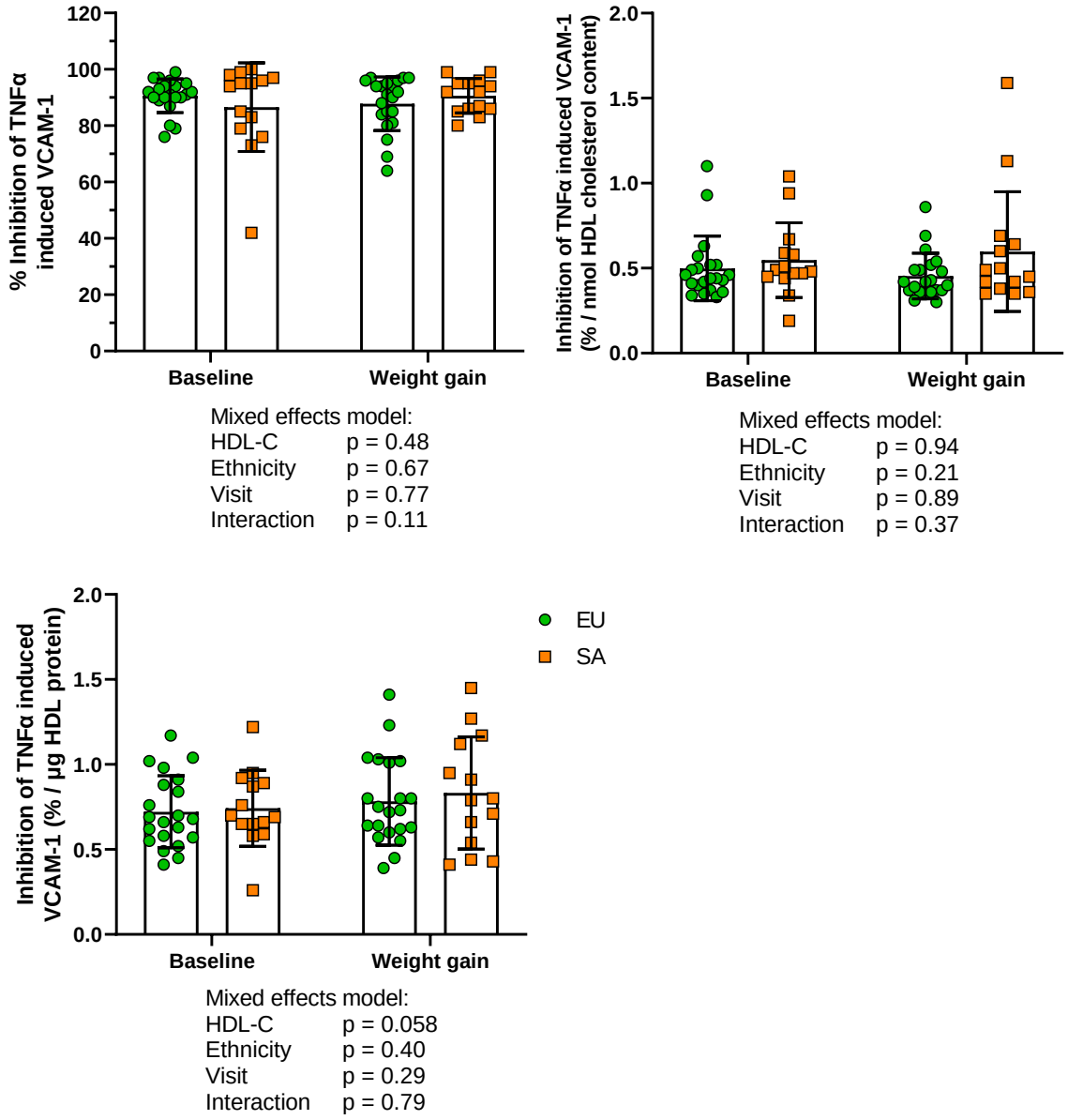

Figure 8-26 The anti-inflammatory function of HDL from white Europeans and South Asians after weight gain: Data expressed as mean ± SD. Comparisons were made by mixed effects model followed by *post hoc* Tukey test. Statistical significance was assumed at $p < 0.05$ for pairwise comparisons .

8.4 Discussion

This chapter set out to understand the HDL compositional and functional differences between white Europeans and South Asians and in their response to weight gain and subsequent weight loss in a longitudinal study of young and healthy white European and South Asian men. There were very minor changes in HDL composition but no changes in HDL function with weight gain and weight loss in Europeans. Despite the weight loss time point being excluded from analysis in South Asians due to the lack of participants, European HDL was markedly different to South Asian HDL in terms of proteome both at baseline and with weight gain, but these differences did not influence South Asian HDL function.

The effect of weight gain and subsequent weight loss on the HDL of healthy, young adult white Europeans was first examined. HDL apoAI and total cholesterol content were not changed by weight gain or weight loss. This was likely a result of the modest, non-pathological weight gain; BMI increased by an average of 1.4 kg/m^2 from baseline which was still well within the healthy BMI range of between 18.5 and 24.9 kg/m^2. This equated to an average 6.4% increase in weight. However, a study of HDL turnover with weight gain (approximately 9.5%) based on a fast-food diet found a significant increase in plasma apoAI post-hyperalimentation (Lindström et al., 2011), at odds with the findings of this chapter. This may be due to the method of weight gain, as the study used high saturated fat fast-food consumption while the GlasVEGAs study used predominantly high sugar snacks. In a study comparing HDL protein and lipids after consumption of both high saturated fat and high carbohydrate test meals, HDL apoAI content increased after a high saturated fat meal but was not altered after a high carbohydrate meal, while HDL total cholesterol content was unchanged (Averill et al., 2020). Both of these studies were much smaller than the present study and included female participants, which limits the ability to relate these studies to the present findings. HDL total protein did not change with weight gain or weight loss, again likely due to the modest changes in body weight in this study. Differences were observed in HDL total protein among the men in the M-FAT study (chapter 7), but the three groups assessed had marked differences in body composition which were not observed in the present chapter. Weight gain did not induce changes in the SAA-1 content of HDL, but

weight loss appeared to reduce HDL SAA-1. One individual increased SAA-1 substantially with weight loss, though there was no technical reason to remove this datapoint. It may be that this individual had underlying immune activity at this visit, increasing the expression of acute phase proteins including SAA-1. The loss of five men to follow up at the weight loss study visit may have reduced the statistical power to detect the reduction in SAA-1 with weight loss.

There were changes in the HDL size distribution with weight gain and weight loss in European men. After weight loss, the proportion of HDL 2b increased back to the pre-weight gain baseline, though the reduction in HDL 2b from baseline was not statistically significant. There was considerable variability in the proportion of HDL 2b at each study visit compared to the more uniform distribution of the other four HDL subclasses. This may reflect the fact that HDL 2b is the most cholesteryl ester laden and is continuously remodelled by lipases and the liver to re-distribute or remove these from the circulation. The proportion of the smallest HDL, HDL 3c, was increased by weight gain, suggesting either increased HDL synthesis by the liver in response to overfeeding, or increased HDL de-lipidation by lipases. Finally, the HDL 2/3 ratio, taking into account all of the HDL subclasses, was increased by weight loss. A longer-term study of lipoprotein subclass distribution found no changes in HDL size after weight loss following a 9-month weight maintenance programme in obese individuals (Lecheminant et al., 2010), while a year-long study of weight loss on HDL size distribution found that the changes in HDL size similar to the present chapter were mediated by metabolic changes outside of weight loss itself (Williams et al., 1992). This may explain the modest differences in HDL size observed in the present chapter.

Proteomic analysis of HDL samples in Europeans found only two proteins with weight loss induced changes, PON-1 and ZAG, perhaps expected given the lack of separation between the study visits in the OPLS-DA model. There were no changes in the LFQ intensity of any apolipoprotein, HDL remodelling protein or immune proteins associated with HDL. The reduction in the protein level of PON-1 is concomitant with the findings of Rector et al., (2007) in adults with characteristics of the metabolic syndrome, and perhaps reflects a reduced need for the antioxidant enzyme with the improved systemic physiology associated with weight loss. ZAG is an adipokine known for its ability to mobilize lipids

directly and by increasing the activity of lipases, as well as its role in adipose tissue browning and relationship to insulin sensitivity (reviewed by Wei et al., (2019)). ZAG stimulated the production of adiponectin by cultured adipocytes but was downregulated with increased total fat mass (Mracek et al., 2010), indicating a role in lipid homeostasis. The increase in ZAG in the HDL of European men post-weight loss suggests a change in energy-balance towards the use of triglyceride and increased turnover of lipoproteins through increased lipase activity. The increase in ZAG therefore demonstrates improved lipid homeostasis with weight loss. In terms of oxidised HDL proteins identified in this analysis, there was a reduction in the oxidation of methionine 172 of apoAI with weight gain, though this appeared to be driven by two individuals with increased oxidation of this residue at baseline. The spread of the data was similar in each group, as was the median LFQ intensity and as such this finding was likely to be a type I error.

Paraoxonase-1 activity was unchanged with weight gain and weight loss, despite the reduction in its protein level on HDL with weight loss. Other than indicating that weight loss itself perhaps increases the activity of the enzyme and therefore reducing the amount of enzyme necessary, the lack of change in activity is likely due to the modest weight gain of this study. Other studies have shown conflicting data on PON-1 activity and body weight, with decreases in PON-1 activity in both overweight and obese individuals (Doğan et al., 2021) and no effect of obesity described by Tabur et al., (2010). The PON-1/SAA-1 ratio was also unchanged by weight gain and weight loss suggesting that the overall functionality of HDL was not affected by this intervention. This finding was confirmed by the assessment of HDL anti-inflammatory function in endothelial cells. Whether corrected for HDL cholesterol content or HDL protein content, the ability of HDL to inhibit TNFα induced adhesion molecule expression was unchanged by weight gain or weight loss. A study with 3.2% weight loss in obese men found that HDL better prevented monocyte chemotactic activity, suggesting an improvement in HDL anti-inflammatory with weight loss when the baseline is pathological obesity (Roberts et al., 2006).

To summarise the findings in European men, HDL composition and function was preserved with weight gain and not improved by weight loss. The size and

proteomic changes in HDL were likely a response to shifting metabolic demands with the modest weight gain and weight loss observed in this study. It may be that for changes in HDL composition and function to occur in European men, a much greater weight gain and more dramatic weight loss is required.

In contrast to the European cohort, South Asians were markedly more insulin resistant after weight gain and their fasting insulin greatly increased despite a similar level of weight gain. South Asian HDL apoAI, total cholesterol, total protein and SAA-1 content were all unchanged compared to white European HDL at baseline and with weight gain. This matches the findings of Bakker et al., (2016), who found no differences in HDL composition between Europeans and South Asians both young and middle-aged by nuclear magnetic resonance spectrometry. However, unlike this published study, the present chapter found marked differences in HDL protein composition between Europeans and South Asians, both by ethnicity irrespective of weight gain and where South Asians responded differently to weight gain.

OPLS-DA models comparing Europeans and South Asians at baseline and after weight gain showed clear separation between the ethnicities and suggested that HDL proteins contributed significantly to the observed separation alongside demographic measures. Four apolipoproteins were significantly different between Europeans and South Asians. Irrespective of weight gain, South Asians had increased HDL apoAIV, perhaps suggesting an altered response to dietary fat intake. ApoAIV production is increased in the intestine in response to the ingestion of fat which implies that South Asians are hyper-responsive in this regard. ApoAIV transfers to HDL through interaction with chylomicron remnants, so increased apoAIV on HDL could be indicating increased chylomicron lipolysis. ApoAIV increases the activity of CETP similarly to ApoAI (Main et al., 1996) which may indicate that South Asians have increased remodelling and turnover of HDL. There is evidence that apoAIV increases insulin secretion by pancreatic ß-cells (Wang et al., 2012) in response to glucose; South Asians are known to be predisposed to insulin resistance and the increase in HDL apoAIV may be a compensatory mechanism to maintain glucose homeostasis. The LPL inhibitor apoCIII was increased in European HDL but reduced in South Asian HDL with weight gain. ApoCIII is active in inhibiting lipoprotein and hepatic lipase when on

triglyceride-rich lipoproteins like chylomicrons, VLDL and LDL, with HDL acting as a reservoir and distributor of apoCIII among lipoproteins (reviewed by Chan et al., (2008)). This finding suggests that with weight gain in Europeans apoCIII is sequestered on HDL to increase the activity of LPL and HL, therefore maintaining plasma triglyceride processing in response to increased dietary lipid. In South Asians this fails to happen; weight gain decreased HDL apoCIII, suggesting lipase activity is decreased therefore increasing retention of triglyceride-rich lipoproteins in plasma. The change in apoCIII with weight gain negatively correlated with the change in liver fat fraction, which implies that excess triglyceride in South Asians is deposited in the liver as a compensatory mechanism, despite the young age and good health of these participants. The antioxidant apoD was increased after weight gain in South Asian HDL, which may be a protective response given the increased oxidative stress in this group at lower blood glucose levels and younger age than comparable Europeans (Brady et al., 2012). There is evidence in mouse models that overexpression of apoD increases hepatic triglyceride storage without consequence on plasma triglyceride levels (Sanchez and Ganfornina, 2021), though these findings have not been investigated in human subjects. There was no correlation between apoD and liver fat fraction in the present study. Finally, HDL apoF tended to decrease in European HDL but increase in South Asian HDL with weight gain. This may be a similar phenomenon as was seen in the IGR group of the M-FAT study (section 7.3.6), where decreased HDL apoF implies increased LDL apoF where it inhibits CETP and increases hepatic LDL uptake to counteract rising plasma triglycerides. It appears that this protective mechanism does not occur in South Asians where HDL CETP also increases with weight gain. HDL lipid composition was not performed in this study, but it may be expected that the weight gain increase in CETP may enrich HDL with triglyceride as a pathogenic compensatory response to rising plasma triglycerides. Taken together, these changes in HDL apolipoproteins and remodelling proteins may reflect altered lipoprotein metabolism in South Asians that contributes to the observation that at a lower BMI, South Asians have increased ectopic liver fat compared to Europeans (Iliodromiti et al., 2023). This altered lipoprotein metabolism may contribute to the overall predisposition of South Asians to develop T2DM, particularly as it has been observed in young and healthy men with a mean 1.5 kg/m^2 increase in BMI.

The proposed mechanism of altered lipoprotein metabolism in Europeans and South Asians is summarised in figures 8-27 and 8-28 respectively.

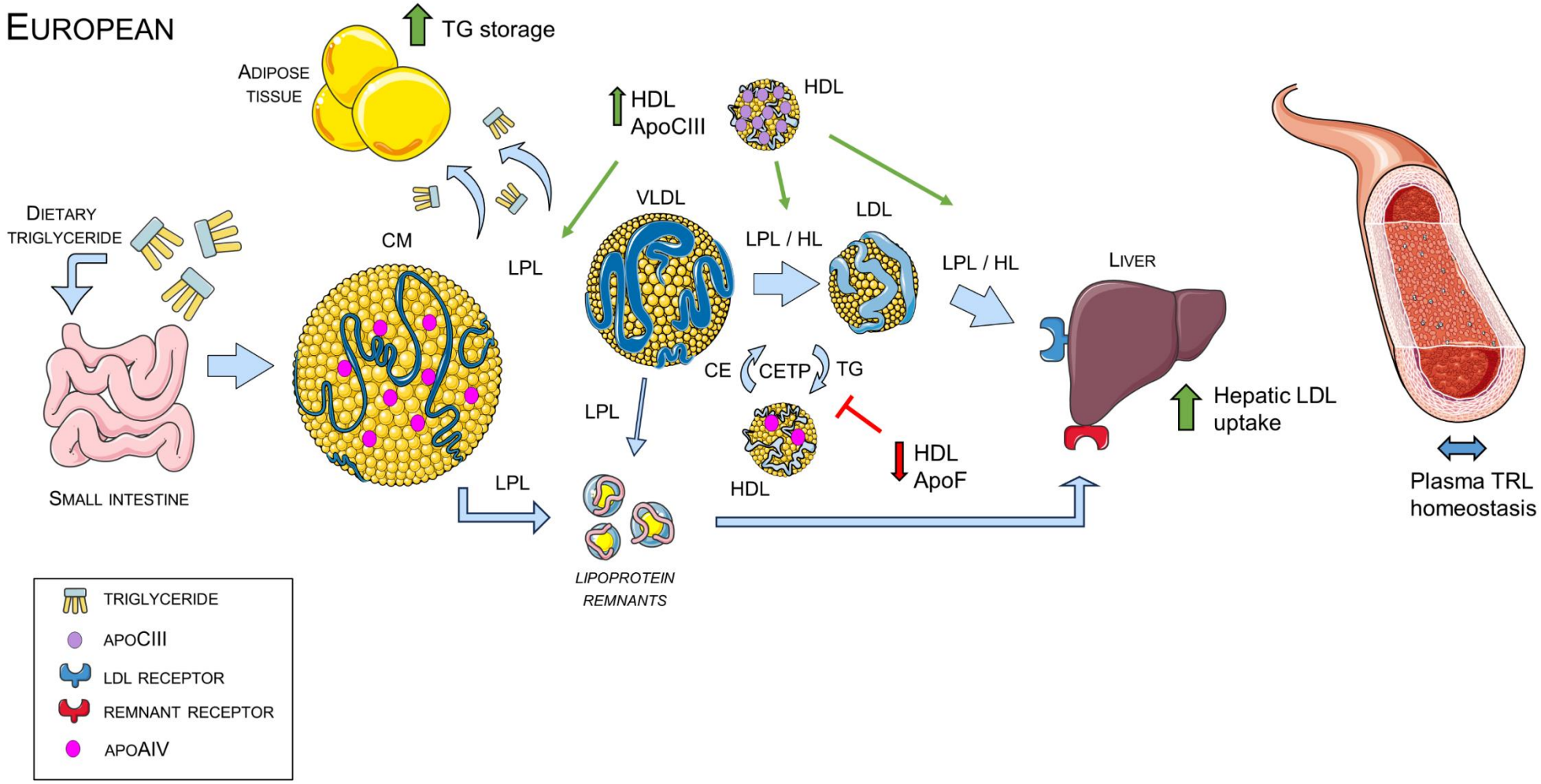

Figure 8-27 Proposed mechanism of triglyceride handling after weight gain in Europeans After weight gain in Europeans, increased HDL apoCIII leads to increased lipase activity while decreased HDL apoF and apoAIV results in the inhibition of CETP. ApoAIV, apolipoprotein AIV; ApoCIII, apolipoprotein CIII; ApoF, apolipoprotein F; CM, chylomicron; LPL, lipoprotein lipase; VLDL, very low-density lipoprotein; HL, hepatic lipase; CE, cholesteryl ester; CETP, cholesteryl ester transfer protein; HDL, high-density lipoprotein; low-density lipoprotein; TG, triglyceride; TRL, triglyceride-rich lipoprotein.

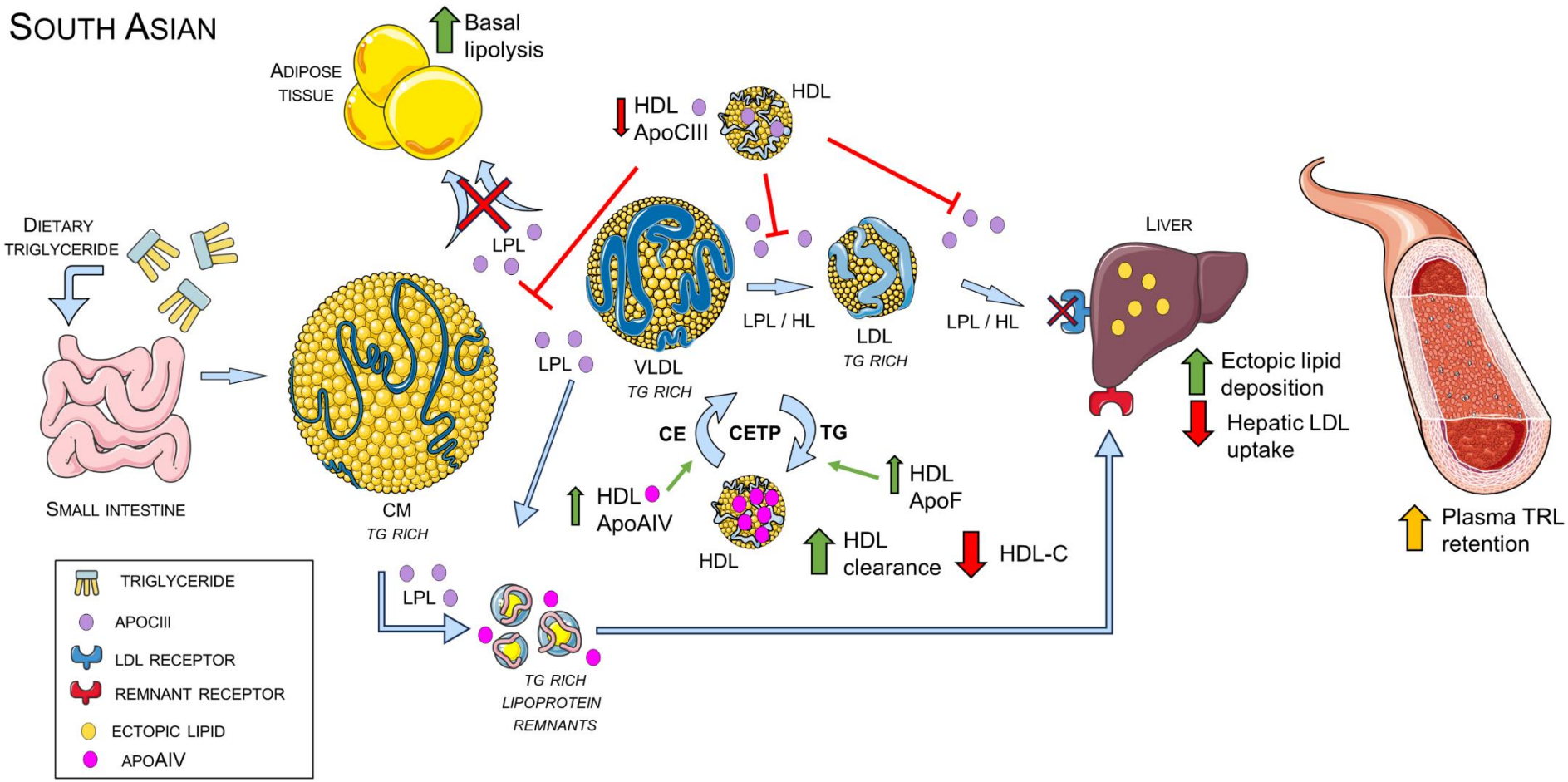

Figure 8-28 Proposed mechanism of triglyceride handling after weight gain in South Asians In South Asians, weight gain decreases HDL apoCIII resulting in reduced lipase activity. Reduced lipase activity results in the formation of triglyceride rich remnants which are taken up by the liver. Increased CETP activity due to increased HDL apoAIV and apoF results in triglyceride enriched HDL and reduced hepatic LDL uptake. Taken together these changes result in increased plasma triglyceride-rich lipoprotein retention, which when coupled with increased basal adipocyte lipolysis results in hepatic fat deposition. ApoAIV, apolipoprotein AIV; ApoCIII, apolipoprotein CIII; ApoF, apolipoprotein F; CM, chylomicron; LPL, lipoprotein lipase; VLDL, very low-density lipoprotein; HL, hepatic lipase; CE, cholesteryl ester; CETP, cholesteryl ester transfer protein; HDL, high-density lipoprotein; low-density lipoprotein; TG, triglyceride; TRL, triglyceride-rich lipoprotein.

The five immune related proteins identified on HDL were all higher in South Asians compared to Europeans irrespective of weight loss, suggesting that South Asians have an increased immune response. Non-diabetic, healthy adult South Asians have increased plasma levels of complement C3 (Siezenga et al., 2009) and C-reactive protein (Chambers et al., 2001) compared to European counterparts. As these two acute-phase reactants are increased in South Asians, it can be inferred that the increase in inflammatory proteins on HDL is a function of the systemic increase in the plasma concentration of these proteins. The adipokines RBP4 and ZAG were both higher in South Asian HDL. RBP4 is increased with insulin resistance (Klöting et al., 2007); it increases adipocyte basal lipolysis and reduces the ability of insulin to suppress lipolysis (which also leads to ectopic liver fat accumulation) and has been implicated in immune stimulation (Kilicarslan et al., 2020). The higher RBP4 in South Asian HDL corroborates the fact that South Asians are more predisposed to insulin resistance and may contribute to this phenotype (Mukhopadhyay et al., 2006). The inflammatory nature of RBP4 may also partly explain the increased immune-related proteins on HDL; RBP4 treated macrophages secrete more TNFα, which in turn increases acute phase protein synthesis (Kilicarslan et al., 2020). The higher ZAG on South Asian HDL may be a compensatory response to counteract the negative effects of RBP4 and adverse lipoprotein metabolism indicated by the altered apolipoprotein make-up of South Asian HDL.

There were six further proteins with differences between European and South Asian men. PON-1 protein levels were not different between European and South Asian HDL irrespective of weight gain, matching the findings of Connelly et al., (2012) in renal transplant patients. Alpha-1B-glycoprotein was increased in young people with type 1 diabetes mellitus, but its function is not yet fully understood (Gourgari et al., 2019) which makes its higher abundance in South Asian HDL difficult to interpret. Carbonic anhydrase was more abundant on South Asian HDL compared to European HDL. This enzyme is postulated to influence insulin secretion by ß-cells by manipulating intracellular pH (Baldini and Avnet, 2019), perhaps contributing to the substantial increase in fasting insulin in South Asians post weight gain. Pigment-epithelium derived factor is highly expressed in the liver and was shown in animal models to protect from steatosis (reviewed by Huang et al., (2018)); the decrease in the abundance of

PEDF after weight gain in South Asian HDL may be a factor in the increased insulin resistance and ectopic liver fat accumulation seen in this group. Finally, protein AMBP (the precursor to alpha-1-microglobulin and bikunin) and vitronectin were more abundant in South Asian HDL compared to European HDL. Each of these proteins are involved in inflammation (Schvartz et al., 1999; Akerstrom et al., 2000; Fries and Blom, 2000) and likely reflect the systemically increased inflammation in South Asians.

Whether corrected for HDL protein or HDL cholesterol content, PON-1 arylesterase activity did not differ by ethnicity or by weight gain which concurs with the findings of Connelly et al., (2012), with the ratio of PON-1 activity to SAA-1 content also unchanged in this context. This suggests that HDL functionality was not different between Europeans and South Asians and that weight gain did not impact HDL function differently in the two ethnicities. This was confirmed by the lack of differences in the anti-inflammatory activity of HDL on endothelial cells between the ethnicities, whether based on HDL apoAI or corrected for total protein or total cholesterol, despite the differences in HDL protein composition as assessed by proteomic analysis. This confirms the findings of Bakker et al., (2016) in a group of subjects of the same age as recruited in the GlasVEGAs study. Much like this published study, the present chapter did not find ethnicity differences in HDL subclass distribution, only a reduction in HDL 2b and HDL 2/3 ratio with weight gain irrespective of ethnicity. There was an altered response of HDL 2a to weight gain by ethnicity, where HDL 2a tended to increase with weight gain in South Asians, but in terms of proportion of total HDL this was a small shift and likely represents an increase in HDL 2a as a result of reduction in HDL 2b. Given the increase in CETP with weight gain in South Asian HDL, it was expected that HDL size would decrease more than European HDL as a result of increased triglyceride transfer to HDL, followed by HDL shrinkage due to lipase activity (Brinton et al., 1994). The lack of change in HDL size may be due to the increased inhibition of HL by apoCIII in South Asians.

To summarise the findings when comparing European and South Asian HDL and their respective responses to weight gain, the core measures of HDL composition were not different between the two ethnicities. Protein composition of HDL differed by ethnicity and in response to weight gain, particularly in proteins

related to lipid metabolism, but HDL function was unchanged between the two ethnicities. This suggests that HDL may be a marker of impaired lipid metabolism in South Asians, despite the modest weight gain and young age of the participants.

The primary strength of this study was the repeated measures design, allowing each individual to be their own control, adding statistical power to detect changes in the variables measured. Acute effects of altered diet or exercise on HDL was accounted for by an energy neutral diet for three days prior to each visit. However, the GlasVEGAs study was powered based on a one standard deviation difference between the groups. This is a large difference, which may have masked subtle HDL differences due to the study population being too small. Many of the published studies cited in this chapter describe overweight or obese study groups, while even after weight gain the participants in the GlasVEGAs study were still of a healthy weight. It may be that the weight gain was insufficient to reveal changes in HDL function or size, though changes in HDL protein composition were readily detected. It would be unethical to induce more serious weight gain in young healthy men, especially in the South Asian cohort who are particularly susceptible to weight gain induced complications. Cholesterol efflux capacity of HDL and measurement of the other plasma lipoproteins was not performed in this study and so the association of the lipoprotein metabolism associated proteins on HDL with its efflux capacity and the consequences on other lipoproteins was not possible.

In conclusion, this chapter revealed that moderate weight gain and weight loss was all but inconsequential to European HDL composition and function, with the minor changes in two proteins and weight gain induced changes in HDL size reflecting a physiological adjustment in metabolic demand. HDL protein composition differed between European and South Asian HDL without changes in HDL function, suggesting that HDL acts as a marker of aberrant lipoprotein metabolism and triglyceride handling in South Asians and offering a potential mechanism explaining the increased ectopic liver fat observed in this ethnicity. These changes occurred in young, healthy men with an average 1.5 unit increase in BMI, providing some context to the vastly different age and BMI of onset of type 2 diabetes mellitus and the increased cardiometabolic risk in South Asians.

Future studies might focus on specific interactions between the different lipoproteins and the liver in a similar cohort, such as by using stable isotope-labelled fatty acids (in a similar manner to (Green et al., 2022)). Including female Europeans and South Asians may reveal sex and ethnicity dependent differences in the HDL response to weight gain.

9 General Discussion

The incidence of obesity, its comorbidities and consequences has been rapidly increasing throughout the world, particularly in Western countries and South Asia (Blüher, 2019). Concomitant with the increased prevalence of obesity is a marked increase in the prevalence of insulin resistance and T2DM (Danaei et al., 2011), which has a myriad of metabolic and vascular consequences ultimately accruing to CVD risk. It has long been established that HDL-C is an inverse predictor of CVD risk (Gordon, William P. Castelli, et al., 1977), and that T2DM is associated with reduced HDL-C (Lopes-Virella et al., 1977). Pharmacological interventions to increase HDL-C failed to decrease CVD risk, thus moving focus towards HDL functions on the vasculature. I therefore hypothesised that HDL composition and function is improved with insulin sensitivity and worsened with insulin resistance. In this context, this thesis had two major aims; to establish the effects of insulin sensitive and insulin resistant conditions on HDL composition and function, and to test whether HDL composition and function is changed under conditions where insulin resistance is ameliorated by diet/exercise or worsened by weight gain. These aims were met using a number of cross-sectional and longitudinal archival studies encompassing a broad range of insulin resistance.

Contrary to my initial hypothesis, it appeared that HDL composition was not modified by insulin resistance *per se* but was a reflection of systemic physiology, whether healthy or pathological. HDL could be described as a scavenger; its primary purpose is the scavenging of excess peripheral cholesterol for recycling or removal. HDL is therefore in contact with a variety of tissues, cell types and plasma proteins, which likely leads to HDL picking up new components reflective of its current environment. In the same manner, HDL is in contact with other lipoproteins and their remnants, altering HDL protein and lipid composition and therefore also acting as a marker of metabolic function with respect to the lipoprotein cascade. In terms of HDL composition, this thesis focussed on three major conditions of altered insulin resistance: pregnancy and its complications, middle-aged men with varying degrees of insulin resistance, and young healthy men of two different ethnicities with known differences in metabolic disease risk. A summary of the findings in each grouping can be found in figure 9-1.

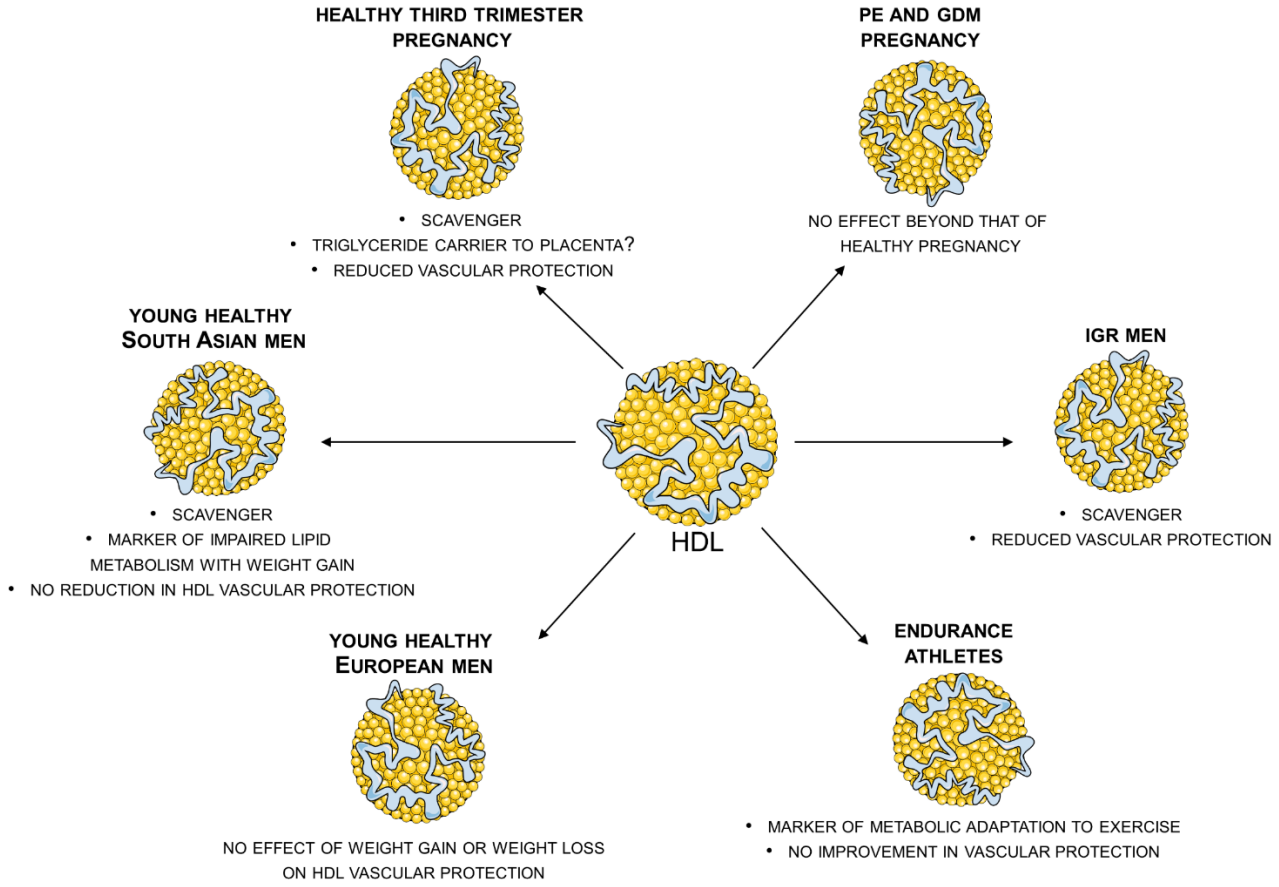

Figure 9-1 Summary of the role of HDL in the groups studied in this thesis. Clockwise from top-left: in healthy third trimester pregnancy, HDL scavenges plasma proteins and triglycerides. HDL may scavenge triglyceride for subsequent delivery to the placenta. HDL vascular function was decreased in third trimester pregnancy, and pregnancy complications did not have an effect on HDL beyond that of healthy pregnancy. HDL also acts as a scavenger in IGR men and like in pregnancy resulted in reduced HDL vascular functions. There was not an improvement in HDL vascular function in endurance athletes though HDL composition reflected the metabolic adaptation to exercise. In young healthy European men, weight gain and weight loss had no impact upon HDL vascular function. In South Asians, HDL composition suggests HDL is a scavenger in this group. Weight gain did not reduce HDL vascular function in South Asians, though did alter HDL composition to reflect impaired lipid metabolism. PE, preeclampsia; GDM, gestational diabetes mellitus; IGR, impaired glucose regulation.

Pregnancy is characterised by inflammation and an altered metabolic environment (Sulaiman et al., 2016). HDL composition was not different between healthy pregnancy and those complicated by GDM despite previous work in this laboratory demonstrating a number of alterations in HDL composition through healthy gestation, predominantly in proteins linked to immunity, coagulation and lipid handling (Patanapirunhakit, 2023). This suggests that GDM does not alter HDL composition any more than the background supraphysiological changes that occur in late healthy gestation. Women who develop GDM have almost 10 times the risk of developing type 2 diabetes mellitus later in life (Vounzoulaki et al., 2020), suggesting that GDM is a window into future metabolic health, though it appears that HDL is not involved in this additional risk. In the previous work, HDL composition returned to the pre-pregnant baseline in all measures by 13-weeks post-partum (Patanapirunhakit, 2023). It might be the case that there is a difference in HDL composition following GDM pregnancy due to a lack of HDL recovery, though this was not measured in this cross-sectional study. Pregnancy is a relatively short-term condition at 40 weeks; these findings demonstrate that changes in HDL composition occur quickly with altered physiology. In late healthy pregnancy, HDL anti-inflammatory function decreased, with no effect of preeclampsia or GDM on HDL anti-inflammatory function compared to healthy pregnancy.

There were a number of changes in HDL composition observed in the male groups studied in this thesis. The cross-sectional M-FAT study discussed in chapter 7 contained the most phenotypically distinct groups, including insulin sensitive endurance athletes through to insulin resistant IGR men. HDL apoAI was lowest in the IGR men, possibly due to the acute-phase reactant SAA-1 replacing apoAI (Miida et al., 1999). Inflammation is known to contribute to insulin resistance (as reviewed by Lumeng and Saltiel, (2011)). Of the nine proteins identified on HDL with significant differences between the study groups, five were more abundant on IGR HDL and were involved in immunity, inflammation and coagulation. This suggests that in these pre-diabetic men HDL is mirroring the inflammatory environment in which it exists. On the other hand, HDL apoAI and cholesterol content were highest in the endurance athletes, likely part of the metabolic adaption required for exercise given the antioxidant and cholesterol efflux properties of apoAI. Two of the nine aforementioned proteins,

apoD and transthyretin, were more abundant on athlete HDL compared to control. Exercise initially increases oxidative stress, however conditioned athletes such as those participating in the M-FAT study adapt to an antioxidant phenotype (Radak et al., 2008). The higher apoD and uniformity of apoAII abundance observed on athlete HDL likely reflects this adaptation, while higher transthyretin abundance in endurance athlete HDL likely reflects an exercise-induced increase in its substrate thyroxine (Refsum and Strömme, 1979). Interestingly, despite the much higher fasting and 2-hour fasting glucose concentration in IGR men, glycation and methionine oxidation of HDL apoAI was higher in endurance athletes, perhaps a consequence of the increased metabolic demands of exercise. The effect of these post-translational modifications of HDL proteins in athletes is unclear, though the literature suggests that these may be protective of muscle during exercise (Riechman et al., 2009; Shao, 2012). HDL PON-1 activity was reduced in IGR men, as was HDL anti-inflammatory function. There was no improvement in either measure of HDL function in endurance athletes.

Further evidence of HDL composition reflecting systemic physiology can be found in the GlasVEGAs study discussed in chapter 8, which compared young healthy Europeans and South Asians after weight gain and weight loss. In the European cohort, weight loss was associated with a reduction in HDL PON-1 abundance and an increase in ZAG abundance, possibly reflecting improved oxidation status and lipid mobilisation with weight loss. When comparing European and South Asian HDL, major differences in HDL protein composition were observed. Five proteins which were related to inflammation and immunity and two adipokines were more abundant on South Asian HDL. Crucially, these differences were ethnicity driven, not induced by weight gain and its concomitant increase in insulin resistance observed in South Asians, perhaps implicating genetic factors leading to their eventual detection on HDL. Previous work in this laboratory found a number of differences in gene expression in the adipose tissue of this cohort of men, where the South Asians had higher expression of inflammatory genes such as TNFα and a lower expression of genes related to lipid turnover compared to their European counterparts (Gao, 2023). However, a genome-wide association study (GWAS) found that 95 genetic loci associated with clinical lipids did not differ by ethnicity between Europeans and South Asians (Teslovich et al., 2010),

though this was a cross-sectional GWAS which did not include any intervention that may alter blood lipids. Three apolipoproteins related to lipid handling through the lipoprotein cascade were different between Europeans and South Asians; apoAIV was higher in South Asian HDL irrespective of weight gain while apoCIII decreased and apoF increased on South Asian HDL after weight gain. Given the changes in genes related to lipid turnover observed by Gao (2023), it is likely that there is some genetic determination of aberrant lipid handling in South Asians, though it is unclear how this might be related to CVD risk or treatment. A Mendelian randomisation study found that though a single nucleotide polymorphism in the *APOCIII* gene associated with increased plasma triglycerides increased the risk of coronary artery disease in Indians by 3 %, loss of function mutations in the same gene that reduced plasma triglyceride concentration by 39 % did not reduce the risk of CVD in Indians but did so in Europeans (Goyal et al., 2021). There were no differences in post-translational modification of HDL proteins between Europeans and South Asians or with weight gain, despite the oxidative and glycation stresses associated with increasing insulin resistance. HDL antioxidant and anti-inflammatory function was not affected by weight gain or by ethnicity. In summary, the findings of this thesis suggest that HDL composition is a function of systemic physiology. Measurement of the lipoprotein cascade is challenging given it is in constant flux depending on energy balance and fed/fasting state. The changes observed in HDL apolipoproteins may act as an integrative marker of the functioning of the lipoprotein cascade, given HDL interactions with the other lipoproteins, the liver and adipose tissue.

HDL vascular protective function also appears to be dependent on systemic physiology possibly via changes in HDL composition. Where HDL contained coagulation and immunity related proteins, as was the case in IGR men and late pregnancy, HDL vascular function was decreased. However, it appears that there was a ceiling of HDL vascular function where improvement in general health and fitness did not necessarily lead to an improvement in already-healthy individuals. This is supported by the observation in chapter 7 that only IGR men exhibited lower HDL antioxidant function based on PON-1 activity, while endurance athletes did not differ from healthy controls. Weight loss also did not improve HDL antioxidant function in healthy young men after modest weight

gain, though this may not be the case in those already overweight or obese and insulin resistant. Healthy gestation and preeclampsia did not alter PON-1 activity (Patanapirunhakit, 2023), and as such it is perhaps unsurprising that GDM pregnancy also did not impact upon HDL antioxidant function. Interestingly, with the exception of 16 weeks of healthy gestation, HDL vascular anti-inflammatory function is maintained at the same dose of apoAI, even in IGR men. However, as the number of apoAI molecules per HDL particle is highly heterogenous and may differ both within and between individuals, this may have resulted in cells being exposed to larger amounts of HDL cholesterol and protein. Correction for HDL cholesterol content therefore facilitated a whole particle measurement of HDL anti-inflammatory function, while correction for HDL protein accounted for all HDL proteins rather than solely apoAI. When corrected for HDL cholesterol and protein content, this thesis found that late pregnancy and IGR had decreased HDL anti-inflammatory function, perhaps due to the presence of larger immune and coagulation-related proteins interfering with the binding of apoAI and other vasoactive agents, such as S1P, to their receptor targets. However, in endurance athletes and in young Europeans and South Asians, HDL anti-inflammatory function was not improved compared to their relevant controls.

In endurance athletes, alterations in the protein composition of HDL were few in number, with two apolipoproteins with antioxidant functions normally present on healthy HDL more abundant in this group. Like HDL from the IGR men in chapter 7, HDL from the young South Asians in chapter 8 did have a greater abundance of immune and coagulation related proteins compared to European HDL, though in these individuals there was no impact on HDL vascular function. It may be that as South Asians age their HDL accumulates more of these proteins and a reduction in HDL anti-inflammatory function may then be observed, or that there are alterations in endothelial physiology in middle-aged IGR men not yet apparent in the healthy young individuals.

While lifestyle interventions improve HDL vascular function in those with existing cardiovascular or metabolic disease (reviewed by Ruiz-Ramie et al., (2019)), this thesis suggests that there is a natural upper limit to HDL vascular anti-inflammatory function. It also suggests there is no effect of HDL composition on anti-inflammatory function in healthy individuals. It may be that there are

differences in endothelial expression of HDL receptors or modified intra-cellular signalling that alter the response to HDL in IGR and late pregnancy, though this was not explored in this thesis. It is likely the case that other functions of HDL, such as reverse cholesterol transport and lipid transfers, are more important to HDL-mediated vascular protection particularly in light of the changes in lipid handling apolipoproteins observed in this thesis. This may particularly be the case in situations where HDL vascular anti-inflammatory function was expected to improve but did not, as was the case with endurance athletes; their HDL had more abundant apoAII, which is known to enhance ABCA1 mediated cholesterol efflux (Melchior et al., 2017), and more of the thyroid hormone transporter transthyretin. Thyroid hormones have beneficial effects on hepatic lipid metabolism and increase the expression of SRB1, required for cholesterol efflux to HDL from peripheral cells (reviewed by Sinha et al (2018)).

There were some limitations to this exploration of HDL composition and function. This thesis focussed on HDL protein composition, given the wide variety of functions HDL-associated proteins have been shown to confer (Beazer et al., 2020). The label-free quantitation method used to interpret the nLC-MS/MS spectra results in relative values, calculated based upon the abundance of every protein identified in all samples in a given mass-spectrometry run. The nature of this technique means that more highly abundant proteins can obscure less abundant proteins. This can particularly affect HDL proteomics given that apoAI accounts for the overwhelming majority of HDL protein content, followed by apoAII. Less abundant proteins may have been assigned an LFQ intensity of zero; this does not necessarily mean that the protein was not detected but that its abundance was relatively low. This may have limited the power to detect differences in the abundance of rarer proteins. The isolation of HDL using methods based on density has the drawback of potentially co-isolating contaminating plasma extracellular vesicles (EVs, reviewed Beazer et al (2020)). EVs are endocytosed from cells and carry a cargo of lipids, proteins and ribonucleic acid (RNA) to facilitate cell-cell communication. It may be that some of the proteins detected in this study are EV-associated rather than HDL associated. Patanapirunhakit (2023) performed a pilot assessment of the impact of EVs on HDL protein composition and found considerable overlap in the proteins detected. However, as summarised by Beazer et al., (2020), sequential

density ultracentrifugation remains the gold standard technique to isolate HDL for compositional and functional analyses. Ultracentrifugation can dislodge loosely associated HDL proteins (Melchior, Street, et al., 2021), which may mean that the HDL particles used to stimulate endothelial cells *in vitro* were not wholly reflective of the particle *in vivo*, with the underestimation of impaired or improved HDL function a potential consequence.

HDL is also made up of a number of lipid species not measured in this work, including phospholipids, sphingomyelin and its metabolites including ceramides and fatty acids, all of which have effects on a host of vascular functions (Kajani et al., 2018). HDL lipids also impact upon HDL morphology, affecting HDL size and the ability of HDL components to interact with remodelling enzymes like CETP and LCAT and with the vascular endothelial surface (Malajczuk and Mancera, 2023). There were not however major changes in HDL size distribution between the study groups assessed or in anti-inflammatory function outside of IGR men and late pregnancy on a whole particle basis, perhaps suggesting that these remodelling enzymes are not at play. A GWAS found a number of genetic loci associated with the blood lipidome in a population of Pakistanis but not in Europeans, including two loci associated with sphingomyelin synthesis and loci associated with LPL, HL and their regulation by angiopoietin-like proteins (Harshfield et al., 2021), suggesting that an exploration of HDL and broader lipoprotein lipid composition is warranted in these ethnic groups. The HDL samples used in this thesis were sent to collaborators in the Netherlands for sphingolipid analyses, however the data was not available in time for inclusion in this thesis. In healthy late gestation, there was an increase in HDL long-chain ceramides (Patanapirunhakit, 2023), though it is unclear whether this was related to an adaptation for delivery or to the characteristic late pregnancy insulin resistance. It may be the case that changes in the lipid composition of HDL may be linked to the proposed scavenger function of HDL.

There are a number of other functions of HDL protective of the vasculature that were not measured in this study. The primary function of HDL is reverse cholesterol transport, which can be measured in cholesterol efflux assays using labelled cholesterol loaded macrophages or apoB containing lipoproteins. HDL cholesterol efflux capacity is an inverse predictor of cardiovascular disease

independent of HDL-C (Rohatgi et al., 2014). It might be the case that the larger HDL observed in late gestation and in athletes is related to improved cholesterol efflux capacity. HDL antioxidant function was assessed by PON-1 activity assay, though PON-1 exerts its effects predominantly in the interstitial spaces (Mackness et al., 1997) which may limit the utility of plasma HDL PON-1 activity measures. HDL apoAI and apoD also have antioxidant effects, as do HDL neutral lipids, which were not assessed in the PON-1 activity assay. It may therefore be useful to measure the antioxidant function of the whole HDL particle, for example by monitoring HDL inhibition of the formation of conjugated dienes in LDL induced by copper sulphate (De Juan-Franco et al., 2009). It is unclear whether or not HDL has a role in coagulation or is a bystander, given the detection of proteins involved in this pathway on HDL. Previous work in this laboratory attempted to develop an assay of HDL anti-thrombotic activity based on pro-thrombin generation, though this proved challenging due to the salt content of the HDL isolation buffers (Patanapirunhakit, 2023).

Increasingly genetic techniques including GWAS and Mendelian randomisation studies have been used to interrogate the relationship between HDL and cardiovascular disease risk. These approaches are particularly pertinent given the lack of improvement in cardiovascular risk after pharmacologically raising HDL-C. There is a general consensus that genes linked to HDL concentrations are not associated with adverse cardiovascular outcomes nor are causal in clinical manifestations of CVD, perhaps explaining the failure of HDL-C raising therapy to improve cardiovascular risk (White et al., 2016; Vitali et al., 2017; Richardson et al., 2020; Kjeldsen et al., 2022). The limited differences observed in HDL function despite changes in HDL protein composition in this thesis may reflect this emergent consensus. Vitali et al., (2017) argue that as a static marker of an everchanging metabolic environment, HDL-C is not likely to be causally protective against cardiovascular disease; this thesis argues that HDL protein composition may instead be a marker of said metabolic environment. When corrected for apoB-containing lipoproteins, the effect estimates of HDL-C and apoAI on CVD development were drastically reduced to non-significance (Richardson et al., 2020), suggesting that apoB-containing lipoproteins have a more important role in CVD risk than HDL. The present study observed that a number of HDL proteins were likely derived from interactions with apoB-

containing lipoproteins and their remnants, lending further weight to the concept of HDL as a bystander merely reflecting wider lipoprotein metabolism.

One explanation for the predictive nature of low HDL-C for CVD risk could be attributed to the intrinsic inverse relationship between HDL-C and the plasma concentrations of apoB-containing lipoproteins (Kjeldsen et al., 2022). Increased plasma apoB-containing lipoproteins, and therefore elevated triglycerides, result in an increased concentration of triglyceride-rich lipoprotein remnants due to competition for hydrolysis by LPL. Through the actions of CETP, triglyceride derived from the remnant pool is exchanged for HDL cholesteryl ester, resulting in smaller, denser HDL readily hydrolysed and cleared by hepatic lipase, thus increasing plasma HDL turnover and ultimately reducing HDL concentration. The Diabetes Remission Clinical Trial performed at the Universities of Glasgow and Newcastle investigated whether weight loss through a low energy diet in T2DM patients could lead to remission of T2DM (Lean et al., 2018). After two years of follow up, hepatic VLDL production and plasma VLDL triglycerides were reduced compared to baseline, while HDL-C increased to a similar level to non-T2DM controls (Al-Mrabeh et al., 2020), lending further credence to the importance of plasma triglycerides on HDL concentration. A comprehensive analysis of both HDL protein and lipid composition, particularly HDL triglyceride content, and functions in a similar cohort may corroborate the findings of the present thesis.

It has been hypothesised that the increase in plasma HDL-C observed during pregnancy, particularly at the establishment of the placental circulation, is of improved function (Sulaiman et al., 2016). This thesis showed that, instead, HDL vascular protective function is diminished in pregnancy, following on from previous work in this laboratory which found an increase in lipid-handling, coagulation and immunity related proteins on HDL (Patanapirunhakit, 2023). Revisiting that hypothesis in light of the present findings and the relationship between HDL-C and triglyceride suggests that rather than having improved function, the newly synthesised HDL may contribute to a larger HDL pool which provides a reservoir of plasma triglycerides in late pregnancy available for placental transfer. Figure 9-2 plots both maternal plasma HDL-C and triglycerides through pregnancy on the same axes (Sulaiman et al., 2016).

The peak in HDL-C at 20 weeks of gestation is timed as triglycerides begin to rise, before a plateau during the peak of triglyceride concentration. HDL-C does not begin to decrease until 10 weeks post-partum, after the nadir in plasma triglyceride. Together with the pregnancy-associated decrease in hepatic lipase activity (Sattar et al., 1997), HDL as a triglyceride reservoir may protect from the deposition of excess hepatic fat and the associated maternal risks (including acute fatty liver of pregnancy, preeclampsia and haemolysis, elevated liver enzymes and low platelets (HELLP) syndrome (Nelson et al., 2021)) while maintaining plasma triglyceride availability for placental transfer. An analysis of HDL lipids in the same cohort found HDL triglyceride content increases through gestation while HDL total cholesterol content decreases (Zamai et al., 2020), corroborating this new hypothesis.

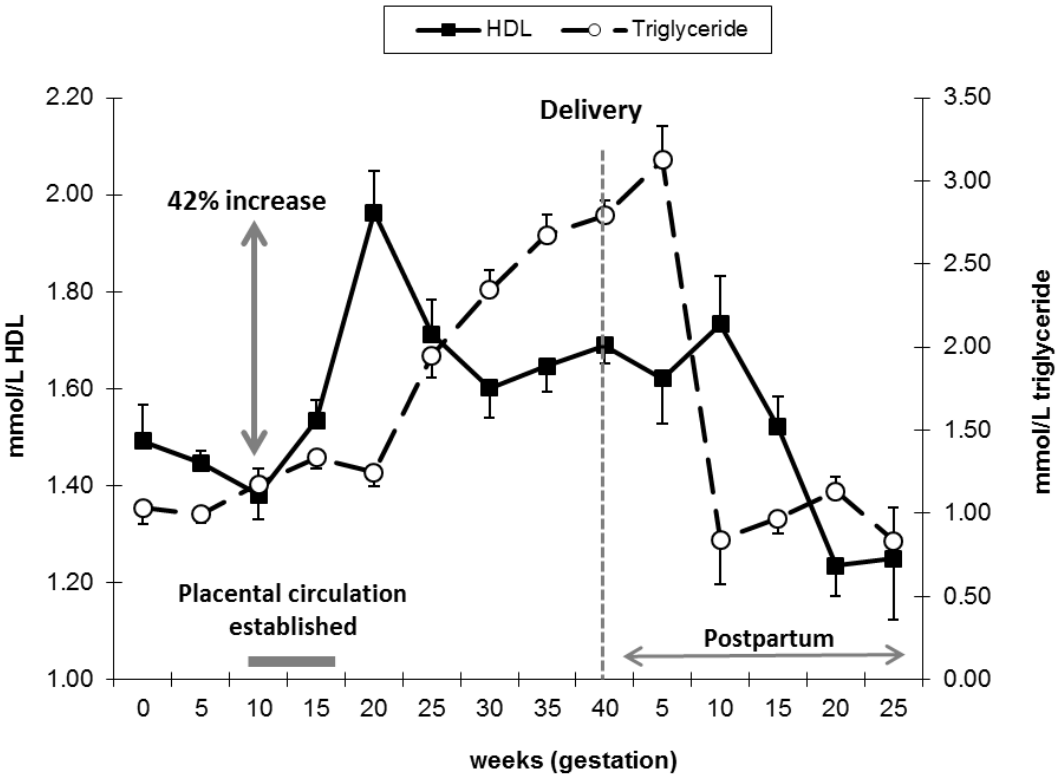

Figure 9-2 Maternal plasma HDL-cholesterol and plasma triacylglycerol concentrations during pregnancy and post-partum. Data from a series of overlapping longitudinal and cross-sectional studies carried out in our laboratory. Lipid measurements were carried out in the Department of Vascular Biochemistry of the University of Glasgow, a Centre for Disease Control (CDC) UK laboratory for the Lipid Standardization Programme (cholesterol, triacylglycerol, HDL-cholesterol) and the CDC Reference Laboratory for cholesterol and HDL-cholesterol, thus lipid measurements are standardized over time. Reproduced with permission of Portland Press, Ltd. from Wan N. Wan Sulaiman, Muriel J. Caslake, Christian Delles, Helen Karlsson, Monique T. Mulder, Delyth Graham, Dilys J. Freeman; Does high-density lipoprotein protect vascular function in healthy pregnancy?. Clin Sci (Lond) 1 April 2016; 130 (7): 491–497; permission conveyed through Copyright Clearance Center, Inc.

This observation that HDL composition reflects systemic and metabolic physiology with limited changes in antioxidant and anti-inflammatory function has implications on interventions aimed at increasing or improving HDL, particularly as those interventions typically also have wider effects on plasma lipids. The findings in this thesis add to the growing consensus that targeting HDL is unlikely to improve cardiovascular outcomes and that treating the underlying pathophysiology remains the optimal course of action. There is a doubtful and cautionary tone to recent review and commentary articles authored by leaders in the HDL field. Rodriguez et al., (2019) fundamentally question the biological purpose of HDL, while several others argue that any potential therapies targeting HDL must be linked to an HDL function demonstrated to be causal to CVD (Hovingh et al., 2015; März et al., 2017; von Eckardstein et al., 2023). Future studies should therefore focus on HDL cholesterol efflux function, and HDL interactions with apoB containing lipoproteins, as well as tissues and organs involved in the lipoprotein cascade such as adipose tissue and the liver.

In conclusion, this thesis suggests that HDL is a scavenger particle, removing excess cholesterol from the periphery. HDL also scavenges proteins from plasma and apoB-containing lipoproteins reflective of the systemic environment and accepts triglyceride and other lipids from the apoB-containing lipoprotein pool when plasma triglycerides are elevated, such as observed in late pregnancy (Sulaiman et al., 2016; Patanapirunhakit, 2023) and in insulin resistance linked dyslipidaemia such as in T2DM. These changes in HDL composition can potentially worsen but not improve HDL functionality. Improving the systemic and metabolic environment by treating the underlying pathophysiology may therefore return HDL composition and function back to its physiological normal.

Appendices

Chapter 6 – List of proteins with glycated residues identified on HDL from the GDM study. Types of glycation are shown underlined within the table.

Protein Name	Position(s) within protein
Fructosyl-lysine	
Apolipoprotein B-100	41
Apolipoprotein C-I	38
Platelet basic protein	38, 42
Serum amyloid A-4 protein	26
Sex hormone-binding globulin	342
Vitronectin	37, 59
Nε-Carboxymethyl-lysine	
Apolipoprotein C-I	36
Cathelicidin antimicrobial peptide	36
Fibrinogen beta chain	458
Platelet basic protein	38, 42
Serotransferrin	163
N1-(5-hydro-4-imidazolon-2-yl) ornithine	
Alpha-1-acid glycoprotein 2	38
Apolipoprotein B-100	26
Beta-2-glycoprotein 1	58
Complement C3	1391
Complement C4-B	269
Platelet basic protein	15, 43
Vitronectin	64
Nε-(1-Carboxyethyl)lysine	
Apolipoprotein B-100	934, 949, 3995
Beta-2-glycoprotein 1	52
Clusterin	114
Leucine-rich alpha-2-glycoprotein	10
Platelet basic protein	38
Vitronectin	25, 37, 59
Nδ-(5-hydro-5-methyl-4-imidazolon2-yl)-ornithine	
Apolipoprotein B-100	5, 233, 931, 2043
Apolipoprotein(a)	4155, 4158, 4174
Inter-alpha-trypsin inhibitor heavy chain H4	5
Platelet basic protein	4, 15
Sex hormone-binding globulin	101, 104
Vitronectin	64

Continued overleaf

Protein Name	Position(s) within protein
Argpyrimidine	
Alpha-1-acid glycoprotein 2	38
Apolipoprotein B-100	5, 26, 3291, 3311
Apolipoprotein C-I	2
Apolipoprotein(a)	3608
Complement C3	1376
Phospholipid transfer protein	235
Platelet basic protein	4, 15
Vitronectin	5, 64
Pyrroline	
Alpha-1-acid glycoprotein 1	42
Apolipoprotein B-100	41
Clusterin	118
Leucine-rich alpha-2-glycoprotein	10, 41
Platelet basic protein	38
Serotransferrin	167
Vitronectin	59
Imidazoline B	
Clusterin	127
Fibrinogen alpha chain	263
Fibrinogen beta chain	376
Platelet basic protein	4, 15
Serotransferrin	162
Serum amyloid A-4 protein	37
Vitronectin	64
1-Alkyl-2-formyl-3,4-glycosyl-pyrrole	
Alpha-1-acid glycoprotein 1	148
Alpha-1-acid glycoprotein 2	126, 138, 148, 153
Apolipoprotein(a)	4174, 4192
Beta-2-glycoprotein 1	62
Clusterin	114, 118, 123
Complement C3	1419, 1427
Hemopexin	234, 239 256
Serotransferrin	143
Serum amyloid A-4 protein	26
Sorting nexin-29	283
Vitronectin	37, 59, 395, 398, 421

List of References

Abarca-Gómez, L., Abdeen, Z.A., Hamid, Z.A., Abu-Rmeileh, N.M., Acosta-Cazares, B., Acuin, C., Adams, R.J., Aekplakorn, W., Afsana, K., Aguilar-Salinas, C.A., Agyemang, C., Ahmadvand, A., Ahrens, W., Ajlouni, K., Akhtaeva, N., Al-Hazzaa, H.M., Al-Othman, A.R., Al-Raddadi, R., Al Buhairan, F., Al Dhukair, S., Ali, M.M., Ali, O., Alkerwi, A., Alvarez-Pedrerol, M., Aly, E., Amarapurkar, D.N., Amouyel, P., Amuzu, A., Andersen, L.B., Anderssen, S.A., Andrade, D.S., Ängquist, L.H., Anjana, R.M., Aounallah-Skhiri, H., Araújo, J., Ariansen, I., Aris, T., Arlappa, N., Arveiler, D., Aryal, K.K., Aspelund, T., Assah, F.K., Assunção, M.C.F., Aung, M.S., Avdicová, M., Azevedo, A., Azizi, F., Babu, B. V, Bahijri, S., Baker, J.L., Balakrishna, N., Bamoshmoosh, M., Banach, M., Bandosz, P., Banegas, J.R., Barbagallo, C.M., Barceló, A., Barkat, A., Barros, A.J., Barros, M.V., Bata, I., Batieha, A.M., Batista, R.L., Batyrbek, A., Baur, L.A., Beaglehole, R., Romdhane, H. Ben, Benedics, J., Benet, M., Bennett, J.E., Bernabe-Ortiz, A., Bernotiene, G., Bettiol, H., Bhagyalaxmi, A., Bharadwaj, S., Bhargava, S.K., Bhatti, Z., Bhutta, Z.A., Bi, H., Bi, Y., Biehl, A., Bikbov, M., Bista, B., Bjelica, D.J., Bjerregaard, P., Bjertness, E., Bjertness, M.B., Björkelund, C., Blokstra, A., Bo, S., Bobak, M., Boddy, L.M., Boehm, B.O., Boeing, H., Boggia, J.G., Boissonnet, C.P., Bonaccio, M., Bongard, V., Bovet, P., Braeckevelt, L., Braeckman, L., Bragt, M.C., Brajkovich, I., Branca, F., Breckenkamp, J., Breda, J., Brenner, H., Brewster, L.M., Brian, G.R., Brinduse, L., Bruno, G., Bueno-de-Mesquita, H.B., Bugge, A., Buoncristiano, M., Burazeri, G., Burns, C., de León, A.C., Cacciottolo, J., Cai, H., Cama, T., Cameron, C., Camolas, J., Can, G., Cândido, A.P.C., Capanzana, M., Capuano, V., Cardoso, V.C., Carlsson, A.C., Carvalho, M.J., Casanueva, F.F., Casas, J.-P., Caserta, C.A., Chamukuttan, S., Chan, A.W., Chan, Q., Chaturvedi, H.K., Chaturvedi, N., Chen, C.-J., Chen, F., Chen, H., Chen, S., Chen, Z., Cheng, C.-Y., Chetrit, A., Chikova-Iscener, E., Chiolero, A., Chiou, S.-T., Chirita-Emandi, A., Chirlaque, M.-D., Cho, B., Cho, Y., Christensen, K., Christofaro, D.G., Chudek, J., Cifkova, R., Cinteza, E., Claessens, F., Clays, E., Concin, H., Confortin, S.C., Cooper, C., Cooper, R., Coppinger, T.C., Costanzo, S., Cottel, D., Cowell, C., Craig, C.L., Crujeiras, A.B., Cucu, A., D'Arrigo, G., d'Orsi, E., Dallongeville, J., Damasceno, A., Damsgaard, C.T., Danaei, G., Dankner, R., Dantoft, T.M., Dastgiri, S., Dauchet, L., Davletov, K., De Backer, G., De Bacquer, D., De Curtis, A., de Gaetano, G., De Henauw, S., de Oliveira, P.D., De Ridder, K., De Smedt, D., Deepa, M., Deev, A.D., Dehghan, A., Delisle, H., Delpeuch, F., Deschamps, V., Dhana, K., Di Castelnuovo, A.F., Dias-da-Costa, J.S., Diaz, A., Dika, Z., Djalalinia, S., Do, H.T., Dobson, A.J., Donati, M.B., Donfrancesco, C., Donoso, S.P., Döring, A., Dorobantu, M., Dorosty, A.R., Doua, K., Drygas, W., Duan, J.L., Duante, C., Duleva, V., Dulskiene, V., Dzerve, V., Dziankowska-Zaborszczyk, E., Egbagbe, E.E., Eggertsen, R., Eiben, G., Ekelund, U., El Ati, J., Elliott, P., Engle-Stone, R., Erasmus, R.T., Erem, C., Eriksen, L., Eriksson, J.G., la Peña, J.E., Evans, A., Faeh, D., Fall, C.H., Sant'Angelo, V.F., Farzadfar, F., Felix-Redondo, F.J., Ferguson, T.S., Fernandes, R.A., Fernández-Bergés, D., Ferrante, D., Ferrari, M., Ferreccio, C., Ferrieres, J., Finn, J.D., Fischer, K., Flores, E.M., Föger, B., Foo, L.H., Forslund, A.-S., Forsner, M., Fouad, H.M., Francis, D.K., Franco, M. do C., Franco, O.H., Frontera, G., Fuchs, F.D., Fuchs, S.C., Fujita, Y., Furusawa, T., Gaciong, Z., Gafencu, M., Galeone, D., Galvano, F., Garcia-de-la-Hera,

M., Gareta, D., Garnett, S.P., Gaspoz, J.-M., Gasull, M., Gates, L., Geiger, H., Geleijnse, J.M., Ghasemian, A., Giampaoli, S., Gianfagna, F., Gill, T.K., Giovannelli, J., Giwercman, A., Godos, J., Gogen, S., Goldsmith, R.A., Goltzman, D., Gonçalves, H., González-Leon, M., González-Rivas, J.P., Gonzalez-Gross, M., Gottrand, F., Graça, A.P., Graff-Iversen, S., Grafnetter, D., Grajda, A., Grammatikopoulou, M.G., Gregor, R.D., Grodzicki, T., Grøntved, A., Grosso, G., Gruden, G., Grujic, V., Gu, D., Gualdi-Russo, E., Guallar-Castillón, P., Guan, O.P., Gudmundsson, E.F., Gudnason, V., Guerrero, R., Guessous, I., Guimaraes, A.L., Gulliford, M.C., Gunnlaugsdottir, J., Gunter, M., Guo, X., Guo, Y., Gupta, P.C., Gupta, R., Gureje, O., Gurzkowska, B., Gutierrez, L., Gutzwiller, F., Hadaegh, F., Hadjigeorgiou, C.A., Si-Ramlee, K., Halkjær, J., Hambleton, I.R., Hardy, R., Kumar, R.H., Hassapidou, M., Hata, J., Hayes, A.J., He, J., Heidinger-Felso, R., Heinen, M., Hendriks, M.E., Henriques, A., Cadena, L.H., Herrala, S., Herrera, V.M., Herter-Aeberli, I., Heshmat, R., Hihtaniemi, I.T., Ho, S.Y., Ho, S.C., Hobbs, M., Hofman, A., Hopman, W.M., Horimoto, A.R., Hormiga, C.M., Horta, B.L., Houti, L., Howitt, C., Htay, T.T., Htet, A.S., Htike, M.M.T., Hu, Y., Huerta, J.M., Petrescu, C.H., Huisman, M., Husseini, A., Huu, C.N., Huybrechts, I., Hwalla, N., Hyska, J., Iacoviello, L., Iannone, A.G., Ibarluzea, J.M., Ibrahim, M.M., Ikeda, N., Ikram, M.A., Irazola, V.E., Islam, M., Ismail, A. al-S., Ivkovic, V., Iwasaki, M., Jackson, R.T., Jacobs, J.M., Jaddou, H., Jafar, T., Jamil, K.M., Jamrozik, K., Janszky, I., Jarani, J., Jasienska, G., Jelakovic, A., Jelakovic, B., Jennings, G., Jeong, S.-L., Jiang, C.Q., Jiménez-Acosta, S.M., Joffres, M., Johansson, M., Jonas, J.B., Jørgensen, T., Joshi, P., Jovic, D.P., Józwiak, J., Juolevi, A., Jurak, G., Jureša, V., Kaaks, R., Kafatos, A., Kajantie, E.O., Kalter-Leibovici, O., Kamaruddin, N.A., Kapantais, E., Karki, K.B., Kasaeian, A., Katz, J., Kauhanen, J., Kaur, P., Kavousi, M., Kazakbaeva, G., Keil, U., Boker, L.K., Keinänen-Kiukaanniemi, S., Kelishadi, R., Kelleher, C., Kemper, H.C., Kengne, Andre P, Kerimkulova, A., Kersting, M., Key, T., Khader, Y.S., Khalili, D., Khang, Y.-H., Khateeb, M., Khaw, K.-T., Khouw, I.M., Kiechl-Kohlendorfer, U., Kiechl, S., Killewo, J., Kim, J., Kim, Y.-Y., Klimont, J., Klumbiene, J., Knoflach, M., Koirala, B., Kolle, E., Kolsteren, P., Korrovits, P., Kos, J., Koskinen, S., Kouda, K., Kovacs, V.A., Kowlessur, S., Koziel, S., Kratzer, W., Kriemler, S., Kristensen, P.L., Krokstad, S., Kromhout, D., Kruger, H.S., Kubinova, R., Kuciene, R., Kuh, D., Kujala, U.M., Kulaga, Z., Kumar, R.K., Kunešová, M., Kurjata, P., Kusuma, Y.S., Kuulasmaa, K., Kyobutungi, C., La, Q.N., Laamiri, F.Z., Laatikainen, T., Lachat, C., Laid, Y., Lam, T.H., Landrove, O., Lanska, V., Lappas, G., Larijani, B., Laugsand, L.E., Lauria, L., Laxmaiah, A., Bao, K.L.N., Le, T.D., Lebanan, M.A.O., Leclercq, C., Lee, Jeannette, Lee, Jeonghee, Lehtimäki, T., León-Muñoz, L.M., Levitt, N.S., Li, Y., Lilly, C.L., Lim, W.-Y., Lima-Costa, M.F., Lin, H.-H., Lin, X., Lind, L., Linneberg, A., Lissner, L., Litwin, M., Liu, J., Loit, H.-M., Lopes, L., Lorbeer, R., Lotufo, P.A., Lozano, J.E., Luksiene, D., Lundqvist, A., Lunet, N., Lytsy, P., Ma, G., Ma, J., Machado-Coelho, G.L., Machado-Rodrigues, A.M., Machi, S., Maggi, S., Magliano, D.J., Magriplis, E., Mahaletchumy, A., Maire, B., Majer, M., Makdisse, M., Malekzadeh, R., Malhotra, R., Rao, K.M., Malyutina, S., Manios, Y., Mann, J.I., Manzato, E., Margozzini, P., Markaki, A., Markey, O., Marques, L.P., Marques-Vidal, P., Marrugat, J., Martin-Prevel, Y., Martin, R., Martorell, R., Martos, E., Marventano, S., Masoodi, S.R., Mathiesen, E.B., Matijasevich, A., Matsha, T.E., Mazur, A., Mbanya, J.C.N., McFarlane, S.R., McGarvey, S.T., McKee,

M., McLachlan, S., McLean, R.M., McLean, S.B., McNulty, B.A., Yusof, S.M., Mediene-Benchekor, S., Medzioniene, J., Meirhaeghe, A., Meisfjord, J., Meisinger, C., Menezes, A.M.B., Menon, G.R., Mensink, G.B., Meshram, I.I., Metspalu, A., Meyer, H.E., Mi, J., Michaelsen, K.F., Michels, N., Mikkel, K., Miller, J.C., Minderico, C.S., Miquel, J.F., Miranda, J.J., Mirkopoulou, D., Mirrakhimov, E., Mišigoj-Durakovic, M., Mistretta, A., Mocanu, V., Modesti, P.A., Mohamed, M.K., Mohammad, K., Mohammadifard, N., Mohan, V., Mohanna, S., Yusoff, Muhammad Fadhli Mohd, Molbo, D., Møllehave, L.T., Møller, N.C., Molnár, D., Momenan, A., Mondo, C.K., Monterrubio, E.A., Monyeki, K.D.K., Moon, J.S., Moreira, L.B., Morejon, A., Moreno, L.A., Morgan, K., Mortensen, E.L., Moschonis, G., Mossakowska, M., Mostafa, A., Mota, J., Mota-Pinto, A., Motlagh, M.E., Motta, J., Mu, T.T., Muc, M., Muiesan, M.L., Müller-Nurasyid, M., Murphy, N., Mursu, J., Murtagh, E.M., Musil, V., Nabipour, I., Nagel, G., Naidu, B.M., Nakamura, H., Námešná, J., Nang, E.E.K., Nangia, V.B., Nankap, M., Narake, S., Nardone, P., Navarrete-Muñoz, E.M., Neal, W.A., Nenko, I., Neovius, M., Nervi, F., Nguyen, C.T., Nguyen, N.D., Nguyen, Q.N., Nieto-Martínez, R.E., Ning, G., Ninomiya, T., Nishtar, S., Noale, M., Noboa, O.A., Norat, T., Norie, S., Noto, D., Nsour, M. Al, O'Reilly, D., Obreja, G., Oda, E., Oehlers, G., Oh, K., Ohara, K., Olafsson, Ö., Olinto, M.T.A., Oliveira, I.O., Oltarzewski, M., Omar, M.A., Onat, A., Ong, S.K., Ono, L.M., Ordunez, P., Ornelas, R., Ortiz, A.P., Osler, M., Osmond, C., Ostojic, S.M., Ostovar, A., Otero, J.A., Overvad, K., Owusu-Dabo, E., Paccaud, F.M., Padez, C., Pahomova, E., Pajak, A., Palli, D., Palloni, A., Palmieri, L., Pan, W.-H., Panda-Jonas, S., Pandey, A., Panza, F., Papandreou, D., Park, S.-W., Parnell, W.R., Parsaeian, M., Pascanu, I.M., Patel, N.D., Pecin, I., Pednekar, M.S., Peer, N., Peeters, P.H., Peixoto, S.V., Peltonen, M., Pereira, A.C., Perez-Farinos, N., Pérez, C.M., Peters, A., Petkeviciene, J., Petrauskiene, A., Peykari, N., Pham, S.T., Pierannunzio, D., Pigeot, I., Pikhart, H., Pilav, A., Pilotto, L., Pistelli, F., Pitakaka, F., Piwonska, A., Plans-Rubió, P., Poh, B.K., Pohlabeln, H., Pop, R.M., Popovic, S.R., Porta, M., Portegies, M.L., Posch, G., Poulimeneas, D., Pouraram, H., Pourshams, A., Poustchi, H., Pradeepa, R., Prashant, M., Price, J.F., Puder, J.J., Pudule, I., Puiu, M., Punab, M., Qasrawi, R.F., Qorbani, M., Bao, T.Q., Radic, I., Radisauskas, R., Rahman, Mahfuzar, Rahman, Mahmudur, Raitakari, O., Raj, M., Rao, S.R., Ramachandran, A., Ramke, J., Ramos, E., Ramos, R., Rampal, L., Rampal, S., Rascon-Pacheco, R.A., Redon, J., Reganit, P.F.M., Ribas-Barba, L., Ribeiro, R., Riboli, E., Rigo, F., de Wit, T.F.R., Rito, A., Ritti-Dias, R.M., Rivera, J.A., Robinson, S.M., Robitaille, C., Rodrigues, D., Rodríguez-Artalejo, F., del Cristo Rodriguez-Perez, M., Rodríguez-Villamizar, L.A., Rojas-Martinez, R., Rojroongwasinkul, N., Romaguera, D., Ronkainen, K., Rosengren, A., Rouse, I., Roy, J.G., Rubinstein, A., Rühli, F.J., Ruiz-Betancourt, B.S., Russo, P., Rutkowski, M., Sabanayagam, C., Sachdev, H.S., Saidi, O., Salanave, B., Martinez, E.S., Salmerón, D., Salomaa, V., Salonen, J.T., Salvetti, M., Sánchez-Abanto, J., Sandjaja, Sans, S., Marina, L.S., Santos, D.A., Santos, I.S., Santos, O., dos Santos, R.N., Santos, R., Saramies, J.L., Sardinha, L.B., Sarrafzadegan, N., Saum, K.-U., Savva, S., Savy, M., Scazufca, M., Rosario, A.S., Schargrodsky, H., Schienkiewitz, A., Schipf, S., Schmidt, C.O., Schmidt, I.M., Schultsz, C., Schutte, A.E., Sein, A.A., Sen, A., Senbanjo, I.O., Sepanlou, S.G., Serra-Majem, L., Shalnova, S.A., Sharma, S.K., Shaw, J.E., Shibuya, K., Shin, D.W., Shin, Y., Shiri, R., Siani, A., Siantar, R., Sibai, A.M., Silva, A.M., Silva, D.A.S., Simon, M.,

Simons, J., Simons, L.A., Sjöberg, A., Sjöström, M., Skovbjerg, S., Slowikowska-Hilczer, J., Slusarczyk, P., Smeeth, L., Smith, M.C., Snijder, M.B., So, H.-K., Sobngwi, E., Söderberg, S., Soekatri, M.Y., Solfrizzi, V., Sonestedt, E., Song, Y., Sørensen, T.I., Soric, M., Jérome, C.S., Soumare, A., Spinelli, A., Spiroski, I., Staessen, J.A., Stamm, H., Starc, G., Stathopoulou, M.G., Staub, K., Stavreski, B., Steene-Johannessen, J., Stehle, P., Stein, A.D., Stergiou, G.S., Stessman, J., Stieber, J., Stöckl, D., Stocks, T., Stokwiszewski, J., Stratton, G., Stronks, K., Strufaldi, M.W., Suárez-Medina, R., Sun, C.-A., Sundström, J., Sung, Y.-T., Sunyer, J., Suriyawongpaisal, P., Swinburn, B.A., Sy, R.G., Szponar, L., Tai, E.S., Tammesoo, M.-L., Tamosiunas, A., Tan, E.J., Tang, X., Tanser, F., Tao, Y., Tarawneh, M.R., Tarp, J., Tarqui-Mamani, C.B., Tautu, O.-F., Braunerová, R.T., Taylor, A., Tchibindat, F., Theobald, H., Theodoridis, X., Thijs, L., Thuesen, B.H., Tjonneland, A., Tolonen, H.K., Tolstrup, J.S., Topbas, M., Topór-Madry, R., Tormo, M.J., Tornaritis, M.J., Torrent, M., Toselli, S., Traissac, P., Trichopoulos, D., Trichopoulou, A., Trinh, O.T., Trivedi, A., Tshepo, L., Tsigga, M., Tsugane, S., Tulloch-Reid, M.K., Tullu, F., Tuomainen, T.-P., Tuomilehto, J., Turley, M.L., Tynelius, P., Tzotzas, T., Tzourio, C., Ueda, P., Ugel, E.E., Ukoli, F.A., Ulmer, H., Unal, B., Uusitalo, H.M., Valdivia, G., Vale, S., Valvi, D., van der Schouw, Y.T., Van Herck, K., Van Minh, H., van Rossem, L., Van Schoor, N.M., van Valkengoed, I.G., Vanderschueren, D., Vanuzzo, D., Vatten, L., Vega, T., Veidebaum, T., Velasquez-Melendez, G., Velika, B., Veronesi, G., Verschuren, W.M., Victora, C.G., Viegi, G., Viet, L., Viikari-Juntura, E., Vineis, P., Vioque, J., Virtanen, J.K., Visvikis-Siest, S., Viswanathan, B., Vlasoff, T., Vollenweider, P., Völzke, H., Voutilainen, S., Vrijheid, M., Wade, A.N., Wagner, A., Waldhör, T., Walton, J., Bebakar, W.M.W., Mohamud, W.N.W., Wanderley, R.S., Wang, M.-D., Wang, Q., Wang, Y.X., Wang, Y.-W., Wannamethee, S.G., Wareham, N., Weber, A., Wedderkopp, N., Weerasekera, D., Whincup, P.H., Widhalm, K., Widyahening, I.S., Wiecek, A., Wijga, A.H., Wilks, R.J., Willeit, J., Willeit, P., Wilsgaard, T., Wojtyniak, B., Wong-McClure, R.A., Wong, J.Y., Wong, J.E., Wong, T.Y., Woo, J., Woodward, M., Wu, F.C., Wu, J., Wu, S., Xu, H., Xu, L., Yamborisut, U., Yan, W., Yang, X., Yardim, N., Ye, X., Yiallouros, P.K., Yngve, A., Yoshihara, A., You, Q.S., Younger-Coleman, N.O., Yusoff, F., Yusoff, Muhammad Fadhli M, Zaccagni, L., Zafiropulos, V., Zainuddin, A.A., Zambon, S., Zampelas, A., Zamrazilová, H., Zdrojewski, T., Zeng, Y., Zhao, D., Zhao, W., Zheng, W., Zheng, Y., Zholdin, B., Zhou, M., Zhu, D., Zhussupov, B., Zimmermann, E., Cisneros, J.Z., Bentham, J., Di Cesare, M., Bilano, V., Bixby, H., Zhou, B., Stevens, G.A., Riley, L.M., Taddei, C., Hajifathalian, K., Lu, Y., Savin, S., Cowan, M.J., Paciorek, C.J., Chirita-Emandi, A., Hayes, A.J., Katz, J., Kelishadi, R., Kengne, Andre Pascal, Khang, Y.-H., Laxmaiah, A., Li, Y., Ma, J., Miranda, J.J., Mostafa, A., Neovius, M., Padez, C., Rampal, L., Zhu, A., Bennett, J.E., Danaei, G., Bhutta, Z.A. and Ezzati, M. 2017. Worldwide trends in body-mass index, underweight, overweight, and obesity from 1975 to 2016: a pooled analysis of 2416 population-based measurement studies in 128·9 million children, adolescents, and adults. *The Lancet*. **390**(10113), pp.2627–2642.

Abildgaard, J., Ploug, T., Al-Saoudi, E., Wagner, T., Thomsen, C., Ewertsen, C., Bzorek, M., Pedersen, B.K., Pedersen, A.T. and Lindegaard, B. 2021. Changes in abdominal subcutaneous adipose tissue phenotype following

menopause is associated with increased visceral fat mass. *Scientific Reports*. **11**(1), p.14750.

Ades, E.W., Candal, F.J., Swerlick, R.A., George, V.G. and Summers, S. 1992. HMEC-1: Establishment of an Immortalized Human Microvascular Endothelial Cell Line. *The Journal of Investigative Dermatology*. **99**(6), pp.683–690.

Agouni, A., He, A., Ducluzeau, P.H., Mostefai, H.A., Draunet-busson, C., Leftheriotis, G., Heymes, C. and Martinez, M.C. 2008. Endothelial Dysfunction Caused by Circulating Microparticles from Patients with Metabolic Syndrome. *American Journal of Pathology*. **173**(4), pp.1210–1219.

Akerstrom, B., Logdberg, L., Berggard C, T., Osmark, P. and Lindqvist, A. 2000. alpha-1-Microglobulin: a yellow-brown lipocalin. *Biochimica et Biophysica Acta*. **1482**, pp.172–184.

Allan, C.M. and Taylor, J.M. 1996. Expression of a novel human apolipoprotein (apoC-IV) causes hypertriglyceridemia in transgenic mice. *Journal of Lipid Research*. **37**, pp.1510–1518.

Alpert, M.A. 2001. Obesity cardiomyopathy: Pathophysiology and evolution of the clinical syndrome *In*: *American Journal of the Medical Sciences*. Lippincott Williams and Wilkins, pp.225–236.

Altman, D.G. and Bland, J.M. 1983. Measurement in Medicine: The Analysis of Method Comparison Studies. *Journal of the Royal Statistical Society. Series D (The Statistician)*. **32**(3), pp.307–317.

Alvarez, J.J., Montelongo, A., Iglesias, A., Lasunción, M.A. and Herrera, E. 1996. Longitudinal study on lipoprotein profile, high density lipoprotein subclass, and postheparin lipases during gestation in women. *Journal of Lipid Research*. **37**(2), pp.299–308.

American Diabetes Association 2017. Management of Diabetes in Pregnancy: Standards of Medical Care in Diabetes—2018. *Diabetes Care*. **41**(Supplement_1), pp.S137–S143.

Annema, W., Nijstad, N., Tölle, M., de Boer, J.F., Buijs, R.V.C., Heeringa, P., van der Giet, M. and Tietge, U.J.F. 2010. Myeloperoxidase and serum amyloid A contribute to impaired in vivo reverse cholesterol transport during the acute phase response but not group IIA secretory phospholipase A2[S]. *Journal of Lipid Research*. **51**(4), pp.743–754.

Annema, W. and Tietge, U.J.F. 2011. Role of Hepatic Lipase and Endothelial Lipase in High-Density Lipoprotein—Mediated Reverse Cholesterol Transport. *Current Atherosclerosis Reports*. **13**(3), pp.257–265.

Annema, W., Willemsen, H.M., de Boer, J.F., Dikkers, A., van der Giet, M., Nieuwland, W., Muller Kobold, A.C., van Pelt, L.J., Slart, R.H.J.A., van der Horst, I.C.C., Dullaart, R.P.F., Tio, R.A. and Tietge, U.J.F. 2016. HDL function is impaired in acute myocardial infarction independent of plasma HDL cholesterol levels. *Journal of Clinical Lipidology*. **10**(6), pp.1318–1328.

Arai, T., Yamashita, S., Hirano, K., Sakai, N., Kotani, K., Fujioka, S., Nozaki, S., Keno, Y., Yamane, M. and Shinohara, E. 1994. Increased plasma cholesteryl ester transfer protein in obese subjects. A possible mechanism for the reduction of serum HDL cholesterol levels in obesity. *Arteriosclerosis and Thrombosis: A Journal of Vascular Biology*. **14**(7), pp.1129–1136.

Arner, P. 2005. Human fat cell lipolysis: Biochemistry, regulation and clinical role. *Best Practice and Research: Clinical Endocrinology and Metabolism*. **19**(4), pp.471–482.

Arsenault, B.J., Lemieux, I., Després, J.P., Wareham, N.J., Stroes, E.S.G., Kastelein, J.J.P., Khaw, K.T. and Boekholdt, S.M. 2010. Comparison between gradient gel electrophoresis and nuclear magnetic resonance

spectroscopy in estimating coronary heart disease risk associated with LDL and HDL particle size. *Clinical Chemistry*. **56**(5), pp.789–798.

Ashby, D.T., Rye, K.-A., Clay, M.A., Vadas, M.A., Gamble, J.R. and Barter, P.J. 1998. Factors Influencing the Ability of HDL to Inhibit Expression of Vascular Cell Adhesion Molecule-1 in Endothelial Cells. *Arterioscler Thromb Vasc Biol*. **18**, pp.1450–1455.

Ashcroft, F.M. and Rorsman, P. 1990. ATP-sensitive K+ channels: a link between B-cell metabolism and insulin secretion. *Biochemical Society Transactions*. **18**(1), pp.109–111.

Attrill, E., Ramsay, C., Ross, R., Richards, S., Sutherland, B.A., Keske, M.A., Eringa, E. and Premilovac, D. 2020. Metabolic-vascular coupling in skeletal muscle: A potential role for capillary pericytes? *Clinical and Experimental Pharmacology and Physiology*. **47**(3), pp.520–528.

Averill, M., Rubinow, K.B., Cain, K., Wimberger, J., Babenko, I., Becker, J.O., Foster-Schubert, K.E., Cummings, D.E., Hoofnagle, A.N. and Vaisar, T. 2020. Postprandial remodeling of high-density lipoprotein following high saturated fat and high carbohydrate meals. *Journal of Clinical Lipidology*. **14**(1), pp.66-76.e11.

Avila, C., Holloway, A.C., Hahn, M.K., Morrison, K.M., Restivo, M., Anglin, R. and Taylor, V.H. 2015. An Overview of Links Between Obesity and Mental Health. *Current obesity reports*. **4**(3), pp.303–310.

Aviram, M., Rosenblat, M., Bisgaier, C.L., Newton, R.S., Primo-Parmo, S.L. and La Du, B.N. 1998. Paraoxonase inhibits high-density lipoprotein oxidation and preserves its functions. A possible peroxidative role for paraoxonase. *The Journal of Clinical Investigation*. **101**(8), pp.1581–1590.

Baker, C. 2023. *Obesity statistics*.

Bakker, L.E.H., Boon, M.R., Annema, W., Dikkers, A., van Eyk, H.J., Verhoeven, A., Mayboroda, O.A., Jukema, J.W., Havekes, L.M., Meinders, A.E., Willems van Dijk, K., Jazet, I.M., Tietge, U.J.F. and Rensen, P.C.N. 2016. HDL functionality in South Asians as compared to white Caucasians. *Nutrition, Metabolism and Cardiovascular Diseases*. **26**(8), pp.697–705.

Baldini, N. and Avnet, S. 2019. The effects of systemic and local acidosis on insulin resistance and signaling. *International Journal of Molecular Sciences*. **20**(1).

Barter, P.J., Caulfield, M., Eriksson, M., Grundy, S.M., Kastelein, J.J.P., Komajda, M., Lopez-Sendon, J., Mosca, L., Tardif, J.-C., Waters, D.D., Shear, C.L., Revkin, J.H., Buhr, K.A., Fisher, M.R., Tall, A.R. and Brewer, B. 2007. Effects of Torcetrapib in Patients at High Risk for Coronary Events. *New England Journal of Medicine*. **357**(21), pp.2109–2122.

Bassini, A., Sartoretto, S., Jurisica, L., Magno-França, A., Anderson, L., Pearson, T., Razavi, M., Chandran, V., Martin, L.R., Jurisica, I. and Cameron, L.C. 2022. Sportomics method to assess acute phase proteins in Olympic level athletes using dried blood spots and multiplex assay. *Scientific Reports*. **12**(1).

Baumfeld, Y., Novack, L., Wiznitzer, A., Sheiner, E., Henkin, Y., Sherf, M. and Novack, V. 2015. Pre-conception dyslipidemia is associated with development of preeclampsia and gestational diabetes mellitus. *PLoS ONE*. **10**(10).

Beazer, J.D. and Freeman, D.J. 2022. Estradiol and HDL Function in Women – A Partnership for Life. *The Journal of Clinical Endocrinology & Metabolism*. **107**(5), pp.e2192–e2194.

Beazer, J.D., Patanapirunhakit, P., Gill, J.M.R., Graham, D., Karlsson, H., Ljunggren, S., Mulder, M.T. and Freeman, D.J. 2020. High-density lipoprotein's vascular protective functions in metabolic and cardiovascular disease – could extracellular vesicles be at play? *Clinical Science*. **134**(22), pp.2977–2986.

Becher, T., Palanisamy, S., Kramer, D.J., Eljalby, M., Marx, S.J., Wibmer, A.G., Butler, S.D., Jiang, C.S., Vaughan, R., Schöder, H., Mark, A. and Cohen, P. 2021. Brown adipose tissue is associated with cardiometabolic health. *Nature Medicine*. **27**(1), pp.58–65.

Belfort, R., Mandarino, L., Kashyap, S., Wirfel, K., Pratipanawatr, T., Berria, R., DeFronzo, R.A. and Cusi, K. 2005. Dose-Response Effect of Elevated Plasma Free Fatty Acid on Insulin Signaling. *Diabetes*. **54**(6), pp.1640–1648.

Bellamy, L., Casas, J.-P., Hingorani, A.D. and Williams, D. 2009. Type 2 diabetes mellitus after gestational diabetes: a systematic review and meta-analysis. *The Lancet*. **373**(9677), pp.1773–1779.

van den Berg, R.A., Hoefsloot, H.C.J., Westerhuis, J.A., Smilde, A.K. and van der Werf, M.J. 2006. Centering, scaling, and transformations: Improving the biological information content of metabolomics data. *BMC Genomics*. **7**.

Berneis, K.K. and Krauss, R.M. 2002. Metabolic origins and clinical significance of LDL heterogeneity. *Journal of Lipid Research*. **43**(9), pp.1363–1379.

Besler, C., Heinrich, K., Rohrer, L., Doerries, C., Riwanto, M., Shih, D.M., Chroni, A., Yonekawa, K., Stein, S., Schaefer, N., Mueller, M., Akhmedov, A., Daniil, G., Manes, C., Templin, C., Wyss, C., Maier, W., Tanner, F.C., Matter, C.M., Corti, R., Furlong, C., Lusis, A.J., Von Eckardstein, A., Fogelman, A.M., Lüscher, T.F. and Landmesser, U. 2011. Mechanisms underlying adverse effects of HDL on eNOS-activating pathways in patients with coronary artery disease. *Journal of Clinical Investigation*. **121**(7), pp.2693–2708.

Beulens, J.W.J., Rutters, F., Rydén, L., Schnell, O., Mellbin, L., Hart, H.E. and Vos, R.C. 2019. Risk and management of pre-diabetes. *European Journal of Preventive Cardiology*. **26**(2_suppl), pp.47–54.

Bird, S.R. and Hawley, J.A. 2017. Update on the effects of physical activity on insulin sensitivity in humans. *BMJ Open Sport & Exercise Medicine*. **2**(1), p.e000143.

Björntorp, P. 1990. 'Portal' adipose tissue as a generator of risk factors for cardiovascular disease and diabetes. *Arteriosclerosis: An Official Journal of the American Heart Association, Inc.* **10**(4), pp.493–496.

Blanco-Vaca, F., Via, David P, Yang, Chao-yuh, Massey, John B, Pownall, Henry J, Via, D P, Yang, C-y, Massey, J B, Pownall, H J and Lipid, lipoproteins J. 1992. Characterization of disulfide-linked heterodimers containing apolipoprotein D in human plasma lipoproteins Characterization of disulfide-linked heter-odimers containing apolipoprotein D in human plasma. *Journal of Lipid Research*. **33**, pp.1785–1796.

Blüher, M. 2019. Obesity: global epidemiology and pathogenesis. *Nature Reviews Endocrinology*. **15**(5), pp.288–298.

Boden, W.E., Probstfield, J.L., Anderson, T., Chaitman, B.R., Desvignes-Nickens, P., Koprowicz, K., McBride, R., Teo, K. and Weintraub, W. 2011. Niacin in Patients with Low HDL Cholesterol Levels Receiving Intensive Statin Therapy. *New England Journal of Medicine*. **365**(24), pp.2255–2267.

Boraschi, D., Del Giudice, G., Dutel, C., Ivanoff, B., Rappuoli, R. and Grubeck-Loebenstein, B. 2010. Ageing and immunity: Addressing immune senescence to ensure healthy ageing. *Vaccine*. **28**(21), pp.3627–3631.

Bradford, M.M. 1976. A rapid and sensitive method for the quantitation of microgram quantities of protein utilizing the principle of protein-dye binding. *Analytical Biochemistry*. **72**, pp.248–254.

Brady, E.M., Webb, D.R., Morris, D.H., Khunti, K., Talbot, D.S.C., Sattar, N. and Davies, M.J. 2012. Investigating endothelial activation and oxidative stress in relation to glycaemic control in a multiethnic population. *Experimental Diabetes Research*. **2012**.

Brand, T., van den Munckhof, I.C.L., van der Graaf, M., Schraa, K., Dekker, H.M., Joosten, L.A.B., Netea, M.G., Riksen, N.P., de Graaf, J. and Rutten, J.H.W. 2021. Superficial vs Deep Subcutaneous Adipose Tissue: Sex-Specific Associations With Hepatic Steatosis and Metabolic Traits. *The Journal of Clinical Endocrinology & Metabolism*. **106**(10), pp.e3881–e3889.

Bray, G.A. 1987. Overweight Is Risking Fate: Definition, Classification, Prevalence, and Risks. *Annals of the New York Academy of Sciences*. **499**(1), pp.14–28.

Brehm, A., Krssak, M., Schmid, A.I., Nowotny, P., Waldhäusl, W. and Roden, M. 2006. Increased Lipid Availability Impairs Insulin-Stimulated ATP Synthesis in Human Skeletal Muscle. *Diabetes*. **55**(1), pp.136–140.

Brinton, E.A., Eisenberg, S. and Breslow, J.L. 1994. Human HDL Cholesterol Levels Are Determined by ApoA-I Fractional Catabolic Rate, Which Correlates Inversely With Estimates of HDL Particle Size Effects of Gender, Hepatic and Lipoprotein Lipases, Triglyceride and Insulin Levels, and Body Fat Distribution. *Arteriosclerosis and Thrombosis*. **14**(5), pp.707–720.

Brown, M.A., Lindheimer, M.D., de Swiet, M., Assche, A. Van and Moutquin, J.-M. 2001a. The Classification and Diagnosis of the Hypertensive Disorders of Pregnancy: Statement from the International Society for the Study of Hypertension in Pregnancy (ISSHP). *Hypertension in Pregnancy*. **20**(1), ix–xiv.

Brown, M.A., Lindheimer, M.D., de Swiet, M., Assche, A. Van and Moutquin, J.-M. 2001b. The Classification and Diagnosis of the Hypertensive Disorders of Pregnancy: Statement from the International Society for the Study of Hypertension in Pregnancy (ISSHP). *Hypertension in Pregnancy*. **20**(1), ix–xiv.

Brown, S.H.J., Eather, S.R., Freeman, D.J., Meyer, B.J. and Mitchell, T.W. 2016. A Lipidomic Analysis of Placenta in Preeclampsia: Evidence for Lipid Storage. *PLOS ONE*. **11**(9), pp.e0163972-.

Burger, D., Turner, M., Xiao, F., Munkonda, M.N., Akbari, S. and Burns, K.D. 2017. High glucose increases the formation and pro-oxidative activity of endothelial microparticles. *Diabetologia*. **60**(9), pp.1791–1800.

Bursill, C.A., Castro, M.L., Beattie, D.T., Nakhla, S., van der Vorst, E., Heather, A.K., Barter, P.J. and Rye, K.-A. 2010. High-Density Lipoproteins Suppress Chemokines and Chemokine Receptors In Vitro and In Vivo. *Arteriosclerosis, Thrombosis, and Vascular Biology*. **30**(9), pp.1773–1778.

Camilli, C., Hoeh, A.E., De Rossi, G., Moss, S.E. and Greenwood, J. 2022. LRG1: an emerging player in disease pathogenesis. *Journal of Biomedical Science*. **29**(6).

Camuzcuoglu, H., Toy, H., Cakir, H., Celik, H. and Erel, O. 2009. Decreased Paraoxonase and Arylesterase Activities in the Pathogenesis of Future Atherosclerotic Heart Disease in Women with Gestational Diabetes Mellitus. *Journal of Women's Health*. **18**, pp.1435–1439.

Cardner, M., Yalcinkaya, M., Goetze, S., Luca, E., Balaz, M., Hunjadi, M., Hartung, J., Shemet, A., Kränkel, N., Radosavljevic, S., Keel, M., Othman,

A., Karsai, G., Hornemann, T., Claassen, M., Liebisch, G., Carreira, E., Ritsch, A., Landmesser, U., Krützfeldt, J., Wolfrum, C., Wollscheid, B., Beerenwinkel, N., Rohrer, L. and von Eckardstein, A. 2020. Structure-function relationships of HDL in diabetes and coronary heart disease. *JCI Insight*. **5**(1).

Carreau, A., Kieda, C. and Grillon, C. 2011. Nitric oxide modulates the expression of endothelial cell adhesion molecules involved in angiogenesis and leukocyte recruitment. *Experimental Cell Research*. **317**(1), pp.29–41.

Cartolano, F.D.C., Dias, G.D., Miyamoto, S. and Damasceno, N.R.T. 2022. Omega-3 Fatty Acids Improve Functionality of High-Density Lipoprotein in Individuals With High Cardiovascular Risk: A Randomized, Parallel, Controlled and Double-Blind Clinical Trial. *Frontiers in Nutrition*. **8**.

Casella-Filho, A., Chagas, A.C.P., Maranhão, R.C., Trombetta, I.C., Cesena, F.H.Y., Silva, V.M., Tanus-Santos, J.E., Negrão, C.E. and da Luz, P.L. 2011. Effect of Exercise Training on Plasma Levels and Functional Properties of High-Density Lipoprotein Cholesterol in the Metabolic Syndrome. *The American Journal of Cardiology*. **107**(8), pp.1168–1172.

Casey, B.M., Lucas, M.J., McIntire, D.D. and Leveno, K.J. 1997. Pregnancy Outcomes in Women With Gestational Diabetes Compared With the General Obstetric Population. *Obstetrics & Gynecology*. **90**(6), pp.869–873.

Cawley, J. and Meyerhoefer, C. 2012. The medical care costs of obesity: An instrumental variables approach. *Journal of Health Economics*. **31**(1), pp.219–230.

Di Cesare, M., Bentham, J., Stevens, G.A., Zhou, B., Danaei, G., Lu, Y., Bixby, H., Cowan, M.J., Riley, L.M., Hajifathalian, K., Fortunato, L., Taddei, C., Bennett, J.E., Ikeda, N., Khang, Y.H., Kyobutungi, C., Laxmaiah, A., Li, Y., Lin, H.H., Miranda, J.J., Mostafa, A., Turley, M.L., Paciorek, C.J., Gunter, M., Ezzati, M., Abdeen, Z.A., Hamid, Z.A., Abu-Rmeileh, N.M., Acosta-Cazares, B., Adams, R., Aekplakorn, W., Aguilar-Salinas, C.A., Ahmadvand, A., Ahrens, W., Ali, M.M., Alkerwi, A., Alvarez-Pedrerol, M., Aly, E., Amouyel, P., Amuzu, A., Andersen, L.B., Anderssen, S.A., Andrade, D.S., Anjana, R.M., Aounallah-Skhiri, H., Ariansen, I., Aris, T., Arlappa, N., Arveiler, D., Assah, F.K., Avdicová, M., Azizi, F., Babu, B. V., Balakrishna, N., Bandosz, P., Banegas, J.R., Barbagallo, C.M., Barceló, A., Barkat, A., Barros, M. V., Bata, I., Batieha, A.M., Batista, R.L., Baur, L.A., Beaglehole, R., Romdhane, H. Ben, Benet, M., Bernabe-Ortiz, A., Bernotiene, G., Bettiol, H., Bhagyalaxmi, A., Bharadwaj, S., Bhargava, S.K., Bhatti, Z., Bhutta, Z.A., Bi, H.S., Bi, Y., Bjerregaard, P., Bjertness, E., Bjertness, M.B., Björkelund, C., Blake, M., Blokstra, A., Bo, S., Bobak, M., Boddy, L.M., Boehm, B.O., Boeing, H., Boissonnet, C.P., Bongard, V., Bovet, P., Braeckman, L., Bragt, M.C.E., Brajkovich, I., Branca, F., Breckenkamp, J., Brenner, H., Brewster, L.M., Brian, G.R., Bruno, G., Bueno-De-Mesquita, H.B., Bugge, A., Burns, C., De León, A.C., Cacciottolo, J., Cama, T., Cameron, C., Camolas, J., Can, G., Cândido, A.P.C., Capuano, V., Cardoso, V.C., Carvalho, M.J., Casanueva, F.F., Casas, J.P., Caserta, C.A., Castetbon, K., Chamukuttan, S., Chan, A.W., Chan, Q., Chaturvedi, H.K., Chaturvedi, N., Chen, C.J., Chen, F., Chen, H., Chen, S., Chen, Z., Cheng, C.Y., Chetrit, A., Chiolero, A., Chiou, S.T., Chirita-Emandi, A., Cho, Y., Christensen, K., Chudek, J., Cifkova, R., Claessens, F., Clays, E., Concin, H., Cooper, C., Cooper, R., Coppinger, T.C., Costanzo, S., Cottel, D., Cowell, C., Craig, C.L., Crujeiras, A.B., D'Arrigo, G., D'Orsi, E., Dallongeville, J., Damasceno, A., Damsgaard, C.T., Dankner, R., Dauchet,

L., De Backer, G., De Bacquer, D., De Gaetano, G., De Henauw, S., De Smedt, D., Deepa, M., Deev, A.D., Dehghan, A., Delisle, H., Delpeuch, F., Dhana, K., Di Castelnuovo, A.F., Dias-Da-Costa, J.S., Diaz, A., Djalalinia, S., Do, H.T.P., Dobson, A.J., Donfrancesco, C., Döring, A., Doua, K., Drygas, W., Egbagbe, E.E., Eggertsen, R., Ekelund, U., El Ati, J., Elliott, P., Engle-Stone, R., Erasmus, R.T., Erem, C., Eriksen, L., De La Peña, J.E., Evans, A., Faeh, D., Fall, C.H., Farzadfar, F., Felix-Redondo, F.J., Ferguson, T.S., Fernández-Bergés, D., Ferrante, D., Ferrari, M., Ferreccio, C., Ferrieres, J., Finn, J.D., Fischer, K., Flores, E.M., Föger, B., Foo, L.H., Forslund, A.S., Fortmann, S.P., Fouad, H.M., Francis, D.K., Do Carmo Franco, M., Franco, O.H., Frontera, G., Fuchs, F.D., Fuchs, S.C., Fujita, Y., Furusawa, T., Gaciong, Z., Gafencu, M., Gareta, D., Garnett, S.P., Gaspoz, J.M., Gasull, M., Gates, L., Geleijnse, J.M., Ghasemian, A., Giampaoli, S., Gianfagna, F., Giovannelli, J., Giwercman, A., Goldsmith, R.A., Gross, M.G., Rivas, J.P.G., Gorbea, M.B., Gottrand, F., Graff-Iversen, S., Grafnetter, D., Grajda, A., Grammatikopoulou, M.G., Gregor, R.D., Grodzicki, T., Grøntved, A., Gruden, G., Grujic, V., Gu, D., Guan, O.P., Gudnason, V., Guerrero, R., Guessous, I., Guimaraes, A.L., Gulliford, M.C., Gunnlaugsdottir, J., Guo, X.H., Guo, Y., Gupta, P.C., Gureje, O., Gurzkowska, B., Gutierrez, L., Gutzwiller, F., Halkjær, J., Hardy, R., Kumar, R.H., Hayes, A.J., He, J., Hendriks, M.E., Cadena, L.H., Heshmat, R., Hihtaniemi, I.T., Ho, S.Y., Ho, S.C., Hobbs, M., Hofman, A., Hormiga, C.M., Horta, B.L., Houti, L., Htay, T.T., Htet, A.S., Htike, M.M.T., Hu, Y., Hussieni, A.S., Huu, C.N., Huybrechts, I., Hwalla, N., Iacoviello, L., Iannone, A.G., Ibrahim, M.M., Ikram, M.A., Irazola, V.E., Islam, M., Iwasaki, M., Jackson, R.T., Jacobs, J.M., Jafar, T., Jamil, K.M., Jamrozik, K., Jasienska, G., Jiang, C.Q., Joffres, M., Johansson, M., Jonas, J.B., Jørgensen, T., Joshi, P., Juolevi, A., Jurak, G., Jureša, V., Kaaks, R., Kafatos, A., Kalter-Leibovici, O., Kapantais, E., Kasaeian, A., Katz, J., Kaur, P., Kavousi, M., Keil, U., Boker, L.K., Kelishadi, R., Kemper, H.H.C.G., Kengne, A.P., Kersting, M., Key, T., Khader, Y.S., Khalili, D., Khaw, K.T.H., Khouw, I.M.S.L., Kiechl, S., Killewo, J., Kim, J., Kiyohara, Y., Klimont, J., Kolle, E., Kolsteren, P., Korrovits, P., Koskinen, S., Kouda, K., Koziel, S., Kratzer, W., Krokstad, S., Kromhout, D., Kruger, H.S., Kula, K., Kulaga, Z., Kumar, R.K., Kusuma, Y.S., Kuulasmaa, K., Laamiri, F.Z., Laatikainen, T., Lachat, C., Laid, Y., Lam, T.H., Landrove, O., Lanska, V., Lappas, G., Laugsand, L.E., Le Nguyen Bao, K., Le, T.D., Leclercq, C., Lee, Jeannette, Lee, Jeonghee, Lehtimäki, T., Rampal, L., León-Munoz, L.M., Lim, W.Y., Lima-Costa, M.F., Lin, X., Linneberg, A., Lissner, L., Litwin, M., Liu, J., Lorbeer, R., Lotufo, P.A., Lozano, J.E., Luksiene, D., Lundqvist, A., Lunet, N., Lytsy, P., Ma, G., Machi, S., Maggi, S., Magliano, D.J., Makdisse, M., Malekzadeh, R., Malhotra, R., Rao, K.M., Manios, Y., Mann, J.I., Manzato, E., Margozzini, P., Markey, O., Marques-Vidal, P., Marrugat, J., Martin-Prevel, Y., Martorell, R., Masoodi, S.R., Matsha, T.E., Mazur, A., Mbanya, J.C.N., McFarlane, S.R., McGarvey, S.T., McKee, M., McLachlan, S., McLean, R.M., McNulty, B.A., Md Yusof, S., Mediene-Benchekor, S., Meirhaeghe, A., Meisinger, C., Mendes, L.L., Menezes, A.M.B., Mensink, G.B.M., Meshram, I.I., Metspalu, A., Mi, J., Michaelsen, K.F., Mikkel, K., Miller, J.C., Miquel, J.F., Mišigoj-Duraković, M., Mohamed, M.K., Mohammad, K., Mohammadifard, N., Mohan, V., Yusoff, M.F.M., Molbo, D., Møller, N.C., Molnár, D., Mondo, C.K., Monterrubio, E.A., Monyeki, K.D.K., Moreira, L.B., Morejon, A., Moreno, L.A., Morgan, K., Mortensen, E.L., Moschonis, G., Mossakowska, M., Mota, J., Motlagh, M.E.,

Motta, J., Mu, T.T., Muiesan, M.L., Müller-Nurasyid, M., Murphy, N., Mursu, J., Murtagh, E.M., Musa, K.I., Musil, V., Nagel, G., Nakamura, H., Námešná, J., Nang, E.E.K., Nangia, V.B., Nankap, M., Narake, S., Navarrete-Muñoz, E.M., Nenko, I., Neovius, M., Nervi, F., Neuhauser, H.K., Nguyen, N.D., Nguyen, Q.N., Nieto-Martínez, R.E., Ning, G., Ninomiya, T., Nishtar, S., Noale, M., Norat, T., Noto, D., Al Nsour, M., O'Reilly, D., Ochoa-Avilés, A.M., Oh, K., Olayan, I.H., Olinto, M.T.A., Oltarzewski, M., Omar, M.A., Onat, A., Ordunez, P., Ortiz, A.P., Osler, M., Osmond, C., Ostojic, S.M., Otero, J.A., Overvad, K., Paccaud, F.M., Padez, C., Pajak, A., Palli, D., Palloni, A., Palmieri, L., Panda-Jonas, S., Panza, F., Parnell, W.R., Parsaeian, M., Pednekar, M.S., Peeters, P.H., Peixoto, S.V., Pereira, A.C., Pérez, C.M., Peters, A., Peykari, N., Pham, S.T., Pigeot, I., Pikhart, H., Pilav, A., Pilotto, L., Pistelli, F., Pitakaka, F., Piwonska, A., Piwonski, J., Plans-Rubió, P., Poh, B.K., Porta, M., Portegies, M.L.P., Poulimeneas, D., Pradeepa, R., Prashant, M., Price, J.F., Puiu, M., Punab, M., Qasrawi, R.F., Qorbani, M., Bao, T.Q., Radic, I., Radisauskas, R., Rahman, M., Raitakari, O., Raj, M., Rao, S.R., Ramachandran, A., Ramke, J., Ramos, R., Rampal, S., Rasmussen, F., Redon, J., Reganit, P.F.M., Ribeiro, R., Riboli, E., Rigo, F., De Wit, T.F.R., Ritti-Dias, R.M., Rivera, J.A., Robinson, S.M., Robitaille, C., Rodríguez-Artalejo, F., Del Cristo Rodriguez-Perez, M., Rodríguez-Villamizar, L.A., Rojas-Martinez, R., Rojroongwasinkul, N., Romaguera, D., Ronkainen, K., Rosengren, A., Rouse, I., Rubinstein, A., Rühli, F.J., Rui, O., Ruiz-Betancourt, B.S., Horimoto, A.R.V.R., Rutkowski, M., Sabanayagam, C., Sachdev, H.S., Saidi, O., Salanave, B., Martinez, E.S., Salomaa, V., Salonen, J.T., Salvetti, M., Sánchez-Abanto, J., Sandjaja, Sans, S., Santos, D.A., Santos, O., Dos Santos, R.N., Santos, R., Sardinha, L.B., Sarrafzadegan, N., Saum, K.U., Savva, S.C., Scazufca, M., Rosario, A.S., Schargrodsky, H., Schienkiewitz, A., Schmidt, I.M., Schneider, I.J., Schultsz, C., Schutte, A.E., Sein, A.A., Sen, A., Senbanjo, I.O., Sepanlou, S.G., Shalnova, S.A., Shaw, J.E., Shibuya, K., Shin, Y., Shiri, R., Siantar, R., Sibai, A.M., Silva, A.M., Silva, D.A.S., Simon, M., Simons, J., Simons, L.A., Sjostrom, M., Slowikowska-Hilczer, J., Slusarczyk, P., Smeeth, L., Smith, M.C., Snijder, M.B., So, H.K., Sobngwi, E., Söderberg, S., Soekatri, M.Y.E., Solfrizzi, V., Sonestedt, E., Sørensen, T.I.A., Sorić, M., Jérome, C.S., Soumare, A., Staessen, J.A., Starc, G., Stathopoulou, M.G., Staub, K., Stavreski, B., Steene-Johannessen, J., Stehle, P., Stein, A.D., Stergiou, G.S., Stessman, J., Stieber, J., Stöckl, D., Stocks, T., Stokwiszewski, J., Stratton, G., Strufaldi, M.W., Sun, C.A., Sundström, J., Sung, Y.T., Sunyer, J., Suriyawongpaisal, P., Swinburn, B.A., Sy, R.G., Szponar, L., Tai, E.S., Tammesoo, M.L., Tamosiunas, A., Tang, L., Tang, X., Tanser, F., Tao, Y., Tarawneh, M., Tarp, J., Tarqui-Mamani, C.B., Taylor, A., Tchibindat, F., Thijs, L., Thuesen, B.H., Tjonneland, A., Tolonen, H.K., Tolstrup, J.S., Topbas, M., Topór-Madry, R., Torrent, M., Traissac, P., Trichopoulou, A., Trichopoulos, D., Trinh, O.T.H., Trivedi, A., Tshepo, L., Tulloch-Reid, M.K., Tuomainen, T.P., Tuomilehto, J., Tynelius, P., Tzotzas, T., Tzourio, C., Ueda, P., Ukoli, F.A.M., Ulmer, H., Unal, B., Valdivia, G., Vale, S., Valvi, D., Van Der Schouw, Y.T., Van Herck, K., Van Minh, H., Van Valkengoed, I.G.M., Vanderschueren, D., Vanuzzo, D., Vatten, L., Vega, T., Velasquez-Melendez, G., Veronesi, G., Monique Verschuren, W.M., Viegi, G., Viet, L., Viikari-Juntura, E., Vineis, P., Vioque, J., Virtanen, J.K., Visvikis-Siest, S., Viswanathan, B., Vollenweider, P., Voutilainen, S., Vrijheid, M., Wade, A.N., Wagner, A., Walton, J., Mohamud, W.N.W., Wang, M.D., Wang, Q.,

Wang, Y.X., Wannamethee, S.G., Wareham, N., Weerasekera, D., Whincup, P.H., Widhalm, K., Widyahening, I.S., Wiecek, A., Wilks, R.J., Willeit, J., Wojtyniak, B., Wong, J.E., Wong, T.Y., Woo, J., Woodward, M., Wu, F.C., Wu, J.F., Wu, S.L., Xu, H., Xu, L., Yamborisut, U., Yan, W., Yang, X., Yardim, N., Ye, X., Yiallouros, P.K., Yoshihara, A., You, Q.S., Younger-Coleman, N.O., Yusoff, A.F., Zainuddin, A.A., Zambon, S., Zdrojewski, T., Zeng, Y., Zhao, D., Zhao, W., Zheng, Y., Zhou, M., Zhu, D., Zimmermann, E. and Cisneros, J.Z. 2016. Trends in adult body-mass index in 200 countries from 1975 to 2014: A pooled analysis of 1698 population-based measurement studies with 19.2 million participants. *The Lancet*. **387**(10026), pp.1377–1396.

Chambers, J.C., Eda, S., Bassett, P., Karim, Y., Thompson, S.G., Ruth Gallimore, J., Pepys, M.B. and Kooner, J.S. 2001. C-Reactive Protein, Insulin Resistance, Central Obesity, and Coronary Heart Disease Risk in Indian Asians From the United Kingdom Compared With European Whites. *Circulation*. **104**, pp.145–150.

Chan, D.C., Chen, M.M., Ooi, E.M.M. and Watts, G.F. 2008. An ABC of apolipoprotein C-III: A clinically useful new cardiovascular risk factor? *International Journal of Clinical Practice*. **62**(5), pp.799–809.

Charla, E., Mercer, J., Maffia, P. and Nicklin, S.A. 2020. Extracellular vesicle signalling in atherosclerosis. *Cellular Signalling*. **75**, p.109751.

Charlton, F., Gabriele Bobek, X., Stait-Gardner, T., Price, W.S., Mirabito Colafella, K.M., Xu, B., Makris, A., Rye, K.-A., Hennessy, A. and Colafella, M.K. 2017. The protective effect of apolipoprotein in models of trophoblast invasion and preeclampsia. *Am J Physiol Regul Integr Comp Physiol*. **312**, pp.40–48.

Chen, L.Y. and Mehta, J.L. 1994. Inhibitory effect of high-density lipoprotein on platelet function is mediated by increase in nitric oxide synthase activity in platelets. *Life Sciences*. **55**(23), pp.1815–1821.

Cheung, M.C. and Albers, J.J. 1984. Characterization of lipoprotein particles isolated by immunoaffinity chromatography. Particles containing A-I and A-II and particles containing A-I but no A-II. *Journal of Biological Chemistry*. **259**(19), pp.12201–12209.

Choi, C.H.J., Barr, W., Zaman, S., Model, C., Park, A., Koenen, M., Lin, Z., Szwed, S.K., Marchildon, F., Crane, A., Carroll, T.S., Molina, H. and Cohen, P. 2022. LRG1 is an adipokine that promotes insulin sensitivity and suppresses inflammation. *eLife*. **11**.

Choi, J.W., Im, M.W. and Pai, S.H. 2002. Nitric Oxide Production Increases during Normal Pregnancy and Decreases in Preeclampsia. *Annals of Clinical & Laboratory Science*. **32**(3), pp.257–263.

Christison, J.K., Rye, K.A. and Stocker, R. 1995. Exchange of oxidized cholesteryl linoleate between LDL and HDL mediated by cholesteryl ester transfer protein. *Journal of Lipid Research*. **36**(9), pp.2017–2026.

Christoffersen, C., Obinata, H., Kumaraswamy, S.B., Galvani, S., Ahnström, J., Sevvana, M., Egerer-Sieber, C., Muller, Y.A., Hla, T., Nielsen, L.B. and Dahlbäck, B. 2011. Endothelium-protective sphingosine-1-phosphate provided by HDL-associated apolipoprotein M. *Proceedings of the National Academy of Sciences*. **108**(23), pp.9613–9618.

Chung, D.W., Chen, J., Ling, M., Fu, X., Blevins, T., Parsons, S., Le, J., Harris, J., Martin, T.R., Konkle, B.A., Zheng, Y. and Lopez, J.A. 2016. High-density lipoprotein modulates thrombosis by preventing von Willebrand factor self-Association and subsequent platelet adhesion. *Blood*. **127**(5), pp.637–645.

Claire Wang, Y., McPherson, K., Marsh, T., Gortmaker, S.L. and Brown, M. 2011. *Obesity 2 Health and economic burden of the projected obesity trends in the USA and the UK* [Online]. Available from: www.thelancet.com.

Clausen, T.D., Mathiesen, E.R., Hansen, T., Pedersen, O., Jensen, D.M., Lauenborg, J. and Damm, P. 2008. High Prevalence of Type 2 Diabetes and Pre-Diabetes in Adult Offspring of Women With Gestational Diabetes Mellitus or Type 1 Diabetes: The role of intrauterine hyperglycemia. *Diabetes Care*. **31**(2), pp.340–346.

Clemente-Postigo, M., Queipo-Ortuño, M.I., Fernandez-Garcia, D., Gomez-Huelgas, R., Tinahones, F.J. and Cardona, F. 2011. Adipose Tissue Gene Expression of Factors Related to Lipid Processing in Obesity. *PLOS ONE*. **6**(9), pp.e24783-.

Cockerill, G.W., Rye, K.A., Gamble, J.R., Vadas, M.A. and Barter, P.J. 1995. High-density lipoproteins inhibit cytokine-induced expression of endothelial cell adhesion molecules. *Arteriosclerosis, Thrombosis, and Vascular Biology*. **15**(11), pp.1987–1994.

Cohn, J.S., Rodriguez, C., Jacques, H., Tremblay, M. and Davignon, J. 2004. Storage of human plasma samples leads to alterations in the lipoprotein distribution of apoC-III and apoE. *Journal of Lipid Research*. **45**(8), pp.1572–1579.

Conn, V.S., Koopman, R.J., Ruppar, T.M., Phillips, L.J., Mehr, D.R. and Hafdahl, A.R. 2014. Insulin Sensitivity Following Exercise Interventions: Systematic Review and Meta-Analysis of Outcomes Among Healthy Adults. *Journal of Primary Care & Community Health*. **5**(3), pp.211–222.

Connelly, P.W., Maguire, G.F., Nash, M.M., Rapi, L., Yan, A.T. and Prasad, G.V.R. 2012. Paraoxonase 1 Phenotype and Mass in South Asian versus Caucasian Renal Transplant Recipients. *Journal of Lipids*. **2012**, pp.1–5.

Cornelius, D.C. 2018. Preeclampsia: From inflammation to immunoregulation. *Clinical Medicine Insights: Blood Disorders*. **11**.

Crow, J.A., Meek, E.C., Wills, R.W. and Chambers, J.E. 2018. A case-control study: The association of serum paraoxonase 1 activity and concentration with the development of type 2 diabetes mellitus. *Diabetes/Metabolism Research and Reviews*. **34**(3).

Crowther, C.A., Hiller, J.E., Moss, J.R., McPhee, A.J., Jeffries, W.S. and Robinson, J.S. 2005. Effect of Treatment of Gestational Diabetes Mellitus on Pregnancy Outcomes. *New England Journal of Medicine*. **352**(24), pp.2477–2486.

Csonka, C., Páli, T., Bencsik, P., Görbe, A., Ferdinandy, P. and Csont, T. 2015. Measurement of NO in biological samples. *British Journal of Pharmacology*. **172**(6), pp.1620–1632.

Cushing, E.M., Chi, X., Sylvers, K.L., Shetty, S.K., Potthoff, M.J. and Davies, B.S.J. 2017. Angiopoietin-like 4 directs uptake of dietary fat away from adipose during fasting. *Molecular Metabolism*. **6**(8), pp.809–818.

Cyr, A.R., Huckaby, L. V, Shiva, S.S. and Zuckerbraun, B.S. 2020. Nitric Oxide and Endothelial Dysfunction. *Critical Care Clinics*. **36**(2), pp.307–321.

Danaei, G, Finucane, M., Paciorek, C J, Lu, Y, Singh, G M, Lin, J K, Farzadfar, F, Ba, R., Cowan, M J, Riley, L M, Khang, Y-H, Hubert,) ;, Danaei, Goodarz, Finucane, M.M., Lu, Yuan, Singh, Gitanjali M, Cowan, Melanie J, Paciorek, Christopher J, Lin, John K, Farzadfar, Farshad, Khang, Young-Ho, Stevens, G.A., Rao, M., Ali, M.K., Riley, Leanne M, Robinson, C.A. and Ezzati, M. 2011. National, regional, and global trends in fasting plasma glucose and diabetes prevalence since 1980: systematic analysis of health examination

surveys and epidemiological studies with 370 country-years and 2·7 million participants. *The Lancet*. **378**, pp.31–40.

Danielsson, A., Fagerholm, S., Öst, A., Franck, N., Kjolhede, P., Nystrom, F.H. and Strålfors, P. 2009. Short-Term Overeating Induces Insulin Resistance in Fat Cells in Lean Human Subjects. *Molecular Medicine*. **15**(7), pp.228–234.

Davidson, W.S., Shah, A.S., Sexmith, H. and Gordon, S.M. 2022. The HDL Proteome Watch: Compilation of studies leads to new insights on HDL function. *Biochimica et Biophysica Acta (BBA) - Molecular and Cell Biology of Lipids*. **1867**(2), p.159072.

Davies, B.S.J., Beigneux, A.P., Barnes, R.H., Tu, Y., Gin, P., Weinstein, M.M., Nobumori, C., Nyrén, R., Goldberg, I., Olivecrona, G., Bensadoun, A., Young, S.G. and Fong, L.G. 2010. GPIHBP1 is responsible for the entry of lipoprotein lipase into capillaries. *Cell Metabolism*. **12**(1), pp.42–52.

Davies, I.G., Graham, J.M. and Griffin, B.A. 2003. Rapid Separation of LDL Subclasses by Iodixanol Gradient Ultracentrifugation. *Clinical Chemistry*. **49**(11), pp.1865–1872.

Denimal, D., Monier, S., Brindisi, M.C., Petit, J.M., Bouillet, B., Nguyen, A., Demizieux, L., Simoneau, I., Pais De Barros, J.P., Vergès, B. and Duvillard, L. 2017. Impairment of the ability of hdl from patients with metabolic syndrome but without diabetes mellitus to activate eNOS: Correction by S1P enrichment. *Arteriosclerosis, Thrombosis, and Vascular Biology*. **37**(5), pp.804–811.

Desoye, G. and Nolan, C.J. 2016. The fetal glucose steal: an underappreciated phenomenon in diabetic pregnancy. *Diabetologia*. **59**(6), pp.1089–1094.

Dhar, J. and Chakrabarti, P. 2014. Defining the loop structures in proteins based on composite β-turn mimics. *Protein Engineering, Design and Selection*. **28**(6), pp.153–161.

Dixon, J.L. and Ginsberg, H.N. 1993. Regulation of hepatic secretion of apolipoprotein B-containing lipoproteins: information obtained from cultured liver cells. *Journal of Lipid Research*. **34**(2), pp.167–179.

Doğan, K., Şeneş, M., Karaca, A., Kayalp, D., Kan, S., Gülçelik, N.E., Aral, Y. and Yücel, D. 2021. HDL subgroups and their paraoxonase-1 activity in the obese, overweight and normal weight subjects. *International Journal of Clinical Practice*. **75**(12).

Doherty, T.M., Asotra, K., Fitzpatrick, L.A., Qiao, J.-H., Wilkin, D.J., Detrano, R.C., Dunstan, C.R., Shah, P.K. and Rajavashisth, T.B. 2003. Calcification in atherosclerosis: Bone biology and chronic inflammation at the arterial crossroads. *Proceedings of the National Academy of Sciences*. **100**(20), pp.11201–11206.

Dørup, I., Skajaa, K. and Sørensen, K.E. 1999. Normal pregnancy is associated with enhanced endothelium-dependent flow-mediated vasodilation. *American Journal of Physiology-Heart and Circulatory Physiology*. **276**(3), pp.H821–H825.

Drew, B.G., Duffy, S.J., Formosa, M.F., Natoli, A.K., Henstridge, D.C., Penfold, S.A., Thomas, W.G., Mukhamedova, N., De Courten, B., Forbes, J.M., Yap, F.Y., Kaye, D.M., Ven Hall, G., Febbraio, M.A., Kemp, B.E., Sviridov, D., Steinberg, G.R. and Kingwell, B.A. 2009. High-density lipoprotein modulates glucose metabolism in patients with type 2 diabetes mellitus. *Circulation*. **119**(15), pp.2103–2111.

Drew, B.G., Fidge, N.H., Gallon-Beaumier, G., Kemp, B.E. and Kingwell, B.A. 2004. High-density lipoprotein and apolipoprotein AI increase endothelial NO

synthase activity by protein association and multisite phosphorylation. *Proceedings of the National Academy of Sciences*. **101**(18), pp.6999–7004.
Ebeling, P., Koistinen, H.A. and Koivisto, V.A. 1998. Insulin-independent glucose transport regulates insulin sensitivity. *FEBS Letters*. **436**(3), pp.301–303.
Ebersole, J.L. and Cappelli, D. 2000. Acute-phase reactants in infections and inflammatory diseases. *Periodontology 2000*. **23**(1), pp.19–49.
Ebtehaj, S., Gruppen, E.G., Parvizi, M., Tietge, U.J.F. and Dullaart, R.P.F. 2017. The anti-inflammatory function of HDL is impaired in type 2 diabetes: Role of hyperglycemia, paraoxonase-1 and low grade inflammation. *Cardiovascular Diabetology*. **16**(1), pp.1–9.
von Eckardstein, A., Nordestgaard, B.G., Remaley, A.T. and Catapano, A.L. 2023. High-density lipoprotein revisited: biological functions and clinical relevance. *European Heart Journal*. **44**(16), pp.1394–1407.
Einarson, T.R., Acs, A., Ludwig, C. and Panton, U.H. 2018. Prevalence of cardiovascular disease in type 2 diabetes: A systematic literature review of scientific evidence from across the world in 2007-2017. *Cardiovascular Diabetology*. **17**(1), pp.1–19.
Einbinder, Y., Biron-Shental, T., Agassi-Zaitler, M., Tzadikevitch-Geffen, K., Vaya, J., Khatib, S., Ohana, M., Benchetrit, S. and Zitman-Gal, T. 2018. High-density lipoproteins (HDL) composition and function in preeclampsia. *Archives of Gynecology and Obstetrics*. **298**(2), pp.405–413.
Engin, B., Willis, S.A., Malaikah, S., Sargeant, J.A., Yates, T., Gray, L.J., Aithal, G.P., Stensel, D.J. and King, J.A. 2022. The effect of exercise training on adipose tissue insulin sensitivity: A systematic review and meta-analysis. *Obesity Reviews*. **23**(7), p.e13445.
Ensign, W., Hill, N. and Heward, C.B. 2006. Disparate LDL phenotypic classification among 4 different methods assesing LDL particle characteristics. *Clinical Chemistry*. **52**(9), pp.1722–1727.
Erdmann, J., Kallabis, B., Oppel, U., Sypchenko, O., Wagenpfeil, S. and Schusdziarra, V. 2008. Development of hyperinsulinemia and insulin resistance during the early stage of weight gain. *American Journal of Physiology-Endocrinology and Metabolism*. **294**(3), pp.E568–E575.
Erickson, H.P. 2009. Size and shape of protein molecules at the nanometer level determined by sedimentation, gel filtration, and electron microscopy. *Biological Procedures Online*. **11**(1), pp.32–51.
Escolà-Gil, J.C., Julve, J., Griffin, B.A., Freeman, D. and Blanco-Vaca, F. 2015. HDL and lifestyle interventions *In*: *Handbook of Experimental Pharmacology*. Springer New York LLC, pp.569–592.
Everson, S., Glodberg, D.E., Helmrich, S.P., Lakka, T.A., Lynch, J.W., Kaplan, G.A. and Salonen, J.T. 1998. Weight Gain and the Risk of Developing Insulin Resistance Syndrome. *Diabetes Care*. **21**(10), pp.1637–1643.
Van den Eynde, M.D.G., Streese, L., Houben, A.J.H.M., Stehouwer, C.D.A., Scheijen, J.L.J.M., Schalkwijk, C.G., Hanssen, N.M.J. and Hanssen, H. 2020. Physical activity and markers of glycation in older individuals: Data from a combined cross-sectional and randomized controlled trial (EXAMIN AGE). *Clinical Science*. **134**(9), pp.1095–1105.
Fåhraeus, L., Larsson-Cohn, U. and Wallentin, L. 1985. Plasma lipoproteins including high density lipoprotein subfractions during normal pregnancy. *Obstetrics and Gynecology*. **66**(4), pp.468–472.
Fattah, C., Farah, N., Barry, S.C., O'Connor, N., Stuart, B. and Turner, M.J. 2010. Maternal weight and body composition in the first trimester of

pregnancy. *Acta Obstetricia et Gynecologica Scandinavica*. **89**(7), pp.952–955.

Faulkner, A. 2021. Trans-endothelial trafficking of metabolic substrates and its importance in cardio-metabolic disease. *Biochemical Society Transactions*. **49**(1), pp.507–517.

Ford, E.S. 2005. Risks for All-Cause Mortality, Cardiovascular Disease, and Diabetes Associated With the Metabolic Syndrome: A summary of the evidence. *Diabetes Care*. **28**(7), pp.1769–1778.

Fox, C.S., Massaro, J.M., Hoffmann, U., Pou, K.M., Maurovich-Horvat, P., Liu, C.Y., Vasan, R.S., Murabito, J.M., Meigs, J.B., Cupples, L.A., D'Agostino, R.B. and O'Donnell, C.J. 2007. Abdominal visceral and subcutaneous adipose tissue compartments: Association with metabolic risk factors in the framingham heart study. *Circulation*. **116**(1), pp.39–48.

Fré Nais, R., Ouguerram, K., Maugeais, C., Mahot, P., Maugè Re, P., Krempf, M. and Magot, T. 1997. *High density lipoprotein apolipoprotein AI kinetics in NIDDM: a stable isotope study*.

Fries, E. and Blom, A.M. 2000. Bikunin - not just a plasma proteinase inhibitor. *The International Journal of Biochemistry & Cell Biology* . **32**, pp.125–137.

Frost, M., Nielsen, T.L., Brixen, K. and Andersen, M. 2015. Peak muscle mass in young men and sarcopenia in the ageing male. *Osteoporosis International*. **26**(2), pp.749–756.

Fryirs, M.A., Barter, P.J., Appavoo, M., Tuch, B.E., Tabet, F., Heather, A.K. and Rye, K.-A. 2010. Effects of High-Density Lipoproteins on Pancreatic β-Cell Insulin Secretion. *Arteriosclerosis, Thrombosis, and Vascular Biology*. **30**(8), pp.1642–1648.

Fuki, I. V, Blanchard, N., Jin, W., Marchadier, D.H.L., Millar, J.S., Glick, J.M. and Rader, D.J. 2003. Endogenously Produced Endothelial Lipase Enhances Binding and Cellular Processing of Plasma Lipoproteins via Heparan Sulfate Proteoglycan-mediated Pathway *. *Journal of Biological Chemistry*. **278**(36), pp.34331–34338.

Furlaneto, C.J., Ribeiro, F.P., Hatanaka, E., Souza, G.M., Cassatella, M.A. and Campa, A. 2002. Apolipoproteins A-I and A-II downregulate neutrophil functions. *Lipids*. **37**(9), pp.925–928.

Gaidukov, L., R. I, V., Yacobson, S., Rosenblat, M., Aviram, M. and Tawfik, D.S. 2010. ApoE Induces Serum Paraoxonase PON1 Activity and Stability Similar to ApoA-I. *Biochemistry*. **49**(3), pp.532–538.

Gao, X. 2023. *Adipocyte hyperplasia and hypertrophy in the development of Type 2 Diabetes Mellitus*. University of Glasgow.

Garner, B., Waldeck, A.R., Witting, P.K., Rye, K.-A. and Stocker, R. 1998. Oxidation of High Density Lipoproteins: II. EVIDENCE FOR DIRECT REDUCTION OF LIPID HYDROPEROXIDES BY METHIONINE RESIDUES OF APOLIPOPROTEINS AI AND AII*. *Journal of Biological Chemistry*. **273**(11), pp.6088–6095.

Garvey, W.T., Kwon, S., Zheng, D., Shaughnessy, S., Wallace, P., Hutto, A., Pugh, K., Jenkins, A.J., Klein, R.L. and Liao, Y. 2003. *Effects of Insulin Resistance and Type 2 Diabetes on Lipoprotein Subclass Particle Size and Concentration Determined by Nuclear Magnetic Resonance* [Online]. Available from: http://diabetesjournals.org/diabetes/article-pdf/52/2/453/660528/db0203000453.pdf.

Gastaldelli, A., Toschi, E., Pettiti, M., Frascerra, S., Quiñones-Galvan, A., Sironi, A.M., Natali, A. and Ferrannini, E. 2001. Effect of Physiological Hyperinsulinemia on Gluconeogenesis in Nondiabetic Subjects and in Type 2 Diabetic Patients. *Diabetes*. **50**(8), pp.1807–1812.

Del Gaudio, I., Hendrix, S., Christoffersen, C. and Wadsack, C. 2020. Neonatal HDL counteracts placental vascular inflammation via S1P–S1PR1 axis. *International Journal of Molecular Sciences*. **21**(3).

Gerber, P.A. and Rutter, G.A. 2016. The Role of Oxidative Stress and Hypoxia in Pancreatic Beta-Cell Dysfunction in Diabetes Mellitus. *Antioxidants & Redox Signaling*. **26**(10), pp.501–518.

Goldberg, I.J., Scheraldi, C.A., Yacoub, L.K., Saxena, U. and Bisgaier, C.L. 1990. Lipoprotein ApoC-II activation of lipoprotein lipase. Modulation by apolipoprotein A-IV. *Journal of Biological Chemistry*. **265**(8), pp.4266–4272.

Golizeh, M., Lee, K., Ilchenko, S., Ösme, A., Bena, J., Sadygov, R.G., Kashyap, S. and Kasumov, T. 2017. Increased serotransferrin and ceruloplasmin turnover in diet-controlled patients with type 2 diabetes. *Free Radical Biology and Medicine*. **113**, pp.461–469.

Gordon, S.M. and Remaley, A.T. 2017. High density lipoproteins are modulators of protease activity: Implications in inflammation, complement activation, and atherothrombosis. *Atherosclerosis*. **259**, pp.104–113.

Gordon, T., Castelli, William P, Hjortland, M.C., Kannel, W.B. and Dawber, T.R. 1977. High density lipoprotein as a protective factor against coronary heart disease: The Framingham study. *The American Journal of Medicine*. **62**(5), pp.707–714.

Gordon, T., Castelli, William P., Hjortland, M.C., Kannel, W.B. and Dawber, T.R. 1977. High density lipoprotein as a protective factor against coronary heart disease. The Framingham study. *The American Journal of Medicine*. **62**(5), pp.707–714.

Gourgari, E., Ma, J., Playford, M.P., Mehta, N.N., Goldman, R., Remaley, A.T. and Gordon, S.M. 2019. Proteomic alterations of HDL in youth with type 1 diabetes and their associations with glycemic control: A case-control study. *Cardiovascular Diabetology*. **18**(1).

Goussetis, E., Spiropoulos, A., Tsironi, M., Skenderi, K., Margeli, A., Graphakos, S., Baltopoulos, P. and Papassotiriou, I. 2009. Spartathlon, a 246 kilometer foot race: Effects of acute inflammation induced by prolonged exercise on circulating progenitor reparative cells. *Blood Cells, Molecules, and Diseases*. **42**(3), pp.294–299.

Goyal, S., Tanigawa, Y., Zhang, W., Chai, J.-F., Almeida, M., Sim, X., Lerner, M., Chainakul, J., Ramiu, J.G., Seraphin, C., Apple, B., Vaughan, A., Muniu, J., Peralta, J., Lehman, D.M., Ralhan, S., Wander, G.S., Singh, J.R., Mehra, N.K., Sidorov, E., Peyton, M.D., Blackett, P.R., Curran, J.E., Tai, E.S., van Dam, R., Cheng, C.-Y., Duggirala, R., Blangero, J., Chambers, J.C., Sabanayagam, C., Kooner, J.S., Rivas, M.A., Aston, C.E. and Sanghera, D.K. 2021. APOC3 genetic variation, serum triglycerides, and risk of coronary artery disease in Asian Indians, Europeans, and other ethnic groups. *Lipids in Health and Disease*. **20**(1), p.113.

Graham, J., Higgins, J.A., Gillott, T., Taylor, T., Wilkinsonb, J., Ford, T. and Billington, D. 1996. A novel method for the rapid separation of plasma lipoproteins using self-generating gradients of iodixanol. *Atherosclerosis*. **124**, pp.125–135.

Green, C.J., Marjot, T., Walsby-Tickle, J., Charlton, C., Cornfield, T., Westcott, F., Pinnick, K.E., Moolla, A., Hazlehurst, J.M., McCullagh, J., Tomlinson, J.W. and Hodson, L. 2022. Metformin maintains intrahepatic triglyceride content through increased hepatic de novo lipogenesis. *European Journal of Endocrinology*. **186**(3), pp.367–377.

Griffiths, K., Pazderska, A., Ahmed, M., Mcgowan, A., Maxwell, A.P., Mceneny, J., Gibney, J. and Mckay, G.J. 2017. Type 2 Diabetes in Young Females Results in Increased Serum Amyloid A and Changes to Features of High Density Lipoproteins in Both HDL2 and HDL3. *Journal of Diabetes Research*. **2017**.

Groot, P.H.E., Oerlemans, M.C. and Scheek, L.M. 1978. Triglyceridase and phospholipase A1 activities of rat-heart lepoprotein lipase: Influence of apolipoproteins C-II and C-III. *Biochimica et Biophysica Acta (BBA) - Lipids and Lipid Metabolism*. **530**(1), pp.91–98.

Gruaz, L., Delucinge-Vivier, C., Descombes, P., Dayer, J.-M. and Burger, D. 2010. Blockade of T Cell Contact-Activation of Human Monocytes by High-Density Lipoproteins Reveals a New Pattern of Cytokine and Inflammatory Genes. *PLOS ONE*. **5**(2), pp.e9418-.

Guérin, M., Le Goff, W., Lassel, T.S., Van Tol, A., Steiner, G. and Chapman, M.J. 2001. Proatherogenic Role of Elevated CE Transfer From HDL to VLDL1 and Dense LDL in Type 2 Diabetes. *Arteriosclerosis, Thrombosis, and Vascular Biology*. **21**(2), pp.282–288.

Guglielmi, V., Maresca, L., D'Adamo, M., Di Roma, M., Lanzillo, C., Federici, M., Lauro, D., Preziosi, P., Bellia, A. and Sbraccia, P. 2014. Age-Related Different Relationships between Ectopic Adipose Tissues and Measures of Central Obesity in Sedentary Subjects. *PLOS ONE*. **9**(7), pp.e103381-.

Guh, D.P., Zhang, W., Bansback, N., Amarsi, Z., Birmingham, C.L. and Anis, A.H. 2009. The incidence of co-morbidities related to obesity and overweight: A systematic review and meta-analysis. *BMC Public Health*. **9**.

Haeusler, R.A., McGraw, T.E. and Accili, D. 2018. Biochemical and cellular properties of insulin receptor signalling. *Nature Reviews Molecular Cell Biology*. **19**(1), pp.31–44.

Haid, M., Muschet, C., Wahl, S., Römisch-Margl, W., Prehn, C., Möller, G. and Adamski, J. 2018. Long-Term Stability of Human Plasma Metabolites during Storage at −80 °C. *Journal of Proteome Research*. **17**(1), pp.203–211.

Han, R., Lai, R., Ding, Q., Wang, Z., Luo, X., Zhang, Y., Cui, G., He, J., Liu, W. and Chen, Y. 2007. Apolipoprotein A-I stimulates AMP-activated protein kinase and improves glucose metabolism. *Diabetologia*. **50**(9), pp.1960–1968.

Härdfeldt, J., Cariello, M., Simonelli, S., Ossoli, A., Scialpi, N., Piglionica, M., Pasculli, E., Noia, A., Berardi, E., Suppressa, P., Piazzolla, G., Sabbà, C., Calabresi, L. and Moschetta, A. 2022. Abdominal obesity negatively influences key metrics of reverse cholesterol transport. *Biochimica et Biophysica Acta (BBA) - Molecular and Cell Biology of Lipids*. **1867**(2), p.159087.

Harman, N.L., Griffin, B.A. and Davies, I.G. 2013. Separation of the principal HDL subclasses by iodixanol ultracentrifugation. *Journal of Lipid Research*. **54**(8), pp.2273–2281.

Harrison, K. 1997. Iodixanol as a Density Gradient Medium for the Isolation of Motile Spermatozoa. *Journal of Assisted Reproduction and Genetics*. **14**(7).

Harshfield, E.L., Fauman, E.B., Stacey, D., Paul, D.S., Ziemek, D., Ong, R.M.Y., Danesh, J., Butterworth, A.S., Rasheed, A., Sattar, T., Zameer-ul-Asar, Saleem, I., Hina, Z., Ishtiaq, U., Qamar, N., Mallick, N.H., Yaqub, Z., Saghir, T., Rizvi, S.N.H., Memon, A., Ishaq, M., Rasheed, S.Z., Memon, F.-R., Jalal, A., Abbas, S., Frossard, P., Saleheen, D., Wood, A.M., Griffin, J.L. and Koulman, A. 2021. Genome-wide analysis of blood lipid metabolites in

over 5000 South Asians reveals biological insights at cardiometabolic disease loci. *BMC Medicine*. **19**(1), p.232.

Hawkins, C.L. and Davies, M.J. 2019. Detection, identification, and quantification of oxidative protein modifications. *Journal of Biological Chemistry*. **294**(51), pp.19683–19708.

He, S., Ryu, J., Liu, J., Luo, H., Lv, Y., Langlias, P.R., Wen, J., Dong, F., Sun, Z., Xia, W., Lynch, J.L., Duggirala, R., Nicholson, B.J., Zang, M., Shi, Y., Zhang, F., Liu, F., Bai, J. and Dong, L.Q. 2021. LRG1 is an adipokine that mediates obesity-induced hepatosteatosis and insulin resistance. *Journal of Clinical Investigation*. **131**(24:e148545).

Hergenreider, E., Heydt, S., Tréguer, K., Boettger, T., Horrevoets, A.J.G., Zeiher, A.M., Scheffer, M.P., Frangakis, A.S., Yin, X., Mayr, M., Braun, T., Urbich, C., Boon, R.A. and Dimmeler, S. 2012. Atheroprotective communication between endothelial cells and smooth muscle cells through miRNAs. *Nature Publishing Group*. **14**(3), pp.249–256.

Hernáez, Á., Castañer, O., Elosua, R., Pintó, X., Estruch, R., Salas-Salvadó, J., Corella, D., Arós, F., Serra-Majem, L., Fiol, M., Ortega-Calvo, M., Ros, E., Martínez-González, M.Á., De La Torre, R., López-Sabater, M.C. and Fitó, M. 2017. Mediterranean Diet Improves High-Density Lipoprotein Function in High-Cardiovascular-Risk Individuals. *Circulation*. **135**(7), pp.633–643.

Holzer, M., Kern, S., Trieb, M., Trakaki, A. and Marsche, G. 2017. HDL structure and function is profoundly affected when stored frozen in the absence of cryoprotectants. *Journal of Lipid Research*. **58**(11), pp.2220–2228.

Hovingh, G.K., Rader, D.J. and Hegele, R.A. 2015. HDL re-examined. *Current Opinion in Lipidology*. **26**(2), pp.127–132.

Hsiao, W.-Y. and Guertin, D.A. 2019. De Novo Lipogenesis as a Source of Second Messengers in Adipocytes. *Current Diabetes Reports*. **19**(11), p.138.

Huang, H., Ren, P., Zhao, Y., Weng, H., Jia, C., Yu, F. and Nie, Y. 2023. Low shear stress induces inflammatory response via CX3CR1/NF-κB signal pathway in human umbilical vein endothelial cells. *Tissue and Cell*. **82**.

Huang, J.-K. and Lee, H.-C. 2022. Emerging Evidence of Pathological Roles of Very-Low-Density Lipoprotein (VLDL). *International Journal of Molecular Sciences*. **23**(8).

Huang, K.T., Lin, C.C., Tsai, M.C., Chen, K. Den and Chiu, K.W. 2018. Pigment epithelium-derived factor in lipid metabolic disorders. *Biomedical Journal*. **41**(2), pp.102–108.

Huda, S.S., Forrest, R., Paterson, N., Jordan, F., Sattar, N. and Freeman, D.J. 2014. In Preeclampsia, Maternal Third Trimester Subcutaneous Adipocyte Lipolysis Is More Resistant to Suppression by Insulin Than in Healthy Pregnancy. *Hypertension*. **63**(5), pp.1094–1101.

Huda, S.S., Jordan, F., Bray, J., Love, G., Payne, R., Sattar, N. and Freeman, D.J. 2017. Visceral adipose tissue activated macrophage content and inflammatory adipokine secretion is higher in pre-eclampsia than in healthy pregnancys. *Clinical Science*. **131**(13), pp.1529–1540.

Huda, S.S., Sattar, N. and Freeman, D.J. 2009. Lipoprotein metabolism and vascular complications in pregnancy. *Clinical Lipidology*. **4**(1), pp.91–102.

Hussain, M.M. 2014. Intestinal lipid absorption and lipoprotein formation. *Current Opinion in Lipidology*. **25**(3).

Huuskonen, J., Olkkonen, V.M., Jauhiainen, M. and Ehnholm, C. 2001. The impact of phospholipid transfer protein (PLTP) on HDL metabolism. *Atherosclerosis*. **155**(2), pp.269–281.

Igarashi, J., Erwin, P.A., Dantas, A.P. V, Chen, H. and Michel, T. 2003. VEGF induces S1P1 receptors in endothelial cells: Implications for cross-talk between sphingolipid and growth factor receptors. *Proceedings of the National Academy of Sciences*. **100**(19), pp.10664–10669.

Iliodromiti, S., McLaren, J., Ghouri, N., Miller, M.R., Dahlqvist Leinhard, O., Linge, J., Ballantyne, S., Platt, J., Foster, J., Hanvey, S., Gujral, U.P., Kanaya, A., Sattar, N., Lumsden, M.A. and Gill, J.M.R. 2023. Liver, visceral and subcutaneous fat in men and women of South Asian and white European descent: a systematic review and meta-analysis of new and published data. *Diabetologia*. **66**(1), pp.44–56.

Inoguchi, T., Li, P., Umeda, F., Yu, H.Y., Kakimoto, M., Imamura, M., Aoki, T., Etoh, T., Hashimoto, T., Naruse, M., Sano, H., Utsumi, H. and Nawata, H. 2000. High glucose level and free fatty acid stimulate reactive oxygen species production through protein kinase C--dependent activation of NAD(P)H oxidase in cultured vascular cells. *Diabetes*. **49**(11), pp.1939–1945.

Janeway, C.J., Travers P, Walport M and Shlomchik, M. 2001. *Immunobiology: The Immune System in Health and Disease* 5th ed. New York: Garland Science.

Jansen, F., Yang, X., Baumann, K., Przybilla, D., Schmitz, T., Flender, A., Paul, K., Alhusseiny, A., Nickenig, G. and Werner, N. 2015. Endothelial microparticles reduce ICAM-1 expression in a microRNA-222-dependent mechanism. *Journal of Cellular and Molecular Medicine*. **19**(9), pp.2202–2214.

Jansen, F., Yang, X., Hoelscher, M., Cattelan, A., Schmitz, T., Proebsting, S., Wenzel, D., Vosen, S., Franklin, B.S., Fleischmann, B.K., Nickenig, G. and Werner, N. 2013. Endothelial microparticle-mediated transfer of microRNA-126 promotes vascular endothelial cell repair via spred1 and is abrogated in glucose-damaged endothelial microparticles. *Circulation*. **128**(18), pp.2026–2038.

Jarvie, E., Hauguel-de-Mouzon, S., Nelson, S.M., Sattar, N., Catalano, P.M. and Freeman, D.J. 2010. Lipotoxicity in obese pregnancy and its potential role in adverse pregnancy outcome and obesity in the offspring. *Clinical Science*. **119**(3), pp.123–129.

Jeon, H. and Blacklow, S.C. 2005. Structure and physiologic function of the low-density lipoprotein receptor. *Annual Review of Biochemistry*. **74**(1), pp.535–562.

De Juan-Franco, E., Pérez, A., Ribas, V., Sánchez-Hernández, J.A., Blanco-Vaca, F., Ordóñez-Llanos, J. and Sánchez-Quesada, J.L. 2009. Standardization of a method to evaluate the antioxidant capacity of high-density lipoproteins. *International Journal of Biomedical Science*. **5**(4), pp.402–410.

Jumper, J., Evans, R., Pritzel, A., Green, T., Figurnov, M., Ronneberger, O., Tunyasuvunakool, K., Bates, R., Žídek, A., Potapenko, A., Bridgland, A., Meyer, C., Kohl, S.A.A., Ballard, A.J., Cowie, A., Romera-Paredes, B., Nikolov, S., Jain, R., Adler, J., Back, T., Petersen, S., Reiman, D., Clancy, E., Zielinski, M., Steinegger, M., Pacholska, M., Berghammer, T., Bodenstein, S., Silver, D., Vinyals, O., Senior, A.W., Kavukcuoglu, K., Kohli, P. and Hassabis, D. 2021. Highly accurate protein structure prediction with AlphaFold. *Nature*. **596**(7873), pp.583–589.

Kajani, S., Curley, S. and McGillicuddy, F.C. 2018. Unravelling hdl—looking beyond the cholesterol surface to the quality within. *International Journal of Molecular Sciences*. **19**(7), pp.1–23.

Kalyani, R.R., Metter, E.J., Xue, Q.-L., Egan, J.M., Chia, C.W., Studenski, S., Shaffer, N.C., Golden, S., Al-Sofiani, M., Florez, H. and Ferrucci, L. 2020. The Relationship of Lean Body Mass With Aging to the Development of Diabetes. *Journal of the Endocrine Society*. **4**(7), p.bvaa043.

Kannel, W.B., Castelli, W.P., Gordon, T. and McNamara, P.M. 1971. Serum Cholesterol, Lipoproteins, and the Risk of Coronary Heart Disease: The Framingham Study. *Annals of Internal Medicine*. **74**(1), pp.1–12.

Karlsson, H., Leanderson, P., Tagesson, C. and Lindahl, M. 2005. Lipoproteomics II: Mapping of proteins in high-density lipoprotein using two-dimensional gel electrophoresis and mass spectrometry. *Proteomics*. **5**(5), pp.1431–1445.

Karpe, F., Olivecrona, T., Walldius, G. and Hamsten, A. 1992. Lipoprotein lipase in plasma after an oral fat load: relation to free fatty acids. *Journal of Lipid Research*. **33**(7), pp.975–984.

Kautzky-Willer, A., Prager, R., Waldhäusl, W., Pacini, G., Thomaseth, K., Wagner, O.F., Ulm, M., Streli, C. and Ludvik, B. 1997. Pronounced Insulin Resistance and Inadequate ß-cell Secretion Characterize Lean Gestational Diabetes During and After Pregnancy. *Diabetes Care*. **20**(11), pp.1717–1723.

Kelley, G.A. and Kelley, K. S. 2006. Aerobic exercise and HDL2-C: A meta-analysis of randomized controlled trials. *Atherosclerosis*. **184**(1), pp.207–215.

Kelley, G.A. and Kelley, Kristi S. 2006a. Aerobic exercise and lipids and lipoproteins in men: A meta-analysis of randomized controlled trials. *Journal of Men's Health and Gender*. **3**(1), pp.61–70.

Kelley, G.A. and Kelley, Kristi S. 2006b. Aerobic exercise and lipids and lipoproteins in men: A meta-analysis of randomized controlled trials. *Journal of Men's Health and Gender*. **3**(1), pp.61–70.

Kenchaiah, S., Evans, J.C., Levy, D., Wilson, P.W.F., Benjamin, E.J., Larson, M.G., Kannel, W.B. and Vasan, R.S. 2002. Obesity and the Risk of Heart Failure. *New England Journal of Medicine*. **347**(5), pp.305–313.

El Khoudary, S.R., Aggarwal, B., Beckie, T.M., Hodis, H.N., Johnson, A.E., Langer, R.D., Limacher, M.C., Manson, J.E., Stefanick, M.L., Allison, M.A. and null, null 2020. Menopause Transition and Cardiovascular Disease Risk: Implications for Timing of Early Prevention: A Scientific Statement From the American Heart Association. *Circulation*. **142**(25), pp.e506–e532.

Kilicarslan, M., de Weijer, B.A., Simonyté Sjödin, K., Aryal, P., ter Horst, K.W., Cakir, H., Romijn, J.A., Ackermans, M.T., Janssen, I.M., Berends, F.J., van de Laar, A.W., Houdijk, A.P., Kahn, B.B. and Serlie, M.J. 2020. RBP4 increases lipolysis in human adipocytes and is associated with increased lipolysis and hepatic insulin resistance in obese women. *FASEB Journal*. **34**(5), pp.6099–6110.

Kim, F., Tysseling, K.A., Rice, J., Pham, M., Haji, L., Gallis, B.M., Baas, A.S., Paramsothy, P., Giachelli, C.M., Corson, M.A. and Raines, E.W. 2005. Free Fatty Acid Impairment of Nitric Oxide Production in Endothelial Cells Is Mediated by IKKß. *Arteriosclerosis, Thrombosis, and Vascular Biology*. **25**(5), pp.989–994.

Kimura, T., Tomura, H., Mogi, C., Kuwabara, A., Damirin, A., Ishizuka, T., Sekiguchi, A., Ishiwara, M., Im, D.S., Sato, K., Murakami, M. and Okajima, F. 2006. Role of scavenger receptor class B type I and sphingosine 1-phosphate receptors in high density lipoprotein-induced inhibition of adhesion molecule expression in endothelial cells. *Journal of Biological Chemistry*. **281**(49), pp.37457–37467.

KINNUNEN, P.K.J., RANTA, T., EHNHOLM, C., NIKKILÄ, J.E.A. and SEPPÄLÄ, M. 1980. Activities of post-heparin plasma lipoprotein lipase and hepatic lipase during pregnancy and lactation. *European Journal of Clinical Investigation*. **10**(6), pp.469–474.

Kjeldsen, E.W., Thomassen, J.Q. and Frikke-Schmidt, R. 2022. HDL cholesterol concentrations and risk of atherosclerotic cardiovascular disease – Insights from randomized clinical trials and human genetics. *Biochimica et Biophysica Acta - Molecular and Cell Biology of Lipids*. **1867**(1).

Kleinman, N., Abouzaid, S., Andersen, L., Wang, Z. and Powers, A. 2014. Cohort Analysis Assessing Medical and Nonmedical Cost Associated With Obesity in the Workplace. *Journal of Occupational and Environmental Medicine*. **56**(2).

Klöting, N., Graham, T.E., Berndt, J., Kralisch, S., Kovacs, P., Wason, C.J., Fasshauer, M., Schön, M.R., Stumvoll, M., Blüher, M. and Kahn, B.B. 2007. Serum Retinol-Binding Protein Is More Highly Expressed in Visceral than in Subcutaneous Adipose Tissue and Is a Marker of Intra-abdominal Fat Mass. *Cell Metabolism*. **6**(1), pp.79–87.

Kolka, C.M. 2020. The vascular endothelium plays a role in insulin action. *Clinical and Experimental Pharmacology and Physiology*. **47**(1), pp.168–175.

Komatsu, M., Takei, M., Ishii, H. and Sato, Y. 2013. Glucose-stimulated insulin secretion: A newer perspective. *Journal of Diabetes Investigation*. **4**(6), pp.511–516.

Kontush, A., Lhomme, M. and Chapman, M.J. 2013. High density lipoprotein structure, function, and metabolism: Unraveling the complexities of the HDL lipidome. *Journal of Lipid Research*. **54**(11), pp.2950–2963.

Kontush, A., Lindahl, M., Lhomme, M., Calabresi, L., Chapman, M.J. and Davidson, W.S. 2015. Structure of HDL: Particle Subclasses and Molecular Components BT - High Density Lipoproteins: From Biological Understanding to Clinical Exploitation *In*: A. von Eckardstein and D. Kardassis, eds. Cham: Springer International Publishing, pp.3–51.

Kopprasch, S., Pietzsch, J., Kuhlisch, E. and Graessler, J. 2003. Lack of association between serum paraoxonase 1 activities and increased oxidized low-density lipoprotein levels in impaired glucose tolerance and newly diagnosed diabetes mellitus. *Journal of Clinical Endocrinology and Metabolism*. **88**(4), pp.1711–1716.

Koren-Gluzer, M., Aviram, M., Meilin, E. and Hayek, T. 2011. The antioxidant HDL-associated paraoxonase-1 (PON1) attenuates diabetes development and stimulates ß-cell insulin release. *Atherosclerosis*. **219**(2), pp.510–518.

Kotani, K., Yamada, T. and Gugliucci, A. 2013. Paired measurements of paraoxonase 1 and serum amyloid A as useful disease markers. *BioMed Research International*. **2013**.

Kou, R., Greif, D. and Michel, T. 2002. Dephosphorylation of Endothelial Nitric-oxide Synthase by Vascular Endothelial Growth Factor: IMPLICATIONS FOR THE VASCULAR RESPONSES TO CYCLOSPORIN A*. *Journal of Biological Chemistry*. **277**(33), pp.29669–29673.

Lain, K.Y. and Catalano, P.M. 2007. Metabolic Changes in Pregnancy. *Clinical Obstetrics and Gynecology*. **50**(4).

Lambert, C.R., Black, H.S. and Truscott, G.T. 1996. Reactivity of butylated hydroxytoluene. *Free Radical Biology and Medicine*. **21**(3), pp.395–400.

Lean, M.E.J., Leslie, W.S., Barnes, A.C., Brosnahan, N., Thom, G., McCombie, L., Peters, C., Zhyzhneuskaya, S., Al-Mrabeh, A., Hollingsworth, K.G., Rodrigues, A.M., Rehackova, L., Adamson, A.J., Sniehotta, F.F., Mathers, J.C., Ross, H.M., McIlvenna, Y., Stefanetti, R., Trenell, M., Welsh, P., Kean,

S., Ford, I., McConnachie, A., Sattar, N. and Taylor, R. 2018. Primary care-led weight management for remission of type 2 diabetes (DiRECT): an open-label, cluster-randomised trial. *The Lancet*. **391**(10120), pp.541–551.

Lecheminant, J.D., Smith, B.K., Westman, E.C., Vernon, M.C. and Donnelly, J.E. 2010. Comparison of a reduced carbohydrate and reduced fat diet for LDL, HDL, and VLDL subclasses during 9-months of weight maintenance subsequent to weight loss.

Lee, M.-J. and Fried, S.K. 2010. Depot-Specific Biology of Adipose Tissues: Links to Fat Distribution and Metabolic Risk *In*: *Adipose Tissue in Health and Disease* [Online]., pp.283–306. Available from: https://doi.org/10.1002/9783527629527.ch15.

Lee, M.J., Wu, Y. and Fried, S.K. 2013. Adipose tissue heterogeneity: Implication of depot differences in adipose tissue for obesity complications. *Molecular Aspects of Medicine*. **34**(1), pp.1–11.

Lemmers, R.F.H., van Hoek, M., Lieverse, A.G., Verhoeven, A.J.M., Sijbrands, E.J.G. and Mulder, M.T. 2017. The anti-inflammatory function of high-density lipoprotein in type II diabetes: A systematic review. *Journal of Clinical Lipidology*. **11**(3), pp.712-724.e5.

Lemmers, R.F.H., Martens, N.E.M.A., Maas, A.H., van Vark-van der Zee, L.C., Leijten, F.P.J., Groot-van Ruijven, C.M., van Hoek, M., Lieverse, A.G., Sijbrands, E.J.G., Haak, H.R., Leenen, P.J.M., Verhoeven, A.J.M., Dik, W.A. and Mulder, M.T. 2021. Breakfast partly restores the anti-inflammatory function of high-density lipoproteins from patients with type 2 diabetes mellitus. *Atherosclerosis Plus*. **44**, pp.43–50.

Levels, J.H.M., Geurts, P., Karlsson, H., Marée, R., Ljunggren, S., Fornander, L., Wehenkel, L., Lindahl, M., Stroes, E.S.G., Kuivenhoven, J.A. and Meijers, J.C.M. 2011. High-density lipoprotein proteome dynamics in human endotoxemia. *Proteome Science*. **9**, pp.1–14.

Levy, R.L., White, P.D., Stroud, W.D. and Hillman, C.C. 1946. OVERWEIGHT; Its Prognostic Significance in Relation to Hypertension and Cardiovascular-Renal Diseases. *Journal of the American Medical Association*. **131**(12), pp.951–953.

Lewis, G.F. and Cabana, V.G. 1996. *Postprandial Changes in High-Density Lipoprotein Composition and Subfraction Distribution Are Not Altered in Patients With Insulin-Dependent Diabetes Mellitus*.

Li, X.-A., Titlow, W.B., Jackson, B.A., Giltiay, N., Nikolova-Karakashian, M., Uittenbogaard, A. and Smart, E.J. 2002. High Density Lipoprotein Binding to Scavenger Receptor, Class B, Type I Activates Endothelial Nitric-oxide Synthase in a Ceramide-dependent Manner*. *Journal of Biological Chemistry*. **277**(13), pp.11058–11063.

Liao, X., Lou, B., Ma, J. and Wu, M. 2005. Neutrophils activation can be diminished by apolipoprotein A-I. *Life Sciences*. **77**(3), pp.325–335.

Lin, X., Zhang, X., Guo, J., Roberts, C.K., McKenzie, S., Wu, W.C., Liu, S. and Song, Y. 2015. Effects of exercise training on cardiorespiratory fitness and biomarkers of cardiometabolic health: A systematic review and meta-analysis of randomized controlled trials. *Journal of the American Heart Association*. **4**(7).

Lin, Y.T., Chen, L.K., Jian, D.Y., Hsu, T.C., Huang, W.C., Kuan, T.T., Wu, S.Y., Kwok, C.F., Ho, L.T. and Juan, C.C. 2019. Visfatin promotes monocyte adhesion by upregulating ICAM-1 and VCAM-1 expression in endothelial cells via activation of p38-PI3K-AKT signaling and subsequent ROS production and

IKK/NF-κB activation. *Cellular Physiology and Biochemistry*. **52**(6), pp.1398–1411.

Lincoff, A.M., Nicholls, S.J., Riesmeyer, J.S., Barter, P.J., Brewer, H.B., Fox, K.A.A., Gibson, C.M., Granger, C., Menon, V., Montalescot, G., Rader, D., Tall, A.R., McErlean, E., Wolski, K., Ruotolo, G., Vangerow, B., Weerakkody, G., Goodman, S.G., Conde, D., McGuire, D.K., Nicolau, J.C., Leiva-Pons, J.L., Pesant, Y., Li, W., Kandath, D., Kouz, S., Tahirkheli, N., Mason, D. and Nissen, S.E. 2017. Evacetrapib and Cardiovascular Outcomes in High-Risk Vascular Disease. *New England Journal of Medicine*. **376**(20), pp.1933–1942.

Lindström, T., Kechagias, S., Carlsson, M. and Nystrom, F.H. 2011. Transient increase in HDL-cholesterol during weight gain by hyperalimentation in healthy subjects. *Obesity*. **19**(4), pp.812–817.

Liu, Y. and Morton, R.E. 2020. Apolipoprotein F: a natural inhibitor of cholesteryl ester transfer protein and a key regulator of lipoprotein metabolism. *Current Opinion in Lipidology*. **31**(4), pp.194–199.

Liz, M.A., Gomes, C.M., Saraiva, M.J. and Sousa, M.M. 2007. ApoA-I cleaved by transthyretin has reduced ability to promote cholesterol efflux and increased amyloidogenicity. *Journal of Lipid Research*. **48**(11), pp.2385–2395.

Ljunggren, S.A., Levels, J.H.M., Hovingh, K., Holleboom, A.G., Vergeer, M., Argyri, L., Gkolfinopoulou, C., Chroni, A., Sierts, J.A., Kastelein, J.J., Kuivenhoven, J.A., Lindahl, M. and Karlsson, H. 2015. Lipoprotein profiles in human heterozygote carriers of a functional mutation P297S in scavenger receptor class B1. *Biochimica et Biophysica Acta - Molecular and Cell Biology of Lipids*. **1851**(12), pp.1587–1595.

Lopes van Balen, V.A., van Gansewinkel, T.A.G., de Haas, S., van Kuijk, S.M.J., van Drongelen, J., Ghossein-Doha, C. and Spaanderman, M.E.A. 2017. Physiological adaptation of endothelial function to pregnancy: systematic review and meta-analysis. *Ultrasound in Obstetrics and Gynecology*. **50**(6), pp.697–708.

Lopes-Virella, M.F.L., Stone, P.G. and Colwell, J.A. 1977. Serum High Density Lipoprotein in Diabetic Patients. *Diabetologia*. **13**, pp.285–291.

Lumeng, C.N. and Saltiel, A.R. 2011. Inflammatory links between obesity and metabolic disease. *Journal of Clinical Investigation*. **121**(6), pp.2111–2117.

Lyall, F. and Greer, I.A. 1996. The vascular endothelium in normal pregnancy and pre-eclampsia. *Reviews of Reproduction*. **1**(2), pp.107–116.

Mackness, M.I., Arrol, S., Abbott, C. and Durrington, P.N. 1993. Protection of low-density lipoprotein against oxidative modification by high-density lipoprotein associated paraoxonase. *Atherosclerosis*. **104**(1), pp.129–135.

Mackness, M.I., Mackness, B., Arrol, S., Wood, G., Bhatnagar, D. and Durrington, P.N. 1997. Presence of paraoxonase in human interstitial fluid. *FEBS Letters*. **416**(3), pp.377–380.

Mahmoud, A.M., Wilkinson, F.L., McCarthy, E.M., Moreno-Martinez, D., Langford-Smith, A., Romero, M., Duarte, J. and Alexander, M.Y. 2017. Endothelial microparticles prevent lipid-induced endothelial damage via Akt/eNOS signaling and reduced oxidative stress. *FASEB Journal*. **31**(10), pp.4636–4648.

Mahrooz, A., Khosravi-Asrami, O.F., Alizadeh, A., Mohmmadi, N., Bagheri, A., Kashi, Z., Bahar, A., Nosrati, M. and Mackness, M. 2023. Can HDL cholesterol be replaced by paraoxonase 1 activity in the prediction of severe coronary

artery disease in patients with type 2 diabetes? *Nutrition, Metabolism and Cardiovascular Diseases*. **33**(8), pp.1599–1607.

Main, L.A., Ohnishi, T. and Yokoyama, S. 1996. Activation of human plasma cholesteryl ester transfer protein by human apolipoprotein A-IV. *Biochimica et Biophysica Acta*. **1300**, pp.17–24.

Malajczuk, C.J. and Mancera, R.L. 2023. Unravelling the influence of surface lipids on the structure, dynamics and interactome of high-density lipoproteins. *Biochimica et Biophysica Acta - Biomembranes*. **1865**(8).

Mao, J.Y., Sun, J.T., Yang, K., Shen, W.F., Lu, L., Zhang, R.Y., Tong, X. and Liu, Y. 2017. Serum amyloid A enrichment impairs the anti-inflammatory ability of HDL from diabetic nephropathy patients. *Journal of Diabetes and its Complications*. **31**(10), pp.1538–1543.

März, W., Kleber, M.E., Scharnagl, H., Speer, T., Zewinger, S., Ritsch, A., Parhofer, K.G., von Eckardstein, A., Landmesser, U. and Laufs, U. 2017. HDL cholesterol: reappraisal of its clinical relevance. *Clinical Research in Cardiology*. **106**(9), pp.663–675.

McIntyre, H.D., Catalano, P., Zhang, C., Desoye, G., Mathiesen, E.R. and Damm, P. 2019. Gestational diabetes mellitus. *Nature Reviews Disease Primers*. **5**(1).

Melchior, J.T., Street, S.E., Andraski, A.B., Furtado, J.D., Sacks, F.M., Shute, R.L., Greve, E.I., Swertfeger, D.K., Li, H., Shah, A.S., Lu, L.J. and Davidson, W.S. 2017. Apolipoprotein A-II alters the proteome of human lipoproteins and enhances cholesterol efflux from ABCA1. *Journal of Lipid Research*. **58**(7), pp.1374–1385.

Melchior, J.T., Street, S.E., Vaisar, T., Hart, R., Jerome, J., Kuklenyik, Z., Clouet-Foraison, N., Thornock, C., Bedi, S., Shah, A.S., Segrest, J.P., Heinecke, J.W. and Sean Davidson, W. 2021. Apolipoprotein A-I modulates HDL particle size in the absence of apolipoprotein A-II. *Journal of Lipid Research*. **62**.

Melchior, J.T., Swertfeger, D.K., Morris, J., Street, S.E., Warshak, C.R., Welge, J.A., Remaley, A.T., Catov, J.M., Davidson, W.S. and Woollett, L.A. 2021. Pregnancy is accompanied by larger high density lipoprotein particles and compositionally distinct subspecies. *Journal of Lipid Research*. **62**.

Melikian, N., Chowienczyk, P., MacCarthy, P.A., Williams, I.L., Wheatcroft, S.B., Sherwood, R., Gale, C., Shah, A.M. and Kearney, M.T. 2008. Determinants of endothelial function in asymptomatic subjects with and without the metabolic syndrome. *Atherosclerosis*. **197**(1), pp.375–382.

Mercurio, F. and Manning, A.M. 1999. Multiple signals converging on NF-κB. *Current Opinion in Cell Biology*. **11**(2), pp.226–232.

Miida, T., Yamada, T., Yamadera, T., Ozaki, K., Inano, K. and Okada, M. 1999. Serum amyloid a protein generates preß1 high-density lipoprotein from α-migrating high-density lipoprotein. *Biochemistry*. **38**(51), pp.16958–16962.

Mistry, H.D., Kurlak, L.O., Mansour, Y.T., Zurkinden, L., Mohaupt, M.G. and Escher, G. 2017. Increased maternal and fetal cholesterol efflux capacity and placental CYP27A1 expression in preeclampsia. *Journal of Lipid Research*. **58**(6), pp.1186–1195.

Mocciaro, G., D'Amore, S., Jenkins, B., Kay, R., Murgia, A., Herrera-Marcos, L.V., Neun, S., Sowton, A.P., Hall, Z., Palma-Duran, S.A., Palasciano, G., Reimann, F., Murray, A., Suppressa, P., Sabbà, C., Moschetta, A., Koulman, A., Griffin, J.L. and Vacca, M. 2022. Lipidomic Approaches to Study HDL Metabolism in Patients with Central Obesity Diagnosed with Metabolic Syndrome. *International Journal of Molecular Sciences*. **23**(12).

Mokkala, K., Vahlberg, T., Pellonperä, O., Houttu, N., Koivuniemi, E. and Laitinen, K. 2020. Distinct Metabolic Profile in Early Pregnancy of Overweight and Obese Women Developing Gestational Diabetes. *Journal of Nutrition*. **150**(1), pp.31–37.

Morais Cabral, J.H., Atkins, G.L., Sánchez, L.M., López-Boado, Y.S., López-Otin, C. and Sawyer, L. 1995. Arachidonic acid binds to apolipoprotein D: implications for the protein's function. *FEBS Letters*. **366**(1), pp.53–56.

Moren, X., Lhomme, M., Bulla, A., Sanchez, J.C., Kontush, A. and James, R.W. 2016. Proteomic and lipidomic analyses of paraoxonase defined high density lipoprotein particles: Association of paraoxonase with the anti-coagulant, protein S. *Proteomics - Clinical Applications*. **10**(3), pp.230–238.

Morgan, A.E., Mooney, K.M., Wilkinson, S.J., Pickles, N.A. and Mc Auley, M.T. 2016. Cholesterol metabolism: A review of how ageing disrupts the biological mechanisms responsible for its regulation. *Ageing Research Reviews*. **27**, pp.108–124.

Morgantini, C., Natali, A., Boldrini, B., Imaizumi, S., Navab, M., Fogelman, A.M., Ferrannini, E. and Reddy, S.T. 2011. Anti-inflammatory and Antioxidant Properties of HDLs Are Impaired in Type 2 Diabetes. *Diabetes*. **60**(10), pp.2617–2623.

Morikawa, M., Derynck, R. and Miyazono, K. 2016. TGF-β and the TGF-β Family: Context-Dependent Roles in Cell and Tissue Physiology. *Cold Spring Harbor Perspectives in Biology*. **8**(5).

Mracek, T., Ding, Q., Tzanavari, T., Kos, K., Pinkney, J., Wilding, J., Trayhurn, P. and Bing, C. 2010. The adipokine zinc-α2-glycoprotein (ZAG) is downregulated with fat mass expansion in obesity. *Clinical Endocrinology*. **72**(3), pp.334–341.

Muhammad, L.N. 2023. Guidelines for repeated measures statistical analysis approaches with basic science research considerations. *Journal of Clinical Investigation*. **133**(11).

Muilwijk, M., Ho, F., Waddell, H., Sillars, A., Welsh, P., Iliodromiti, S., Brown, R., Ferguson, L., Stronks, K., Valkengoed, I. van, Pell, J.P., Gray, S.R., Gill, J.M.R., Sattar, N. and Celis-Morales, C. 2019. Contribution of type 2 diabetes to all-cause mortality, cardiovascular disease incidence and cancer incidence in white Europeans and South Asians: findings from the UK Biobank population-based cohort study. *BMJ Open Diabetes Research & Care*. **7**(1), p.e000765.

Mukhopadhyay, B., Forouhi, N.G., Fisher, B.M., Kesson, C.M. and Sattar, N. 2006. A comparison of glycaemic and metabolic control over time among South Asian and European patients with Type 2 diabetes: Results from follow-up in a routine diabetes clinic. *Diabetic Medicine*. **23**(1), pp.94–98.

Müller, M.M. and Griesmacher, A. 2000. Markers of endothelial dysfunction. *Clinical Chemistry and Laboratory Medicine*. **38**(2), pp.77–85.

Muñoz-Vega, M., Massó, F., Páez, A., Carreón-Torres, E., Cabrera-Fuentes, H.A., Fragoso, J.M., Pérez-Hernández, N., Martinez, L.O., Najib, S., Vargas-Alarcón, G. and Pérez-Méndez, Ó. 2018. Characterization of immortalized human dermal microvascular endothelial cells (HMEC-1) for the study of HDL functionality. *Lipids in Health and Disease*. **17**(1), pp.1–8.

Muñoz-Vega, M., Massó, F., Páez, A., Vargas-Alarcón, G., Coral-Vázquez, R., Mas-Oliva, J., Carreón-Torres, E. and Pérez-Méndez, Ó. 2018. HDL-Mediated Lipid Influx to Endothelial Cells Contributes to Regulating Intercellular Adhesion Molecule (ICAM)-1 Expression and eNOS Phosphorylation. *International Journal of Molecular Sciences*. **19**(11), p.3394.

Munro, H.N., Eaton, J.C. and Glen, A. 1949. SURVEY OF A SCOTTISH DIABETIC CLINIC A STUDY OF THE ETIOLOGY OF DIABETES MELLITUS. *The Journal of Clinical Endocrinology & Metabolism*. **9**(1), pp.48–78.

Musliner, T.A., Herbert, P.N. and Kingston, M.J. 1979. Lipoprotein substrates of lipoprotein lipase and hepatic triacylglycerol lipase from human post-heparin plasma. *Biochimica et Biophysica Acta (BBA) - Lipids and Lipid Metabolism*. **575**(2), pp.277–288.

Mutharasan, R.K., Thaxton, C.S., Berry, J., Daviglus, M.L., Yuan, C., Sun, J., Ayers, C., Lloyd-Jones, D.M. and Wilkins, J.T. 2017. HDL efflux capacity, HDL particle size, & high-risk carotid atherosclerosis in a cohort of asymptomatic older adults: The Chicago Healthy Aging Study. *Journal of Lipid Research*. **58**(3), pp.600–606.

Muzakova, V., Beekhof, P.K. and Jansen, E.H.J.M. 2020. Very long-term stability of lipid biomarkers in human serum. *Analytical Biochemistry*. **597**, p.113695.

Naka, K.K., Papathanassiou, K., Bechlioulis, A., Kazakos, N., Pappas, K., Tigas, S., Makriyiannis, D., Tsatsoulis, A. and Michalis, L.K. 2012. Determinants of vascular function in patients with type 2 diabetes. *Cardiovascular Diabetology*. **11**(1), p.127.

Nakazawa, T., Chiba, T., Kaneko, E., Yui, K., Yoshida, M. and Shimokado, K. 2005. Insulin Signaling in Arteries Prevents Smooth Muscle Apoptosis. *Arteriosclerosis, Thrombosis, and Vascular Biology*. **25**(4), pp.760–765.

Nelson, D.B., Byrne, J.J. and Cunningham, F.G. 2021. Acute Fatty Liver of Pregnancy. *Obstetrics & Gynecology*. **137**(3).

Nicholls, S.J., Lundman, P., Harmer, J.A., Cutri, B., Griffiths, K.A., Rye, K.A., Barter, P.J. and Celermajer, D.S. 2006. Consumption of Saturated Fat Impairs the Anti-Inflammatory Properties of High-Density Lipoproteins and Endothelial Function. *Journal of the American College of Cardiology*. **48**(4), pp.715–720.

Nielsen, S., Guo, Z., Johnson, C.M., Hensrud, D.D. and Jensen, M.D. 2004. Splanchnic lipolysis in human obesity. *The Journal of Clinical Investigation*. **113**(11), pp.1582–1588.

Nofer, J.-R., van der Giet, M., Tölle, M., Wolinska, I., von Wnuck Lipinski, K., Baba, H.A., Tietge, U.J., Gödecke, A., Ishii, I., Kleuser, B., Schäfers, M., Fobker, M., Zidek, W., Assmann, G., Chun, J. and Levkau, B. 2004. HDL induces NO-dependent vasorelaxation via the lysophospholipid receptor S1P3. *The Journal of Clinical Investigation*. **113**(4), pp.569–581.

Nofer, J.-R., Walter, M., Kehrel, B., Wierwille, S., Tepel, M., Seedorf, U. and Assmann, G. 1998. HDL3-Mediated Inhibition of Thrombin-Induced Platelet Aggregation and Fibrinogen Binding Occurs via Decreased Production of Phosphoinositide-Derived Second Messengers 1,2-Diacylglycerol and Inositol 1,4,5-tris-Phosphate. *Arteriosclerosis, Thrombosis, and Vascular Biology*. **18**(6), pp.861–869.

Noguchi, H., Ikemoto, T., Naziruddin, B., Jackson, A., Shimoda, M., Fujita, Y., Chujo, D., Takita, M., Kobayashi, N., Onaca, N., Levy, M.F. and Matsumoto, S. 2009. Iodixanol-controlled density gradient during islet purification improves recovery rate in human islet isolation. *Transplantation*. **87**(11), pp.1629–1635.

Norata, G.D., Callegari, E., Marchesi, M., Chiesa, G., Eriksson, P. and Catapano, A.L. 2005. High-Density Lipoproteins Induce Transforming Growth Factor-ß2 Expression in Endothelial Cells. *Circulation*. **111**(21), pp.2805–2811.

Ntuk, U.E., Gill, J.M.R., Mackay, D.F., Sattar, N. and Pell, J.P. 2014. Ethnic-Specific Obesity Cutoffs for Diabetes Risk: Cross-sectional Study of 490,288 UK Biobank Participants. *Diabetes Care*. **37**(9), pp.2500–2507.

Oldoni, F., Cheng, H., Banfi, S., Gusarova, V., Cohen, J.C. and Hobbs, H.H. 2020. ANGPTL8 has both endocrine and autocrine effects on substrate utilization. *JCI Insight*. **5**(17).

Onyiaodike, C.C., Murray, H.M., Zhang, R., Meyer, B.J., Jordan, F., Brown, E.A., Nibbs, R.J.B., Lyall, H., Sattar, N., Nelson, S.M. and Freeman, D.J. 2018. Pre-conception maternal erythrocyte saturated to unsaturated fatty acid ratio predicts pregnancy after natural cycle frozen embryo transfer. *Scientific Reports*. **8**(1), p.1216.

Ortiz-Muñoz, G., Houard, X., Martín-Ventura, J.-L., Ishida, B.Y., Loyau, S., Rossignol, P., Moreno, J.-A., Kane, J.P., Chalkley, R.J., Burlingame, A.L., Michel, J.-B. and Meilhac, O. 2009. HDL antielastase activity prevents smooth muscle cell anoikis, a potential new antiatherogenic property. *The FASEB Journal*. **23**(9), pp.3129–3139.

Otero-Díaz, B., Rodríguez-Flores, M., Sánchez-Muñoz, V., Monraz-Preciado, F., Ordoñez-Ortega, S., Becerril-Elias, V., Baay-Guzmán, G., Obando-Monge, R., García-García, E., Palacios-González, B., Villarreal-Molina, M.T., Sierra-Salazar, M. and Antuna-Puente, B. 2018. Exercise Induces White Adipose Tissue Browning Across the Weight Spectrum in Humans. *Frontiers in Physiology*. **9**.

Otnes, S., Fogh-Andersen, N., Rømsing, J. and Thomsen, H.S. 2017. Analytical interference by contrast agents in biochemical assays. *Contrast Media and Molecular Imaging*. **2017**.

Owen, J.S. and Mulcahy, J. V 2002. ATP-binding cassette A1 protein and HDL homeostasis. *Atherosclerosis Supplements*. **3**(4), pp.13–22.

Palmer, B.F. and Clegg, D.J. 2015. The sexual dimorphism of obesity. *Molecular and Cellular Endocrinology*. **402**, pp.113–119.

Park, C.M., Tillin, T., March, K., Ghosh, A.K., Jones, S., Wright, A., Heasman, J., Francis, D., Sattar, N., Mayet, J., Chaturvedi, N. and Hughes, A.D. 2014. Hyperglycemia Has a Greater Impact on Left Ventricle Function in South Asians Than in Europeans. *Diabetes Care*. **37**(4), pp.1124–1131.

Passos, L.S.A., Lupieri, A., Becker-Greene, D. and Aikawa, E. 2020. Innate and adaptive immunity in cardiovascular calcification. *Atherosclerosis*. **306**, pp.59–67.

Pasternak, Y., Biron-Shental, T., Ohana, M., Einbinder, Y., Arbib, N., Benchetrit, S. and Zitman-Gal, T. 2020. Gestational diabetes type 2: Variation in high-density lipoproteins composition and function. *International Journal of Molecular Sciences*. **21**(17), pp.1–11.

Patanapirunhakit, P. 2023. *High density lipoprotein composition and function in healthy pregnancy and preeclampsia*.[Online] University of Glasgow. Available from: http://theses.gla.ac.uk/83445/.

Patel, S., Puranik, R., Nakhla, S., Lundman, P., Stocker, R., Wang, X.S., Lambert, G., Rye, K.A., Barter, P.J., Nicholls, S.J. and Celermajer, D.S. 2009. Acute hypertriglyceridaemia in humans increases the triglyceride content and decreases the anti-inflammatory capacity of high density lipoproteins. *Atherosclerosis*. **204**(2), pp.424–428.

Pérez-Morga, D., Vanhollebeke, B., Paturiaux-Hanocq, F., Nolan, D.P., Lins, L., Homblé, F., Vanhamme, L., Tebabi, P., Pays, A., Poelvoorde, P., Jacquet, A., Brasseur, R. and Pays, E. 2005. Apolipoprotein L-I Promotes

Trypanosome Lysis by Forming Pores in Lysosomal Membranes. *Science*. **309**(5733), pp.469–472.

Perrin-Cocon, L., Diaz, O., Carreras, M., Dollet, S., Guironnet-Paquet, A., André, P. and Lotteau, V. 2012. High-density lipoprotein phospholipids interfere with dendritic cell Th1 functional maturation. *Immunobiology*. **217**(1), pp.91–99.

Perségol, L., Vergès, B., Gambert, P. and Duvillard, L. 2007. Inability of HDL from abdominally obese subjects to counteract the inhibitory effect of oxidized LDL on vasorelaxation. *Journal of Lipid Research*. **48**(6), pp.1396–1401.

Petersen, K.F., Befroy, D., Dufour, S., Dziura, J., Ariyan, C., Rothman, D.L., DiPietro, L., Cline, G.W. and Shulman, G.I. 2003. Mitochondrial Dysfunction in the Elderly: Possible Role in Insulin Resistance. *Science*. **300**(5622), pp.1140–1142.

Petersen, K.F., Dufour, S., Befroy, D., Lehrke, M., Hendler, R.E. and Shulman, G.I. 2005. Reversal of Nonalcoholic Hepatic Steatosis, Hepatic Insulin Resistance, and Hyperglycemia by Moderate Weight Reduction in Patients With Type 2 Diabetes. *Diabetes*. **54**(3), pp.603–608.

Petrie, J.R., Guzik, T.J. and Touyz, R.M. 2018a. Diabetes, Hypertension, and Cardiovascular Disease: Clinical Insights and Vascular Mechanisms. *Canadian Journal of Cardiology*. **34**(5), pp.575–584.

Petrie, J.R., Guzik, T.J. and Touyz, R.M. 2018b. Diabetes, Hypertension, and Cardiovascular Disease: Clinical Insights and Vascular Mechanisms. *Canadian Journal of Cardiology*. **34**(5), pp.575–584.

Pietzsch, J., Julius, U., Nitzsche, S. and Hanefeld, M. 1998. In Vivo Evidence for Increased Apolipoprotein A-I Catabolism in Subjects With Impaired Glucose Tolerance. *DIABETES*. **47**, pp.1928–1934.

Pol, E. van der, Böing, A.N., Harrison, P., Sturk, A. and Nieuwland, R. 2012. Classification, Functions, and Clinical Relevance of Extracellular Vesicles M. P. Mattson, ed. *Pharmacological Reviews*. **64**(3), p.676.

Pressly, J.D., Gurumani, M.Z., Varona Santos, J.T., Fornoni, A., Merscher, S. and Al-Ali, H. 2022. Adaptive and maladaptive roles of lipid droplets in health and disease. *American Journal of Physiology-Cell Physiology*. **322**(3), pp.C468–C481.

Pugsley, M.K. and Tabrizchi, R. 2000. The vascular system: An overview of structure and function. *Journal of Pharmacological and Toxicological Methods*. **44**(2), pp.333–340.

Rabbani, N., Ashour, A. and Thornalley, P.J. 2016. Mass spectrometric determination of early and advanced glycation in biology. *Glycoconjugate Journal*. **33**(4), pp.553–568.

Radak, Z., Chung, H.Y. and Goto, S. 2008. Systemic adaptation to oxidative challenge induced by regular exercise. *Free Radical Biology and Medicine*. **44**(2), pp.153–159.

Rader, D.J. 2006. Molecular regulation of HDL metabolism and function: implications for novel therapies. *The Journal of Clinical Investigation*. **116**(12), pp.3090–3100.

Rader, D.J., Castro, G., Zech, L.A., Fruchart, J.C. and Brewer, H.B. 1991. In vivo metabolism of apolipoprotein A-I on high density lipoprotein particles LpA-I and LpA-I,A-II. *Journal of Lipid Research*. **32**(11), pp.1849–1859.

Rämet, M.E., Rämet, M., Lu, Q., Nickerson, M., Savolainen, M.J., Malzone, A. and Karas, R.H. 2003. High-density lipoprotein increases the abundance of

eNOS protein in human vascular endothelial cells by increasing its half-life. *Journal of the American College of Cardiology*. **41**(12), pp.2288–2297.

Ramsay, J.E., Ferrell, W.R., Crawford, L., Wallace, A.M., Greer, I.A. and Sattar, N. 2002. Maternal Obesity Is Associated with Dysregulation of Metabolic, Vascular, and Inflammatory Pathways. *The Journal of Clinical Endocrinology & Metabolism*. **87**(9), pp.4231–4237.

Rashid, S. and Genest, J. 2007. Effect of Obesity on High-density Lipoprotein Metabolism. *Obesity*. **15**(12), pp.2875–2888.

Rector, R.S., Warner, S.O., Liu, Y., Hinton, P.S., Sun, G.Y., Cox, R.H., Stump, C.S., Laughlin, M.H., Dellsperger, K.C. and Thomas, T.R. 2007. Exercise and diet induced weight loss improves measures of oxidative stress and insulin sensitivity in adults with characteristics of the metabolic syndrome. *American Journal of Physiology - Endocrinology and Metabolism*. **293**(2).

Reers, C., Erbel, S., Esposito, I., Schmied, B., Büchler, M.W., Nawroth, P.P. and Ritzel, R.A. 2009. Impaired islet turnover in human donor pancreata with aging. *European Journal of Endocrinology*. **160**(2), pp.185–191.

Refsum, H.E. and Strömme, S.B. 1979. Serum thyroxine, triiodothyronine and thyroid stimulating hormone after prolonged heavy excerise. *Scandinavian Journal of Clinical and Laboratory Investigation*. **39**(5), pp.455–459.

Reis, E.S., Mastellos, D.C., Hajishengallis, G. and Lambris, J.D. 2019. New insights into the immune functions of complement. *Nature Reviews Immunology*. **19**(8), pp.503–516.

Rensen, P.C.N. and van Berkel, T.J.C. 1996. Apolipoprotein E Effectively Inhibits Lipoprotein Lipase-mediated Lipolysis of Chylomicron-like Triglyceride-rich Lipid Emulsions in Vitro and in Vivo*. *Journal of Biological Chemistry*. **271**(25), pp.14791–14799.

Ribeiro, I.C.D., Iborra, R.T., Neves, M.Q.T.S., Lottenberg, S.A., Charf, A.M., Nunes, V.S., Negrão, C.E., Nakandakare, E.R., Quintão, E.C.R. and Passarelli, M. 2008. HDL Atheroprotection by aerobic exercise training in type 2 diabetes mellitus. *Medicine and Science in Sports and Exercise*. **40**(5), pp.779–786.

Ricard, N., Bailly, S., Guignabert, C. and Simons, M. 2021. The quiescent endothelium: signalling pathways regulating organ-specific endothelial normalcy. *Nature Reviews Cardiology*. **18**(8), pp.565–580.

Ricci, J.A. and Chee, E. 2005. Lost Productive Time Associated With Excess Weight in the U.S. Workforce. *Journal of Occupational and Environmental Medicine*. **47**(12).

Richardson, T.G., Sanderson, E., Palmer, T.M., Ala-Korpela, M., Ference, B.A., Davey Smith, G. and Holmes, M. V 2020. Evaluating the relationship between circulating lipoprotein lipids and apolipoproteins with risk of coronary heart disease: A multivariable Mendelian randomisation analysis. *PLOS Medicine*. **17**(3), pp.e1003062-.

Richter, R.J., Jarvik, G.P. and Furlong, C.E. 2008. Determination of paraoxonase 1 status without the use of toxic organophosphate substrates. *Circulation. Cardiovascular genetics*. **1**(2), pp.147–152.

Riddell, D.R. and Owen, J.S. 1997. Nitric Oxide and Platelet Aggregation *In*: G. Litwack, ed. *Vitamins & Hormones* [Online]. Academic Press, pp.25–48. Available from: https://www.sciencedirect.com/science/article/pii/S0083672908606391.

Riechman, S.E., Lee, C.W., Chikani, G., Chen, V.C.W. and Lee, T.V. 2009. Cholesterol and Skeletal Muscle Health *In*: Simopoulos. A.P and F. De

Meester, eds. *A Balanced Omega-6/Omega-3 Fatty Acid Ratio, Cholesterol and Coronary Heart Disease.*, pp.71–79.

Riederer, M., Köfeler, H., Lechleitner, M., Tritscher, M. and Frank, S. 2012. Impact of endothelial lipase on cellular lipid composition. *Biochimica et Biophysica Acta (BBA) - Molecular and Cell Biology of Lipids*. **1821**(7), pp.1003–1011.

Roberts, C.K., Ng, C., Hama, S., Eliseo, A.J. and James Barnard, R. 2006. Effect of a short-term diet and exercise intervention on inflammatory/anti-inflammatory properties of HDL in overweight/obese men with cardiovascular risk factors. *J Appl Physiol*. **101**, pp.1727–1732.

Robson, P., Blanninl, A.K., Walsh, N.P., Castel, L.M. and Cleeson, M. 1999. Effects of Exercise Intensity, Duration and Recovery on in vitro Neutrophil Function in Male Athletes. *Int J Sports Med*. **20**, pp.128–135.

Rodriguez, A., Trigatti, B.L., Mineo, C., Knaack, D., Wilkins, J.T., Sahoo, D., Asztalos, B.F., Mora, S., Cuchel, M., Pownall, H.J., Rosales, C., Bernatchez, P., Ribeiro Martins Da Silva, A., Getz, G.S., Barber, J.L., Shearer, G.C., Zivkovic, A.M., Tietge, U.J.F., Sacks, F.M., Connelly, M.A., Oda, M.N., Davidson, W.S., Sorci-Thomas, M.G., Vaisar, T., Ruotolo, G., Vickers, K.C. and Martel, C. 2019. Proceedings of the Ninth HDL (High-Density Lipoprotein) Workshop: Focus on Cardiovascular Disease. *Arteriosclerosis, Thrombosis, and Vascular Biology*. **39**(12), pp.2457–2467.

Rohatgi, A., Khera, A., Berry, J.D., Givens, E.G., Ayers, C.R., Wedin, K.E., Neeland, I.J., Yuhanna, I.S., Rader, D.R., de Lemos, J.A. and Shaul, P.W. 2014. HDL Cholesterol Efflux Capacity and Incident Cardiovascular Events. *New England Journal of Medicine*. **371**(25), pp.2383–2393.

Rohrer, L., Cavelier, C., Fuchs, S., Schlüter, M.A., Völker, W. and von Eckardstein, A. 2006. Binding, internalization and transport of apolipoprotein A-I by vascular endothelial cells. *Biochimica et Biophysica Acta (BBA) - Molecular and Cell Biology of Lipids*. **1761**(2), pp.186–194.

Ronda, N., Bernini, F., Giacosa, R., Gatti, R., Baldini, N., Buzio, C. and Orlandini, G. 2003. Normal human IgG prevents endothelial cell activation induced by TNFa and oxidized low-density lipoprotein atherogenic stimuli. *Clin Exp Immunol*. **133**, pp.219–226.

Ronsein, G.E. and Vaisar, T. 2019. Deepening our understanding of HDL proteome. *Expert Review of Proteomics*. **16**(9), pp.749–760.

Rorsman, P. and Renström, E. 2003. Insulin granule dynamics in pancreatic beta cells. *Diabetologia*. **46**(8), pp.1029–1045.

Ruan, H., Hacohen, N., Golub, T.R., Van Parijs, L. and Lodish, H.F. 2002. Tumor Necrosis Factor-α Suppresses Adipocyte-Specific Genes and Activates Expression of Preadipocyte Genes in 3T3-L1 Adipocytes: Nuclear Factor-κB Activation by TNF-α Is Obligatory. *Diabetes*. **51**(5), pp.1319–1336.

Rubanyi, G.M., Romero, J.C. and Vanhoutte, P.M. 1986. Flow-induced release of endothelium-derived relaxing factor. *American Journal of Physiology-Heart and Circulatory Physiology*. **250**(6), pp.H1145–H1149.

Ruiz, M., Frej, C., Holmér, A., Guo, L.J., Tran, S. and Dahlbäck, B. 2017. High-density lipoprotein-associated apolipoprotein M limits endothelial inflammation by delivering sphingosine-1-phosphate to the sphingosine-1-phosphate receptor 1. *Arteriosclerosis, Thrombosis, and Vascular Biology*. **37**(1), pp.118–129.

Ruiz-Ramie, J.J., Barber, J.L. and Sarzynski, M.A. 2019. Effects of exercise on HDL functionality. *Current Opinion in Lipidology*. **30**(1), pp.16–23.

Saarelainen, H., Laitinen, T., Raitakari, O.T., Juonala, M., Heiskanen, N., Lyyra-Laitinen, T., Viikari, J.S.A., Vanninen, E. and Heinonen, S. 2006. Pregnancy-Related Hyperlipidemia and Endothelial Function in Healthy Women. *Circulation Journal*. **70**(6), pp.768–772.

Sadler, J.B.A., Lamb, C.A., Gould, G.W. and Bryant, N.J. 2016. Iodixanol gradient centrifugation to separate components of the low-density membrane fraction from 3T3-L1 adipocytes. *Cold Spring Harbor Protocols*. **2016**(2), pp.199–200.

Salter, A.M. and Brindley, D.N. 1988. The biochemistry of lipoproteins. *Journal of Inherited Metabolic Disease*. **11**(S1), pp.4–17.

Sanchez, D. and Ganfornina, M.D. 2021. The Lipocalin Apolipoprotein D Functional Portrait: A Systematic Review. *Frontiers in Physiology*. **12**.

Sang, H., Yao, S., Zhang, L., Li, X., Yang, N., Zhao, J., Zhao, L., Si, Y., Zhang, Y., Lv, X., Xue, Y. and Qin, S. 2015. Walk-Run Training Improves the Anti-Inflammation Properties of High-Density Lipoprotein in Patients With Metabolic Syndrome. *The Journal of Clinical Endocrinology & Metabolism*. **100**(3), pp.870–879.

Santamarina-Fojo, S., González-Navarro, H., Freeman, L., Wagner, E. and Nong, Z. 2004. Hepatic Lipase, Lipoprotein Metabolism, and Atherogenesis. *Arteriosclerosis, Thrombosis, and Vascular Biology*. **24**(10), pp.1750–1754.

Sarzynski, M.A., Ruiz-Ramie, J.J., Barber, J.L., Slentz, C.A., Apolzan, J.W., McGarrah, R.W., Harris, M.N., Church, T.S., Borja, M.S., He, Y., Oda, M.N., Martin, C.K., Kraus, W.E. and Rohatgi, A. 2018. Effects of Increasing Exercise Intensity and Dose on Multiple Measures of HDL (High-Density Lipoprotein) Function. *Arteriosclerosis, Thrombosis, and Vascular Biology*. **38**(4), pp.943–952.

Sattar, N., Gaw, A., Packard, C.J. and Greer, I.A. 1996. Potential pathogenic roles of aberrant lipoprotein and fatty acid metabolism in pre-eclampsia. *BJOG: An International Journal of Obstetrics & Gynaecology*. **103**(7), pp.614–620.

Sattar, N., Greer, I.A., Louden, J., Lindsay, G., McConnell, M., Shepherd, J. and Packard, C.J. 1997. Lipoprotein Subfraction Changes in Normal Pregnancy: Threshold Effect of Plasma Triglyceride on Appearance of Small, Dense Low Density Lipoprotein1. *The Journal of Clinical Endocrinology & Metabolism*. **82**(8), pp.2483–2491.

Sawa, Y., Sugimoto, Y., Ueki, T., Ishikawa, H., Sato, A., Nagato, T. and Yoshida, S. 2007. Effects of TNF-α on Leukocyte Adhesion Molecule Expressions in Cultured Human Lymphatic Endothelium. *Journal of Histochemistry & Cytochemistry*. **55**(7), pp.721–733.

Schipper, B.M., Marra, K.G., Zhang, W., Donnenberg, A.D. and Rubin, J.P. 2008. Regional Anatomic and Age Effects on Cell Function of Human Adipose-Derived Stem Cells. *Annals of Plastic Surgery*. **60**(5).

Schlitt, A., Hojjati, M.R., von Gizycki, H., Lackner, K.J., Blankenberg, S., Schwaab, B., Meyer, J., Rupprecht, H.J. and Jiang, X.-C. 2005. Serum sphingomyelin levels are related to the clearance of postprandial remnant-like particles. *Journal of Lipid Research*. **46**(2), pp.196–200.

Schmidt, A., Geigenmüller, S., Völker, W. and Buddecke, E. 2006. The antiatherogenic and antiinflammatory effect of HDL-associated lysosphingolipids operates via Akt → NF-kappaB signalling pathways in human vascular endothelial cells. *Basic Research in Cardiology*. **101**(2), pp.109–116.

Schneider, J., Erren, T., Zgfel, P. and Kaffamik, H. 1990. Metformin-induced changes in serum lipids, lipoproteins, and apoproteins in non-insulin-dependent diabetes mellitus. *Atherosclerosis*. **82**, pp.97–103.

Schorr, M., Dichtel, L.E., Gerweck, A. V., Valera, R.D., Torriani, M., Miller, K.K. and Bredella, M.A. 2018. Sex differences in body composition and association with cardiometabolic risk. *Biology of Sex Differences*. **9**(1).

Schröder, M., Schäfer, R. and Friedl, P. 1997. Spectrophotometric Determination of Iodixanol in Subcellular Fractions of Mammalian Cells. *Analytical Biochemistry*. **244**(1), pp.174–176.

Schvartz, I., Seger, D. and Shaltiel, S. 1999. Molecules in focus Vitronectin. *The International Journal of Biochemistry & Cell Biology* . **31**, pp.539–544.

Schwartz, G.G., Olsson, A.G., Abt, M., Ballantyne, C.M., Barter, P.J., Brumm, J., Chaitman, B.R., Holme, I.M., Kallend, D., Leiter, L.A., Leitersdorf, E., McMurray, J.J. V, Mundl, H., Nicholls, S.J., Shah, P.K., Tardif, J.-C. and Wright, R.S. 2012. Effects of Dalcetrapib in Patients with a Recent Acute Coronary Syndrome. *New England Journal of Medicine*. **367**(22), pp.2089–2099.

Schwartz, R.S., Shuman, W.P., Bradbury, V.L., Cain, K.C., Fellingham, G.W., Beard, J.C., Kahn, S.E., Stratton, J.R., Cerqueira, M.D. and Abrass, I.B. 1990. Body Fat Distribution in Healthy Young and Older Men. *Journal of Gerontology*. **45**(6), pp.M181–M185.

Selemidis, S., Dusting, G.J., Peshavariya, H., Kemp-Harper, B.K. and Drummond, G.R. 2007. Nitric oxide suppresses NADPH oxidase-dependent superoxide production by S-nitrosylation in human endothelial cells. *Cardiovascular Research*. **75**(2), pp.349–358.

Shao, B. 2012. Site-specific oxidation of apolipoprotein A-I impairs cholesterol export by ABCA1, a key cardioprotective function of HDL. *Biochimica et Biophysica Acta - Molecular and Cell Biology of Lipids*. **1821**(3), pp.490–501.

Siezenga, M.A., Chandie Shaw, P.K., Van Der Geest, R.N., Mollnes, T.E., Daha, M.R., Rabelink, T.J. and Berger, S.P. 2009. Enhanced complement activation is part of the unfavourable cardiovascular risk profile in South Asians. *Clinical and Experimental Immunology*. **157**(1), pp.98–103.

Silver, A.E., Beske, S.D., Christou, D.D., Donato, A.J., Moreau, K.L., Eskurza, I., Gates, P.E. and Seals, D.R. 2007. Overweight and Obese Humans Demonstrate Increased Vascular Endothelial NAD(P)H Oxidase-p47phox Expression and Evidence of Endothelial Oxidative Stress. *Circulation*. **115**(5), pp.627–637.

Sinha, R.A., Singh, B.K. and Yen, P.M. 2018. Direct effects of thyroid hormones on hepatic lipid metabolism. *Nature Reviews Endocrinology*. **14**(5), pp.259–269.

Sokooti, S., Flores-Guerrero, J.L., Kieneker, L.M., Heerspink, H.J.L., Connelly, M.A., Bakker, S.J.L. and Dullaart, R.P.F. 2021. HDL Particle Subspecies and Their Association with Incident Type 2 Diabetes: The PREVEND Study. *Journal of Clinical Endocrinology and Metabolism*. **106**(6), pp.1761–1772.

Song, Z., Xiaoli, A.M. and Yang, F. 2018. Regulation and Metabolic Significance of De Novo Lipogenesis in Adipose Tissues. *Nutrients*. **10**(10).

Soran, H., Hama, S., Yadav, R. and Durrington, P.N. 2012. HDL functionality. *Current Opinion in Lipidology*. **23**(4), pp.353–366.

Soski, S.S., Dobutovi, B.D., Sudar, E.M., Obradovi, M.M., Nikoli, D.M., Djordjevic, J.D., Radak, D.J., Mikhailidis, D.P. and Isenovi, E.R. 2011. *Regulation of Inducible Nitric Oxide Synthase (iNOS) and its Potential Role in Insulin Resistance, Diabetes and Heart Failure*.

Sparks, D.L., Davidson, W.S., Lund-Katz, S. and Phillips, M.C. 1995. Effects of the Neutral Lipid Content of High Density Lipoprotein on Apolipoprotein A-I Structure and Particle Stability (*). *Journal of Biological Chemistry*. **270**(45), pp.26910–26917.

Stadler, J.T., van Poppel, M.N.M., Wadsack, C., Holzer, M., Pammer, A., Simmons, D., Hill, D., Desoye, G. and Marsche, G. 2023. Obesity Affects Maternal and Neonatal HDL Metabolism and Function. *Antioxidants*. **12**(1).

Stadler, J.T., Scharnagl, H., Wadsack, C. and Marsche, G. 2023. Preeclampsia Affects Lipid Metabolism and HDL Function in Mothers and Their Offspring. *Antioxidants*. **12**(4).

Stanton, K.M., Kienzle, V., Dinnes, D.L.M., Kotchetkov, I., Jessup, W., Kritharides, L., Celermajer, D.S. and Rye, K.A. 2022a. Moderate-and High-Intensity Exercise Improves Lipoprotein Profile and Cholesterol Efflux Capacity in Healthy Young Men. *Journal of the American Heart Association*. **11**(12).

Stanton, K.M., Kienzle, V., Dinnes, D.L.M., Kotchetkov, I., Jessup, W., Kritharides, L., Celermajer, D.S. and Rye, K.A. 2022b. Moderate-and High-Intensity Exercise Improves Lipoprotein Profile and Cholesterol Efflux Capacity in Healthy Young Men. *Journal of the American Heart Association*. **11**(12).

Steinberg, H.O., Brechtel, G., Johnson, A., Fineberg, N. and Baron, A.D. 1994. Insulin-mediated skeletal muscle vasodilation is nitric oxide dependent. A novel action of insulin to increase nitric oxide release. *The Journal of Clinical Investigation*. **94**(3), pp.1172–1179.

Stewart, F.M., Freeman, D.J., Ramsay, J.E., Greer, I.A., Caslake, M. and Ferrell, W.R. 2007. Longitudinal Assessment of Maternal Endothelial Function and Markers of Inflammation and Placental Function throughout Pregnancy in Lean and Obese Mothers. *The Journal of Clinical Endocrinology & Metabolism*. **92**(3), pp.969–975.

Strawford, A., Antelo, F., Christiansen, M. and Hellerstein, M.K. 2004. Adipose tissue triglyceride turnover, de novo lipogenesis, and cell proliferation in humans measured with 2H2O. *American Journal of Physiology-Endocrinology and Metabolism*. **286**(4), pp.E577–E588.

Subbaiah, P. V and Liu, M. 1993. Role of sphingomyelin in the regulation of cholesterol esterification in the plasma lipoproteins. Inhibition of lecithin-cholesterol acyltransferase reaction. *Journal of Biological Chemistry*. **268**(27), pp.20156–20163.

Sulaiman, W.N., Caslake, M.J., Delles, C., Karlsson, H., Mulder, M.T., Graham, D. and Freeman, D.J. 2016. Does high-density lipoprotein protect vascular function in healthy pregnancy? *Clinical Science*. **130**(7), pp.491–497.

Sun, K., Kusminski, C.M. and Scherer, P.E. 2011. Adipose tissue remodeling and obesity. *Journal of Clinical Investigation*. **121**(6), pp.2094–2101.

Tabur, S., Torun, A.N., Sabuncu, T., Turan, M.N., Celik, H., Ocak, A.R. and Aksoy, N. 2010. Non-diabetic metabolic syndrome and obesity do not affect serum paraoxonase and arylesterase activities but do affect oxidative stress and inflammation. *European Journal of Endocrinology*. **162**(3), pp.535–541.

Tang, C., Liu, Y., Kessler, P.S., Vaughan, A.M. and Oram, J.F. 2009. The Macrophage Cholesterol Exporter ABCA1 Functions as an Anti-inflammatory Receptor*. *Journal of Biological Chemistry*. **284**(47), pp.32336–32343.

Tang, S., Tabet, F., Cochran, B.J., Cuesta Torres, L.F., Wu, B.J., Barter, P.J. and Rye, K.A. 2019. Apolipoprotein A-I enhances insulin-dependent and

insulin-independent glucose uptake by skeletal muscle. *Scientific Reports*. **9**(1).

Taylor, J.K., Carpio-Rivera, E., Chacón-Araya, Y., Grandjean, P.W. and Moncada-Jiménez, J. 2022. The Effects of Acute and Chronic Exercise on Paraoxonase-1 (PON1): A Systematic Review With Meta-Analysis. *Research Quarterly for Exercise and Sport*. **93**(1), pp.130–143.

Teslovich, T.M., Musunuru, K., Smith, A. V., Edmondson, A.C., Stylianou, I.M., Koseki, M., Pirruccello, J.P., Ripatti, S., Chasman, D.I., Willer, C.J., Johansen, C.T., Fouchier, S.W., Isaacs, A., Peloso, G.M., Barbalic, M., Ricketts, S.L., Bis, J.C., Aulchenko, Y.S., Thorleifsson, G., Feitosa, M.F., Chambers, J., Orho-Melander, M., Melander, O., Johnson, T., Li, X., Guo, X., Li, M., Shin Cho, Y., Jin Go, M., Jin Kim, Y., Lee, J.Y., Park, T., Kim, K., Sim, X., Twee-Hee Ong, R., Croteau-Chonka, D.C., Lange, L.A., Smith, J.D., Song, K., Hua Zhao, J., Yuan, X., Luan, J., Lamina, C., Ziegler, A., Zhang, W., Zee, R.Y.L., Wright, A.F., Witteman, J.C.M., Wilson, J.F., Willemsen, G., Wichmann, H.E., Whitfield, J.B., Waterworth, D.M., Wareham, N.J., Waeber, G., Vollenweider, P., Voight, B.F., Vitart, V., Uitterlinden, A.G., Uda, M., Tuomilehto, J., Thompson, J.R., Tanaka, T., Surakka, I., Stringham, H.M., Spector, T.D., Soranzo, N., Smit, J.H., Sinisalo, J., Silander, K., Sijbrands, E.J.G., Scuteri, A., Scott, J., Schlessinger, D., Sanna, S., Salomaa, V., Saharinen, J., Sabatti, C., Ruokonen, A., Rudan, I., Rose, L.M., Roberts, R., Rieder, M., Psaty, B.M., Pramstaller, P.P., Pichler, I., Perola, M., Penninx, B.W.J.H., Pedersen, N.L., Pattaro, C., Parker, A.N., Pare, G., Oostra, B.A., O'donnell, C.J., Nieminen, M.S., Nickerson, D.A., Montgomery, G.W., Meitinger, T., Mcpherson, R., Mccarthy, M.I., Mcardle, W., Masson, D., Martin, N.G., Marroni, F., Mangino, M., Magnusson, P.K.E., Lucas, G., Luben, R., Loos, R.J.F., Lokki, M.L., Lettre, G., Langenberg, C., Launer, L.J., Lakatta, E.G., Laaksonen, R., Kyvik, K.O., Kronenberg, F., König, I.R., Khaw, K.T., Kaprio, J., Kaplan, L.M., Johansson, Å., Jarvelin, M.R., Cecile, A., Ingelsson, E., Igl, W., Kees Hovingh, G., Hottenga, J.J., Hofman, A., Hicks, A.A., Hengstenberg, C., Heid, I.M., Hayward, C., Havulinna, A.S., Hastie, N.D., Harris, T.B., Haritunians, T., Hall, A.S., Gyllensten, U., Guiducci, C., Groop, L.C., Gonzalez, E., Gieger, C., Freimer, N.B., Ferrucci, L., Erdmann, J., Elliott, P., Ejebe, K.G., Döring, A., Dominiczak, A.F., Demissie, S., Deloukas, P., De Geus, E.J.C., De Faire, U., Crawford, G., Collins, F.S., Chen, Y.D.I., Caulfield, M.J., Campbell, H., Burtt, N.P., Bonnycastle, L.L., Boomsma, D.I., Boekholdt, S.M., Bergman, R.N., Barroso, I., Bandinelli, S., Ballantyne, C.M., Assimes, T.L., Quertermous, T., Altshuler, D., Seielstad, M., Wong, T.Y., Tai, E.S., Feranil, A.B., Kuzawa, C.W., Adair, L.S., Taylor, H.A., Borecki, I.B., Gabriel, S.B., Wilson, J.G., Holm, H., Thorsteinsdottir, U., Gudnason, V., Krauss, R.M., Mohlke, K.L., Ordovas, J.M., Munroe, P.B., Kooner, J.S., Tall, A.R., Hegele, R.A., Kastelein, J.J.P., Schadt, E.E., Rotter, J.I., Boerwinkle, E., Strachan, D.P., Mooser, V., Stefansson, K., Reilly, M.P., Samani, N.J., Schunkert, H., Cupples, L.A., Sandhu, M.S., Ridker, P.M., Rader, D.J., Van Duijn, C.M., Peltonen, L., Abecasis, G.R., Boehnke, M. and Kathiresan, S. 2010. Biological, clinical and population relevance of 95 loci for blood lipids. *Nature*. **466**(7307), pp.707–713.

Timasheff, S.N. 1993. THE CONTROL OF PROTEIN STABILITY AND ASSOCIATION BY WEAK INTERACTIONS WITH WATER: How Do Solvents Affect These Processes? *Annu. Rev. Biophys. Biomol. Struct.* **22**, pp.67–97.

Tranquilli, A.L., Brown, M.A., Zeeman, G.G., Dekker, G. and Sibai, B.M. 2013. The definition of severe and early-onset preeclampsia. Statements from the International Society for the Study of Hypertension in Pregnancy (ISSHP). *Pregnancy Hypertension: An International Journal of Women's Cardiovascular Health*. **3**(1), pp.44–47.

Trimarco, V., Izzo, R., Morisco, C., Mone, P., Virginia Manzi, M., Falco, A., Pacella, D., Gallo, P., Lembo, M., Santulli, G. and Trimarco, B. 2022. High HDL (High-Density Lipoprotein) Cholesterol Increases Cardiovascular Risk in Hypertensive Patients. *Hypertension*. **79**(10), pp.2355–2363.

Trivett, C., Lees, Z.J. and Freeman, D.J. 2021. Adipose tissue function in healthy pregnancy, gestational diabetes mellitus and pre-eclampsia. *European Journal of Clinical Nutrition*. **75**(12), pp.1745–1756.

Tudurí, E., Soriano, S., Almagro, L., Montanya, E., Alonso-Magdalena, P., Nadal, Á. and Quesada, I. 2022. The pancreatic β-cell in ageing: Implications in age-related diabetes. *Ageing Research Reviews*. **80**, p.101674.

Vaisar, T., Couzens, E., Hwang, A., Russell, M., Barlow, C.E., DeFina, L.F., Hoofnagle, A.N. and Kim, F. 2018. Type 2 diabetes is associated with loss of HDL endothelium protective functions. *PLoS ONE*. **13**(3), pp.1–16.

Varadi, M., Anyango, S., Deshpande, M., Nair, S., Natassia, C., Yordanova, G., Yuan, D., Stroe, O., Wood, G., Laydon, A., Zídek, A., Green, T., Tunyasuvunakool, K., Petersen, S., Jumper, J., Clancy, E., Green, R., Vora, A., Lutfi, M., Figurnov, M., Cowie, A., Hobbs, N., Kohli, P., Kleywegt, G., Birney, E., Hassabis, D. and Velankar, S. 2022. AlphaFold Protein Structure Database: Massively expanding the structural coverage of protein-sequence space with high-accuracy models. *Nucleic Acids Research*. **50**(D1), pp.D439–D444.

Vats, H., Saxena, R., Sachdeva, M.P., Walia, G.K. and Gupta, V. 2021. Impact of maternal pre-pregnancy body mass index on maternal, fetal and neonatal adverse outcomes in the worldwide populations: A systematic review and meta-analysis. *Obesity Research & Clinical Practice*. **15**(6), pp.536–545.

Vedhachalam, C., Chetty, P.S., Nickel, M., Dhanasekaran, P., Lund-Katz, S., Rothblat, G.H. and Phillips, M.C. 2010. Influence of apolipoprotein (Apo) A-I structure on nascent High Density Lipoprotein (HDL) particle size distribution. *Journal of Biological Chemistry*. **285**(42), pp.31965–31973.

Verma, M., Esht, V., Alshehri, M.M., Aljahni, M., Chauhan, K., Morsy, W.E., Kapoor, N. and Kalra, S. 2023. Factors Contributing to the Change in Overweight/Obesity Prevalence Among Indian Adults: A multivariate decomposition analysis of data from the National Family Health Surveys. *Advances in Therapy*.

Verwer, B.J., Scheffer, P.G., Vermue, R.P., Pouwels, P.J., Diamant, M. and Tushuizen, M.E. 2020. NAFLD is related to Post-prandial Triglyceride-enrichment of HDL Particles in Association with Endothelial and HDL Dysfunction. *Liver International*. **40**(10), pp.2439–2444.

Viljanen, A.P.M., Iozzo, P., Borra, R., Kankaanpää, M., Karmi, A., Lautamäki, R., Järvisalo, M., Parkkola, R., Rönnemaa, T., Guiducci, L., Lehtimäki, T., Raitakari, O.T., Mari, A. and Nuutila, P. 2009. Effect of Weight Loss on Liver Free Fatty Acid Uptake and Hepatic Insulin Resistance. *The Journal of Clinical Endocrinology & Metabolism*. **94**(1), pp.50–55.

Vitali, C., Khetarpal, S.A. and Rader, D.J. 2017. HDL Cholesterol Metabolism and the Risk of CHD: New Insights from Human Genetics. *Current Cardiology Reports*. **19**(12).

Vounzoulaki, E., Khunti, K., Abner, S.C., Tan, B.K., Davies, M.J. and Gillies, C.L. 2020. Progression to type 2 diabetes in women with a known history of gestational diabetes: Systematic review and meta-analysis. *The BMJ*. **369**.

Wagner-Golbs, A., Neuber, S., Kamlage, B., Christiansen, N., Bethan, B., Rennefahrt, U., Schatz, P. and Lind, L. 2019. Effects of Long-Term Storage at −80 °C on the Human Plasma Metabolome. *Metabolites*. **9**(5).

Wahlgren, C.-M., Zheng, W., Shaalan, W., Tang, J. and Bassiouny, H.S. 2009. Human Carotid Plaque Calcification and Vulnerability: Relationship between Degree of Plaque Calcification, Fibrous Cap Inflammatory Gene Expression and Symptomatology. *Cerebrovascular Diseases*. **27**(2), pp.193–200.

Wang, F., Kohan, A.B., Kindel, T.L., Corbin, K.L., Nunemaker, C.S., Obici, S., Woods, S.C., Davidson, W.S. and Tso, P. 2012. Apolipoprotein A-IV improves glucose homeostasis by enhancing insulin secretion. *Proceedings of the National Academy of Sciences of the United States of America*. **109**(24), pp.9641–9646.

Watson, A.D., Berliner, J.A., Hama, S.Y., La Du, B.N., Faull, K.F., Fogelman, A.M. and Navab, M. 1995. Protective effect of high density lipoprotein associated paraoxonase. Inhibition of the biological activity of minimally oxidized low density lipoprotein. *The Journal of Clinical Investigation*. **96**(6), pp.2882–2891.

Wei, X., Liu, X., Tan, C., Mo, L., Wang, H., Peng, X., Deng, F. and Chen, L. 2019. Expression and Function of Zinc-α2-Glycoprotein. *Neuroscience Bulletin*. **35**(3), pp.540–550.

West, R.M. 2022. Best practice in statistics: The use of log transformation. *Annals of Clinical Biochemistry*. **59**(3), pp.162–165.

White, J., Swerdlow, D.I., Preiss, D., Fairhurst-Hunter, Z., Keating, B.J., Asselbergs, F.W., Sattar, N., Humphries, S.E., Hingorani, A.D. and Holmes, M. V. 2016. Association of lipid fractions with risks for coronary artery disease and diabetes. *JAMA Cardiology*. **1**(6), pp.692–699.

White, R.E. 2002. Estrogen and vascular function. *Vascular Pharmacology*. **38**(2), pp.73–80.

Wilkerson, B.A., Grass, G.D., Wing, S.B., Argraves, W.S. and Argraves, K.M. 2012. Sphingosine 1-Phosphate (S1P) Carrier-dependent Regulation of Endothelial Barrier: HIGH DENSITY LIPOPROTEIN (HDL)-S1P PROLONGS ENDOTHELIAL BARRIER ENHANCEMENT AS COMPARED WITH ALBUMIN-S1P VIA EFFECTS ON LEVELS, TRAFFICKING, AND SIGNALING OF S1P1*. *Journal of Biological Chemistry*. **287**(53), pp.44645–44653.

Williams, P.T., Krauss, R.M., Vranizan, K.M., Albers, J.J. and Wood, P.D.S. 1992. *Effects of Weight-Loss by Exercise and by Diet on Apolipoproteins A-I and A-II and the Particle-Size Distribution of High-Density Lipoproteins in Men*.

Wilson, J.R. and Kapoor, S.C. 1993. *Contribution of prostaglandins to exercise-induced vasodilation in humans*.

Wilson, P.G., Thompson, J.C., Shridas, P., McNamara, P.J., de Beer, M.C., de Beer, F.C., Webb, N.R. and Tannock, L.R. 2018. Serum Amyloid A Is an Exchangeable Apolipoprotein. *Arteriosclerosis, Thrombosis, and Vascular Biology*. **38**(8), pp.1890–1900.

Witte, D.R., Taskinen, M.R., Perttunen-Nio, H., Van Tol, A., Livingstone, S. and Colhoun, H.M. 2004. Study of agreement between LDL size as measured by nuclear magnetic resonance and gradient gel electrophoresis. *Journal of Lipid Research*. **45**(6), pp.1069–1076.

Wójtowicz, A., Zembala-Szczerba, M., Babczyk, D., Kołodziejczyk-Pietruszka, M., Lewaczyńska, O. and Huras, H. 2019. Early-and Late-Onset

Preeclampsia: A Comprehensive Cohort Study of Laboratory and Clinical Findings according to the New ISHHP Criteria. *International Journal of Hypertension*. **2019**.

Wolska, A., Reimund, M. and Remaley, A.T. 2020. Apolipoprotein C-II: The re-emergence of a forgotten factor. *Current Opinion in Lipidology*. **31**(3), pp.147–153.

Woollett, L.A., Catov, J.M. and Jones, H.N. 2022. Roles of maternal HDL during pregnancy. *Biochimica et Biophysica Acta - Molecular and Cell Biology of Lipids*. **1867**(3).

Wu, M.-S., Johnston, P., Sheu, -H, Hollenbeck, C.B., Jeng, C.-Y., Goldfine, I.D., Chen, Y.-D.L. and Reaven, C.M. 1990. Effect of Metformin on Carbohydrate and Lipoprotein Metabolism in NIDDM Patients. *Diabetes Care*. **13**, pp.1–8.

Wu, P., Haththotuwa, R., Kwok, C.S., Babu, A., Kotronias, R.A., Rushton, C., Zaman, A., Fryer, A.A., Kadam, U., Chew-Graham, C.A. and Mamas, M.A. 2017. Preeclampsia and Future Cardiovascular Health. *Circulation: Cardiovascular Quality and Outcomes*. **10**(2), p.e003497.

Xiao, C. and Lewis, G.F. 2012. Regulation of chylomicron production in humans. *Biochimica et Biophysica Acta (BBA) - Molecular and Cell Biology of Lipids*. **1821**(5), pp.736–746.

Yamagata, K. 2017. Docosahexaenoic acid regulates vascular endothelial cell function and prevents cardiovascular disease. *Lipids in Health and Disease*. **16**(1).

Yamauchi, T., Kamon, J., Waki, H., Terauchi, Y., Kubota, N., Hara, K., Mori, Y., Ide, T., Murakami, K., Tsuboyama-Kasaoka, N., Ezaki, O., Akanuma, Y., Gavrilova, O., Vinson, C., Reitman, M.L., Kagechika, H., Shudo, K., Yoda, M., Nakano, Y., Tobe, K., Nagai, R., Kimura, S., Tomita, M., Froguel, P. and Kadowaki, T. 2001. The fat-derived hormone adiponectin reverses insulin resistance associated with both lipoatrophy and obesity. *Nature Medicine*. **7**(8), pp.941–946.

Young, J.C., Enslin, J. and Kuca, B. 1989. Exercise intensity and glucose tolerance in trained and nontrained subjects. *Journal of Applied Physiology*. **67**(1), pp.39–43.

Yu, X.-H. and Tang, C.-K. 2022. ABCA1, ABCG1, and Cholesterol Homeostasis *In*: L. Zheng, ed. *HDL Metabolism and Diseases* [Online]. Singapore: Springer Nature Singapore, pp.95–107. Available from: https://doi.org/10.1007/978-981-19-1592-5_7.

Yuana, Y., Levels, J., Grootemaat, A., Sturk, A. and Nieuwland, R. 2014. Co-isolation of extracellular vesicles and high-density lipoproteins using density gradient ultracentrifugation. *Journal of Extracellular Vesicles*. **3**(1), p.23262.

Yuhanna, I.S., Zhu, Y., Cox, B.E., Hahner, L.D., Osborne-Lawrence, S., Lu, P., Marcel, Y.L., Anderson, R.G.W., Mendelsohn, M.E., Hobbs, H.H. and Shaul, P.W. 2001. High-density lipoprotein binding to scavenger receptor-BI activates endothelial nitric oxide synthase. *Nature Medicine*. **7**(7), pp.853–857.

Zabczyk, M., Hondo, L., Krzek, M. and Undas, A. 2013. High-density cholesterol and apolipoprotein AI as modifiers of plasma fibrin clot properties in apparently healthy individuals. *Blood Coagulation & Fibrinolysis*. **24**(1).

Zamai, N., Cortie, C.H., Jarvie, E.M., Onyiaodike, C.C., Alrehaili, A., Francois, M., Freeman, D.J. and Meyer, B.J. 2020. In pregnancy, maternal HDL is specifically enriched in, and carries the highest proportion of, DHA in plasma. *Prostaglandins Leukotrienes and Essential Fatty Acids*. **163**.

Zambon, A., Deeb, S.S., Bensadoun, A., Foster, K.E. and Brunzell, J.D. 2000. In vivo evidence of a role for hepatic lipase in human apoB-containing lipoprotein metabolism, independent of its lipolytic activity. *Journal of Lipid Research*. **41**(12), pp.2094–2099.

Zeljkovic, A., Vekic, J., Spasic, S., Jelic-Ivanovic, Z., Spasojevic-Kalimanovska, V., Gojkovic, T., Ardalic, D., Mandic-Markovic, V., Cerovic, N. and Mikovic, Z. 2013. Changes in LDL and HDL subclasses in normal pregnancy and associations with birth weight, birth length and head circumference. *Maternal and Child Health Journal*. **17**(3), pp.556–565.

Zerrad-Saadi, A., Therond, P., Chantepie, S., Couturier, M., Rye, K.-A., Chapman, M.J. and Kontush, A. 2009. HDL3-Mediated Inactivation of LDL-Associated Phospholipid Hydroperoxides Is Determined by the Redox Status of Apolipoprotein A-I and HDL Particle Surface Lipid Rigidity. *Arteriosclerosis, Thrombosis, and Vascular Biology*. **29**(12), pp.2169–2175.

Zhang, C. and Rawal, S. 2017. Dietary iron intake, iron status, and gestational diabetes. *Am J Clin Nutr*. **106**, pp.1672–80.

Zhang, W.-J., Stocker, R., Mccall, M.R., Forte, T.M. and Frei, B. 2002. Lack of inhibitory effect of HDL on TNFa-induced adhesion molecule expression in human aortic endothelial cells. *Atherosclerosis*. **165**, pp.241–249.

Zhu, Y.P., Shen, T., Lin, Y.J., Chen, B.D., Ruan, Y., Cao, Y., Qiao, Y., Man, Y., Wang, S. and Li, J. 2013. Astragalus polysaccharides suppress ICAM-1 and VCAM-1 expression in TNF-α-treated human vascular endothelial cells by blocking NF-κB activation. *Acta Pharmacologica Sinica*. **34**(8), pp.1036–1042.